Fischer and N-heterocyclic carbene complexes of tungsten(0)

By

René Pretorius

Submitted in partial fulfilment of the degree

MAGISTER SCIENTIAE

In the Faculty of Natural and Agricultural Sciences

UNIVERSITY OF PRETORIA

PRETORIA

Supervisor: Dr. M. Landman

May 2012

DECLARATION

I, René Pretorius, declare that the dissertation, which I hereby submit for the degree Magister Scientiae at the University of Pretoria, is my own work and has not previously been submitted by me for at degree at this or any other tertiary institution.

_____

Signature

_____

Date

To the Creator:

Who am I that You are mindful of me,

Everything I am is because of You.

ACKNOWLEDGEMENTS

Dr. M. Landman - For always believing in us, all your patience, and for being more than just a supervisor. I value your input in my life. Thank you

Theresa - 24 years of looking after me, you never cease to amaze me

Manson - Ek was toe net bang, dankie vir die inspirasie

Mommy - For always listening, and supporting me, no matter what

Roan – The Lab partner, all the late nights, slap chips and the cinnamon doughnuts, you ROCK

Tamzyn and Lauren - The Bubble and The Minion, here is to the Parlotones

The Organics: Chantal, Cara, Stephen, Wynand and Rohen - Coffee, lunch, advice and craziness, you are true friends

Sam and Karl - For all the lessons in chemistry, and life, your advice is priceless

Mr. Eric Palmer - For the beautiful NMR spectra, they always put a smile on my dial

Mr. Dave Liles - For all the crystal structures you patiently correct

Prof v. Rooyen - Thank you for keeping us all sane

Prof Vleggaar - Thank you for the the deuterated solvents and for always assisting with NMRs

Prof Lotz, Nina, Belinda - Thank you for all the advice, and keeping me from blowing something up

Prof Potgieter - Your guidance and advice is precious

Renet - For reminding me there is life outside the lab!

Reinardt - My chemie maatjie, sterkte met dit wat kom

Walter and Bertie - For keeping me company on all those late lab nights

Wolff - You are finally finished. It was a wild ride. Cheers buddy!

TABLE OF CONTENTS

CHAPTER 6: EXPERIMENTAL

APPENDIXES: ATTACHED COMPACT DISK

ABSTRACT

The synthesis of novel Fischer and N-heterocyclic tungsten(0) carbene complexes was endeavoured in this study and resulted in the synthesis, isolation and characterisation of eighteen new complexes.

Sixteen novel Fischer carbene complexes were synthesised. In these complexes, both carbene ligand substituents were varied. Ethoxy as well as amino heteroatom substituents were used. Heteroaryl compounds thiophene and furan were employed as the second substituents on the carbene ligand. Complexes with combinations of these different substituents were synthesised and investigated to assess the influence the various substituents of the carbene ligand may have on the carbene complex itself. In addition, the metal ligand sphere was altered by substitution of one or two carbonyl ligands for either an amine or a phosphine ligand/s. These substitutions resulted in the formation of metal pentacarbonyl, metal tetracarbonyl as well as metal tricarbonyl systems. The complexes were successfully characterised by means of NMR and IR spectroscopy, and in selected cases X-ray diffraction and mass spectrometry.

Synthesis of N-heterocyclic carbene complexes derived from isopropyl and mesityl imidazolium chlorides was attempted. The products were obtained in crude form, but could not be isolated due to decomposition during purification. Two novel decomposition products, which point towards a unique decomposition route, were isolated.

Theoretical models of both the novel Fischer carbene complexes and the N-heterocyclic carbene complexes were calculated. This allowed for identification of infrared modes observed in experimental data. Furthermore, the HOMO and LUMO distributions and the HOMO-LUMO energy gaps were calculated, along with electrostatic potential maps. In all the Fischer carbene complexes the HOMOs were located on the metal centre and the LUMOs on the carbene ligand. In contrast, the HOMO and the LUMO were both located on the metal centre for the N-heterocyclic carbenes. The HOMO-LUMO energy gap decreased as follows:

NHC complexes > Amino Fischer carbene complexes > Ethoxy Fischer carbene complexes

Lastly, in all the complexes studied, the electrostatic potential maps indicated that the highest amount of electron density was found on the carbonyl ligands of these complexes.

Both experimental and theoretical data indicated marked differences in the various classes of compounds, suggesting that these complexes would not only have different reactivities but also be suited to different applications. Experimental studies on reactivity and applications are thus future avenues of study which are made available from these results.

LIST OF COMPOUNDS

KNOWN COMPOUNDS
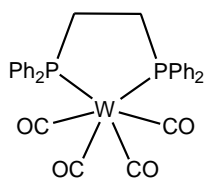
W(CO)₄DPPE
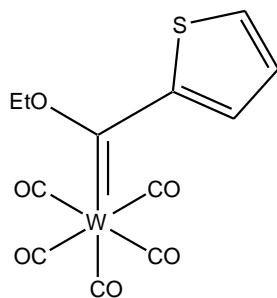
A
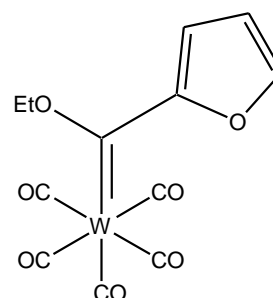
B
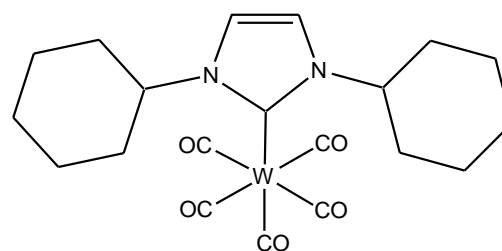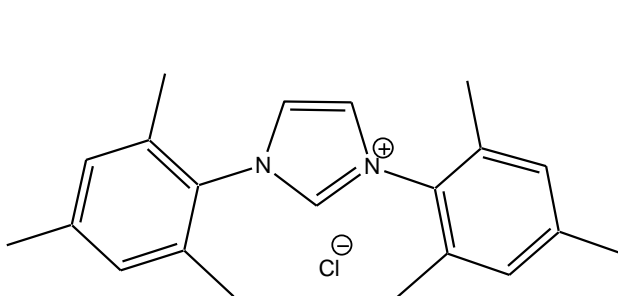
C

NOVEL COMPOUNDS
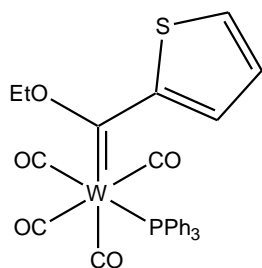
A1

B1

A2

B2

A3

B3

A4

B4

vi
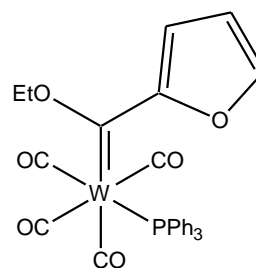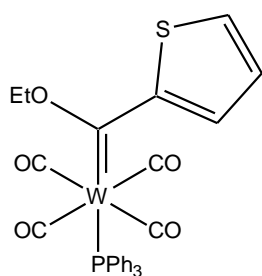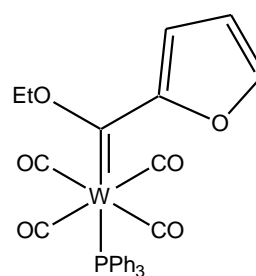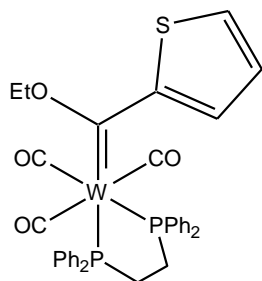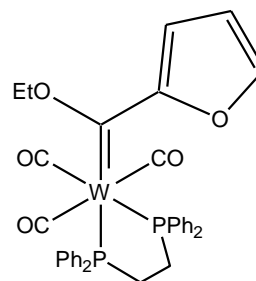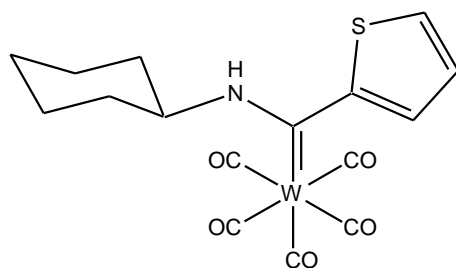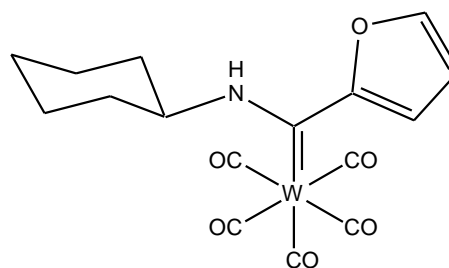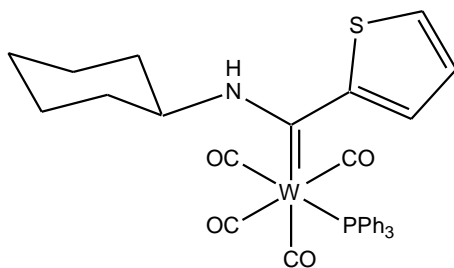
A5
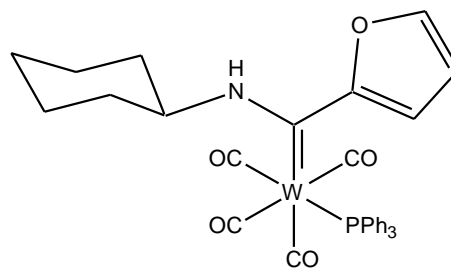
B5
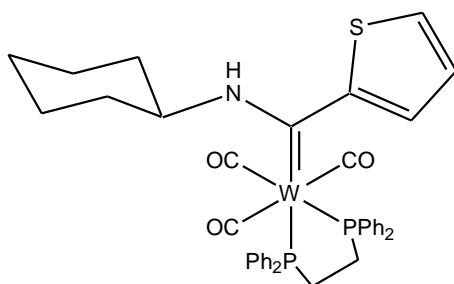
A6
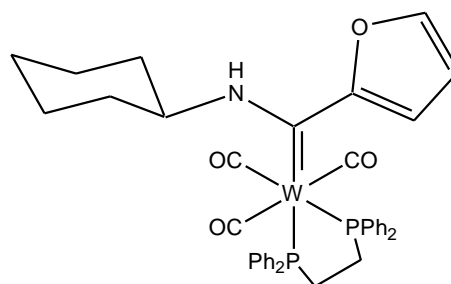
B6
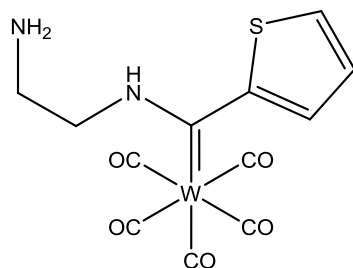
A7
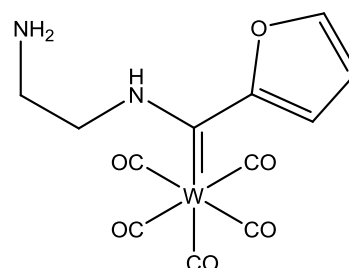
B7
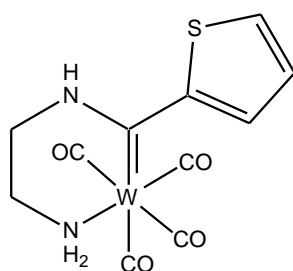
A8
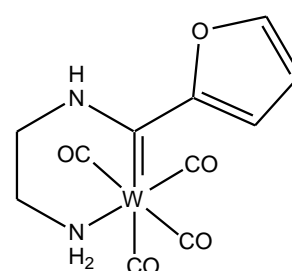
B8
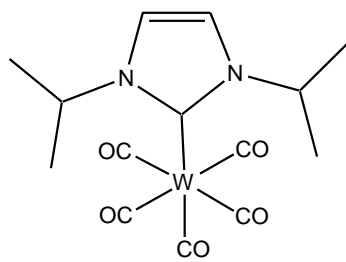
C1
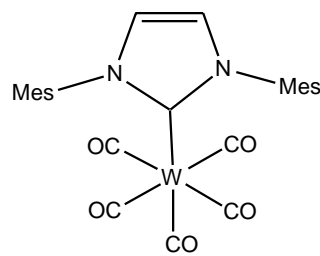
C2
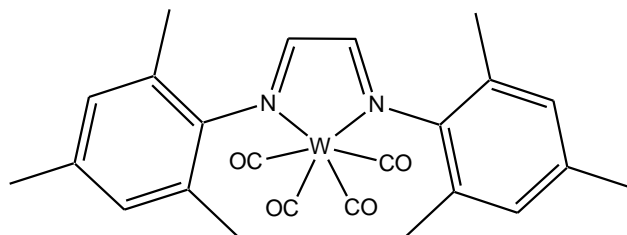
C3
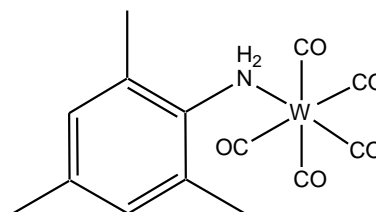
C4

LIST OF ABBREVIATIONS

b	Broad peak
CO	Carbonyl
d	Doublet
ESP	Electrostatic potential
DCM	Dichloromethane
Diglyme	Diglycol methylether
DPPE	Bis(diphenylphosphino)ethane
EN	Ethylenediamine
HOMO	Highest occupied molecular orbital
hr	Hour
ICyc	Imidazolidene cyclohexyl
IMes	Imidazolidene mesityl
IR	Infrared
LUMO	Lowest occupied molecular orbital
m	Multiplet
MeOH	Methanol
min	Minutes
M.S.	Mass spectrometry
mmol	Millimole
^{n}BuLi	^{n}Butyl lithium
NHC	N-Heterocyclic carbene
NMR	Nuclear magnetic resonance
q	Quartet
RT	Room Temperature
t	Triplet
THF	Tetrahydrofuran
XRD	X-ray diffractometry

CHAPTER 1:

INTRODUCTION

In 1963 the first heteroatom stabilized metal carbene complex was synthesised by R.B. King (Figure 1.1).[1,2] This complex was unfortunately characterised incorrectly, and the proper structure was only assigned in 1970.[2] The first fully characterised, stable metal carbene complex, pentacarbonyl[methoxy(phenyl)carbene]tungsten(0) (Figure 1.1), was published in 1964 by Fischer and Maasböl,[3,4] and sparked interest in a new field of organometallic chemistry which has since developed at an immense rate. Today three main classes of carbene complexes are recognized, namely Schrock, Fischer and N-heterocyclic carbenes (NHCs). Each set of carbenes has its own unique characteristics and reactivity patterns. The development of carbene chemistry has been closely linked to the many applications of these complexes. These applications range from fine organic synthesis to catalysis. A brief discussion of the discovery, bonding pattern and reactivity of the Fischer, N-heterocyclic and Schrock carbenes will be given, concluding with the various applications of these complexes.
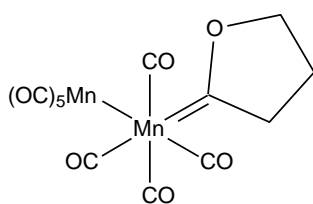
King's Complex: Final structure[1,2]   First Fischer Carbene Complex[3,4]
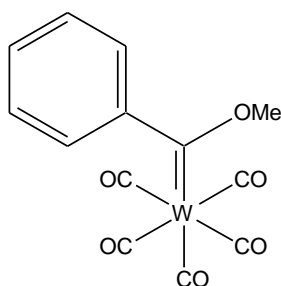
FIGURE 1.1: HISTORIC CARBENE COMPLEXES

1.1 FISCHER CARBENE COMPLEXES

Fischer carbenes were the first carbene complexes to be correctly described in literature.[1–7] Shortly after the initial synthesis and characterisation of the first complex, the chromium analogue was characterised by means of X-ray crystallography, confirming the proposed structure.[5,7] These carbene complexes, along with the complex synthesised by King, are examples of what are today known as Fischer carbene complexes. Fischer carbenes are generally found as ligands to late transition metals in low oxidation states.[1,5,6,8,9] The carbene carbons found for these complexes are singlet carbenes, and are electrophilic. This implies that the bond between the metal and the carbon centre consists of a sigma bonding interaction from the carbene carbon to the metal, and π-backbonding from the metal centre to the carbene carbon (Figure 1.2).[1,2,9,10] An essential characteristic of Fischer carbenes is the presence of at least one heteroatom substituent on the carbene carbon. The heteroatom substituent stabilizes the empty p-orbital on the carbene carbon, stabilizing the singlet state, and decreasing the amount of π-donation required from the metal centre.[1,9,10]

X = Heteroatom
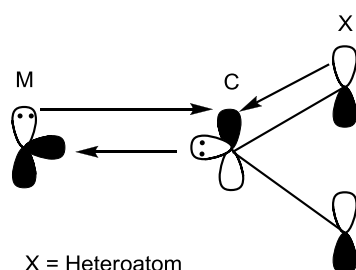
FIGURE 1.2: BONDING PATTERN IN FISCHER CARBENE COMPLEXES

The majority of the electron density from the π-bond is, however, withdrawn by the electron withdrawing metal fragment, causing the electrophilic character of the carbene carbon.[1,5,9,11] The general reactivity pattern found for Fischer carbene complexes is summarised in figure 1.3.

X = Heteroatom
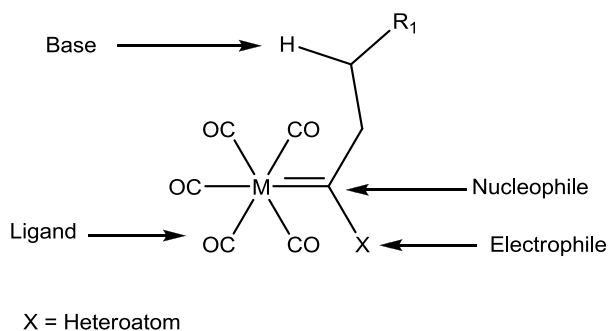
FIGURE 1.3: REACTIVITY PATTERN OF FISCHER CARBENE COMPLEXES[5]

Naturally the carbene centre may be attacked by nucleophiles.[5] Hydrogens found on the α-carbon of the carbene are readily removed by a base, allowing the complex to be available for further reactions.[5,11] Electrophiles may also coordinate to the heteroatom substituent. Lastly, the co-ligand sphere of the metal may be altered.[5,7,12–15]

Heteroatoms are essential for the stabilization of Fischer carbenes and do so in two ways. Firstly, by withdrawing electron density from the carbene carbon through inductive effects, thus stabilizing the σ-nonbonding orbital of the singlet state.[16] Secondly, π-donation from the lone pair found on the heteroatom into the empty p-orbital of the carbene also stabilizes the carbene. This, consequently, reduces the amount of backbonding required from the metal.
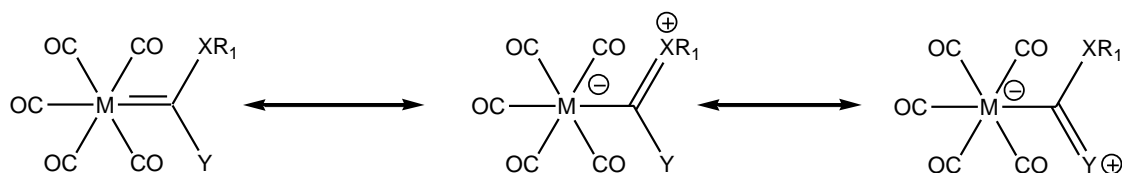
M = Metal, X = Heteroatom, Y = π-Donating substituent

FIGURE 1.4: RESONANCE PATTERNS FOR STABILIZED FISCHER CARBENES

It was thus concluded that π-donation from substituent Y would further increase the stability of the carbene, and subsequently decrease the π-interaction from the metal fragment (Figure 1.4). This has been shown to be true, especially in the case of NHCs.[10,16] Naturally not only heteroatom stabilization was considered for position Y, and thus aryl substituents were also investigated. The first crystal structure of a Fischer carbene was incidently determined on $(CO)_5CrC(OMe)(Ph)$.[5] However, the phenyl ring was not orientated correctly to be involved in π-donation, in the solid state. Thus the focus was shifted to heteroaryl groups, notably the five membered rings of N-methyl pyrrole, furan and thiophene. The addition of a heteroatom to the ring did, in fact, increase stability of the carbene.[17] The increase in stability depended on the heteroatom contained in the ring and stabilization of the carbene is known to increase in the order O < S < NMe.[17] The Fischer carbene tungsten complexes considered during this study were, actually, found to be stable in the presence of air for several days, indicating the increased stability of heteroaryl substituted carbene complexes. Several examples of these complexes are found, including the complete range of Group 6 metals,[17–20] as well as Re and Mn derivatives of these complexes.[21] These substituents also readily lend themselves to synthesis of multimetal complexes[23–25] and unique chelate carbene complexes.[22] The heteroaryl ligands have

furthermore been modified by extension of the aromatic system which allows for novel applications in nanomaterials.[24]

1.2 N-HETEROCYCLIC CARBENE COMPLEXES

N-Heterocyclic carbenes are an extremely popular and useful class of carbenes. Initially they were seen as a type of diamino Fischer carbene. However, the many differences between Fischer carbenes and NHCs have allowed the two classes of carbenes to be distinguished.[10] The first reports of NHC carbenes were by Wanzlick[26] and Öfele[27] in 1968, only four years after the first Fischer carbenes were accurately described (Figure 1.5).
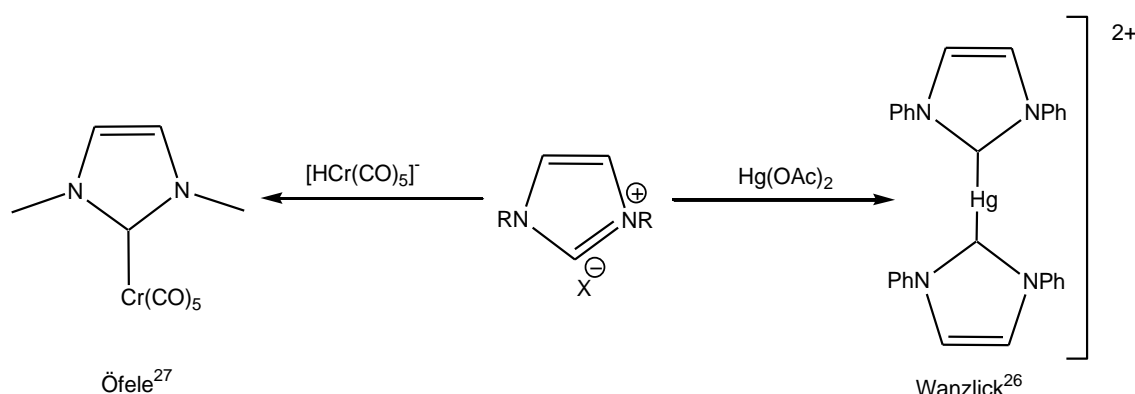
FIGURE 1.5: FIRST NHC COMPLEXES SYNTHESISED BY ÖFELE[27] AND WANZLICK[26]

These were developed mostly with the idea that having two heteroatoms, which can donate electron density, bonded to the carbene centre would increase stability. However, the field of NHC chemistry only truly started to develop after Arduengo was able to synthesise and isolate the first stable free NHCs and their protonated halide precursor salts in 1991 (Figure 1.6(a)).[28] It was found that the larger the steric bulk of the NHC substituent, the higher the stability of the free carbene. Arduengo's discovery allowed for straightforward synthesis of stable free carbenes. This permitted the use of NHCs as catalysts in free form or coordinated to a metal centre. In honour of Arduengo's discovery, NHCs are often called Arduengo carbenes. The development of Grubbs 2 (Figure 1.6(b)) and similar metathesis catalysts,[29,30] in which NHCs proved to be excellent replacements for phosphines,[30–33] granted NHCs a further boost. Today, much attention is given to the understanding and development of free and complexed N-heterocyclic carbenes.

4

1,3-bis(adamantyl)imidazolium chloride

(a)

Grubbs 2 Catalyst

(b)
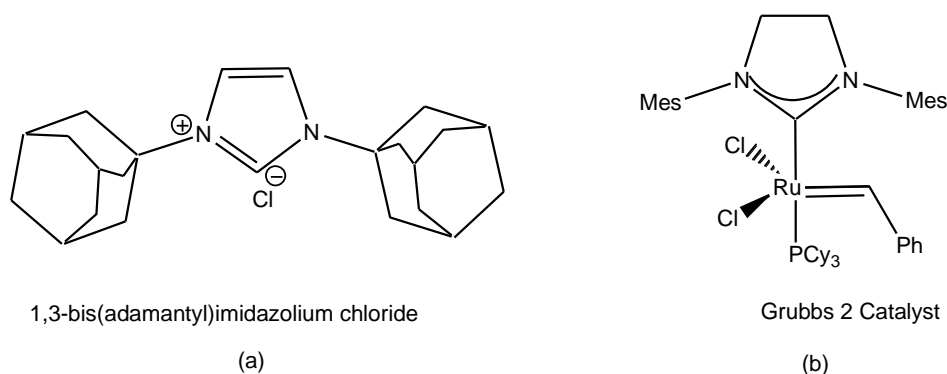
FIGURE 1.6: IMPORTANT DEVELOPMENTS IN NHC CHEMISTRY: (a) FIRST STABLE FREE CARBENE SYNTHESISED BY ARDUENGO[28] AND (b) THE GRUBBS 2 CATALYST[9]

NHCs are generally found complexed to late transition metals,[10] but representative complexes for most metal groups are found.[30] These complexes, in contrast to the Fischer analogues, are bound to the metal centre through σ-donation with negligible π-backdonation.[30,34] It has been shown recently, however, that some π-donation may occur for certain metals.[34]
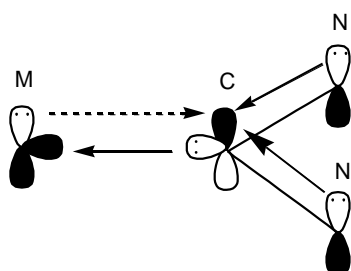
FIGURE 1.7: BONDING INTERACTIONS IN NHC COMPLEXES

The bonding pattern found in NHC complexes is very different from Fischer carbenes. Since NHCs are sometimes described as diamino-substituted Fischer carbenes,[10] it would thus be expected that they have similar bonding patterns. However, the carbene centre is exceedingly well stabilized by π-donation from both nitrogen groups (Figure 1.7).[16] The central NHC ring furthermore forces the nitrogen p-orbitals into the most favourable position for maximum overlap with the empty p-orbitals of the carbene carbon. π-Donation to the carbene also increases the energy gap between the singlet and the triplet state, favouring the more stable singlet electron configuration, similar to Fischer carbene complexes. Lastly, the nitrogen atoms are also σ-withdrawing substituents and stabilize the singlet state by inductive effects.[16] NHC carbenes are thus much more stable, and less reactive than other carbene classes.

5

Much work has been done on Ru, Pt and other late transition metal carbene complexes which are used for catalysis, as is obvious from the many reviews on this topic.[31,35,36] An interesting alternative to these types of complexes is the carbonyl derivatives. Carbonyl-containing NHC metal complexes are generally found for Group 6 and 7 metals.[37–45] However, cobalt carbonyl NHC complexes, with applications in hydroformylation catalysis, have also been synthesised.[46] Carbonyl NHC metal complexes (Figure 1.8) are of interest since the orginal work published by Öfele[27] focused on these molecules and their transformations.

van Rensburg *et.al.*[46]

Lui *et.al.*[44]

R = ^{I}Pr
M = Mn, X = Br
M = Re, X = Cl

Martin *et.al.*[37]

Roberts *et.al.*[45]
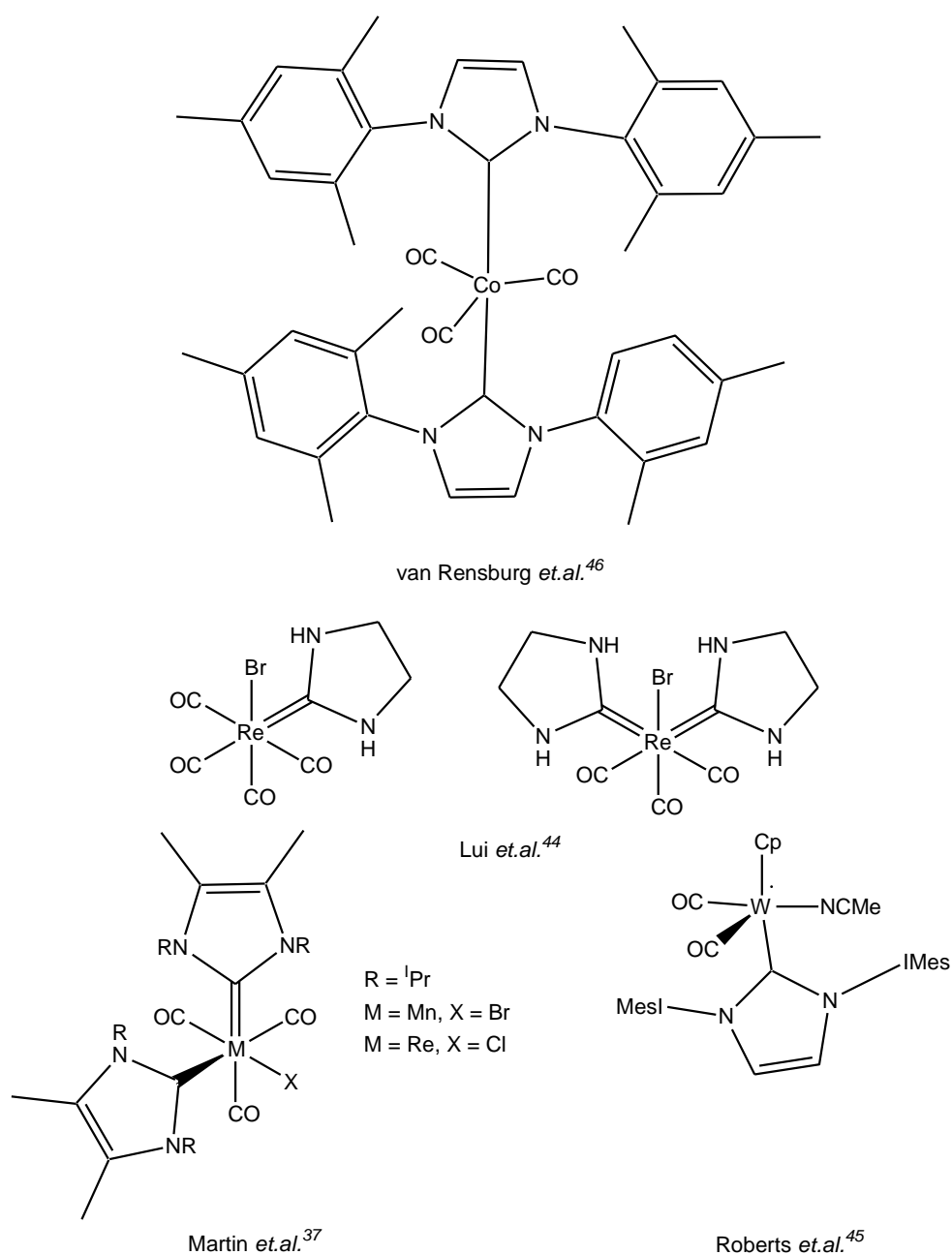
FIGURE 1.8: UNIQUE NHC CARBONYL METAL COMPLEXES

1.3 SCHROCK CARBENE COMPLEXES

The final class of carbenes were discovered by R.R. Schrock. The first Schrock carbene complex was synthesised in 1974, 10 years after the first recognized carbene complex.[1]
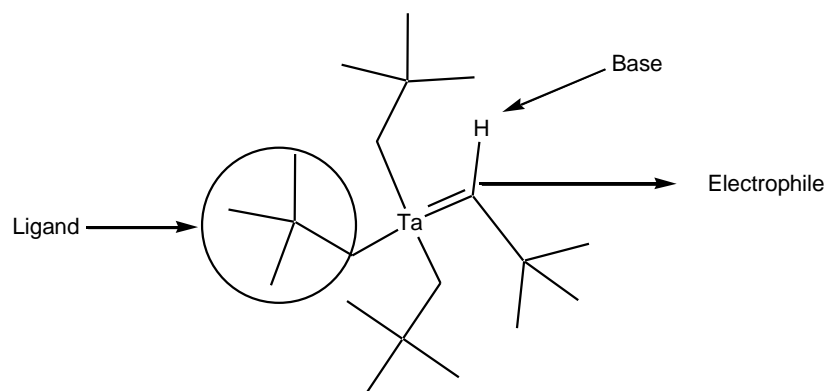
FIGURE 1.9: REPRESENTATIVE SCHROCK CARBENE COMPLEX AND THE REACTIVITY PATTERN FOR THESE COMPLEXES

Schrock carbenes are generally found as ligands to early transitions metals in a high oxidation state.[1] These complexes are characterised by the presence of a hydrogen atom or an alkyl group as the carbene substituents.[1,5,6] These substituents do not favour or stabilize the singlet state, and thus the carbene carbon is found in a triplet state. Schrock carbene complexes therefore have a formal double bond with covalent character between the metal centre and the carbon atom.[6] These complexes do not have heteroatom substituents, and are distinguished in this manner from Fischer carbene complexes.
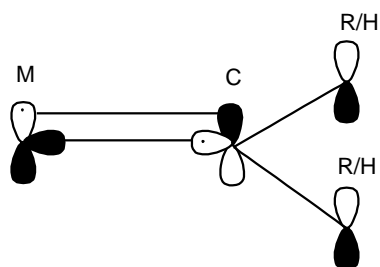
FIGURE 1.10: BONDING PATTERN OBSERVED FOR SCHROCK CARBENE COMPLEXES

7

As a result of this bonding, the carbene carbon is said to be nucleophilic and thus susceptible to attack from electrophiles.[1,5,6] The general reactivity patterns for these complexes also include deprotonation of the carbene carbon, if hydrogen is one of the carbene substituents. Substitution of the other ligands surrounding the metal may also occur (Figure 1.9).[5]

1.4 APPLICATIONS OF CARBENE COMPLEXES

A plethora of reactions and applications have been established for carbene complexes. Each class mentioned above has its own unique applications, but often, more than one carbene is combined in a complex to allow unique reactivity.

Fischer carbenes are applied in several different organic transformations. However, one of the most important applications for Fischer carbenes appears to be the formation of organic ring structures. The Dötz benzannulation reaction[5,47] is the most renowned of these ring forming reactions (Figure 1.11). Benzannulation is used for the production of highly substituted phenols, which are difficult to synthesise by other means. However, a range of organic ring structures ranging from cyclopropane[48] to cycloheptane may be synthesised with Fischer carbenes.[47] Fischer carbenes are also useful for the production of heteroaryl substituted rings such as furan derivatives.[49] Furthermore, these carbenes are essential for the Pauson-Khand reaction, also a cyclization reaction, which frequently involves amino carbenes. Fischer carbenes have additionally been applied to the synthesis of dienol esters,[50] production of ketenes and ketimines,[8] and even complex natural products have been synthesised using these carbenes. Fischer carbenes are not used that often, but have been shown to be useful for metathesis reactions as well.[9,51]

8
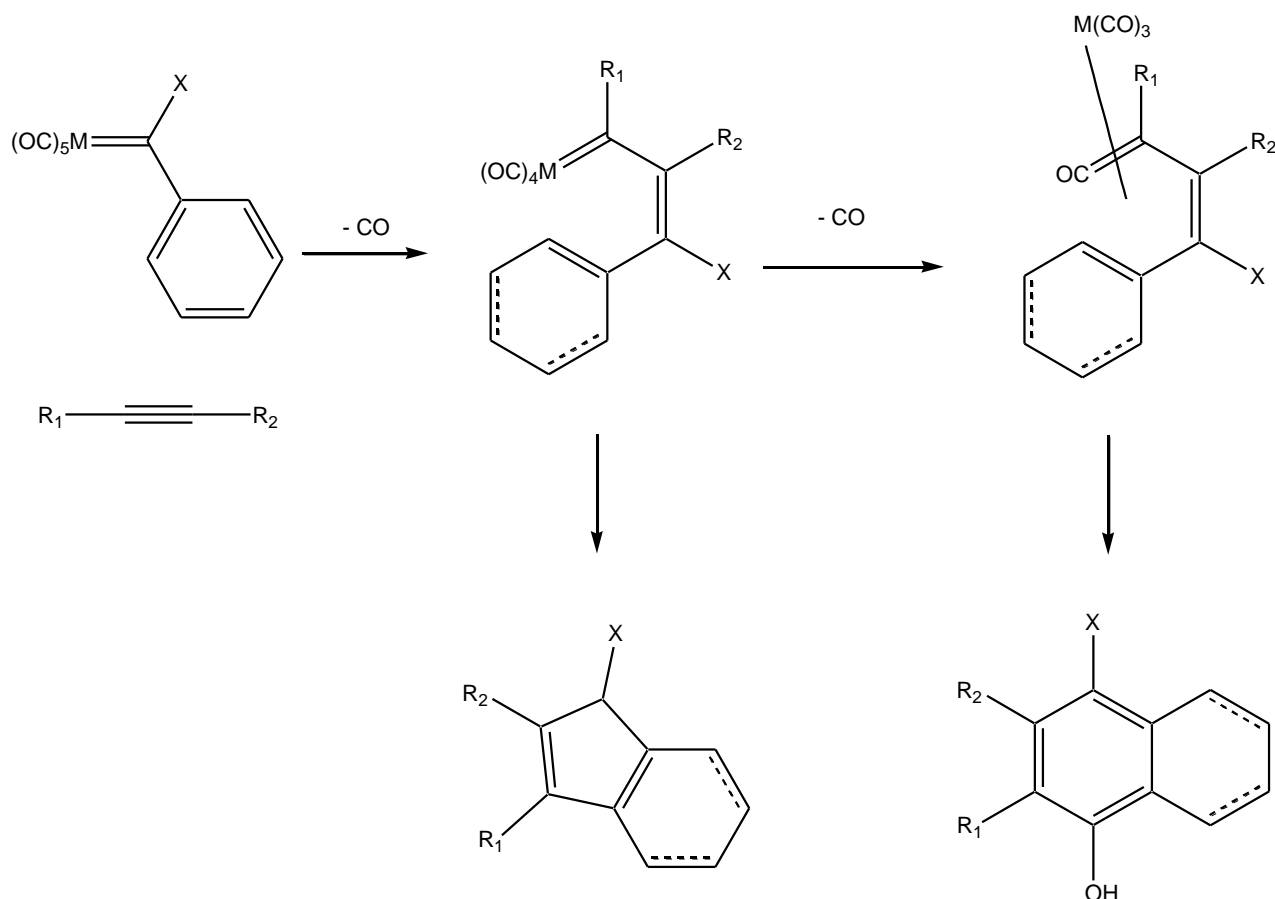
FIGURE 1.11: BENZANNULATION REACTION

Schrock carbenes are best known for their applications as Wittig phosphine ylide replacements[5,8] and applications in catalysis. Like Fischer carbenes, Schrock complexes have also been shown to be useful for the synthesis of cyclopropanes.[5] Fischer carbenes are, however, the preferred reagents for the formation of cyclic organic complexes.

NHC complexes, like Schrock carbenes, find the most applications in metathesis. This is due to the remarkable stability of NHC complexes[16,30,34] and the similarities found between phosphine ligands and NHCs. NHCs have been shown to be useful in Heck and Suzuki couplings and the copolymerisation of ethylene and CO. The transformation of olefin complexes, including cyclopropanation, hydrogenation and hydroformylation of olefins, is catalysed by NHC complexes.[16,30]

The Grubbs 2 catalyst is the most famous metathesis catalyst, and contains NHC ligands. This catalyst does not only use a single carbene ligand, but also incorporates a Schrock carbene (Figure 1.12).

9
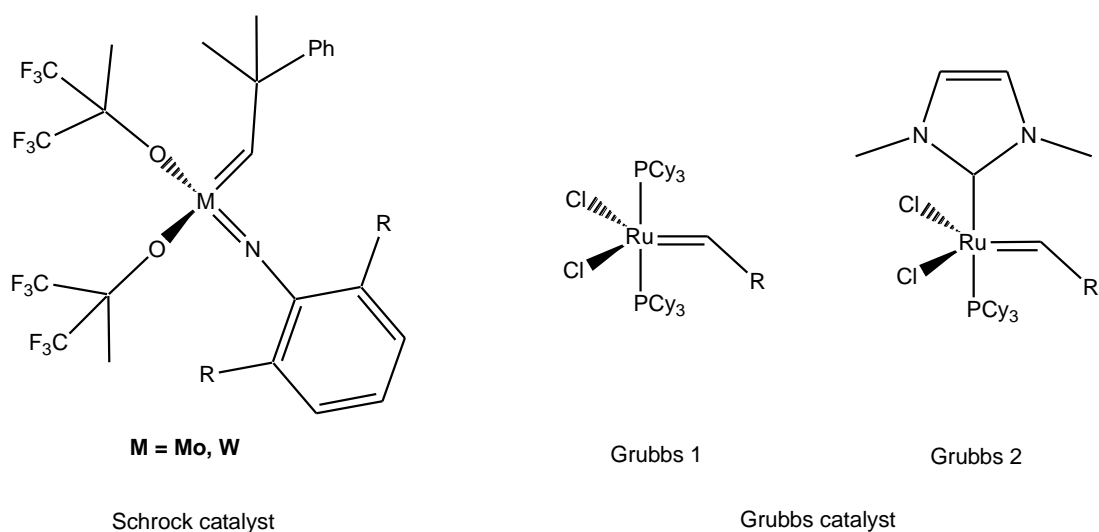
FIGURE 1.12: EXAMPLES OF POPULAR CARBENE-CONTAINING CATALYSTS

Olefin metathesis is extremely important since it allows for several novel transformations of organic complexes and is essential for polymer formation. The significance of these transformations is emphasised by the fact that Chauvin, Schrock and Grubbs were awarded the Noble prize in 2005, for mechanistic and applications-orientated studies on catalysts active in olefin metathesis.[6] Metathesis is defined as the exchange of double bond substituents by breaking and reformation of two double bonds.[52,53] The mechanism for alkene methathesis that is accepted today was developed by Chauvin and further evidence presented by Schrock (Figure 1.13).[6]
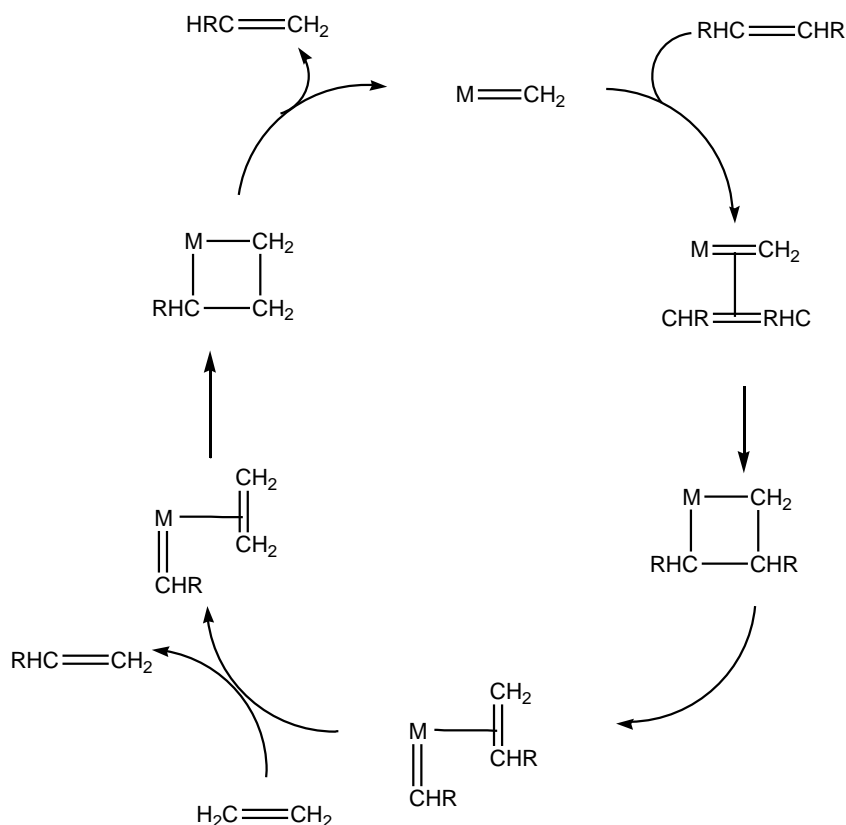
FIGURE 1.13: MECHANISM FOR ALKENE METHATHESIS

Currently the most popular and versatile catalysts are the Schrock tungsten and molybdenum catalysts, and Grubbs catalysts.[52] All three these catalysts contain Schrock components. However, the Grubbs 2 catalysts, which contain NHCs, are preferred since they are more stable and easier to handle.[9] It is generally accepted that most metathesis catalysts of early transition metals are in fact in a high oxidation state.[51] Katz,[51] however, suggests that low oxidations state transition metal complexes may also be used for metathesis. He uses metathesis-active tungsten Fischer carbenes as the main example for his argument (Figure 1.14). It can thus be seen that all three classes of carbenes have metathesis reactions as their common application.
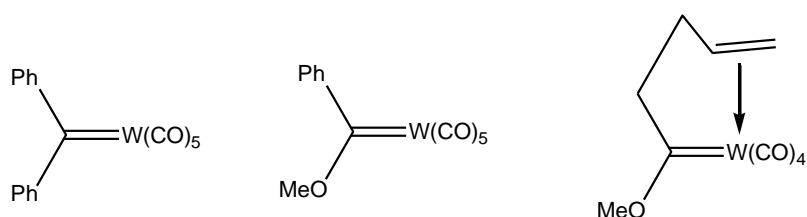
FIGURE 1.14: TUNGSTEN(0) FISCHER CARBENE INITIATORS OF METATHESIS

1.5 AIM OF THIS STUDY

It is clear from the many examples given that carbene metal complexes have a large range of applications. The most notable and the common application found for Fischer, Schrock and NHC complexes are in metathesis reactions. There are, however, fewer examples of catalytic Fischer carbene complexes than metathesis active Schrock and NHC complexes. It was recently shown by Fernández *et.al.*[54] that previously unphotoreactive tungsten Fischer carbene complexes can have increased reactivity by replacement of a carbonyl group on an amino Fischer carbene with a phosphorous ligand. Also, Arrieta *et.al.*[55] found that the energy difference between the HOMO and the LUMO of the carbene complexes can be reduced, and thus the reactivity of the complex increased, by substitution of a carbonyl group with a phosphine ligand. Lastly, it is known that in metal pentacarbonyl Fischer complex, a carbonyl group must be lost to allow for the olefin to coordinate, and metathesis to occur.[51] If one considers all of this information, it can be reasoned that altering the ligand sphere of pentacarbonyl Fischer carbenes with a phosphine would not only increase the reactivity of these complexes, but also facilitate the loss of a ligand, and thus increase catalytic activity. Some examples of Fischer carbene complexes substituted in this manner are found; however, there is a marked void for this research when compared to other avenues of Fischer carbene research.[56,57] The void is especially noteworthy in the case of diphosphine amino Fischer carbene complexes of tungsten(0).[56,57] There are, furthermore, no examples of heteroaryl Fischer carbenes with phosphine substituents. NHCs are also well known for their catalytic capabilities, thus low oxidation state complexes containing NHCs would also have potential catalytic activity. The aim of this study was thus the synthesis and theoretical study of novel heteroaryl Fischer carbene complexes with phosphine substituents and NHC tungsten(0) complexes. The intention was to develop a synthetic route to these complexes and a theoretical comparison of their properties, in order to increase the current knowledge regarding these types of complexes. This will aid the development of novel low oxidation state metal complexes with Fischer and N-heterocyclic carbene ligands.

1.6 REFERENCES

(1)   de Frémont, P.; Marion, N.; Nolan, S. P. *Coord. Chem. Rev.* **2009**, *253*, 862, and references therein.

(2)   Sierra, M. A. *Chem. Rev.* **2000**, *100*, 3591, and references therein.

(3)   Fischer, E. O.; Maasböl, A. *Angew. Chem. Int. Ed.* **1964**, *3*, 580.

(4)   Fischer, E. O.; Maasböl, A. *Angew. Chem.* **1964**, *76*, 645.

(5)   Dötz, K. H. *Angew. Chem. Int. Ed.* **1984**, *23*, 587.

(6)   Elschenbroich, C. *Organometallics*; 3rd ed.; Wiley - VCH: Weinheim, **2011**.

(7)   Mills, O. S.; Redhouse, A. D. *Chem. Commun.* **1966**, 814.

(8)   Herdon, J. W. *Tetrahedron* **2000**, *56*, 237.

(9)   Kotha, S.; Dipak, M. K. *Tetrahedron* **2012**, *68*, 397.

(10)   Fey, N.; Haddow, M. F.; Harvey, J. N.; Mcmullin, C. L.; Orpen, A. G. *Dalton Trans.* **2009**, 8183.

(11)   Wu, Y.-T.; Kurahashi, T.; de Meijere, A. *J. Organomet. Chem.* **2005**, *690*, 5900.

(12)   Werner, H.; Rascher, H. *Inorg. Chim. Acta* **1968**, 181.

(13)   Fischer, E. O.; Aumann, R. *Chem. Ber.* **1969**, *102*, 1495.

(14)   Streubel, R.; Priemer, S.; Jones, P. G. *J. Organomet. Chem.* **2001**, *618*, 423.

(15)   Sierra, M. A.; Fernández, I.; Gomez-Gallego, M.; Torres, M. R.; Cossı, F. P.; Arrieta, A.; Lecea, B.; Poveda, A.; Jimenez-Barbero, J. *J. Am. Chem. Soc.* **2003**, *125*, 9572.

(16)   Bourissou, D.; Guerret, O.; Gabbaı, P.; Bertrand, G. *Chem. Rev.* **2000**, *100*.

(17)   Connor,J. A.; Jones, M. *J. Chem. Soc. (A)* **1971**, 1974.

(18)   Fischer, E. O.; Held, W.; Kreißl, F. R.; Frank, A.; Huttner, G. *Chem. Ber.* **1977**, *110*, 656.

(19)   Olivier, A. J. Novel carbene complexes with pyrrole ligands, University of Pretoria, **2001**.

(20)   Aoki, S.; Fujimura, T.; Nakamura, E. *J. Am. Chem. Soc.* **1992**, *114*, 2985.

(21)   Bezuidenhout, D. I. Synthesis and structural investigations of manganese carbene complexes, University of Pretoria, **2006**.

(22)   van Jaarsveld, N. Synthesis and structure of modified thiophene biscarbene complexes, University of Pretoria, **2009**.

(23)   Crause, C.; Lotz, S. *Dalton Trans.* **2005**, *9*, 1649.

(24)   Landman, M.; Görls, H.; Lotz, S. *J. Organomet. Chem.* **2001**, *617*, 280.

(25)   Bezuidenhout, D. I.; Lotz, S.; Liles, D. C.; van der Westhuizen, B. *Coord. Chem. Rev.* **2012,** *256*, 479.

(26)   Wanzlick, H. W.; Schoenherr, H. J. *Angew. Chem. Int. Ed. Engl.* **1968**, *7*, 141.

(27)   Öfele, K. *J. Organomet. Chem.***1968**, *12*, 42 .

(28)   Arduengo, A. J.; Harlow, R. I.; Kline, M. *J. Am. Chem. Soc.* **1991**, *113*, 361.

(29)   *N-Heterocyclic Carbenes in Synthesis*; Nolan, S. P., Ed.; 1st ed.; Wiley - VCH Verlag GmbH & Co. KGaA: Weinheim, **2006**.

(30)   Herrmann, W. A.; Weskamp, T.; Böhm, V. P. W. *Adv. Organomet. Chem.* **2001**, *48*, 1.

(31)   Singh, R.; Nolan, S. P. *Annu. Rep. Prog. Chem., Sect. B* **2006**, *102*, 168.

(32)   Tapu, D.; Dixon, D. A.; Roe, C. *Chem. Rev.* **2009**, *109*, 3385.

(33)   Wang, F.; Liu, L.-jun; Wang, W.; Li, S.; Shi, M. *Coord. Chem. Rev.* **2012**, *256*, 804.

(34)   Jacobsen, H.; Correa, A.; Poater, A.; Constable, C.; Cavallo, L. *Coord. Chem. Rev.* **2009**, *253*, 687.

(35)   Zinn, F. K.; Viciu, M. S.; Nolan, S. P. *Annu. Rep. Prog. Chem., Sect. B.* **2004**, *100*, 231.

(36)   Boeda, F.; Nolan, S. P. *Annu. Rep. Prog. Chem., Sect. B* **2008**, *104*, 184.

(37)   Martin, T. A.; Ellul, C. E.; Mahon, M. F.; Warren, M. E.; Allen, D.; Whittlesey, M. K. *Organometallics* **2011**, *30*, 2200.

(38)   Kreiter, C. G.; Öfele, K.; Wieser, G. W. *Chem. Ber.* **1976**, *109*, 1749.

(39)   Herrmann, W. A.; Köcher, C.; Gooßen, L. J.; Artus, G. R. J. *Chem. Eur. J.* **1996**, *2*, 1627.

(40)   Nonnenmacher, M.; Kunz, D.; Rominger, F.; Oeser, T. *J. Organomet. Chem.* **2005**, *690*, 5647.

(41)   Ku, R.; Huang, J.; Cho, J.; Kiang, F.; Reddy, K. R.; Chen, Y.; Lee, K.; Lee, J.; Lee, G.; Peng, S.; Liu, S. *Organometallics* **1999**, *18*, 2145.

(42)   Huertos, M. A.; Perez, J.; Riera, L.; Memendez-Velazquez, A. *J. Am. Chem. Soc.* **2008**, *130*, 13530.

(43)   Edwards, P. G.; Hahn, F.E.; Limon, M.; Newman, P. D.; Kariuki, B. M.; Stasch, A. *Dalton Trans.* **2009**, 5115.

(44)   Liu, C.; Chen, D.; Lee, G.; Peng, S.; Liu, S. T. *Organometallics* **1996**, *15*, 1055.

(45)   Roberts, J. A. S.; Franz, J. A.; Eide, E. F. V. D.; Walter, E. D.; Petersen, J. L.; Dubois, D. L.; Bullock, R. M. *J. Am. Chem. Soc.* **2011**, *2*, 14593.

(46)   van Rensburg, H.; Tooze, R. P.; Foster, D. F.; Slawin, A. M. Z. *Inorg. Chem.* **2004**, *43*, 2468.

(47)   Barluenga, J.; Lopez, L. A.; Martinez, S.; Toma, M.; *Tetrahedron* **2000**, *56*, 4967.

(48)   Dötz, K. H.; Fischer, E. O. *Chem. Ber.* **1972**, *105*, 1356.

(49)   Iwasawa, N.; Maeyama, K.; Saitou, M. *J. Am. Chem. Soc.* **1997**, *119*, 1486.

(50)   Neil, S. N. O.; Chisnell, A. C.; Liu, J. *Tetrahedron* **2000**, *56*, 5037.

(51)   Katz, T. J. *Angew. Chem. Int. Ed.* **2005**, 3010.

(52)   Fürstner, A. *Angew. Chem. Int. Ed.* **2000**, *39*, 3012.

(53)   Casey, C. P. *J. Chem. Educ.* **2006**, *83*, 192.

(54)   Fernández, I.; Sierra, M. A.; Gomez-Gallego, M.; Mancheno, M. J.; Cossío, F. P. *Angew. Chem.* **2006**, *118*, 131.

(55)   Arrieta, A.; Cossío, F. P.; Fernández, I.; Gomez-Gallego, M.; Lecea, B.; Mancheno, M. J.; Sierra, M. A. *J. Am. Chem. Soc.* **2000**, *122*, 11509.

(56)   Reinheimer, E. W.; Kantardjieff, K. A.; Herron, S. R.; Tisserat, C. G.; Casalnuovo, J. A. *J. Chem. Crystallogr.* **2003**, *33*, 503.

(57)   Reinheimer, E. W.; Kantardjieff, K. A.; Ouyang, X.; Herron, S. R.; Lu, T.; Casalnuovo, J. A. *J. Chem. Crystallogr.* **2007**, *37*, 507.

CHAPTER 2:

ETHOXY CARBENE COMPLEXES OF TUNGSTEN(0)

2.1 INTRODUCTION

The first recognized carbene complex was $W(CO)_5C(Ph)(OMe)$.[1,2] Since then Fischer carbenes have enjoyed a large amount of attention from both organometallic and organic chemists because of their large range of applications. Several modifications of classical carbonyl derived carbenes have since been attempted. Both the carbene substituents and the ligand sphere of the metal have been altered (Figure 2. 1), allowing modulation of both the reactivity and the stability of these complexes.
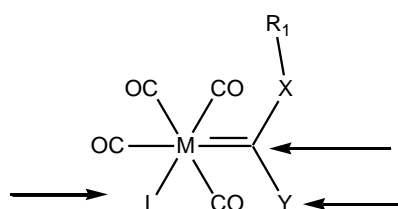
M = Metal   L = Ligand   X = Heteroatom   Y = Substituent R_1 = Alkyl or Aryl Group

FIGURE 2. 1: POTENTIAL SITES FOR FISCHER CARBENE MODIFICATION

Fischer carbenes are generally characterised by the presence of at least one heteratom substituent on the carbene,[3–5] which is represented by X in figure 2.1. X is generally an O, N, or S atom, since these heteroatoms have lone pairs which can stabilize the carbene by π-donation. The substituents found in position Y range from alkyl and aryl derivatives to heteroatoms. Lastly, several modifications of the ligand sphere can be performed. However, to maintain the classical low oxidation state of Fischer carbenes, one would have to focus on neutral ligands.[6,7] For the purpose of this study, heteroaryl ethoxy Fischer carbenes were used as the starting point and modifications to both the

ligand sphere and the heteroatom at position X were made. The importance of the heteroatom for the stabilization of carbenes and the extension of this concept to heteroaryl substituents was discussed in chapter 1. A discussion on the modifications of the ligand sphere will follow, while modifications of X will, however, only be discussed in the following chapter.

Modification of the ligand sphere of carbonyl carbene complexes was studied not long after the discovery of the first metal carbene complex.[8–10] These examples made use of phosphines as alternatives to carbonyl ligands, and it was noted by Fischer that these ligands allowed the complexes higher stability in air than their carbonyl analogues.[8] It is essential that the carbonyl groups should be stubstituted with other strong π-acceptor ligands to maintain the classical Fischer character of these complexes.[6,11] Phosphines are good examples of such ligands, since they are known to be similar to carbonyls, but are much softer ligands than carbonyls.[12–14] Also, the σ-donor, π-acceptor[15] and steric[16] characteristics of phosphines can be regulated by modification of their substituents. Phosphines have many applications in organometallic chemistry, specifically as ligands in homogenous catalysts.[17] In the case of Fischer carbenes, phosphine "chelates", which are tethered to the carbene through the Y ligand,[18] have been synthesised, as well as examples of carbenes bound to polymers through the phosphorous ligand.[19,20] It was also shown that phosphines confer additional reactivity to the carbene complex during reactions with electrophiles, and alter the reactivity pattern during certain organic transformations by varying the stereoselectivity of the complex.[21] The change in stereoselectivity was brought about by the use of a chiral phosphine. Barluenga *et.al.*[12] also noted that phosphine ligands can be used to introduce chirality into a Fischer carbene complex. Phosphine carbene complexes were used by Arrieta *et.al.*[14] to alter the reactivity of Fischer carbene complexes during photocarbonylation reactions and to understand the reaction mechanism better. The examples mentioned here and some additional literature examples of Group 6 phosphine Fischer carbenes are found in figure 2.2.

17

cis and trans isomers
R=Ph or [n]Bu

Arrieta et.al.[14]

1) R = Me, R' = Et, M = Cr
2) R = Ph, R' = Me, M = Cr
3) R = Me, R' = Me, M = W
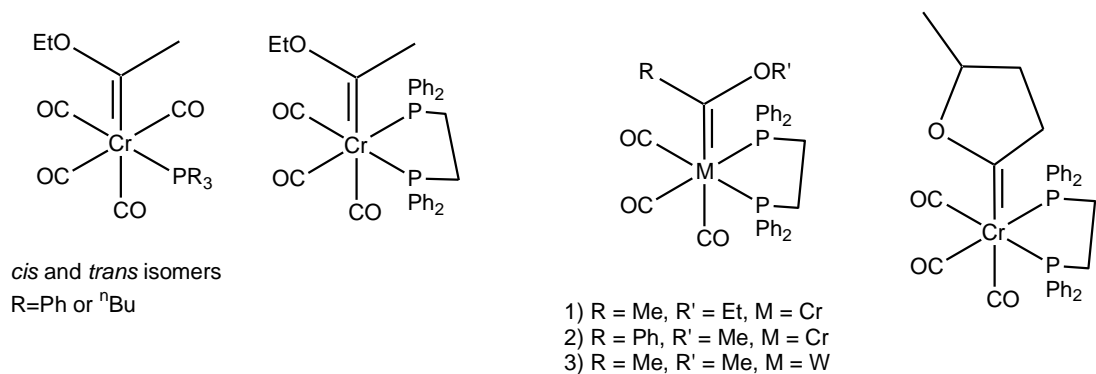
Reinheimer et.al.[22]

cis and trans isomers
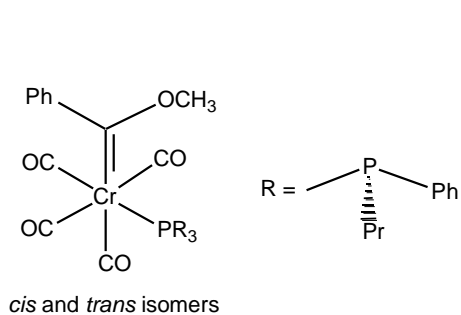
Cooke and Fischer[21]
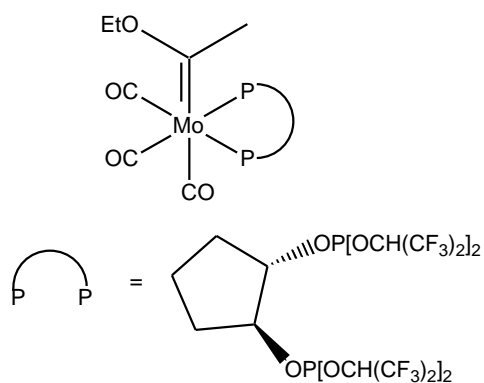
Barluenga et.al.[12]
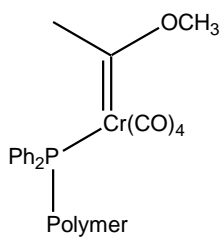
Maiorana et.al.[19]
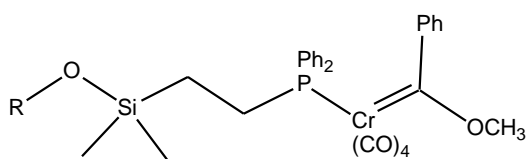
Klapdohr et.al.[20]

FIGURE 2.2: REPRESENTATIVE LITERATURE EXAMPLES OF GROUP 6 PHOSPHINE FISCHER CARBENE COMPLEXES [12,14,19–22]

18

Even though these modifications of Fischer carbenes have been known since the late 1960s, not many examples of these complexes were found in literature. This gap was especially noticable for the diphosphine derivatives.[22] Furthermore, to our knowledge, no examples of heteroaryl phosphine carbenes are known. The combination of altered reactivity of the complex and the catalytic possibility of phosphines, along with the innovative nature of this work made phosphorous ligands the natural choice for our study. Specifically, PPh$_3$ and the corresponding bidentate ligand, DPPE, were used. PPh$_3$ and DPPE were chosen since these are some of the weakest π-donor ligands found in the phosphine range,[11] and would thus allow for maximum modification of the metal ligand sphere characteristics, without altering the Fischer carbene character of the complexes.

2.2 FOCUS OF THIS STUDY

A1 and **B1**   **A2** and **B2**   **A3** and **B3**

Y = S or O
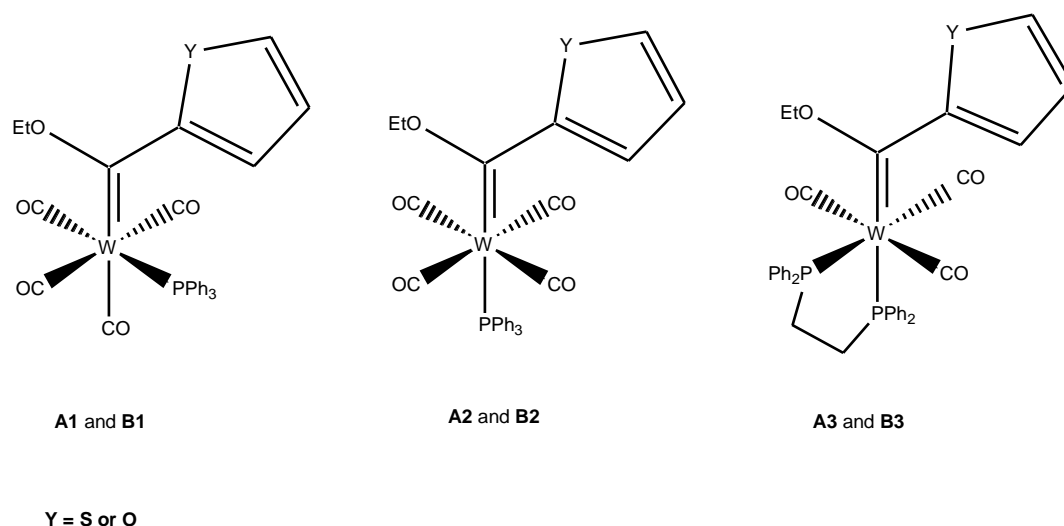
FIGURE 2.3: PHOSPHINE DERIVATIVES OF HETEROARYL ETHOXY TUNGSTEN(0) CARBENE COMPLEXES

Thienyl[23] and furyl[24] ethoxy tungsten carbenes have been synthesised in our laboratories. These were however synthesised for comparison with biscarbene analogues and other derivatives. A similar approach for the synthesis of the monocarbene complexes was used in this study. The pentacarbonyl tungsten(0) monocarbene complexes were synthesised and used for further modifications to yield the desired phosphine derivatives and for comparative purposes. Reactions of the pentacarbonyl tungsten(0) monocarbene complexes (**A** and **B**) with PPh$_3$ and DPPE, respectively, yielded mono- (**A1**, **A2**, **B1** and **B2**) and disubstituted (**A3** and **B3**) carbene complexes (Figure 2.3).

2.3 SYNTHESIS

Fischer carbenes can be synthesised by two methods, namely the original "Fischer route" and the Hegedus-Semmelhack synthesis.[25–27] The classical "Fischer route" is still the most popular and makes use of the addition of lithium salts of organic substituents to the metal carbonyl reagent. This is followed by O-alkylation using hard alkylation agents, thus yielding alkoxycarbenes. The Fischer method finds its greatest limitation in the availability of the organolithium reagent. The Hegedus-Semmelhack synthesis offers an alternative to the Fischer route when such limitations are found. It makes use of the reaction of $K_2[Cr(CO)_5]$ with an acyl chloride or an amide to finally form alkoxy or aminocarbene complexes. For the synthesis of heteroaryl carbenes, the "Fischer route" is most often used, and is well understood in our laboratories.[23,24,28] This method was thus used for the synthesis of the ethoxy Fischer carbene precursors (**A** and **B**) that were used for comparative purposes and further modifications.

The incorporation of phosphines into a Fischer carbene's ligand sphere can be done either before or after the carbene was introduced.[9,10,12,14,21,29,30] If $M(CO)_5PR_3$ is used instead of $M(CO)_6$ during the classical Fischer synthesis, *cis*-tetracarbonyl phosphine carbenes are formed.[10,21] It is suggested that the phosphine reduces the electrophilicity of the *trans*-carbonyl carbon due to the increased backbonding from the metal, thus making it less available to react with the organolithium reagent, hence reducing the chance of the *trans* isomer forming. If the phosphine is coordinated to the carbene complex by the normal carbonyl substitution methods, i.e. thermal or photolytic substitution, then both the *cis* and the *trans* isomers are formed. Literature found for diphosphine ligands only makes use of carbonyl substitution to form the chelates.[9,21,29] In this case, as for the analogous monophosphine complexes, both the *fac* and the *mer* isomers can be obtained.[12,22] Lastly, photolysis tends to yield more side products than thermal substitution, and thus thermal substitution is preferred.[29] For the purposes of our studies thermal carbonyl substitution of the monocarbene was preferred, because it would allow for comparison of the various isomers.
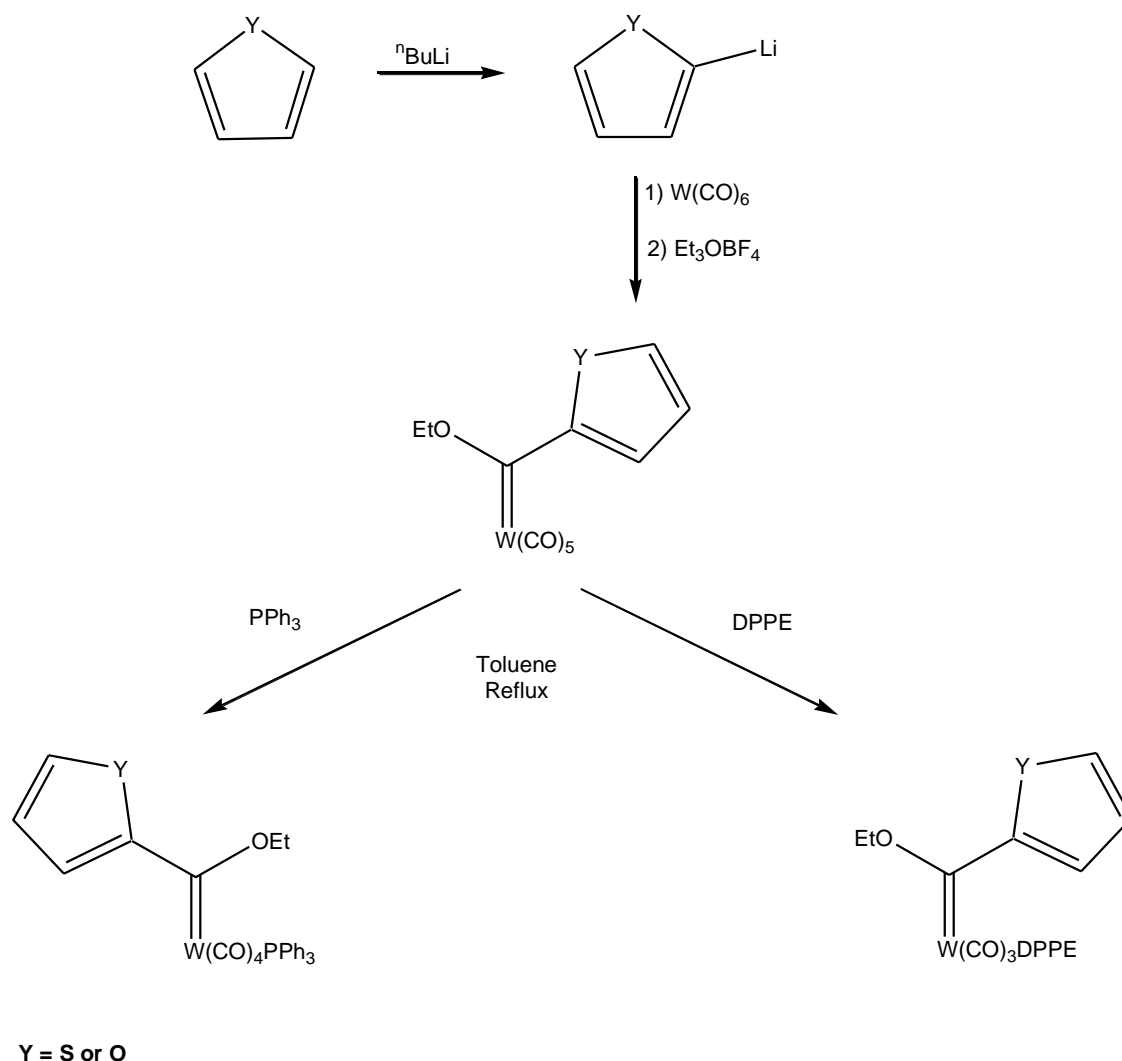
SCHEME 2.1: SYNTHETIC ROUTES TO PROPOSED TUNGSTEN(0) CARBENE COMPLEXES

Monocarbene complexes **A** and **B** were prepared by deprotonation of the corresponding heteroaryl ring at low temperatures, metallation and finally alkylation. This method has been discussed previously and will thus not be discussed here.[23,24,31] Both products were bright red and hence allowed the progress of the subsequent reactions to be followed easily by monitoring the colour change. The phosphine ligands were then introduced into the complex by refluxing the monocarbene complex (**A** or **B**) in toluene with an excess of ligand. In the case of DPPE (complexes **A3** and **B3**), reflux was maintained until all the starting carbene was converted. The reaction times were characteristically 8 hrs or longer. Generally both the *fac* and *mer* isomers (1:3 ratio) were observed on TLC. The *mer* isomer appeared as a yellow-brown spot that was slightly less polar than the red-brown *fac* isomer. Crystals obtained for the *mer* isomer were, however black. This corresponds well with literature, which suggests that both isomers can be obtained, but the *mer* is favoured,[12,22] especially at high reaction temperatures.[12] Column chromatography was attempted on a silica gel column. However, the two isomers could not be separated and appeared to decompose and isomerise further.

21

Thus only crystallization was used for purification. Unfortunately only the *mer* isomer was obtained with this method. During synthesis of monophosphine carbene complexes, Werner and Rascher[9] as well as the Fischer group[32] found several decomposition products which included mono- and diphosphine metal carbonyls. This was due to the formation of an ylide intermediate, where the phosphine coordinated to the carbene before rearranging to yield the product.[32] Similarily, in our reactions, $W(CO)_4DPPE$ crystals were isolated after crystallization from the crude reaction mixtures for **A3** and **B3**, and identified using XRD. This indicates that a similar reaction mechanism for the formation of the diphosphine Fischer carbene complexes may be at work as for the monophosphine Fischer carbene complexes. A synthetic procedure for $W(CO)_4DPPE$ as well as ^{13}C and ^{31}P NMR data are found in literature.[33–35] However, to our knowledge, there is no literature report for the $W(CO)_4DPPE$ crystal structure. This crystal structure for $W(CO)_4DPPE$ is thus presented in this work as a novel crystal. Yields of approximately 40% were obtained for complexes **A3** and **B3**. This seems low; however, when compared to literature, which reports the total yields of both isomers, our yields, which only consider the *mer* isomer, are reasonable.[22] The monophosphine reactions were performed in a similar manner to that of the DPPE reactions, with the exception that the reactions were not allowed to continue until all the monocarbene starting material had been converted. No apparent change in the ratio of the products to the starting material was observed on TLC after approximately 8 hrs. Since the reactions seemed to reach equilibrium, it was decided to stop the reaction to prevent decomposition. The *cis* isomer was generally obtained in tenfold excess to the *trans* isomer. TLCs observed for the crude products of **A1**, **A2**, **B1** and **B2** resembled that of the DPPE complexes. A yellow-brown spot, belonging to the *trans* isomer (**A1** and **B1**), was observed slightly above the red-brown spot, which corresponded to the *cis* isomer (**A2** and **B2**)*.* Separation of the *cis* and *trans* monophosphine ethoxy carbene derivatives proved to be difficult. This is due to the isomerisation equilibrium that exists between the *cis* and the *trans* isomers.[36] In fact, Cooke and Fischer[21] found it impossible to separate the isomers from one another. The isomers were thus separated mostly by means of fraction collection, since separate bands were not readily observed. It appeared that cooler column temperatures facilitated the separation. This is found to be the preferred separation technique in literature.[30] Relatively low yields (≈40%) were obtained when compared to recent literature.[13,30] However, they were comparable to those of the DPPE complexes, and could be expected since complete conversion of the starting material was not achieved. The relatively high amount of *cis* isomer (**A1** and **B1**) present in the *trans* fractions, together with the low yield, made solvent-based characterisation of the *trans* isomers (**A2** and **B2**) exceptionally challenging. For full experimental procedures, please refer to Chapter 6.

2.4 NMR CHARACTERISATION
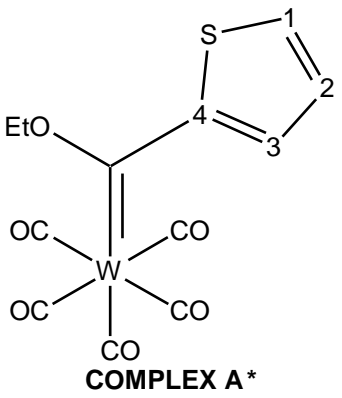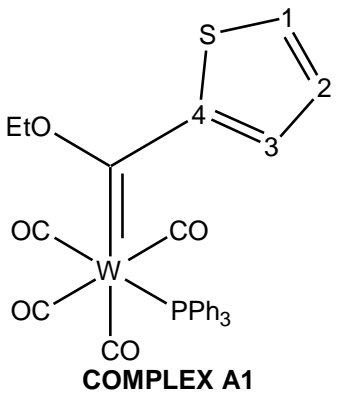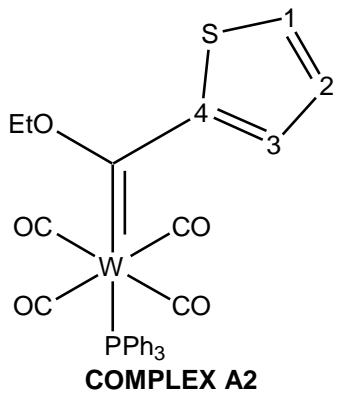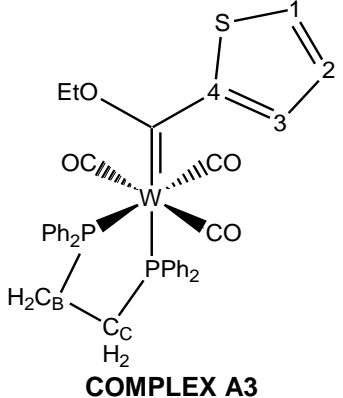
2.4.1 ^{1}H NMR Spectroscopy

^{1}H NMR data for PPh$_3$, DPPE and W(CO)$_4$DPPE is summarised in table 2.1. ^{1}H NMR data for complexes **A1**-**A3** and **B1**-**B3** is summarised in tables 2.2 and 2.3. All solvents used are indicated below the tables.

TABLE 2.1: LIGANDS AND CORRESPONDING TUNGSTEN(0) DERIVATIVES				
Proton	**PPh$_3$**	**DPPE**		**W(CO)$_4$DPPE**
	δ (ppm)	**δ (ppm)**	**J (Hz)**	**δ (ppm)**
CH		2.08　　(t, b)	4.01	2.50 - 2.68　　(m)
Ph	7.33 – 7.40　　(m)	7.24 - 7.35　　(m)		7.30 - 7.44　　(m)
				7.49 - 7.61　　(m)

All spectra were recorded in CDCl$_3$

TABLE 2.2: ^{1}H NMR DATA FOR ETHOXY THIENYL TUNGSTEN(0) DERIVATIVES

Proton	COMPLEX A* δ (ppm)		COMPLEX A* J (Hz)	COMPLEX A1 δ (ppm)		COMPLEX A1 J (Hz)	COMPLEX A2 δ (ppm)		COMPLEX A2 J (Hz)	COMPLEX A3 δ (ppm)		COMPLEX A3 J (Hz)
OCH$_2$**CH$_3$**	1.64	(t)	7.1	1.20	(t)	7.0	1.61	(t)	7.0	1.24	(t)	7.0
O**CH$_2$**CH$_3$	4.98	(q)	7.1	4.53	(dq)	0.5 (J(P-H)) 7.0	4.98	(q)	7.0	4.39	(q)	7.0
H1	7.80	(dd)	0.6 5.0	7.65	(dd)	1.1 5.0	7.65	(ddd)	0.6(J(P-H)) 1.1 5.1	7.63 - 7.70	(m)	
H2	7.20	(dd)	4.3 4.8	6.97	(dd)	4.0 4.8	7.15	(dd)	4.0 5.1	6.84	(dd)	3.9 5.1
H3	8.14	(dd)	0.8 4.1	7.77	(dd)	1.1 4.0	8.01	(ddd)	0.3(J(P-H)) 1.1 4.0	7.53	(dd)	1.1 3.9
P-C$_B$**H$_2$**										2.53 - 2.66	(m)	
P-C$_C$**H$_2$**										2.66 - 2.82	(m)	
P**Ph$_3$**				7.31 - 7.46	(m)		7.32 -7.49	(m)		7.30 - 7.47	(m)	
							7.50 - 7.58	(m)		7.63 - 7.70	(m)	

*Solvents used: * = CDCl$_3$; All other spectra recorded in CD$_2$Cl$_2$*

24

TABLE 2.3: ^{1}H NMR DATA FOR ETHOXY FURYL TUNGSTEN(0) DERIVATIVES

Proton	COMPLEX B* δ (ppm)		COMPLEX B* J (Hz)	COMPLEX B1 δ (ppm)		COMPLEX B1 J (Hz)	COMPLEX B2 δ (ppm)		COMPLEX B2 J (Hz)	COMPLEX B3 δ (ppm)		COMPLEX B3 J (Hz)
OCH_2CH_3	1.62	(t)	7.1	1.36	(t)	7.1	1.60	(t)	7.0	1.35	(t)	7.0
OCH_2CH_3	4.94	(q)	7.1	4.68	(q)	7.1	4.97	(q)	7.0	4.51	(q)	7.0
H1	7.86	(dd)	0.7 / 1.6	7.30 - 7.43	(m)		7.79	(s)		7.11	(dd)	0.8 / 1.7
H2	6.6	(dd)	1.7 / 3.7	6.37	(dd)	1.7 / 3.6	6.55	(dd)	1.7 / 3.5	6.30	(dd)	1.7 / 3.5
H3	7.13	(dd)	0.7 / 3.7	6.80	(dd)	0.8 / 3.6	6.97	(d)	3.5	6.65	(dd)	0.8 / 3.5
$P-C_BH_2$										2.47 -2.80	(m)	
$P-C_CH_2$										2.47 -2.80	(m)	
PPh_3				7.30 - 7.43	(m)		7.32 - 7.48	(m)		7.28 - 7.46	(m)	
							7.52 - 7.60	(m)		7.59 -7.73	(m)	

*Solvents used: * = CDCl₃; All other spectra recorded in CD₂Cl₂*

It should be noted that the proton chemical shifts observed for $W(CO)_4DPPE$ were similar to those reported by Connor *et.al.* for the monodentate $W(CO)_5DPPE$ complex (P-CH$_2$: 2.48 ppm; PPh$_2$: 7.42 ppm).[37] The data did not show any noteworthy trends and thus will not be discussed further.

It can clearly be seen that all resonance peaks observed for all the phosphine carbene derivatives (**A1**-**A3**; **B1**-**B3**) on the heteroaryl group were more upfield than the corresponding resonance peaks of the two monocarbene complexes (**A** and **B**). This correlates well with the data found for monophosphines complexes.[9] It should be noted that the greatest upfield shifts were observed for almost all the proton chemical shifts of the carbene substituents of complexes **A3** and **B3**. Accordingly, this indicated the additive effect of two phosphorous atoms in the complex. Also, for complex **A3** the relative chemical shifts of H1 and H3 were switched when compared to the other thienyl derivatives. This was deduced from the coupling constants observed for these protons. A switch was not observed for complex **B3**. However, the relative order of the rings proton chemical shifts are not in the same order in thienyl[38] and furyl[31] derivatives, and thus one would not expect similar trends. This also points towards a change in the electron environment of the carbene due to the prescence of two phosphorous atoms in the metal ligand sphere, when compared to a single phosphorous substituent. It is furthermore of interest that the *trans* monophosphine complexes (**A2** and **B2**) generally had more downfield shifts for both the furyl and thienyl derivatives. The opposite was found to be true by the Fischer group;[21,29] however, Arrieta *et. al.*[14] observed a similar trend as found in these complexes. It seems that this contradicts the assumption that the metal should have more electron density available for π-backbonding to the carbene, since PPh$_3$ is a weaker π-acceptor than carbonyls. However, since it is known that phosphines and carbenes have similar σ-donor qualities, while carbenes are only slightly better π-acceptors than phosphines,[39] it is suggested that the ligands are essentially in equal competition for the metal electrons. Thus, the influence of the altered ligand sphere is not felt as strongly in the *trans* complexes as it is in the *cis* complexes.

The influence of ^{31}P nuclei on the ^1H NMR spectra varied somewhat. ^{31}P nuclei have a spin ½ and are thus expected to couple to other nuclei with the same spin number, such as ^1H and ^{13}C. Furthermore, phosphorous may couple with nuclei up to five bonds away.[40–42] It is thus reasonable to expect the proton spectra observed for the phosphorous substituted complexes to show indications of these couplings, if the resolution is high enough. The effect of the J(P-H) coupling is clearly seen on the protons of the phosphorous backbone (C_CH_2 and C_BH_2). Multiplets are observed for these proton chemical shifts in contrast to triplet peaks, that would be expected in the absence of the additional phosphorous couplings. When compared to pentacarbonyl complexes **A** and **B**, only complex **A2** and **A3** showed clear differences. Complexes **A3**, **B1**, **B2** and **B3** did show some signs of additional couplings; however, these were not well resolved and were thus not reported. It is significant to note that the additional couplings found could not be due to long range couplings between the carbene

26

substituents as suggested by Darensbourg and Darensbourg (Figure 2.4).[39] Since the couplings are not the same size, the two protons are not coupling to one another.
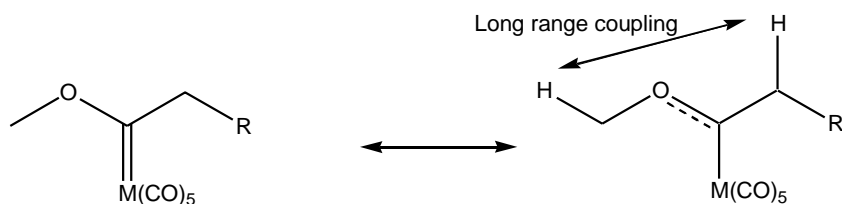
FIGURE 2.4: DIAGRAM OF THE LONG RANGE COUPLING OBSERVED BY DARENSBOURG AND DARENSBOURG

Darensbourg and Darensbourg found that in certain complexes the protons on the alkoxy substituent coupled to protons on the alkyl substituent. This five bond proton coupling was possible due to the unsaturated nature of the bond between the carbene carbon and the oxygen of the alkoxy substituent. It is clear from the coupling constants observed for **A2** and **A3**, that the additional couplings that were observed when compared to **A**, were not due to the effect observed by Darensbourg and Darensbourg. It was thus concluded that J(P-H) couplings were present in complexes **A2** and **A3.**
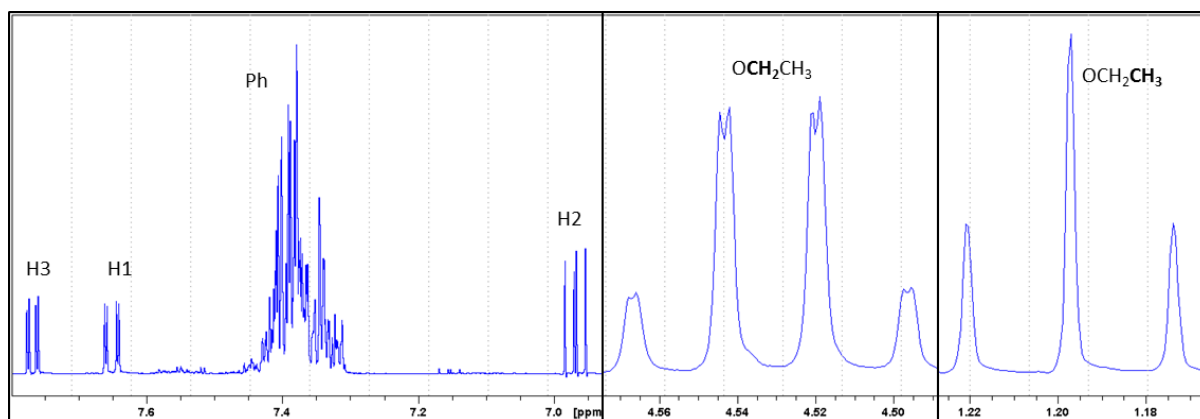
FIGURE 2.5: SELECTED REGIONS OF THE ^{1}H NMR SPECTRUM OF COMPLEX A1

As a general trend, the ^{1}H NMR spectra of the phosphine ligands either did not show a dramatic change or indicated a downfield shift in the chemical resonance peaks when compared to PPh$_3$, DPPE and W(CO)$_4$DPPE. Each ligand will be discussed separately since DPPE has additional protons that are not present in PPh$_3$.

27

Firstly, a slight downfield shift was observed for chemical resonances of the protons found on the phenyl groups of PPh_3 compared to uncoordinated PPh_3. This would correspond with the electronwithdrawing effect of the metal moiety on the ligand upon coordination. Moreover, it is interesting to note that for the *trans* isomers (**A2** and **B2**), two multiplets were observed for the chemical shift of the phenyl protons, in contrast to the *cis* isomers (**A1** and **B1**) which showed only one multiplet. The more downfield multiplet observed for the phenyl groups on complex **A2** and **B2** integrates for six protons, while the upfield multiplet integrates for nine protons. If one assumes that the proton shifts follow the same order as the carbon chemical shifts, it is suggested that the more downfield multiplet for the phenyl protons of complexes **A2** and **B2** corresponded to the protons closest to the phosphorous atoms. This indicates that, not only the protons found on the carbene substituents in the *trans* isomers (**A2** and **B2**), but also the phenyl groups are more deshielded when compared with the *cis* isomers (**A1** and **B1**). The phenyl groups found on DPPE showed a similar shift in the protons closest to phosphorous atoms for all three metal chelates studied ($W(CO)_4DPPE$, **A3** and **B3**). This trend illustrated the influence of the electron withdrawing metal fragment on the ligand upon coordination. The largest change in chemical shift was observed upon coordination of the free ligand to tungsten carbonyl to form $W(CO)_4DPPE$. However, there did not appear to be a significant difference between chemical resonances observed for the phenyl protons of $W(CO)_4DPPE$, **A3** and **B3**. This suggests that chelation to the metal centre produces the greatest change in the proton chemical resonances of the ligand. C_BH_2 and C_CH_2 did not have the same chemical resonances values. This shows the different chemical environments of the groups *trans* and *cis* to the carbene in complexes **A3** and **B3**. The information gained from the monophosphine derivatives and comparisons made with ^{13}C assignments were used to determine the assignment of the multiplets for C_BH_2 and C_CH_2. The more downfield multiplet was thus allocated to C_BH_2, the protons of the carbon on the phosphorous atom found *trans* to the carbene, and the C_AH_2 multiplet was assigned to the protons of the carbon attached to the phosphorous moiety *cis* to the carbene.

In conclusion, it can be said that the greatest changes in the proton NMR spectra were seen for the carbene substituents when the pentacarbonyl carbene complexes (**A** and **B**) and the phosphine derivatives (**A1**-**A3**, and **B1**-**B3**) were compared. In contrast, the proton chemical shifts observed for the phosphorous ligands showed modest alterations. However, it is likely that the untidy nature of proton spectra for the phenyl rings, due to P-H couplings, reduces the amount of change one can observe for these protons.

2.4.2 ^{13}C NMR Spectroscopy
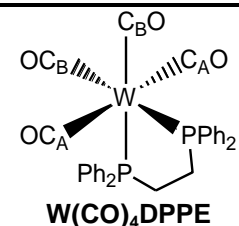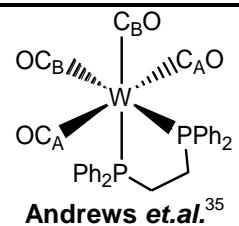
Numbering for the phenyl ring found on the phosphine ligands was done as follows:
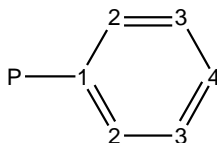
All couplings indicated in the tables below are J(P-C) couplings unless otherwise noted.

Please note that the ^{13}C spectrum for complex **B2** contained almost equal amounts of the *cis* and the *trans* isomers. This is due to isomerisation that occurs for the monophoshine complexes. The isomerisation effect was higher for this complex than the corresponding thiophene derivative since it could not be obtained as purely. These peaks were thus assigned by comparison with those found for complex **B1**, as well as by comparing the trend found between complex **A1** and complex **A2.** These assignments are thus only tentative. Most of the comparisons and discussions will thus focus on the thienyl complexes, since these peaks could be assigned unambiguously.

The various DPPE components in the carbene complexes were named according to the carbonyl that the closest phosphorous had displaced. This was done to emphasise the correlation between the phosphorous and the *trans* carbonyl. It also allows for a direct comparison between the monophosphine and the diphosphine complexes, since the carbonyl groups with the same code have the same orientation relative to the phosphines and the carbene.

29

TABLE 2.4: ^{13}C NMR DATA FOR LIGANDS AND CORRESPONDING TUNGSTEN(0) DERIVATIVES

Carbon	PPh$_3$		DPPE		W(CO)$_4$DPPE		Andrews et.al.[35]	
	δ (ppm)	J (Hz)	δ (ppm)	J (Hz)	δ (ppm)	J (Hz)	δ (ppm)	J (Hz)
PCH$_2$			23.8 (d)	35.81	29.8 (dd)	13.6	29.7 (dd)	14.5
						29.8		27.3
P**C**1	137.1 (d)	10.7	138.1 (m)		136.1 (d)	39.7	135.6 (d)	39.0
P**C**2	133.7 (d)	19.5	132.7 (d)	9.37	131.6 (d)	10.0	131.8 (d)	9.7
P**C**3	128.5 (d)	6.9	128.4 (d, b)	3.24	128.9 (d)	9.7	128.9 (d)	12.2
P**C**4	128.7 (s)		128.6 (b)		130.0 (s)		130.2 (d)	1.8
C$_A$O					201.3 (dd)	6.4	201.9 (dd)	6.7
						6.8		6.8
C$_B$O					208.2 (dd)	7.1	208.8 (d)	23.9
						23.1		
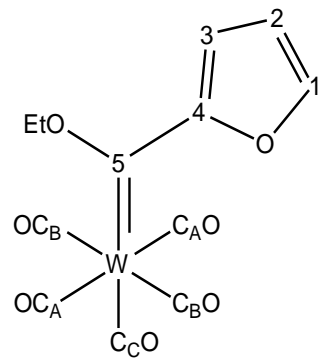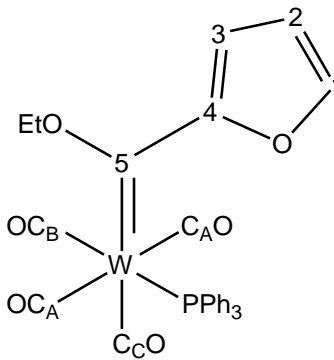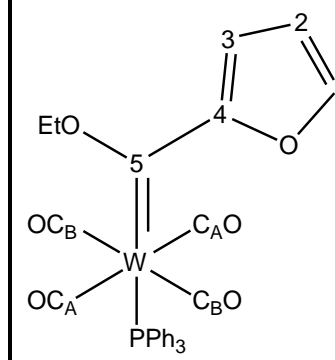
All spectra were recorded in CDCl$_3$

The magnitude of J(P-X), with X= C, H, W, and P are dependent on a number of factors. These include stereochemistry of the molecule, number of bonds separating the atoms, and the electronic environment of the phosphorous atoms.[40–42] The J(P-X) couplings may vary from 0 to 300 Hz.[42]

30

TABLE 2.5: ^{13}C NMR DATA FOR THIENYL TUNGSTEN(0) DERIVATIVES

Carbon	COMPLEX A* δ (ppm)		COMPLEX A1 δ (ppm)		J (Hz)	COMPLEX A2 δ (ppm)		J (Hz)
OCH$_2$**CH$_3$**	15.0	(s)	14.8	(s)		15.4	(s)	
O**CH$_2$**CH$_3$	78.6	(s)	77.8	(d)	1.8	76.2	(s)	
C1	136.0	(s)	133.1	(s)		131.9	(s)	
C2	129.0	(s)	128.7	(s)		128.9	(s)	
C3	141.5	(s)	140.2	(s)		138.9	(s)	
C4	158.3	(s)	159.9	(s)		161.1	(s)	
C5	290.7	(s)	294.5	(d)	7.0	283.7	(d)	15.3
P**C1**			135.9	(d)	38.3	137.8	(d)	38.9
P**C2**			133.7	(d)	11.8	133.7	(d)	11.8
P**C3**			129.0	(d)	9.7	128.9	(d)	9.5
P**C4**			130.4	(d)	1.7	130.2	(d)	1.6
C$_A$O	197.6 (126.4 Hz)[#]	(t)	203.8	(d)	6.8	205.2	(d)	6.4
C$_B$O	197.6 (126.4 Hz)[#]	(t)	207.3	(d)	24.0	205.2	(d)	6.4
C$_C$O	202.5	(s)	211.4	(d)	6.5			
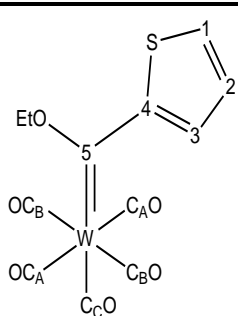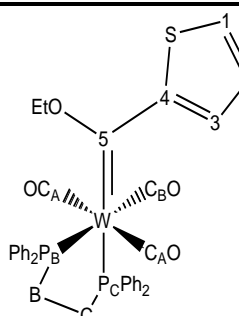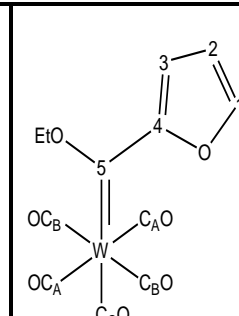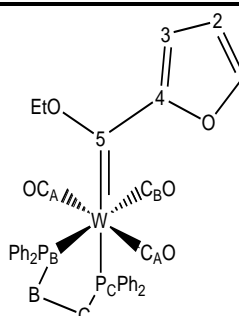
= J(W-C)   Solvents used: * = CDCl$_3$; All other spectra recorded in CD$_2$Cl$_2$

	TABLE 2.6: ^{13}C NMR DATA FOR FURYL TUNGSTEN(0) DERIVATIVES						
Carbon	COMPLEX B*			COMPLEX B1		COMPLEX B2	
	δ (ppm)			δ (ppm)	J (Hz)	δ (ppm)	J (Hz)
OCH$_2$**CH$_3$**	15.1	(s)		15.3 (s)		15.6 (s)	
O**CH$_2$**CH$_3$	78.4	(s)		77.4 (s)		76.0 (s)	
C1	150.0	(s)		148.5 (s)		147.8 (s)	
C2	113.4	(s)		112.1 (s)		111.2 (s)	
C3	113.4	(s)		113.3 (s)		113.1 (s)	
C4	166.2	(s)		167.1 (s)		167.5 (s)	
C5	284.8	(s)		289.0 (dd)	6.9 105.4[#]	278.5 (s)	
PC1				136.5 (d)	38.2	138.1 (d)	37.6
PC2				133.8 (d)	11.8	134.0 (d)	4.3
PC3				128.8 (d)	9.5	129.0 (d)	9.1
PC4				130.4 (d)	1.7	130.3 (s)	
C$_A$O	197.4	(s)		203.8 (dt)	6.9 128.0[#]	205.0 (d)	5.5
C$_B$O	197.4	(s)		207.5 (dt)	24.4 146.7[#]	205.0 (d)	5.5
C$_C$O	203.4	(s)		212.3 (dt)	6.7 115.5[#]		

*# = J(W-C)   Solvents used: * = CDCl$_3$; All other spectra recorded in CD$_2$Cl$_2$*

32

TABLE 2.7: ^{13}C NMR DATA FOR DPPE TUNGSTEN(0) DERIVATIVES

Carbon	COMPLEX A* δ (ppm)	COMPLEX A3 δ (ppm)	COMPLEX A3 J (Hz)	COMPLEX B* δ (ppm)	COMPLEX B3 δ (ppm)	COMPLEX B3 J (Hz)
OCH$_2$**CH$_3$**	15.0 (s)	15.4 (s)		15.1 (s)	15.5 (s)	
O**CH$_2$**CH$_3$	78.6 (s)	75.2 (s)		78.4 (s)	74.6 (s)	
C1	136.0 (s)	134.9 (s)		149.9 (s)	144.9 (s)	
C2	129.0 (s)	127.6 (s)		113.4 (s)	112.3 (s)	
C3	141.5 (s)	127.9 (s)		113.4 (s)	107.3 (s)	
C4	158.3 (s)	163.8 (d)	6.7	166.2 (s)	170.0 (s)	
C5	290.7 (s)	284.4 (dd)	6.3 / 19.9	284.9 (s)	279.1 (dd)	6.2 / 18.8
PC$_B$H$_2$		30.7 (dd)	13.6 / 24.3		30.1 (dd)	14.0 / 24.6
PC$_C$H$_2$		33.0 (dd)	17.6 / 28.1		32.5 (dd)	17.6 / 28.1
P$_B$C1		137.1 (dd)	2.5 / 34.7		137.3 (dd)	2.5 / 35.0
P$_C$C1		138.7 (d)	35.3		138.5 (dd)	2.1 / 34.8
P$_B$C2		132.4 (d)	11.2		132.2 (d)	11.2
P$_C$C2		133.0 (d)	11.7		132.7 (d)	11.2
P$_B$C3		129.1 (s)			128.8 (d)	9.1
P$_C$C3		129.2 (s)			129.0 (d)	10.8
P$_B$C4		130.1 (s)			130.2 (s)	
P$_C$C4		130.6 (s)			129.9 (d)	1.7
C$_A$O	197.6 (t) (126.4 Hz)[#]	208.2 (dd)	5.9 / 6.7	197.4 (s)	208.1 (d)	6.3
C$_B$O	202.5 (s)	217.0 (dd)	7.2 / 23.8	203.4 (s)	217.8 (dd)	7.2 / 24.1
C$_C$O	202.5 (s)			203.4 (s)		

= J(W-C)   Solvents used: * = CDCl$_3$; All other spectra recorded in CD$_2$Cl$_2$

33

The carbon spectra will now be discussed firstly for the monophosphine carbene derivatives, then DPPE derivatives and lastly a comparison of these complexes will be made. As is expected, the most valuable information that was obtained from all the spectra was derived from the carbonyl groups and thus a large part of the discussion will focus on this. It should be noted that the data found for W(CO)$_4$DPPE correlated well with that found by Andrews *et. al.*[33] Thus no further discussion of this complex will be done. Firstly, however emphasis needs to be placed on the fact that both J(P-C) and J(W-C) couplings were observed in the carbon spectra. ^{13}C, ^{31}P and ^{183}W all have spin ½ nuclei. This implies that these nuclei can couple during NMR measurements, and subsequently, the chemical resonances observed for these nuclei will have coupling patterns.[40–42] Couplings between phosphorous and carbon are observed as doublets similar to the case of J(H-H). Tungsten couplings, in contrast, are observed as two small satellite peaks centred on the central carbon peak. J(W-C) is the difference in Hz between these two satellites. W-C are thus less readily observed than P-C couplings, since the satellites are small and often cannot be distinguished from the background noise.

The trends found for **A1-A3** and **B1**-**B3** will, firstly, be discussed in terms of the changes in resonance seen for the phenyl groups found on the phosphine ligands, secondly the changes seen in the carbene ligand resonances will be noted and finally the changes observed for the carbonyl chemical shifts mentioned. The phenyl groups did not show significant chemical shift differences between the free ligand and the coordinated ligand for complexes **A1-A3** and **B1**-**B3**. A downfield shift is observed for the chemical resonance of PC1-PC4. However, if one compares DPPE, W(CO)$_4$DPPE, **A2-A3** and **B2**-**B3** it is clear that the downfield shift is due to chelation to the metal, and not due to the prescence of the carbene ligand. This correlates well with the data seen for ^{1}H NMR resonances, and was fully explained in section 2.4.1.

The carbene ligand, in contrast to the phenyl groups, did show changes in the carbon chemical shifts when **A** and **B** are compared to **A1-A3** and **B1**-**B3**, respectively. In general, if complexes **A1**, **A2**, **B1** and **B2** are compared to their respective monocarbenes (**A** and **B**), the carbene substituent's carbon resonance peaks were generally more upfield in complexes **A1**, **A2**, **B1**, and **B2**. The *trans* isomers (**A2** and **B2**) had more upfield carbene carbon chemical shifts than the *cis* isomers (**A1** and **B1**). This points towards the difference between the σ-donor, π-acceptor qualities of carbonyls and phosphines. Phosphines are stronger σ-donors and weaker π-acceptors than carbonyls, thus more electron density will be available for π-backbonding between the metal and the carbene carbon. Increased electron density on the carbene carbon will be reflected as an upfield shift in the carbon NMR spectrum. Most importantly, a coupling was seen on the methylene carbon of **A1.** Therefore the coupling found in the ^{1}H NMR spectrum (Table 2.2) could in fact be due to the phosphorous couplings.

34

As mentioned, the most dramatic changes in the carbon spectra were seen in the carbonyl region. For the tungsten(0) pentacarbonyl monocarbene complexes one finds two sets of carbonyl peaks, which are easily distinguished by height and chemical shift. These carbonyls are more downfield than in the corresponding hexacarbonyl, with the *trans* CO being found most downfield.[44] Furthermore, the chemical shift value for a carbonyl group is dependent on the substituent *trans* to the carbonyl and follows the following trend:

CO < phosphite < phosphine, arsine < amine < carbene
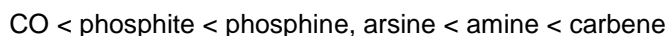
It was also shown that carbonyl groups can be distinguished by the size differences in J(P-C) coupling.[10,30,45] A *trans* carbonyl has a larger J(P-C) coupling constant (24 Hz) than a *cis* carbonyl (6-7 Hz). Lastly, one would expect a single carbonyl resonance peak for the *trans* isomers, while the *cis* isomers should have three carbonyl chemical resonances with a relative ratio of 1:1:2, which corresponds to three different environments. This was found to be the case for the complexes studied (**A1**, **A2**, **B1** and **B2**). Excellent correlation was, furthermore, found for the coupling constants between the thienyl and the furyl derivatives. It was also noted that the values for the chemical resonance peaks for C_AO and C_BO of **A1** and **B1** were the average of the values for the corresponding carbonyl chemical resonance peaks in **A1** and **B1**. This indicates the combined influence of the carbene and phosphine on ligands on the carbonyls. The spectra thus correlate well with expected results.

The [1]J(W-C) couplings found should also be noted. These couplings were not seen in all the spectra due to relatively small size of these peaks, which is aggravated by the phosphorous couplings. It was however, observed on the spectrum of **B1** (Figure 2.6); not only for the carbonyls, but also the carbene carbon. The coupling was found as a doublet of triplets for the carbonyls and a doublet of doublets for the carbene carbon. All these couplings were over 100 Hz, as would be expected, and are similar to those found in literature for analoguos monophosphine carbene complexes.[30,45] Most importantly, however, is the difference in these couplings, which can be ascribed to the *trans* influence. The *trans* influence is the ability of a ligand to weaken the metal-ligand bond of the ligand *trans* to it.[46] Buchner and Schenk[46] found that the smaller the [1]J(W-C) of a carbonyl, the larger the *trans* influence of the ligand *trans* to it. The [1]J(W-C) couplings for **B1** decreased in the following order: $C_BO > C_AO > C_CO$. This indicates that the *trans* influence increases as follows: phosphine < carbonyl < carbene. This is similar to the order found by Buchner and Schenk.[46]
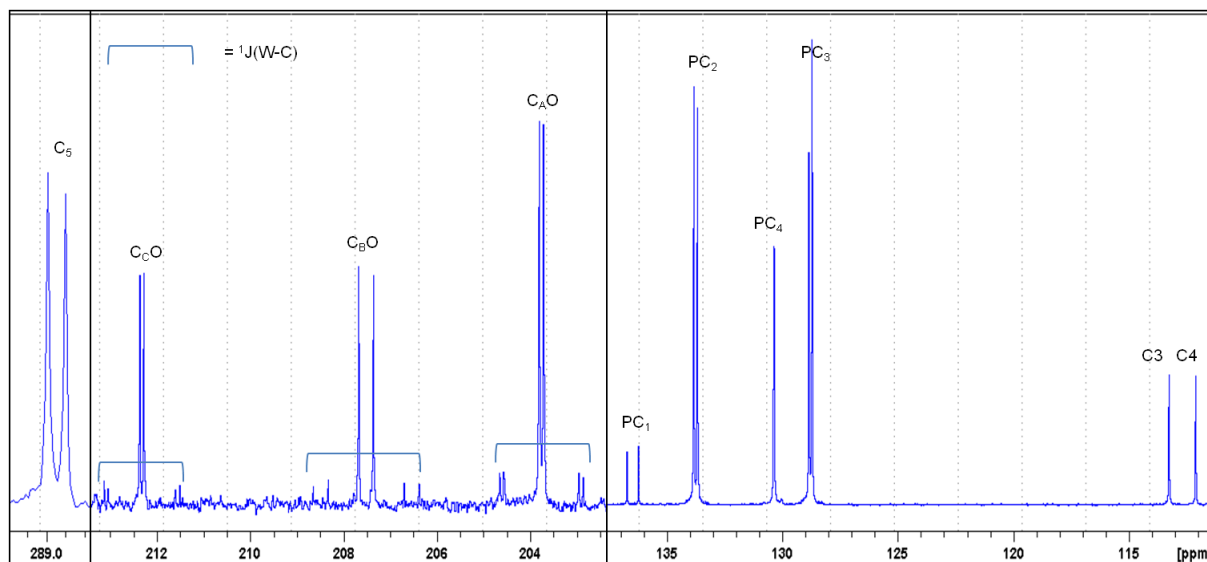
FIGURE 2.6: SELECTED REGIONS ON THE ^{13}C NMR SPECTRUM OF COMPLEX B1

The DPPE complexes will now be discussed. Once again the assignment of the carbon peaks in the aromatic region was facilitated by comparison of the furyl and thienyl derivatives, as for the **A1**, **A2**, **B1** and **B2** carbenes. C1 and C3 both displayed upfield shifts for the carbon resonance peaks relative to **A** and **B**. In complexes **A3** and **B3**, C3 was shifted between 8 and 13 ppm upfield relative to the corresponding carbon resonance peaks in **A** and **B**. C3 is most affected by electron donation from the heteroaryl ring to the carbene carbon. The upfield shift thus suggests that less electron density is donated from the heteroaryl ring to the carbene in complexes **A3** and **B3**, which may indicate that the phosphorous ligands allow more electron density to be available for the carbene than do the carbonyl ligands. The influence of two phosphine ligands on the carbene ligand can thus be seen clearly on the ^{13}C NMR spectra.

The DPPE subtituents were significantly affected by the unsymmetrical substitution of the *mer* isomer. All the phenyl carbon resonance peaks were doubled. By comparison with the monophosphine derivatives and the patterns observed for the carbonyls, it was concluded that the part of the ligand *trans* to the carbene (P_CPh_2 and P_CCH_2) corresponded to the more downfield shifts. Excluding the doubling of the peaks, no significant alteration was found for the resonance peaks of the phenyl substituents. The coupling constants did, however, vary, but once again this was merely due to the unsymmetrical nature of the complex.

Additional J(P-C) couplings were observed for carbons close to the phosphorous atoms when compared with W(CO)$_4$DPPE and the monophosphine derivatives (**A1**-**A2** and **B1**-**B2**). This is expected since the two phosphorous atoms are in different environments and thus each would couple

uniquely. The carbons resonance peaks for **A3** and **B3** that showed additional couplings were C5 and PC1. P_BCH_2 and P_CCH_2 had different coupling constants when compared to $W(CO)_4DPPE$. The change in the coupling constants is consistent with an altered chemical environment for each of the phosphorous atoms. For C5 it is suggested that the smaller coupling is to the *cis* phosphorous atom, while the larger coupling is to the *trans* phosphorous atom. This was concluded from comparisons with the monophosphine derivatives (**A1**, **A2**, **B1** and **B2**). The additional couplings observed for PC1 are suggested to be due to long range coupling with the phosphorous nuclei.

The resonances of the carbonyl groups also indicated variation when compared to $W(CO)_4DPPE$. Two distinct peaks were expected and observed for the carbonyl ligands (C_AO and C_BO). The carbonyls were found at almost exactly the same shift values for both carbene derivatives (**A3** and **B3**), indicating that a change from the furyl to the thienyl carbene substituent has little effect on carbon chemical shifts observed for the carbonyl groups. Assignments were made in the same manner as described for the monophosphine complexes. Hence, C_AO, or the carbonyls *trans* to one another, were observed upfield from the carbonyl group (C_BO) *trans* to the phosphorous atom. The C_BO carbonyls further showed a distinctive large coupling to the *trans* phosphorous atom (J(P-C)= ±24Hz) and a small coupling to the *cis* phosphorous atom (J(P-C) =7.2). The assignments could thus be verified on the basis of the shift values and coupling constants. In comparison with all other complexes, the carbonyls of **A3** and **B3** had the most downfield shift values. This can be seen as an additive effect of multiple carbonyl substitutions. Also, downfield shifts of carbonyls are indicative of increased metal π-bonding,[46] as would be expected for a greater degree of carbonyl substitution. The carbonyl chemical resonances also agree with the *trans* influence as described for the monophosphine carbene complexes, and indicate that these complexes can be used to study the properties of multiple ligands in a single complex.

It can thus be concluded, that in general, the additive influence of an additional phosphorous atom can be seen in the resonances of the carbene and the carbonyl ligands. Futhermore, the spectra reflect the asymmetrical nature of the isomer, and thus confirm the isomeric assignment, as the *mer* isomer.

2.4.3 ^{31}P NMR Spectroscopy

Chemical shifts of ^{31}P nuclei are known to be sensitive to the chemical environment surrounding the atoms, and are even useful for elucidation of stereochemistry.[47] The ^{31}P NMR data for the complexes synthesised and relevant comparative data is found in table 2.8. Phosphorous atoms of **A3** and **B3** were given the same assignments as used for the corresponding groups in the ^{13}C NMR data.

37

TABLE 2.8: ^{31}P NMR DATA FOR ETHOXY TUNGSTEN(0) DERIVATIVES		δ (ppm)	J(P-P) (Hz)	J(P-W) (Hz)
PPh$_3$*		-5.40		
W(CO)$_5$PPh$_3$[40]		20.6		280.0
A1		25.00		233.6
A2		22.78		209.3
B1		25.25		236.3
B2		25.00		235.3
DPPE*		-12.57		
W(CO)$_4$DPPE*		40.70	5.5[33]	230.4
A3	P$_C$	41.18	7.8	181.7
	P$_B$	42.26	7.8	223.1
B3	P$_C$	40.51	7.9	181.8
	P$_B$	41.66	7.7	224.2

*Solvents used: * = CDCl$_3$; All other spectra recorded in CD$_2$Cl$_2$*

Firstly, it should be noted that the data found for W(CO)$_4$DPPE correlated well with that found in literature,[33,35,48] although the ^{2}J(P-P) coupling was not observed.

For the monophosphine derivatives (**A1**, **A2**, **B1** and **B2**), the chemical shifts found for the ^{31}P nuclei are all more downfield than the resonances of either the ligand or W(CO)$_5$PPh$_3$. The data found for the *cis* isomers (**A1** and **B1**) correlates well with those of similar ethoxy complexes found in literature.[30] Furthermore, it was seen that the chemical shift values for the *trans* isomers (**A2** and **B2**) are lower than those found for the corresponding *cis* isomers (**A1** and **B1**). Since altering the group *trans* to the phosphorous atom has been shown to influence the ^{31}P shift, this difference is to be expected. On comparing chemical shift values for the *cis* and *trans* isomers, it is observed that the phosphorous resonance is shifted more upfield when the phosphorous atom is found *trans* to a carbene ligand (as for **A2** and **B2**) compared to the resonance when the phosphorous atom is found *trans* to a carbonyl ligand (as for **A1** and **B1**). This can again be explained by the σ-donor, π-acceptor properties of the *trans* ligand: carbene < carbonyl. Therefore, in the *cis* complexes (**A1** and **B1**) , the carbonyl ligand is a better π-acceptor ligand and competes for electron density from the metal, leaving the phosphorous atom deshielded. In *trans* complexes , the carbene ligand is similar to the phosphine ligand in π-accepting ability. Hence, the more upfield chemical shift observed for **A2** and **B2**. It is also interesting to note the large difference in ^{1}J(P-W) observed for **A1** and **A2**.[49] Both the chemical shifts observed for a ^{31}P nuclei as well as P-M couplings are considered to consist of σ- and π-components.[50] For P-M couplings, the σ-influence is generally considered to be altered by the substituent on the phosphine ligand, while the π-influence is affected by the ligand *trans* to the

phosphine. If one correlates this trend with that of the *trans* ligand influence, then it can be seen that the stronger the *trans* influencing ligand opposite the phosphorous atom, the smaller the ^{1}J(W-P).[49] It was further suggested that this parameter can be used to determine the W-P bond length. Thus an increase in ^{1}J(W-P) correlates to a decrease in W-P bond length and vice versa.[40] This suggests that the W-P bonds for the *trans* monophosphine complexes (**A2** and **B2**) should be longer than the corresponding bonds in the *cis* isomers (**A1** and **B1**) if only the *trans* influence is considered. However, since carbonyl ligands are stronger π-acceptors than carbene ligands, the opposite may in fact be true. XRD studies regarding these effects are thus suggested for future work, in order to determine which has the stronger influence.
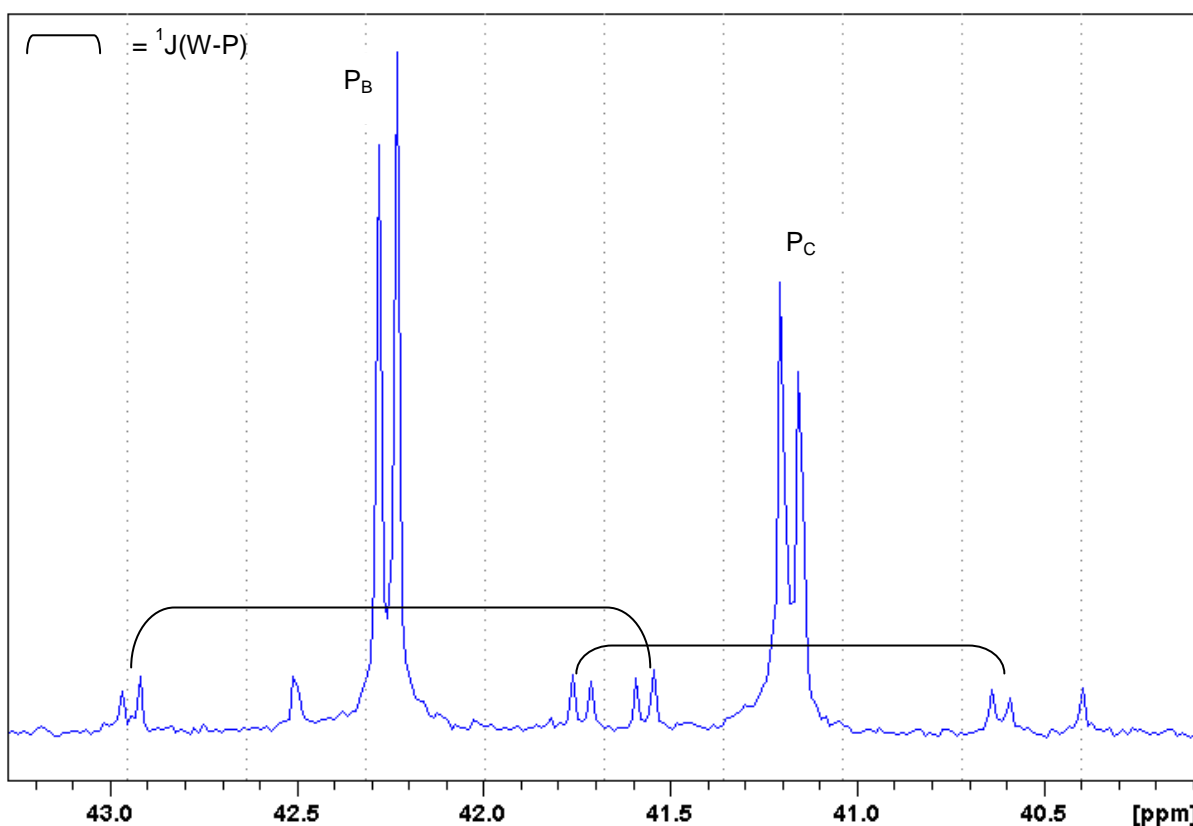
FIGURE 2.7: ^{31}**P NMR SPECTRUM FOR COMPLEX A3**

On considering the DPPE derivatives (**A3** and **B3**), two peaks were seen for each of the complexes, as would be expected for phosphorous atoms in non-equivalent positions. By comparison with the monophosphines, the assignments could be easily deduced. The spectra of **A3** (Figure 2.7) and **B3** both showed the differences for the ^{1}J(W-P) couplings seen between **A1** and **A2**. This once again suggests that the *trans* ligand influence is at work. Thus it is expected that due to decreased electron density on the metal centre, the P_C-W bond should be longer than the corresponding bond length in W(CO)$_4$DPPE, if this is the only influence considered. However, once again the π-acceptor capabilities of the carbonyl ligands and carbene ligand need to be considered.

39

2.5 IR SPECTROSCOPY

TABLE 2.9: IR STRETCHING FREQUENCIES FOR TUNGSTEN COMPLEXES (cm^{-1})			
Pentacarbonyls			
W(CO)$_5$PPh$_3$[45]	2071 (A_1^1)	1979 (B_1)	1943 (E)	1940 (A_1^2)
A	2066 (A_1^1)	1916 (B_1, E, A_1^2)		
B	2067 (A_1^1)	1920 (B_1, E, A_1^2)		
Tetracarbonyls			
W(CO)$_4$DPPE	2013 (A_1^1)	1920(A_1^2)	1886 (B_1)	1872 (B_2)
A1	2009 (A_1^1)	1914 (B_2)	1894 (A_1^2)	1883 (B_1)
B1	2009 (A_1^1)	1921 (B_2)	1888 (A_1^2)	1860 (B_1)
A2	2017 (A_1)	1944 (B_1)	1892 (E)	
B2	2019 (A_1)	1941 (B_1)	1884 (E)	
Tricarbonyls *mer*			
A3	1966 (A_1^1)	1866 (B_1)	1846 (A_1^2)	
B3	1962 (A_1^1)	1866 (B_1)	1841 (A_1^2)	

All spectra recorded in KBr (with the exception of literature)

IR stretching modes for complexes **A1**-**A3** and **B1**-**B3** were assigned by comparison with theoretical vibrational spectra. Assignments for known complexes were found in literature.

The IR data was divided into sections based on the CO substitution to facilitate the understanding of the different systems. The values found for the tungsten pentacarbonyl carbene derivatives agreed relatively well with those reported in literature.[24,31,51] No band overlap was observed in literature, however the spectra for literature complexes were recorded in hexane and thus differences noted are most likely due to different media used for collection.
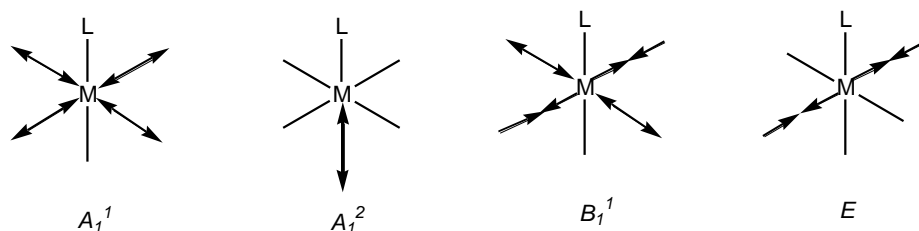
FIGURE 2.8: IR-ACTIVE MODES FOR METAL PENTACARBONYL SYSTEMS

40

Metal pentacarbonyl systems are expected to have C_{4v} symmetry with three active bands.[44] However, the presence of a bulky L ligand such as a carbene can result in a fourth band being seen. The IR bands that can be observed are thus as follows (in order of decreasing wavenumber): A_1^1, B_1, E and A_1^2 (Figure 2.8). This is clearly reflected in the literature data for $W(CO)_4PPh_3$. However, complexes **A** and **B** do not reflect this due to extensive overlap of the various bands. Only the A_1^1 band could be assigned unambiguously. The second band represents overlap of the other three expected bands.

(a) IR-active modes for *cis*-[M(CO)$_4$L$_1$L$_2$]

(b) IR-active modes for *trans*-[M(CO)$_4$L$_1$L$_2$]
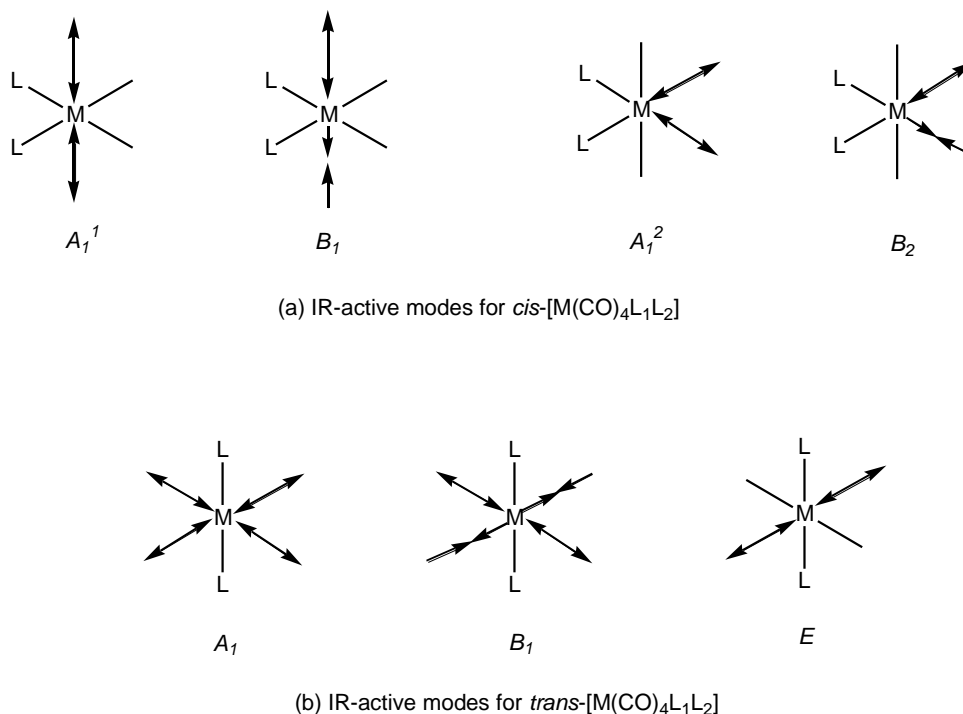
FIGURE 2.9: IR-ACTIVE MODES FOR (a) CIS AND (b) TRANS-[M(CO)$_4$L$_1$L$_2$] COMPLEXES

Metal tetracarbonyl systems (M(CO)$_4$ L$_1$L$_2$) show varying symmetry patterns which depend both on the substitution pattern and the nature of the ligand L. W(CO)$_4$DPPE data agreed relatively well with the data found in literature (2016 cm^{-1}, 1921 cm^{-1}, 1901 cm^{-1}, 1876 cm^{-1}).[52] For *cis* tetracarbonyl systems where L$_1 \neq$ L$_2$, C_S symmetry of the metal moiety is found.[10,44] This allows for four IR active modes: A_1^1, A_1^2, B_1 and B_2 (Figure 2.9). *Trans* substituted M(CO)$_4$ L$_1$L$_2$ complexes where L$_1 \neq$ L$_2$, have A_1, B_1, and E bands derived from C_{4v} symmetry of the metal moiety.[10,29,44] Complex **A2** did not show all IR active bands, most likely due to excessive overlap. Complex **B2** did, however, show the expected pattern. The different stereochemistries for the carbene complexes can, in conclusion, be differentiated easily on the basis of IR spectroscopy.

41
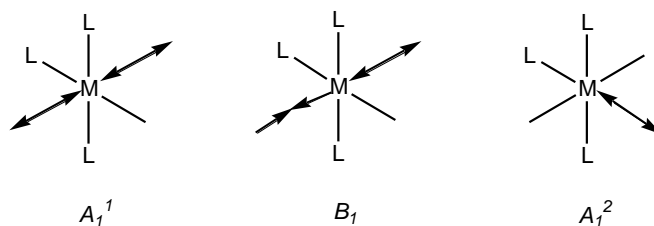
FIGURE 2.10: IR-ACTIVE MODES FOR *MER*-[M(CO)$_3$L$_1$L$_2$L$_3$] COMPLEXES

Metal tricarbonyl systems in which L$_1 \neq$L$_2 \neq$L$_3$ are expected to have three IR active modes with C_S symmetry for the metal moiety (Figure 2.10). Complexes **A3** and **B3** both showed three bands on their spectra, the $A_1{}^1$, B_1 and $A_1{}^2$ bands.[44,53] It could thus be shown from IR spectroscopy that the *mer* isomer for **A3** and **B3** were indeed isolated, in contrast to the *fac* isomer, which would have only two IR active bands.

The A_1 band in metal pentacarbonyl systems is seen as the distinctive CO frequency.[45] If this frequency is considered as distinctive for all the carbonyl systems studied, then a correlation between the compounds can be made. There is a marked decrease in the wavenumber of the A_1 band with each successive carbonyl substitution, which correlates well with increased electron density being available for metal π-backbonding to the carbonyl groups. Phosphine ligands are weaker π-acceptors than carbonyls. Thus, substitution of a carbonyl with a phosphine would result in increased π-donation from the metal to the carbonyl groups. Increased metal-carbon bond character would decrease the carbon-oxygen bond character, and thus the wavenumber observed for the carbonyl stretching frequencies would decrease (Structure a, Figure 2.11).

L= weaker π-acceptor e.g. PR$_3$ L= strong π-acceptor e.g. CO
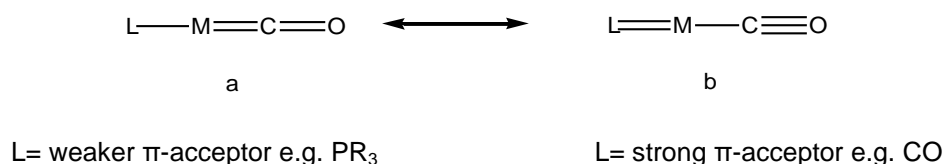
FIGURE 2.11: π-METAL INTERACTIONS BETWEEN LIGAND(L) AND CARBONYL GROUPS

The differences between the *cis* and the *trans* isomers are obviously due to the different substitution patterns. In the *trans* isomer the CO groups are all trans to one another and thus cannot benefit as much from the altered ligand sphere. In conclusion, it can thus be seen that each set of complexes has a distinctive IR pattern which can be used for identification, and reflects the changes in metal π-donation.

42

2.6 XRD: CRYSTAL STRUCTURE ANALYSIS

W(CO)₄DPPE   **Complex A3**
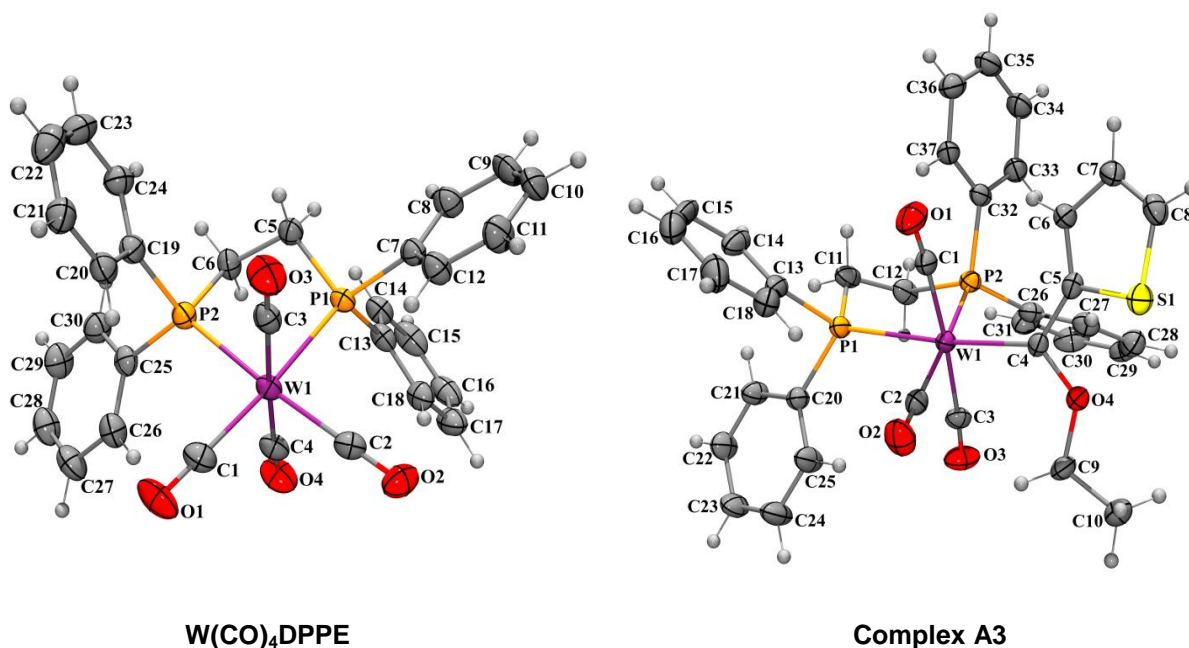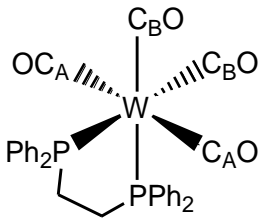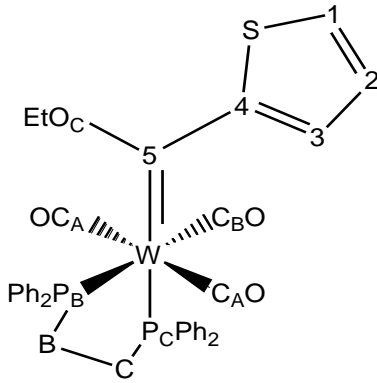
FIGURE 2.12: ORTEP PLOT REPRESENTATIONS OF THE CRYSTAL STRUCTURES OF **W(CO)₄DPPE** AND COMPLEX **A3**

The discussion of the crystal structures will commence with a comparison of the W(CO)₄DPPE crystal with the Mo derivative,[34] and then follow on to compare the carbene DPPE complex (**A3**) with this structure. All atom labels used during the discussion refer to those shown in table 2.10.

The Mo and W crystal structures showed striking similarities. Firstly, it was seen that the key bond angles and bond lengths rarely deviated more than 2° and 0.05 Å, respectively, from one another.[34] This correlation indicates that no large deviations are seen for the W derivative that would set it apart from the other Group 6 derivatives, the Mo analogue in particular.

TABLE 2.10 SELECTED DATA FOR THE CRYSTAL STRUCTURES OF W(CO)₄DPPE AND A3		
	W(CO)₄DPPE	**Complex A3**
Bond Length (Å)		
W-C5		2.118
W-C$_A$O	2.031	2.015
W-C$_B$O	1.987	1.982
C5-C4		1.457
C4-C3		1.379
C3-C2		1.422
C2-C1		1.331
C1-S		1.709
C4-S		1.742
W-P$_B$	2.495	2.493
W-P$_C$		2.514
Torsion angles (°)		
W-C5-C4-O$_C$		172.9
W-C5-C4-C3		-24.8

Complex **A3** showed interesting deviations when compared with literature results for the *fac* isomer of found by Reinheimer *et.al.*[22] This group found that the ethoxy group would nestle between the phenyl substituents of DPPE, and the ethoxy group was in the *E* conformation. In our case, the ethoxy group was situated furthest away from the DPPE group, and was found in the more favourable and more common *Z* conformation. It is suggested that the *mer*-substitution allowed this more favourable Z conformation since the steric factors which forced the *E* conformer are not present, in complex **A3**.

The W-P bond lengths showed changes when **A3** was compared to W(CO)₄DPPE. The W-P$_B$ bond length was 2.493 Å, while the average bond length in W(CO)₄DPPE was 2.495 Å. This is not a significant difference and indicates little change in bond order. The W-P$_C$ bond length, however, was 2.514 Å, showing a slight increase in bond length. This correlates well with NMR data which suggests that the carbene ligand has a greater *trans* influence than the carbonyl groups and thus W-P$_C$ should be longer than W-P$_B$. In **A3**, the W-C5 bond is longer than the W-CO bonds. This is indicative of larger

44

double bond character for the W-CO bond than the W-$C_{carbene}$ bond. W-C_AO is much shorter than W-C_BO. Since phosphines are weaker π-acceptors than carbonyls, more π-backbonding should be present for W-C_BO bond than the W-C_AO bond, causing the difference in bond lengths. Lastly if the length of the bonds in the heteroaryl ring are compared, it is clear the the thienyl substituent is not symmetrical. This indicates that electron density is being withdrawn from the heteroaryl ring, thereby distorting the bond lengths.

When comparing the **A3** bond angles to the W(CO)$_4$DPPE bond angles, a few interesting differences were noted. The P-W-P angle was not altered significantly. However, the angle between the phosphorous atom and the carbene carbon (P_B-W-C5) was 99.31°, correspond to a 10° deviation from the perfect octahedral structure. This is clearly a structural requirement to prevent steric interactions between the carbene substituents and the phenyl rings of the phosphorous atom.
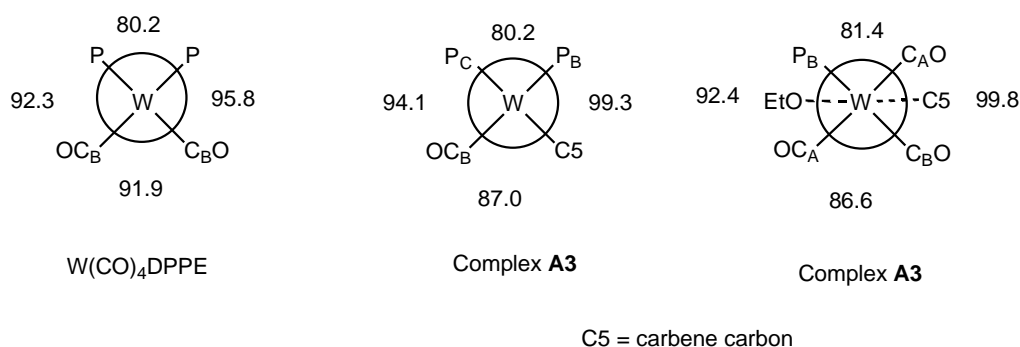
FIGURE 2.13: SELECTED BOND ANGLES(°) FOR W(CO)$_4$DPPE AND A3

The large deviation from 90° seen for the phosphorous bite angle for both W(CO)$_4$DPPE and **A3** is due to the 5-membered ring structure formed by tungsten and the DPPE ligand, which limits this angle. This was the largest deviation from octahedral geometry that was noticed in W(CO)$_4$DPPE. This indicates minimal deviations from the perfect octahedral geometry and optimal arrangement around the metal centre. In contrast, **A3** did not only show deviation from the perfect octahedral geometry for the phosphorous bite angle, but also in the rest of the molecule. Deviations due to steric requirements of the carbene ligand and the phosphine ligand resulted in further deviations, as shown in figure 2.13. The carbene substituents are staggered between C_AO, C_BO and P_B. The bonds between these atoms therefore deviate from the perfect octahedral geometry to allow the carbene substituents to nestle between these groups.

45

2.7 THEORETICAL CALCULATIONS

The theoretical discussion of this chapter will focus on determining the distribution of the HOMO and LUMO orbitals, and the corresponding energy gap between these two orbitals. Electrostatic potential maps were calculated in order to better understand the electron distribution in the complexes. Only the thienyl derivatives (**A1**-**A3**) are shown and discussed in the section since the furyl carbene complexes (**B1**-**B2**) showed similar trends.

HOMO A1: E = -0.192 Hartrees   HOMO A2: E = -0.186 Hartrees   HOMO A3: E = -0.169 Hartrees

LUMO A1: E = -0.080 Hartrees   LUMO A2: E = -0.072 Hartrees   LUMO A3: E = -0.058 Hartrees
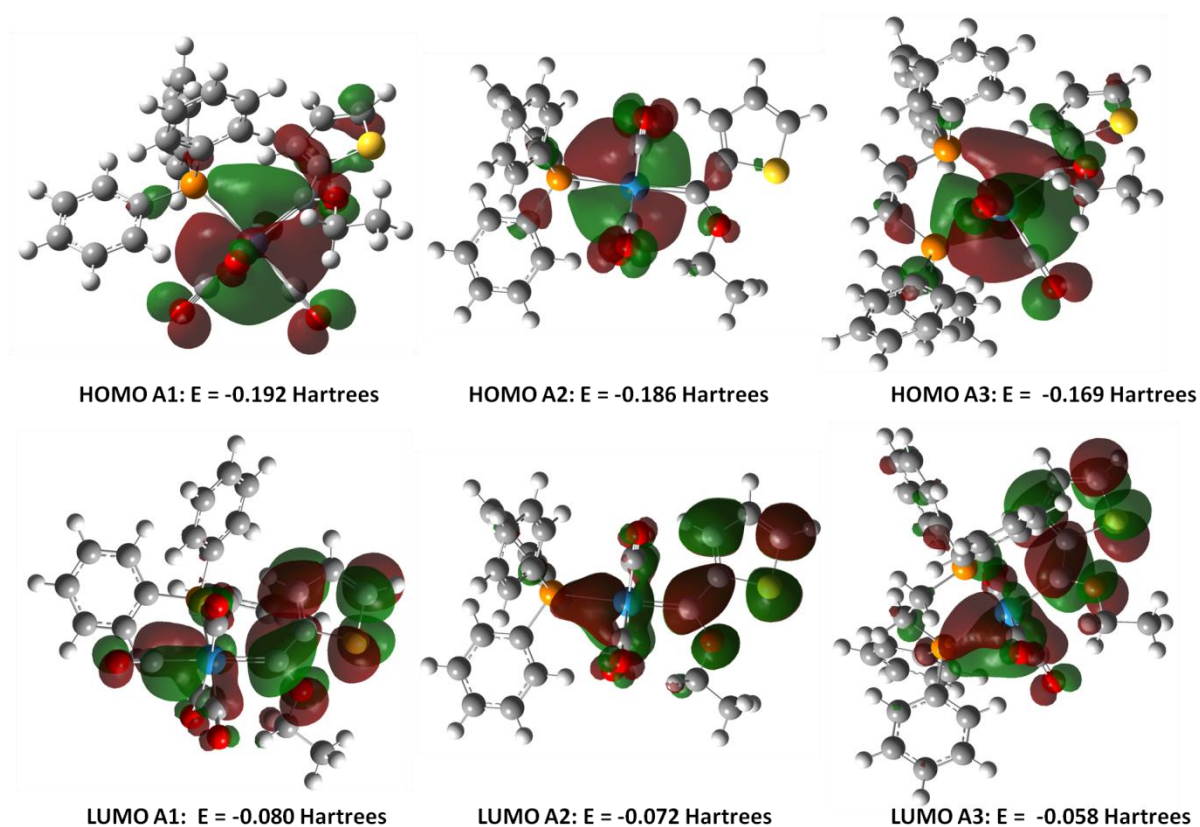
FIGURE 2.14: HOMO AND LUMO DIAGRAMS CALCULATED FOR OPTIMIZED COMPLEXES A1-A3 (1 HARTREE = 2600 KJ/MOL)

The HOMOs for complexes **A1**-**A3** were mostly centred around the metal, with only minor components being present on the carbon atoms of the heteroaryl carbene substituent. The LUMOs, in contrast, were localised on the heteroaryl carbene substituent's atoms, the carbene carbon and the oxygen atom of the carbene substituent. The LUMO was also localised along the metal-ligand bond *trans* to the carbene ligand. The atoms with the highest amount of HOMO contribution are expected to be the most likely point for electrophilic attack. Conversely, nucleophilic attack will be focused on the

46

atoms which have the largest LUMO contribution. The HOMO-LUMO distribution therefore suggests that electrophilic attack will be directed toward the metal centre. Nucleophilic attack will be directed towards the carbene carbon, and potentially the bond *trans* to the carbene ligand. Since Fischer carbenes are known to be electrophilic,[3,54] the theoretical results support experimental data.

Complex **A1**   Complex **A2**   Complex **A3**

Electron Density

High   Low
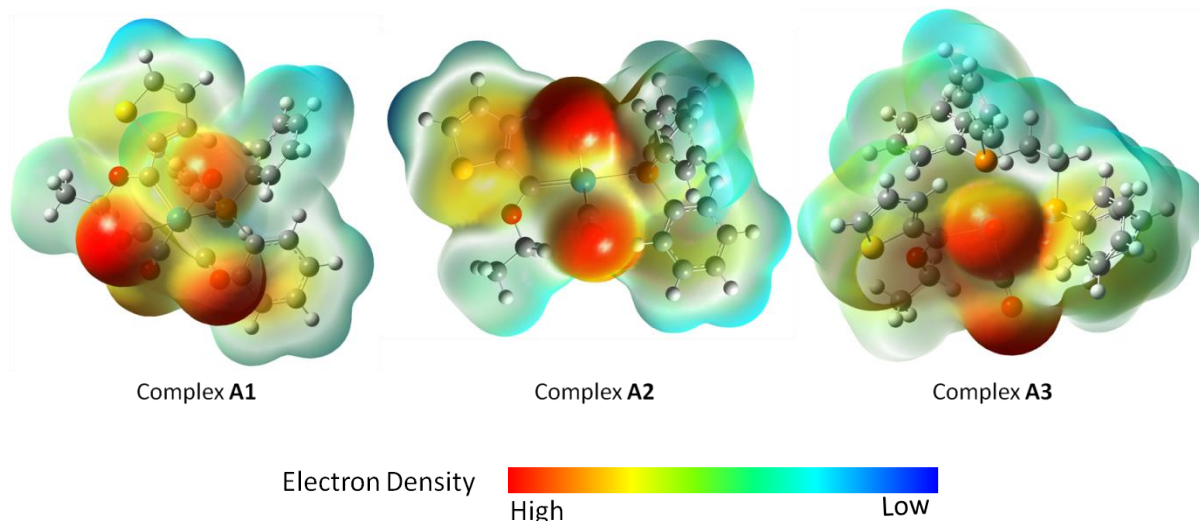
FIGURE 2.15: ESP MAPS CALCULATED FOR OPTIMIZED COMPLEXES A1-A3

ESP maps calculated for complexes **A1-A3** are presented in figure 2.15. The highest electron density is located on the carbonyl ligands in all three cases. In complex **A1**, electron density is concentrated on one side, and thus this molecule will have a dipole. However, in complexes **A2** and **A3** the areas of high electron density are engulfed by the areas of low electron density, and the electron density distribution is almost symmetrical. This firstly indicates that complexes **A2** and **A3** will have a smaller dipole than complex **A1**. The differences in polarity between **A1** and **A2** are seen during synthesis, where **A2** is found to be less polar than **A1** as is expected from the ESP maps.

TABLE 2.11: ENERGY DIFFERENCE BETWEEN HOMOS AND LUMOS	
COMPLEX	**ENERGY GAP (KJ / MOL)**
Complex A1	294.1
Complex A2	299.3
Complex A3	291.4

The HOMO-LUMO energy gap is known to be an indication of the reactivity of the complex.[14] This energy gap was shown to be useful in dertermining changes in reactivity of Fischer carbene

47

complexes upon substitution with different phosphine ligands in photocarbonylation reactions. The HOMO-LUMO energy gap for the complexes summarised in table 2.11 decreases as follows:

A2 > A1 > A3

These energy gaps are not significantly different but do allow for a tentative trend in reactivity to be suggested. Diphosphinated complexes are expected to have a lower HOMO-LUMO energy difference since two strong σ-donors are found in the complex when compared to monophosphinated complex. It is consequently expected that **A3** should have the smallest HOMO-LUMO gap, as was found. However, the additive effect of two substituted carbonyls would cause complex **A3** to be less reactive than complex **A1** and **A2** as successive carbonyl substitution becomes exponentially more difficult with each substitution.[14] Complex **A2** is also expected to be less reactive than complex **A1**, since it has the largest HOMO-LUMO gap. The *trans* placement of the phosphine and carbene ligands clearly reduce the reactivity of the complexes. The data thus suggests that complex **A1** is likely to be the most reactive of the three complexes.

2.8 CONCLUSION

Synthesis and characterisation of complexes **A1**-**A3** and **B1**-**B3** could be achieved satisfactorily. These complexes clearly showed that the characteristics of the complexes were altered by changing the substituents in the ligand sphere from carbonyls to phosphines. ^{1}H-, ^{13}C- and ^{31}P NMR spectroscopy confirmed that the proposed complexes were synthesised successfully. Further evidence supporting the proposed structures is found in XRD characterisation of complex **A3**. Theoretical calculations indicated that the HOMO orbitals were centred on the metal centre, while the LUMO orbitals were on the carbene ligand. The metal centre will thus be the preferred location for electrophilic attack, and the carbene ligand the preferred location for nucleophilic attack. ESP maps indicated that the highest concentration of electron density is always found on the carbonyl ligands. Complex **A1** is likely to be the most reactive complex, if one considers the HOMO-LUMO energy difference as well as ligand substitution. It can thus be concluded that varying the metal ligand sphere and the carbene substituents is handy for altering the characteristics of the tungsten Fischer carbene complexes, and may be used to tune reactivity patterns. Future work from these studies would include determination of the crystal structure of complexes **A1**-**A2** and **B1**-**3**, to allow the trend for the *trans* influence of the various ligands as suggested from NMR data to be confirmed. Lastly, experimental data, which allows for the comparison of complexes **A1**-**A3** and **B1**-**B3** is needed to confirm the expected reactivity trends, and thus suggested for future studies.

2.9 REFERENCES

(1)   Fischer, E. O.; Maasböl, A. *Angew. Chem.* **1964**, *76*, 645.

(2)   Fischer, E. O.; Maasböl, A. *Angew. Chem. Int. Edit* **1964**, *3*, 580.

(3)   de Frémont, P.; Marion, N.; Nolan, S. P. *Coord. Chem. Rev.* **2009**, *253*, 862.

(4)   Sierra, M. A. *Chem. Rev.* **2000**, *100*, 3591.

(5)   Fey, N.; Haddow, M. F.; Harvey, J. N.; Mcmullin, C. L.; Orpen, A. G. *Dalton Trans.* **2009**, 8183.

(6)   Dötz, K. H. *Angew. Chem. Int. Ed.* **1984**, *23*, 587.

(7)   Jimenez-Halla, J. O. C.; Solá, M. *Chem. Eur. J.* **2009**, *15*, 12503.

(8)   Mills, O. S.; Redhouse, A. D. *Chem. Commun.* **1966**, 814.

(9)   Werner, H.; Rascher, H. *Inorg. Chim. Acta* **1968**, *2*, 181.

(10)   Fischer, E. O.; Aumann, R. *Chem. Ber.* **1969**, *102*, 1495.

(11)   Elschenbroich, C. *Organometallics*; 3rd ed.; Wiley - VCH: Weinheim, **2011**.

(12)   Barluenga, J.; Muniz, K.; Tomas, M.; Ballesteros, A.; Garcia - Granda, S. *Organometallics* **2003**, *22*, 1756.

(13)   Sierra, M. A.; Fernández, I.; Gomez-Gallego, M.; Torres, M. R.; Cossı, F. P.; Arrieta, A.; Lecea, B.; Poveda, A.; Jimenez-Barbero, J. *J. Am. Chem. Soc.* **2003**, *125*, 9572.

(14)   Arrieta, A.; Cossío, F. P.; Fernández, I.; Gomez-Gallego, M.; Lecea, B.; Mancheno, M. J.; Sierra, M. A. *J. Am. Chem. Soc.* **2000**, *122*, 11509.

(15)   Crotti, C.; Farnetti, E.; Celestino, T.; Stener, M.; Fontana, S. *Organometallics* **2004**, *23*, 5219.

(16)   Brown, T. L.; Lee, K. J. *Coord. Chem. Rev.* **1993**, *128*, 89.

(17)   Herrmann, W. A.; Goossen, L. J.; Artus, G. R. J. *Organometallics* **1997**, *2*, 2472.

(18)   Fernández, I.; Sierra, M. A.; Gomez-Gallego, M.; Mancheno, M. J.; Cossío, F. P. *Angew. Chem.* **2006**, *118*, 131.

49

(19)   Maiorana, S.; Seneci, P.; Rossi, T.; Bladoli, C.; Ciraco, M.; de Magistris, E.; Licandro, E.; Papagni, A.; Provera, S.; Baldoli, C.; Povera, S. *Tetrahedron Lett.* **1999**, *40*, 3635.

(20)   Klapdohr, S.; Dötz, K. H.; Assenmacher, W.; Hoffbauer, W.; Hüsing, N.; Nieger, M.; Pfeiffer, J.; Popall, M.; Schubbert, U.; Trimmel, G. *Tetrahedron Lett.* **1999**, *40*, 3635.

(21)   Cooke, M. D.; Fischer, E. O. *J. Organomet. Chem.* **1973**, *56*, 279.

(22)   Reinheimer, E. W.; Kantardjieff, K. A.; Herron, S. R.; Tisserat, C. G.; Casalnuovo, J. A. *J. Chem. Crystallogr.* **2003**, *33*, 503.

(23)   Terblans, Y. M.; Roos, H. M.; Lotz, S. *J. Organomet. Chem.* **1998**, *566*, 133.

(24)   Crause, C.; Görls, H.; Lotz, S. *Dalton Trans.* **2005**, 1649.

(25)   Dötz, K. H.; Stendel, J. *Chem. Rev.* **2009**, *109*, 3227.

(26)   Wu, Y.-T.; Kurahashi, T.; de Meijere, A. *J. Organomet. Chem.* **2005**, *690*, 5900.

(27)   Dötz, K. H.; Tomuschat, P. *Chem. Soc. Rev.* **1999**, *28*, 187.

(28)   Landman, M.; Görls, H.; Lotz, S. *J. Organomet. Chem.* **2001**, *617*, 280.

(29)   Fischer, E. O.; Fischer, H. *Chem. Ber.* **1974**, *107*, 657.

(30)   Streubel, R.; Priemer, S.; Jones, P. G. *J. Organometal. Chem.* **2001**, *618*, 423.

(31)   Crause, C. Synthesis and application of carbene complexes with heteroaromatic substituents, University of Pretoria, **2004**.

(32)   Fischer, E. O.; Fischer, H.; Kreissl, F. R. *J. Organomet. Chem.* **1974**, *64*, C41.

(33)   Andrews, G. T.; Colquhoun, I. J.; Mcfarlane, W. *Polyhedron* **1983**, *2*, 783.

(34)   Bookham, J. L.; McFarlane, W.; Thornton-Pett, M.; Jones, S. *J. Chem. Soc. Dalton Trans.* **1990**, 3621.

(35)   Andrews, G. T.; Colquhoun, I. J.; McFarlane, W.; Grim, S. *J. Chem. Soc. Dalton Trans.* **1982**, 2353.

(36)   Fischer, E. O.; Fischer, H.; Werner, H. *Angew. Chem. Int. Ed.* **1972**, *11*, 644.

(37)   Connor, J. A.; Day, J. P.; Jones, E. M.; McEwen, G. K. *J.Chem.Soc. Dalton Trans.* **1973**, 347.

(38)   Aoki, S.; Fujimura, T.; Nakamura, E. *J. Am. Chem. Soc.* **1992**, *114*, 2985.

(39)   Darensbourg, M. Y.; Darensbourg, D. J. *Inorg. Chem.* **1970**, *9*, 32.

(40)   Pregosin, P. S.; Kunz, R. W. *^{31}P and ^{13}C NMR of Transition Metal Phosphine Complexes*; Diehl, P.; Fluck, E.; Kosfeld, R., Eds.; 1st ed.; Springer - Verlag: Berlin, **1979**.

(41)   *Phosphorus-31 NMR: Principles and Applications*; Gorenstein, D. G., Ed.; 1st ed.; Academic Press Inc.: London, **1984**.

(42)   *Handbook of Phosphorous-31 Nuclear Magnetic Resonance Data*; Tebby, J. C., Ed.; 1st ed.; CRC Press, Inc.: Boston, **1991**.

(43)   B. P. P.; Badertscher, M.; Pretsch, E.; Bühlmann, P. *Structure determination of organic compounds*; 4th ed.; Springer - Verlag: Berlin, **2009**.

(44)   Braterman, P. S. *Metal Carbonyl Spectra*; 1st ed.; Academic Press Inc.: London, **1975**.

(45)   Guns, M. F.; Claeys, E. G.; van der Kelen, G. P. *J. Mol.Stuct.* **1979**, *54*, 101.

(46)   Buchner, W.; Schenk, W. A. *Inorg. Chem.* **1984**, *23*, 132.

(47)   Twyman, R. M. In *NMR Spectrorscopy - Applicable Elements*; **2005**; pp. 278.

(48)   Grim, S.; Briggs, W. L.; Barth, R. C.; Tolman, C. A.; Jesson, J. P. *Inorg. Chem.***1974**, *13,* 1095.

(49)   Schenk, W. A.; Buchner, W. *Inorg. Chim. Acta* **1983**, *70*, 189.

(50)   Mathieu, R.; Lenzi, M.; Poilblanc, R. *Inorg. Chem.* **1970**, *9*, 2030.

(51)   van Staden, M. Synthesis and structure of bithiophene complexes, University of Pretoria, **2001**.

(52)   Chatt, J.; Watson, H. R. *J. Chem. Soc.* **1960**, 4980.

(53)   Fischer, E. O.; Richter, K. *Chem. Ber.* **1976**, *109*, 2547.

(54)   Kotha, S.; Dipak, M. K. *Tetrahedron* **2012**, *68*, 397.

CHAPTER 3:

AMINO CARBENE COMPLEXES OF TUNGSTEN(0)

3.1 INTRODUCTION

Fischer carbenes are known to be electrophilic and are thus open to nucleophilic attack on the carbene carbon.[1–3] This naturally would allow for modification of the carbene. Alkoxy carbenes are readily altered in this manner by nucleophilic attack, which generally leads to substitution of the alkoxy substituent. Nucleophiles that may be used to substitute alkoxy groups include amines, thiols, and aryllitium salts, and lead to the formation of amino, thio- and aryl-carbene complexes, respectively (Scheme 3.1).[1,4]
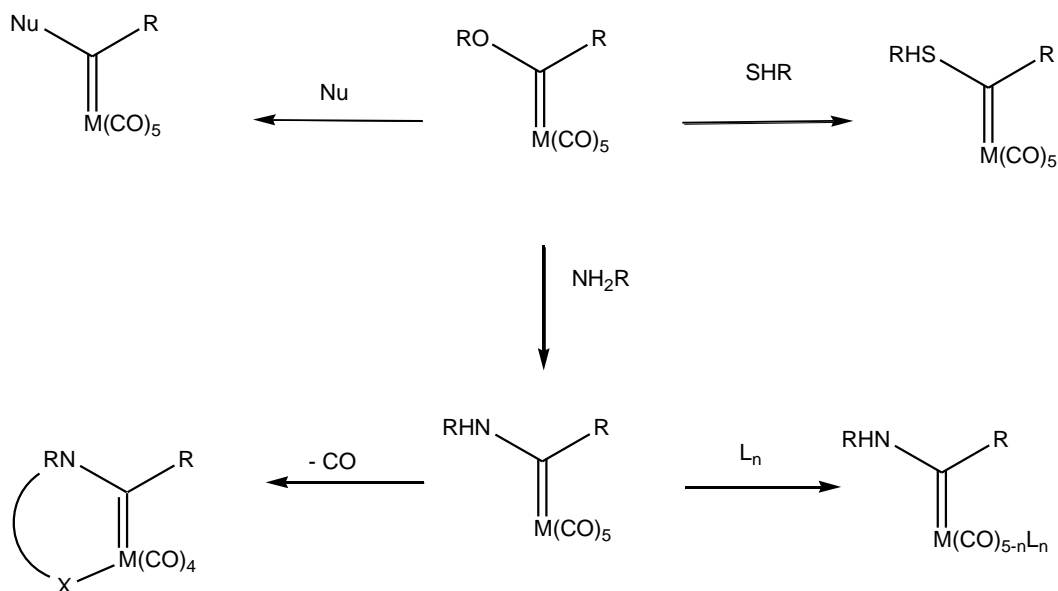
SCHEME 3.1: MODIFICATION OF ETHOXY FISCHER CARBENES BY NUCLEOPHILIC ATTACK ON THE HETEROATOM

Of these modifications, aminolysis has been used most extensively,[5] for various reasons. Firstly, the reactivity of thiocarbenes resemble ethoxy carbenes and consequently this modification does not have as large an effect on the complex as aminolysis.[5] Thiols are also unpleasant to work with. Substitution with aryl groups, in contrast, requires the lithium intermediates and the reaction is more demanding than aminolysis. Aryl substitution further alters the carbene to resemble a Schrock carbene, and hence does not increase the stability of the complex as much as amino groups do. Amines are as a result preferred for nucleophilic attack of alkoxy carbenes, because of the relative ease of the reaction and the increased stability of the products.

Amino carbenes were synthesised not long after the first stable alkoxy carbene.[6] These products were obtained by aminolysis of the corresponding alkoxy carbene. Since this time, much attention has been given to the aminolysis reaction, as well as alternative methods to synthesise amino carbenes. Aminolysis of alkoxy Fischer carbenes occurs in a similar fashion to the reaction of an ester with an amine, and is also base catalysed.[5–7] The original methodology has been extended to allow primary, secondary and even tertiary amines to be used for the production of amino carbenes. Alternative methods for the production of amino carbenes include the Hedgedus synthesis[8] (Scheme 3.2) and nucleophilic attack of isocyanide metal complexes.[3]

$M(CO)_6 + C_8K \longrightarrow [M(CO)_5^-] +$

O double bond, R_1—C—NR_2 $\longrightarrow$ $(OC)_5M=$ carbene with NR_2 and R_1

R_1 = alkyl, aryl, vinyl
R_2 = H, alkyl
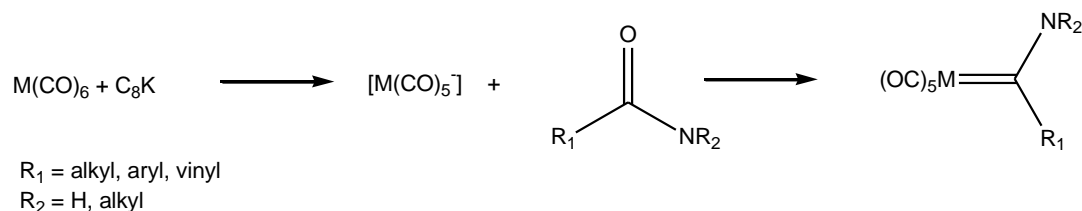
SCHEME 3.2: HEDGEDUS-SEMMELHACK SYNTHESIS OF AMINO CARBENES

Nucleophilic attack of a carbonyl group with an amino lithium salt, for example LDA, will also produce amino carbenes.[9] However, classical aminolysis still remains the easiest method for producing amino carbenes. Modification of the ligand sphere as well as the amino substituent has developed extensively since the first aminolysis product was reported, and has led to many novel applications (Figure 3.1). These applications include polymer-bound amino chromium Fischer carbene complexes.[10] Also, the activation of photochemical inert tungsten carbene complexes was achieved by modification of an amino carbene's ligand sphere.[11] Lastly, amino carbenes are used in the Pauson-Khand cyclization reaction.[12]

Maiorana *et.al.*[10]

Stumpf *et.al.*[13]

Heat

hv

Fernandez *et.al.*[11]

Streubel *et.al.*[14]
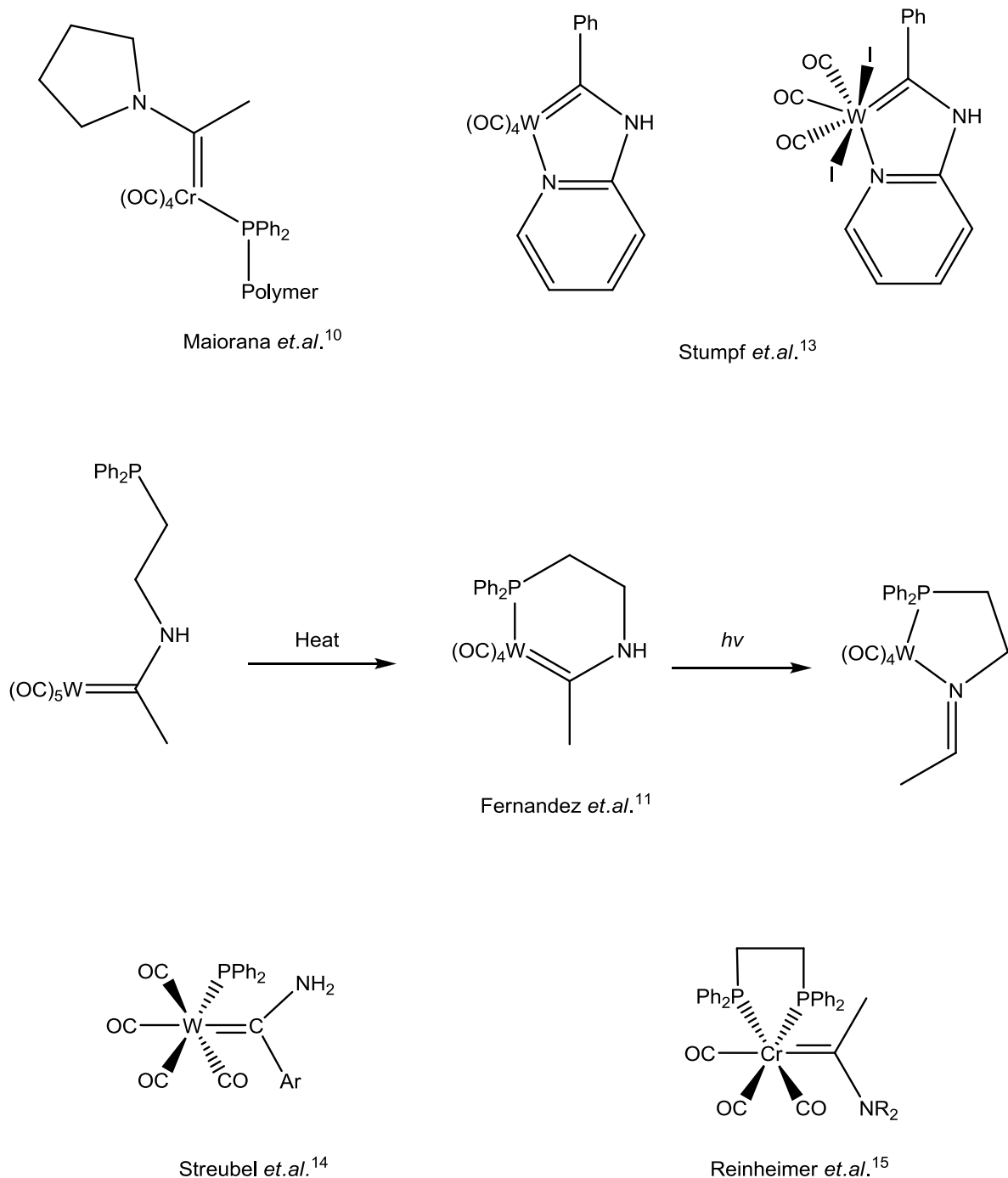
Reinheimer *et.al.*[15]

FIGURE 3.1: REPRESENTATIVE AMINO CARBENES WITH ALTERED LIGAND SPHERES[10,11,13–15]

As is seen in figure 3.1 above, examples of amino carbenes with altered ligand spheres are found in literature. However, as is noted by Reinheimer *et.al.*[15] not much work has been done with regards to phosphinated amino Fischer carbenes. These complexes are, however, particularly useful. Streubel *et.al.* made use of altering the ligand sphere with a phosphine to understand the mechanism of the formation of *2H*-azaphosphirene complexes.[14] This void in literature is especially notable for diphosphine amino carbenes such as complex **A6** and **B6** (Figure 3.2).[15] Also, no literature examples

54

of amino heteroaryl Fischer carbenes containing phosphines or amines in the ligand sphere are known. Synthesis of heteroaryl amino carbenes containing phosphines and amines in the ligand sphere were thus proposed as the focus of this study, an area of Fischer carbene chemistry that has been almost completely neglected in literature until now.

3.2 FOCUS OF THIS STUDY
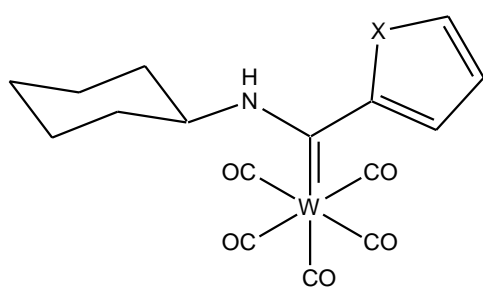
A4 and **B4**
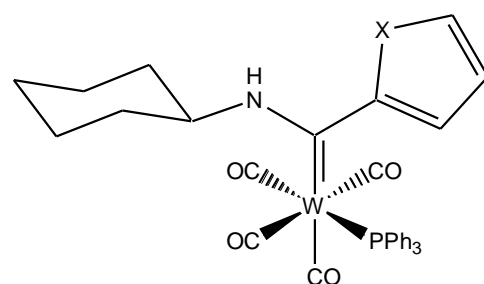
A5 and **B5**
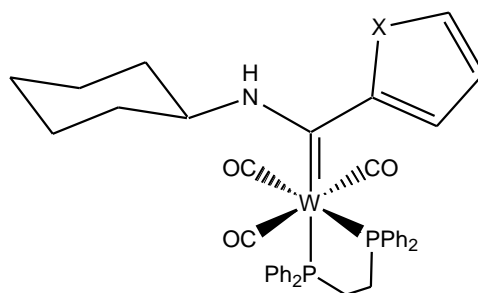
A6 and **B6**
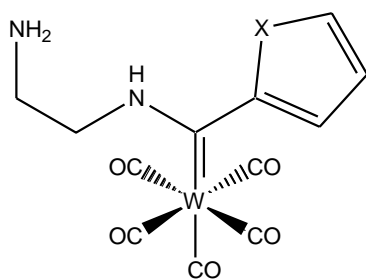
A7 and **B7**
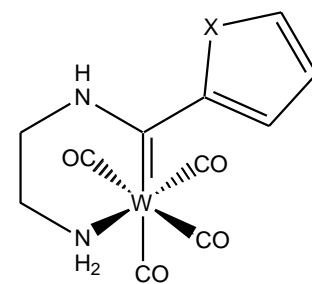
A8 and **B8**

X = S,O

FIGURE 3.2: OVERVIEW OF THE VARIOUS AMINO CARBENE COMPLEXES SYNTHESISED

The focus of this study was the synthesis of amino derivatives of the ethoxy carbene complexes discussed in chapter 2. Two different amines were used for aminolysis, namely cylcohexylamine and ethylenediamine. Cyclohexylamine is a sterically demanding group, and very few examples of amino carbene complexes with this substituent are found in literature.[16] It was therefore decided to use this amine for the transformation of ethoxy heteroaryl tungsten(0) pentacarbonyl carbenes, as well as the triphenylphosphine and diphenylphosphine ethoxy heteroaryl carbenes. The influence of a sterically demanding group and an amine substituent could thus be determined simultaneously for these complexes. Ethylenediamine, in contrast, was only used to modify the ethoxy heteroaryl tungsten(0) pentacarbonyl carbenes (**A** and **B**). This ligand is unique since it has two nitrogen groups. These can both be used for aminolysis, thereby allowing two complexes to be linked,[17] or if the reaction conditions are controlled correctly, a chelate may be formed. Aminolysis of complex **A** and **B**, followed by the formation of an amino chelate was chosen as the focus for this section of the study. It allowed for comparison between aminolysis products. More importantly, though, this allowed for comparison of the effect of σ-donors (amines) and σ-donor, π-acceptors (phosphines) on the properties of the carbene complexes.

3.3 SYNTHESIS
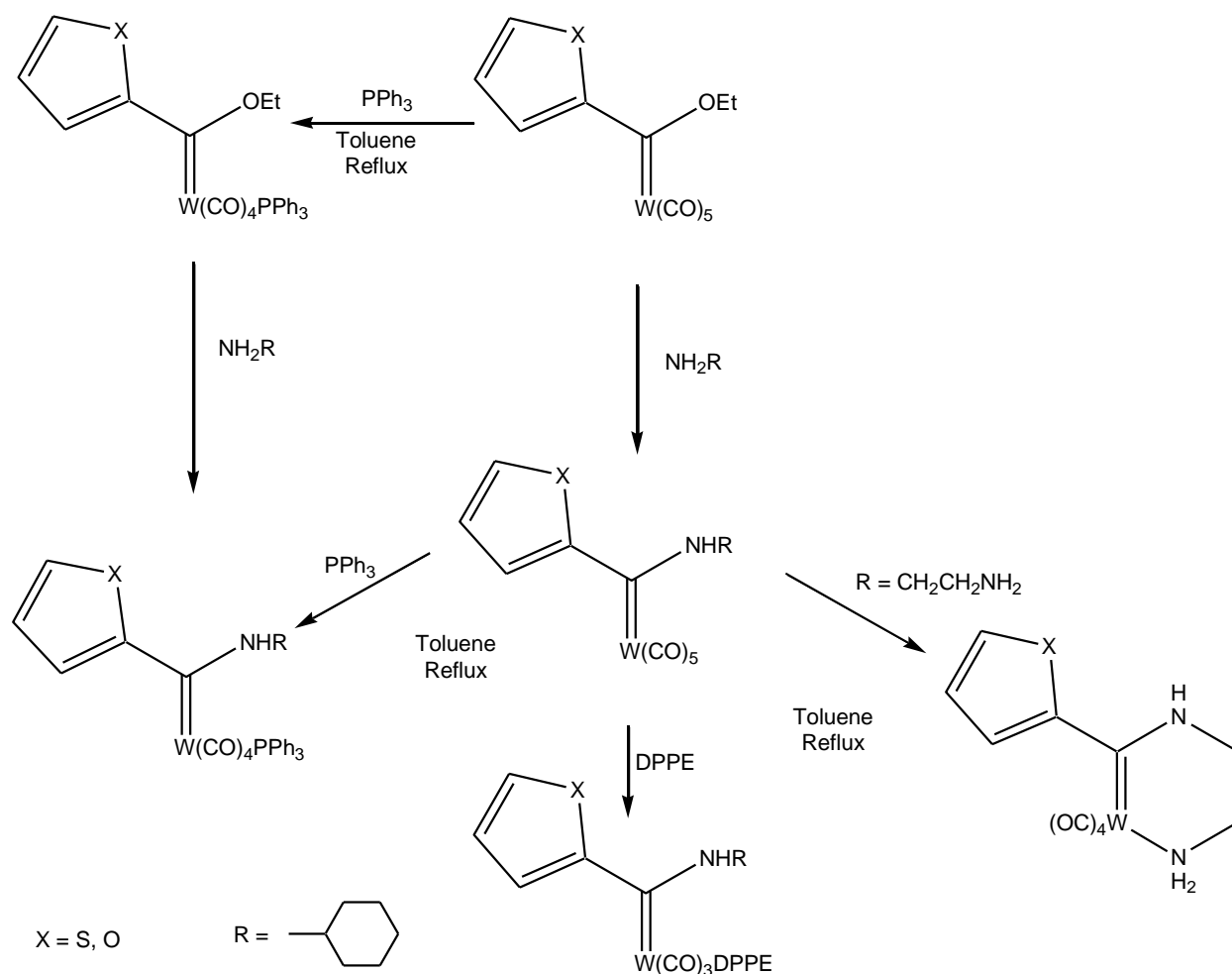
SCHEME 3.3: SYNTHESIS OF TUNGSTEN(0) AMINO CARBENE COMPLEXES

A summary of the procedures used to synthesise the various amino carbenes discussed in this chapter is found in scheme 3.3 above. Full synthetic procedures are given in chapter 6.

Complexes **A4**, **B4**, **B5**, **A7** and **B7** were synthesised using classical aminolysis methods.[1,3,18] The required amine was thus added to a solution of the ethoxy monocarbene complexes (**A**, **B**, and **B1**) at room temperature. For complexes **A4**, **B4** and **B5** ether or THF was used as solvent. Generally ethers are the preferred solvents for aminolysis. This is due to the increased reaction rate because of the stabilisation of the reaction intermediates. DCM was used instead of ether for the synthesis of complex **A7** and **B7**. Purification of these complexes was found to be complicated when ethers were

used as solvents. It is possible that the solvent molecules became trapped due to hydrogen bonding with the free NH_2-moiety that was present in **A7** and **B7.** However, this reaction occurred readily in both DCM and toluene, thus these solvents were used. Purification of **A7** and **B7** was not needed since the reaction went to completion. These reactions could be followed easily by observing the colour change. Generally the bright red ethoxy tungsten(0) pentacarbonyl heteroaryl carbene (**A** and **B**) solution would change to a bright yellow colour.

Aminolysis of the ethoxy phosphine carbenes was not possible for all the phosphine derivatives. Thus, complexes **A5**, **A6** and **B6** could only be synthesised by substitution of a carbonyl group on the corresponding amino carbene complexes **A4** and **B4**. These reactions were also easy to follow since the reaction mixture would change from bright yellow to orange. However, these reactions did not have high yields. Low yields were found either due to heat sensitivity of the products (**A5**) or steric demands of the complex (**A6** and **B6**). The furyl monophosphine amino carbene **B5** was, however, synthesised by aminolysis of the ethoxy monophosphine carbene complex **B1**. This reaction was hard to follow, since the colour change was not readily observed due to low conversion of the ethoxy carbene to the amino carbene. Aminolysis of ethoxy phosphine carbenes has been described in literature.[14,19] Lastly, it was not possible to separate the *fac* and *mer* isomers of complexes **A6** and **B6**. These complexes did not crystallize readily, and thus could not be purified in the same manner as the ethoxy analogues (**A3** and **B3**). Also, as for **A3** and **B3**, the isomers of complexes **A6** and **B6** could not be separated by means of silica gel chromatography, since the isomers could not be distinguished from one another.

The conversion of complexes **A7** and **B7** to complexes **A8** and **B8**, respectively, was performed easily. It merely required heating the reaction mixture to allow for substitution of a carbonyl. The product precipitated out of solution as an orange solid, allowing for effortless purification. **A8** and **B8** were not readily soluble in solvents such as hexane and DCM.

3.4 NMR CHARACTERISATION

Altering the heteroatom substituent on the carbene is expected to have a large effect on all of the spectra recorded for the complexes. Amino groups are known to be better π-donor substituents on carbenes than ethoxy groups.[18,20,21] The carbene carbon and the heteroaryl substituent should thus be more shielded in amino carbenes than in ethoxy carbenes.

3.4.1 NMR Characterisation for cylcohexylaminocarbene complexes of tungsten(0)
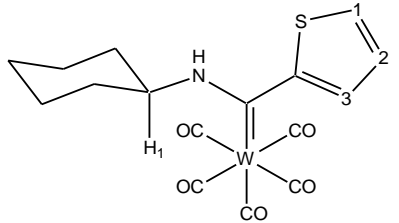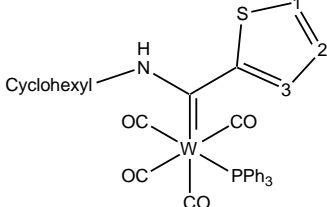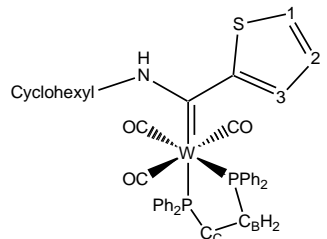
Solvents used for the various complexes are indicated below the respective tables. The *fac* and *mer* isomers of complex **A6** and **B6** could not be separated, thus only tentative assignments could be made for these complexes.

^{1}H NMR Spectroscopy

^{1}H NMR data for complexes **A4**-**A6** and **B4**-**B6** is summarised in tables 3.1 and 3.2. Assignments of heteroaryl proton chemical shifts were made by comparison with ethoxy carbene complexes discussed in chapter 2.
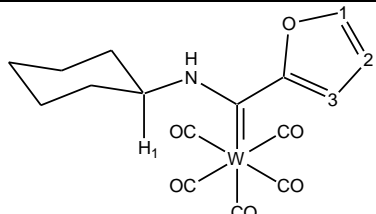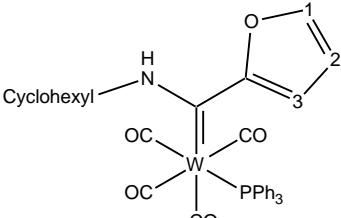
TABLE 3.1: ^{1}H NMR Data for Cyclohexylamino Thienyl Tungsten(0) Derivatives

PROTON	COMPLEX A4* ISOMER A δ (ppm)		J (Hz)	COMPLEX A4* ISOMER B δ (ppm)		J (Hz)	COMPLEX A5 δ (ppm)		J (Hz)	COMPLEX A6 δ (ppm)		J (Hz)
H1	7.50	(dd)	1.2 / 5.1	7.46	(dd)	1.1 / 5.0	7.33 - 7.43	(m)		7.02 - 7.45	(m)	
H2	7.12	(dd)	3.8 / 5.1	7.07	(dd)	3.7 / 5.0	6.97	(dd)	3.7 / 5.0	6.91	(dd)	3.6 / 4.9
H3	7.34	(dd)	1.2 / 3.8	6.93	(dd)	1.1 / 3.7	7.12	(dd)	1.2 / 3.7	6.52	(dd)	1.2 / 3.5
N-CHexyl	1.10 - 2.20	(m)		1.10 - 2.20	(m)		1.06 - 1.30 (m); 1.58 - 1.75 (m)			1.15 - 1.90	(m)	
CHexyl-H$_1$	4.35 - 4.52	(m)		3.73 - 3.86	(m)		4.02 - 4.13	(m)		3.90 - 4.05	(m)	
N-H	8.30	(s, b)		8.64	(s, b)		8.10	(s, b)		8.40	(s, b)	
P-C$_B$H$_2$										2.20 - 2.50	(m)	
P-C$_C$H$_2$										2.55 - 2.85	(m)	
PPh$_3$							7.33 - 7.43	(m)		7.02 - 7.45 (m); 7.57 - 7.72 (m)		

Solvents used: * = CDCl$_3$; All other spectra recorded in CD$_2$Cl$_2$

TABLE 3.2: ¹H NMR DATA FOR CYCLOHEXYLAMINO FURYL TUNGSTEN(0) DERIVATIVES

PROTON	COMPLEX B4* ISOMER A δ (ppm)	J (Hz)	ISOMER B δ (ppm)	J (Hz)	COMPLEX B5 δ (ppm)	J (Hz)	COMPLEX B6 δ (ppm)	J (Hz)
H1	7.51 (d)	1.4	7.68 (dd)	0.6 / 1.8	7.21 - 7.46 (m)		7.03 (s)	
H2	6.57 (dd)	1.8 / 3.6	6.60 (dd)	1.8 / 3.6	6.26 (dd)	1.8 / 3.6	6.26 (dd)	1.5 / 3.2
H3	7.38 (dd)	0.5 / 3.6	7.25 (dd)	0.6 / 3.6	6.82 (d)	3.6	6.65 (s)	
N-CHexyl	1.12 - 2.15 (m)		1.12 - 2.15 (m)		1.10 – 1.35 (m) / 1.15 – 1.80 (m)		1.12 – 1.90 (m)	
CHexyl-H₁	4.31 - 4.42 (m)		4.09 - 4.22 (m)		4.15 - 4.32 (m)		4.15 - 4.30 (m)	
N-H	8.93 (s, b)		8.13 (s, b)		8.75 (s, b)		8.59 (s, b)	
P-C$_B$H₂							2.22 – 2.50 (m)	
P-C$_C$H₂							2.22 – 2.50 (m)	
PPh₃					7.21 - 7.46 (m)		7.25 - 7.45 (m)	
					(m)		7.55 - 7.75 (m)	

Solvents used: * = CDCl₃; All other spectra recorded in CD₂Cl₂

61

The ^{1}H NMR spectra indicated several interesting changes due to the replacement of the ethoxy group with a cyclohexylamine moiety. Firstly, and most notably, the order of the proton chemical shifts changed for the thienyl derivatives, when compared to the ethoxy complexes (Table 2.2). Protons in the same relative relationship to one another have the same coupling constants. Assignments for H1 and H3 could be made by examining the coupling constants. The assignments clearly showed an inversion of the proton chemical shifts, relative to one another. The altered relative chemical shifts observed for H1 and H3 indicate the large effect aminolysis has on the carbene carbon. This order was also noted for the Cr analogue by Connor *et.al.*[22] In general, for both the thienyl (**A4**-**A6**) and the furyl (**B4**-**B6**) derivatives, the proton chemical shifts of the heteroaryl ring on the amino carbene had a more upfield resonance when compared to the ethoxy carbenes. As mentioned in the introduction to this section, the nitrogen atom of the cyclohexylamine substituent is better able to donate electron density to the carbene centre than the oxygen atom of the ethoxy group.[18,20,22,23] Consequently, it is expected that less π-donation is required from the heteroaryl ring to the carbene carbon atom. The protons of the heteroaryl ring will be more shielded and have more upfield shifts for the amino carbene when compared to the ethoxy derivatives. It is important to note that for both complex **A4** and **B4**, two isomers were observed. Isomer *B* was found in a lower concentration than Isomer *A* in both cases. However, the concentration difference was much more pronounced for the thienyl derivative than the furyl derivative. Two isomers were also observed for amino dimanganese thienyl and furyl complexes.[24,25] Amino carbenes are known to occur in both *syn* and *anti* conformations (Figure 3.3).[20,22,26]

Resonance form I   *Resonance form II*
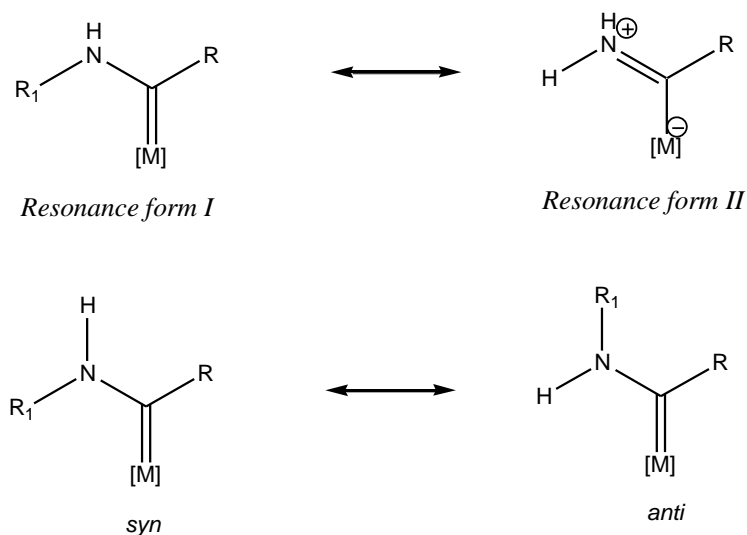
syn   *anti*

FIGURE 3.3: RESONANCE FORMS OF *SYN* AND *ANTI* CONFIGURATIONS OF THE AMINO CARBENE SUBSTITUENT

62

These isomers occur due to the restricted rotation about the N-C$_{carbene}$ bond, which has double bond character due to π-donation from the nitrogen atom to the carbene carbon (Figure 3.3). Also, the heteroaryl ring may have the heteroatom either facing to or away from the metal centre. There are hence four different isomers which are possible for **A4** and **B4** (Figure 3.4).

Conformer 1; *syn*   Conformer 2; *anti*

Conformer 3; *syn*   Conformer 4; *anti*
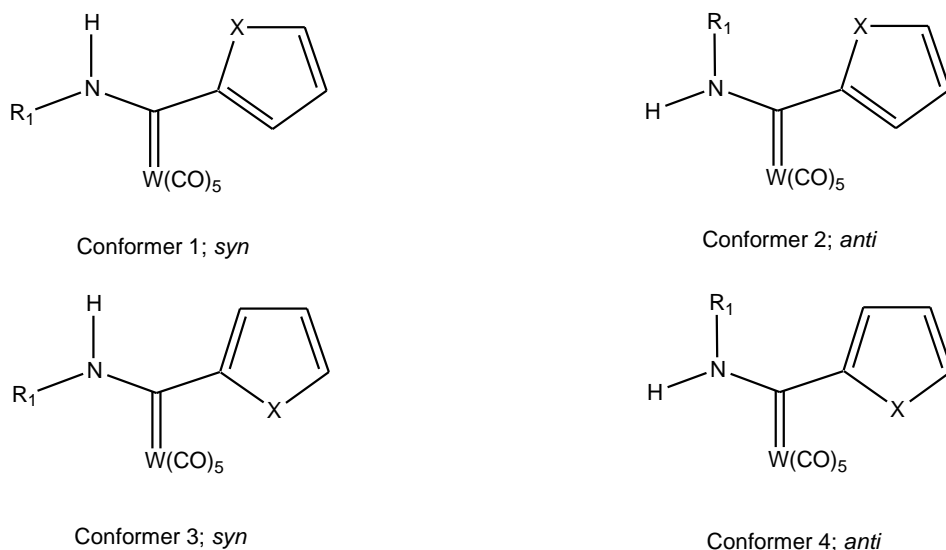
R$_1$ = Cyclohexyl

FIGURE 3.4: FOUR POSSIBLE ISOMERS FOR COMPLEXES A4 AND B4

It was noted by Streubel,[14] and Moser and Fischer[26] that the chemical resonance observed for the amino proton of *syn* amino carbenes is lower than in *anti* amino carbenes. The downfield shift observed for the *anti* amino proton is due to deshielding of the proton by the metal centre. Comparison of the chemical shifts of N-H and CHexyl-H$_1$ found for isomers *A* and *B* of **A4** indicates that isomer *A* has a *syn* amino conformation, while isomer *B* has the *anti* amino conformation. The chemical resonance observed for H3 of **A4** is shifted more upfield in isomer *B* than in isomer *A,* which indicates two different conformations for the heteroaryl ring. H1 would be shifted most downfield when closest to the metal centre. This leads to the conclusion that isomer *A* of **A4** has a conformation similar to conformer 1 in figure 3.4, isomer *B* of **A4** has the same conformation as conformer 4. The crystal structure found for complex **A4** is also the major isomer in solution, i.e. conformer 1. Similar reasoning did not hold for the furyl derivative, **B4.** The preferred conformation could not be deduced from the ^{1}H NMR data. However, it is clear that different conformations are preferred for complex **A4** than complex **B4.** However, since only a single isomer, corresponding to conformer 1 (Figure 3.4) was observed in the crystal structures of both derivatives (**A4** and **B4**), it is suggested that this phenomenon occurs mainly in solution. Furthermore, the characterisation and identification of both complexes can be still be achieved, and thus the isomerisation was not problematic. Determination of

the various effects and the reasons for the isomers, as well as the differences in the trends observed for the thienyl and furyl derivatives is a study by itself and will not be discussed here.
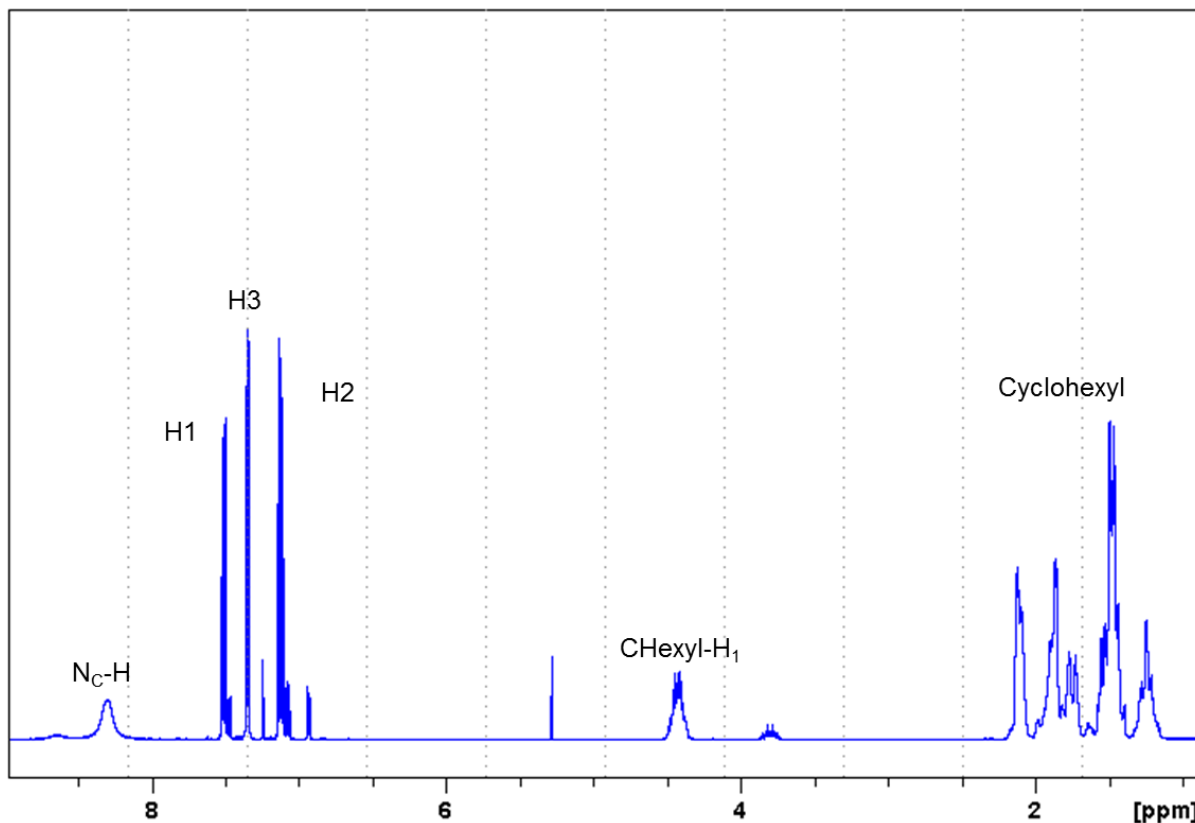
FIGURE 3.5: ^{1}H NMR SPECTRUM OF COMPLEX A4 (ASSIGNMENTS FOR ISOMER *A* SHOWN)

The phosphine derivatives (**A5**, **A6**, **B5** and **B6**) of the amino carbenes showed similar trends to the ethoxy analogues discussed in chapter 2. The same arguments used for the changes observed in the ethoxy carbenes apply to the amino carbenes, and will thus not be discussed again.
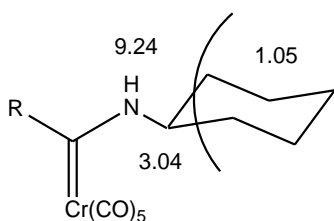
FIGURE 3.6: SELECTED ^{1}H NMR DATA FOR CYCLOHEXYLAMINO CHROMIUM PENTACARBONYL CARBENE (δ, PPM) [22]

64

When compared with a cylcohexylamino chromium carbene synthesised by Connor *et.al.*[22] (Figure 3.6), a similar trend in the proton chemical shifts is observed as for the complexes in this study. The shifts are, however, more upfield in the complex synthesised by Connor *et.al.*, than those summarised in tables 3.1 and 3.2. The difference is most likely due to different R groups present on the carbene, as well as the different metals, Cr *vs.* W.
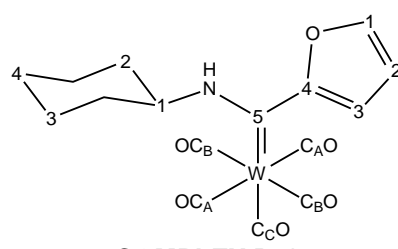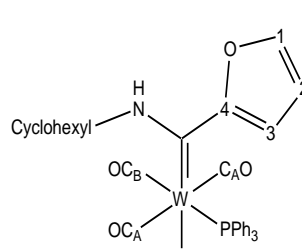
^{13}C NMR Spectroscopy

^{13}C NMR data for complexes **A4**-**A6** and **B4**-**B5** is summarised in tables 3.3 and 3.4. Complex **B6** was not included in the tables due to the poor quality of the spectra, because of the presence of both the *fac* and the *mer* isomers.

TABLE 3.3: ^{13}C NMR DATA FOR CYCLOHEXYLAMINO THIENYL TUNGSTEN(0) DERIVATIVES

COMPLEX A4 / COMPLEX A4* / COMPLEX A5 / COMPLEX A6

CARBON	COMPLEX A4* ISOMER A δ (ppm)	J (Hz)	ISOMER B δ (ppm)	J (Hz)	COMPLEX A5 δ (ppm)	J (Hz)	COMPLEX A6 δ (ppm)	
C1	129.5 (s)		127.8 (s)		128.2 (s)		126.5	(s)
C2	126.9 (s)		127.3 (s)		127.3 (s)		113.7	(s)
C3	128.1 (s)		124.2 (s)		127.6 (s)		121.0	(s)
C4	157.0 (s)		150.2 (s)		159.0 (s)		159.5	(s)
C5	235.0 (t)	90.8[#]	245.7 (t)	90.8[#]	245.2 (d)	6.9	n.o.	
NC1	64.9 (s)		59.5 (s)		64.0 (s)		58.7	(s)
NC2	33.0 (s)		33.3 (s)		33.5 (s)		32.0	(s)
NC3	24.9 (s)		24.7 (s)		25.1 (s)		25.3	(s)
NC4	24.4 (s)		24.2 (s)		25.7 (s)		24.4	(s)
P_BC_1					137.0 (d)	36.4	136.8 (39.2 Hz)[#]	(d)
P_CC_1							140.1 (34.7 Hz)[#]	(d)
P_BC_2					134.1 (d)	11.8	132.1	(s)
P_CC_2							132.2	(s)
P_BC_3					128.9 (d)	9.3	128.7	(s)
P_CC_3							128.8	(s)
P_BC_4					130.6 (s)		130.6	(s, b)
P_CC_4							130.6	(s, b)
C_AO	198.2 (t)	127.0[#]	198.7 (t)	127.8[#]	204.6 (d)	6.8	208.7	(s)
C_BO	198.2 (t)	127.0[#]	198.7 (t)	127.8[#]	208.2 (d)	25.6	216.9	(s)
C_CO	202.8 (t)	127.1[#]	203.5 (s)		210.6 (d)	5.4		

= J(W-C)   Solvents used: * = CDCl$_3$; All other spectra recorded in CD$_2$Cl$_2$

TABLE 3.4: ^{13}C NMR DATA FOR CYCLOHEXYLAMINO FURYL TUNGSTEN(0) DERIVATIVES

COMPLEX B4*

COMPLEX B5

CARBON	ISOMER *A*		ISOMER *B*		COMPLEX B5	
	δ (ppm)	J (Hz)	δ (ppm)	J (Hz)	δ (ppm)	J (Hz)
C1	144.1 (s)		145.8 (s)		145.0 (s)	
C2	113.7 (s)		113.3 (s)		113.4 (s)	
C3	126.3 (s)		126.4 (s)		123.8 (s)	
C4	159.1 (s)		157.6 (s)		160.6 (d)	1.8
C5	219.3 (s)		225.7 (s)		228.8 (d)	7.8
NC1	64.3 (s)		61.1 (s)		63.4 (s)	
NC2	33.1 (s)		33.2 (s)		33.5 (s)	
NC3	24.5 (s)		24.3 (s)		25.0 (s)	
NC4	25.3 (s)		25.3 (s)		25.6 (s)	
PC$_1$					136.5 (d)	36.3
PC$_2$					134.0 (d)	11.7
PC$_3$					128.7 (d)	8.9
PC$_4$					130.3 (d)	1.6
C$_A$O	198.4 (t)	126.9#	199.1 (t)	122.2#	204.9 (d)	6.9
C$_B$O	198.4 (t)	126.9#	199.1 (t)	122.2#	208.4 (d)	26.5
C$_C$O	202.4 (s)		202.8 (s)		210.1 (d)	5.6

*# = J(W-C)   Solvents used: * = CDCl$_3$; All other spectra recorded in CD$_2$Cl$_2$*

The ^{13}C NMR spectra show similar trends to those found for the ^{1}H NMR spectra, when the cyclohexylamino carbenes are compared to the ethoxy carbenes. The thienyl and furyl heteroaryl rings had more upfield carbon resonances in the amino carbene complexes than in the ethoxy carbenes. This once again correlates with less electron density being donated from the heteroaryl ring to the carbene centre. The most notable change is the large upfield shift (50 – 60ppm) for the carbene carbon resonance, C5. This indicates the increased backbonding from the amine to the carbene when compared to the ethoxy group. Similar decreases were noted in literature when ethoxy substituents were replaced with amines.[22,23] As explained above for the ^{1}H NMR, increased π-donation from the amino group when compared to the ethoxy group, decreases π-contribution needed from the heteroaryl ring, resulting in the upfield shift of the carbene carbon resonance.
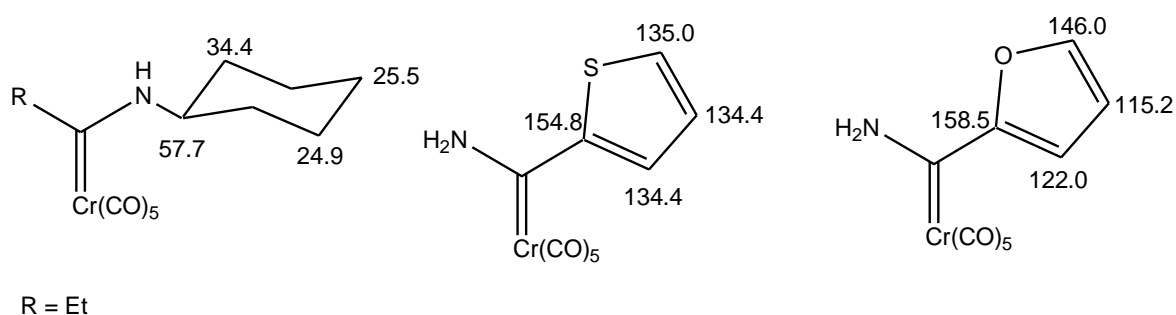
FIGURE 3.7: SELECTED ^{13}C NMR DATA FOR REPRESENTATIVE CHROMIUM CARBENE COMPLEXES (δ, PPM)[22]

The carbon spectra of complexes **A4** and **B4**, as for the proton spectra, indicated that two isomers were present in the solution. The carbon chemical shifts observed for the cyclohexyl ring and the heteroaryl rings once again follow a similar trend to that observed in literature (Figure 3.7).[22] It is interesting to note that the change from an ethoxy carbene to an amino carbene is not reflected in the carbonyl shifts of the complexes in this study. However, other aromatic tungsten carbenes also do not show a significant difference in the carbonyl shifts when the ethoxy group is substituted for an amino substituent.[14,27] It has been suggested by Connor *et.al.* that the larger orbitals found on tungsten do not distribute modifications of the ligand sphere to the carbonyl groups as efficiently as in the chromium analogues.[22] However, striking similarities are found for the carbonyl chemical shifts of amino carbenes found in literature (Figure 3.8), and those summarised in tables 3.3 and 3.4. The carbene chemical shifts ranged from 218 ppm to 246 ppm. These shifts are lower than those observed in literature (Figure 3.8).[11,14]
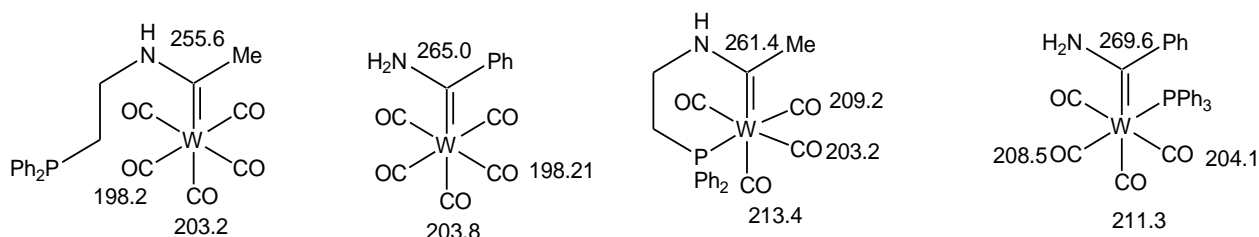
FIGURE 3.8: SELECTED ^{13}C NMR DATA FOR REPRESENTATIVE TUNGSTEN CARBENE COMPLEXES (δ, PPM)[11,14]

Changes for the amino carbene complexes when carbonyl groups were substituted for phosphines were similar to those found for the ethoxy carbene complexes in chapter 2. The carbonyl resonances observed for complexes **A5** and **B5** furthermore indicated that the *cis* isomer formed for both the furyl and thienyl complexes. This is obvious from the presence of three distinct carbonyl chemical shifts and the values of the coupling constants. A complete discussion on the use of carbon resonances to distinguish between *cis* and *trans* isomers, and importance of the coupling constants, was given in chapter 2. The significance of the *cis* isomer forming is obvious when one compares the methods used to synthesise the thienyl and furyl compounds. The thienyl derivative (**A5**) was prepared by substitution of a carbonyl group on the amino carbene complex (**A4**) while the furyl derivative (**B5**) was prepared by aminolysis of the furyl ethoxy phosphine complex. This corresponds well with literature where it was found that only the *cis* isomer is formed for photochemical addition of phosphines to amino carbene complexes.[19]

69
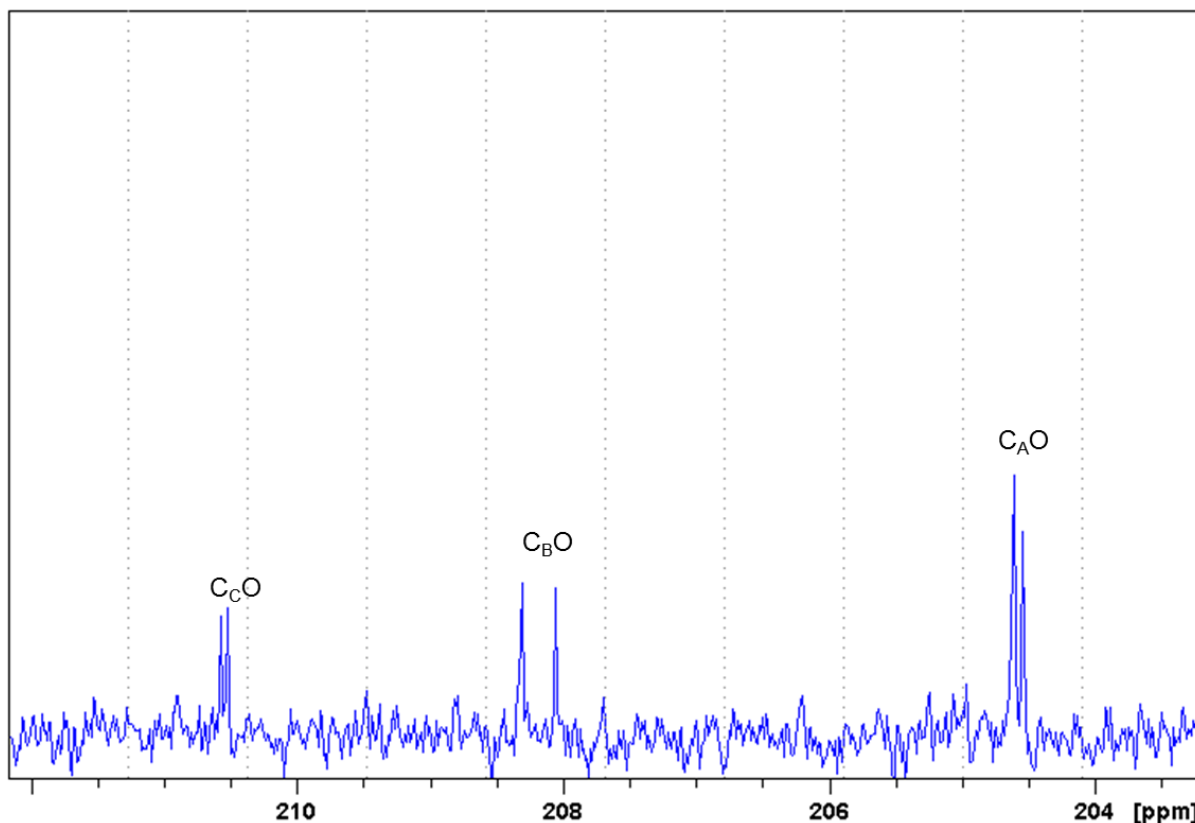
FIGURE 3.9: CARBONYL REGION OF ^{13}C NMR SPECTRUM FOR COMPLEX A5

^{31}P NMR Spectroscopy

^{31}P NMR data for complexes **A4**-**A6** and **B4**-**B6** is summarised in table 3.5. Corresponding ligand data is summarised in table 2.7.

TABLE 3.5: ^{31}P NMR DATA			
Complex	**δ (ppm)**	**J (P-W) (Hz)**	**J (P-P) (Hz)**
A5	24.3	233.0	
B5	24.1	231.7	
A6 P$_B$	45.5	n.o	11.7
A6 P$_C$	40.1	n.o	11.6
B6 P$_B$	46.3	222.9	13.6
B6 P$_C$	39.0	n.o.	13.4

All spectra recorded in CD$_2$Cl$_2$
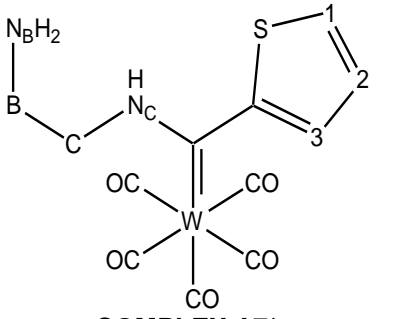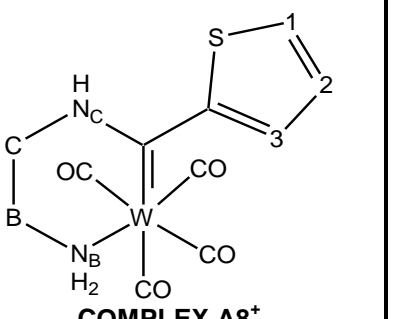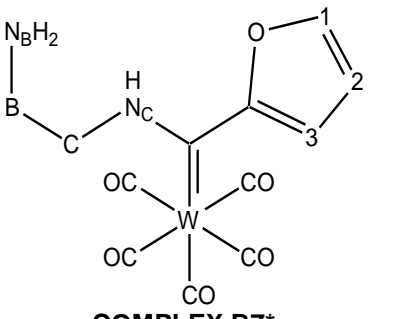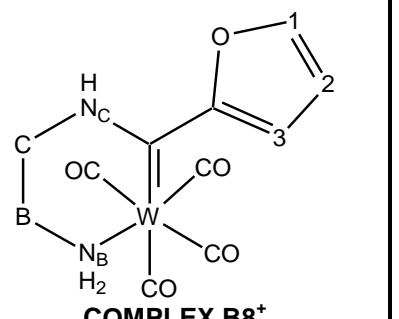
^{31}P NMR data for the corresponding ethoxy carbene complexes is found in table 2.8. For both the furyl and thienyl complexes, the phosphorous peaks are shifted approximately 1 ppm upfield for the

amino carbene complexes when compared to the ethoxy carbene complexes. This doesn't follow the expected trend seen in literature for similar aryl amino carbenes.[14] A downfield shift of approximately 0.6 ppm was observed by Streubel *et.al.*[14] for the phosphorous resonance when the ethoxy group was substituted for NH_2. However, it has been suggested by Schenk and Buchner[28] that if a carbonyl is substituted by a phosphine in a *cis* complex, an upfield shift for the phosphorous resonance is observed. This upfield shift in the phosphorous resonance increases with an increase in the size of the new ligand. Since cyclohexylamine is a much larger amine than NH_2 used by Streubel et.al, it is suggested that the large upfield shift seen for the complexes discussed here, is due to the steric bulkiness of the cyclohexylamine group. No significant variations were observed between the ethoxy and amino carbenes for the ^1J(W-P) couplings. However, since the group *trans* to the phosphorous atom does not alter for the ethoxy- and amino carbene complexes, the ^1J(W-P) couplings are not expected to change.[28]

3.4.2 NMR Characterisation for ethylenediamino tungsten(0) complexes

^{1}H- and ^{13}C NMR data for complexes **A7**-**A8** and **B7**-**B8** are summarised in tables 3.6 and 3.7, respectively. Assignments of heteroaryl proton chemical shifts were made by comp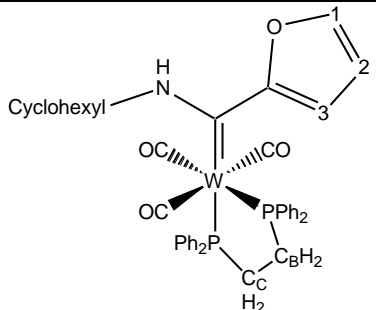arison with ethoxy carbene complexes discussed in chapter 2. All solvents used are indicated below the corresponding table.
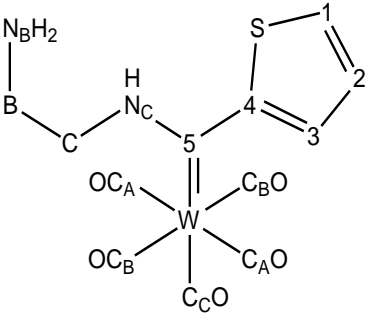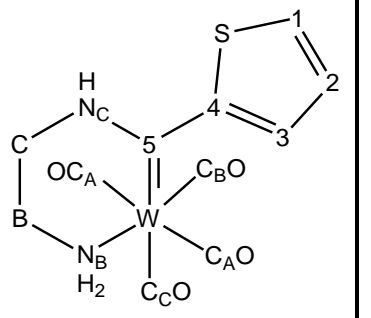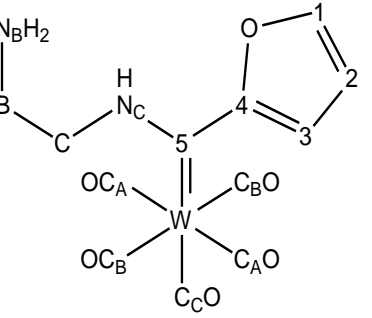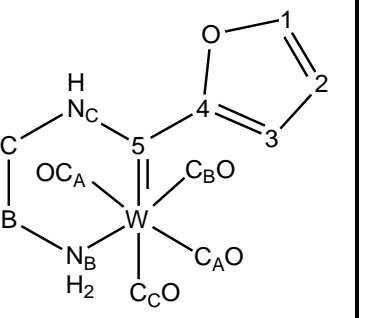
	TABLE 3.6: ^{1}H NMR DATA FOR ETHYLENEDIAMINO TUNGSTEN(0) DERIVATIVES							
PROTON	COMPLEX A7*			COMPLEX A8$^+$			COMPLEX B7*	COMPLEX B8$^+$	
	δ (ppm)		J (Hz)	δ (ppm)		J (Hz)	δ (ppm)	δ (ppm)	J (Hz)
H1	7.52	(dd)	1.2 5.1	7.69	(dd)	1.19 5.08	7.38 (s)	7.66 (dd)	0.5 1.8
H2	7.12	(dd)	3.8 5.1	7.18	(dd)	3.81 5.07	6.56 (s)	6.60 (dd)	1.8 3.6
H3	7.43	(dd)	1.2 3.8	7.49	(dd)	1.16 3.82	7.54 (s)	7.52 (dd)	0.6 3.6
N_B-**CH$_2$**	3.14 - 3.16	(m)		2.66 – 2.76	(m)		3.15 (m)	3.61 – 3.67 (m)	
N_C-**CH$_2$**	3.94 - 3.98	(m)		3.58 – 3.65	(m)		3.95 (m)	2.66 – 2.73 (m)	
N_B-**H$_2$**	1.72	(s, b)		3.39	(s, b)		1.70 (s, b)	3.36 (s,b)	
N_C-**H**	9.52	(s, b)		9.68	(s, b)		9.89 (s, b)	9.93 (s, b)	

= J(W-C)   Solvents used: * = CDCl$_3$; $^+$ = CD$_3$CN; All other spectra recorded in CD$_2$Cl$_2$

72

	COMPLEX A7* δ (ppm)	COMPLEX A8+ δ (ppm)	COMPLEX B7* δ (ppm)	COMPLEX B8+ δ (ppm)
TABLE 3.7: ^{13}C NMR DATA FOR ETHYLENEDIAMINO TUNGSTEN(0) DERIVATIVES				
CARBON				
C1	130.0	132.7	144.4	145.9
C2	127.4	126.7	113.6	114.4
C3	128.1	128.9	125.7	125.8
C4	157.0	156.1	159.6	n.o.
C5	237.6	246.9	223.2	235.4
N_C**C**	55.9	52.3	55.8	52.1
N_B**C**	40.23	40.8	40.6	41.2
C_A**O**	198.5 (127.3 Hz)[#]	205.8	198.6 (126.0Hz)[#]	206.0
C_B**O**	198.5 (127.3 Hz)[#]	213.3	198.6 (126.0Hz)[#]	214.0
C_C**O**	202.7	216.0	202.3	215.8

= J(W-C)   Solvents used: * = CDCl₃; + = CD₃CN; All other spectra recorded in CD₂Cl₂

The ^{1}H- and ^{13}C NMR spectra recorded confirm the proposed structures for the ethylenediamine carbene complexes. As can be seen from figure 3.10 below, similar trends and resonances were observed by Moretó *et.al.*[17]

^{1}H NMR Data ^{13}C NMR Data
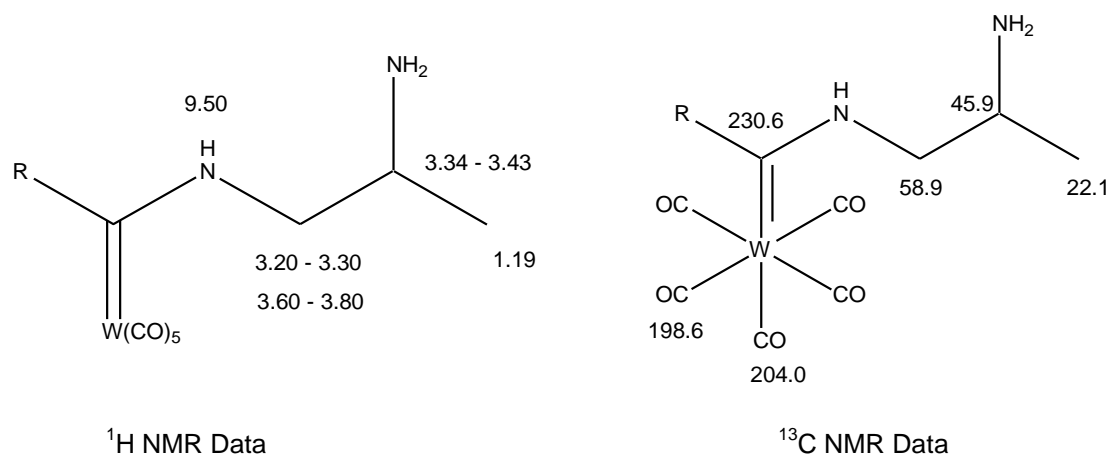
FIGURE 3.10: SELECTED NMR DATA FOR LITERATURE COMPLEXES AS DESCRIBED BY MORETÓ *ET.AL.*[17] (δ, PPM)

Both the ^{13}C spectra of the thienyl and furyl complexes also showed an alteration of the order of the heteroaryl ring resonances. This correlates with the trend found for the cylcohexylamine thienyl complexes (**A4** and **A5**) discussed previously.
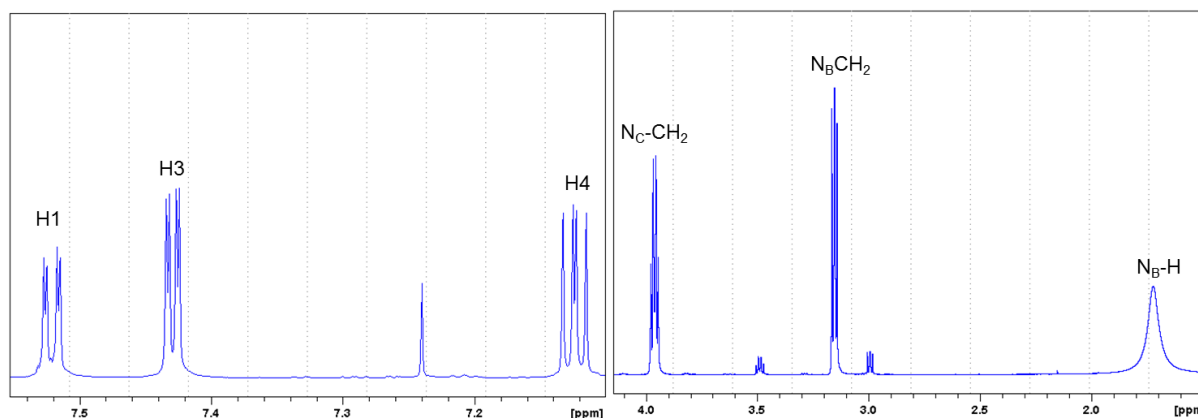
FIGURE 3.11: SELECTED ^{1}H NMR SPECTRA FOR COMPLEX A7

Complexes **A8** and **B8** both show a large downfield shift for N_BH_2. This indicates deshielding of the protons due to coordination of N_B to the metal, as would be expected. Furthermore, the chemical

74

resonances noted for the ^{13}C NMR data of the heteroaryl ring components of complexes **A8** and **B8** were shifted downfield when compared to **A7** and **B7**.This could indicate increased electron donation from the heteroaryl carbene substituent to the carbene centre, however it is more likely that the changes were due to solvent shifts. If the ^{13}C NMR of **A7** and **A8** (Figure 3.12) are compared, one can clearly observe the changes that occur in the molecule when chelation occurs. Firstly, three carbonyl peaks are observed for complexes **A8** and **B8**, as one would expect for three non-equivalent carbonyl groups. The carbon resonance peaks associated with the carbonyl groups are further downfield in complex **A8** than in complex **A7**. The chemical shifts associated with carbonyl groups are greater for the carbonyl group *trans* to the ligand and increase as follows: phosphine < amine < carbene. **A8** and **B8** clearly indicate that this trend was followed since the resonance peak associated with C_BO, which is *trans* to the amine, is only 3 ppm upfield from that of C_CO, which is *trans* to the carbene. Lastly, the ^{13}C resonance peak for the carbene carbon, C5, is shifted downfield when complex **A8** is compared to complex **A7**. This suggests that the carbene more deshielded in **A8** than in **A7**. A similar trend was noted in literature for phosphine chelate carbenes (Figure 3.8).[11]
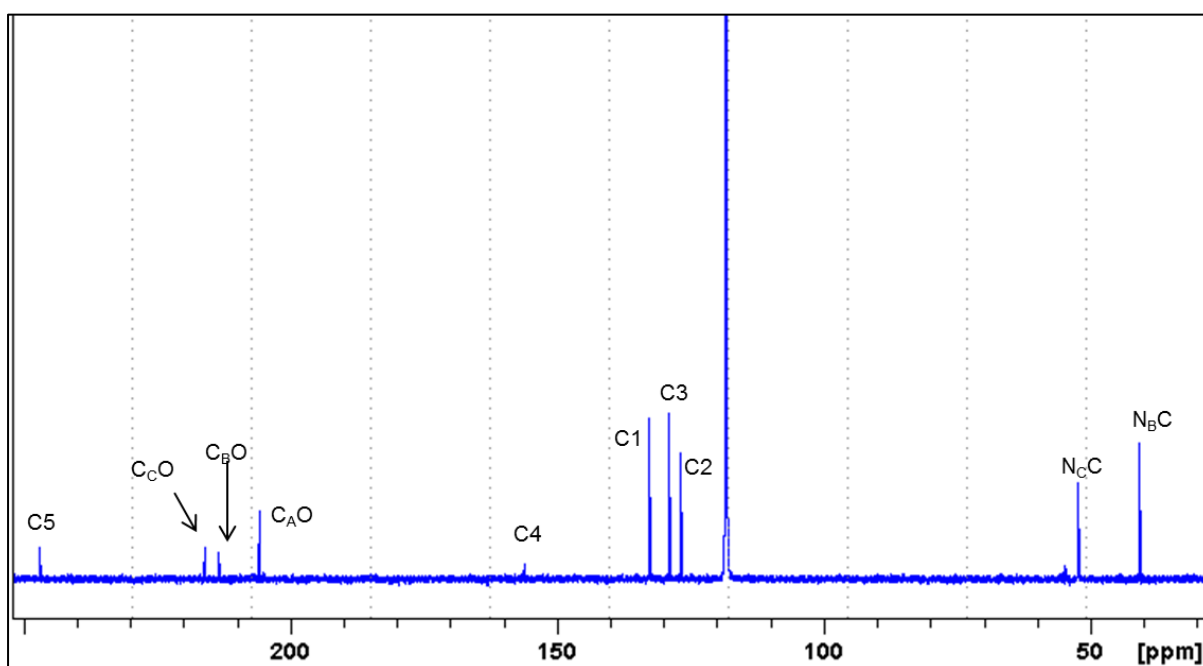
FIGURE 3.12: ^{13}C NMR SPECTRUM FOR COMPLEX **A8**

3.5 IR SPECTROSCOPY

TABLE 3.8: IR STRETCHING FREQUENCIES FOR TUNGSTEN COMPLEXES (cm^{-1})			
Pentacarbonyls			
A4	2061 (A_1^1)	1972 (B_1)	1950 (A_1^2)	1906 (E)
B4	2059 (A_1^1)	1966 (B_1)	1908 (A_1^2)	1882 (E)
A7	2059(A_1^1)	1916 (A_1^2,B_1 and E)		
B7	2058(A_1^1)	1972(B_1)	1910(A_1^2)	1892(E)
Tetracarbonyls			
A5	2002 (A_1^1)	1894 (A_1^2)	1870 (B_1)	1860 (B_2)
B5	2001 (A_1^1)	1875 (A_1^2, B_1 and B_2)		
A8	2008 (A_1^1)	1943 (A_1^2)	1906 (B_1)	1858 (B_2)
B8	2006 (A_1^1)	1934 (A_1^2)	1904 (B_1)	1862 (B_2)
Tricarbonyls			
A6	1916 (A_1^1)	1829 (A_1^2 and B_1)		
B6	1914 (A_1^1)	1821 (A_1^2 and B_1)		

All spectra recorded in KBr

Assignments of the IR active bands were made with the assistance of theoretical calculations for the vibrational spectra of the complexes found in table 3.8. Comparison of the symmetrical stretching frequency A_1^1 will be used for comparison of the complexes.[29] If the complexes **A4** to **A6** and **B4** to **B6** are compared, a decrease in the wavenumber of A_1^1 is observed as the number of phosphine ligands increases. This clearly is a sign of increased π-metal backbonding between the metal centre and the carbonyl groups. Phosphines are weaker π-acceptors than carbonyls and thus are less able to benefit from π-donation from the metal than carbonyl groups. Increasing the number of phosphine ligands, will thus increase π-donation to the carbonyl groups and decrease the wavenumber as observed. Amines are only σ-donors and not π-acceptors, and will also increase π-donation from the metal centre to carbonyl groups, thereby resulting in a decrease in wavenumber. Comparison of complex **A7** and **B7** with the corresponding amino chelates, **A8** and **B8**, indicate the expected decrease in wavenumber for the A_1^1 stretching frequency (table 3.8).

76

3.6 XRD: CRYSTAL STRUCTURE ANALYSIS

A4

B4

A5

B8
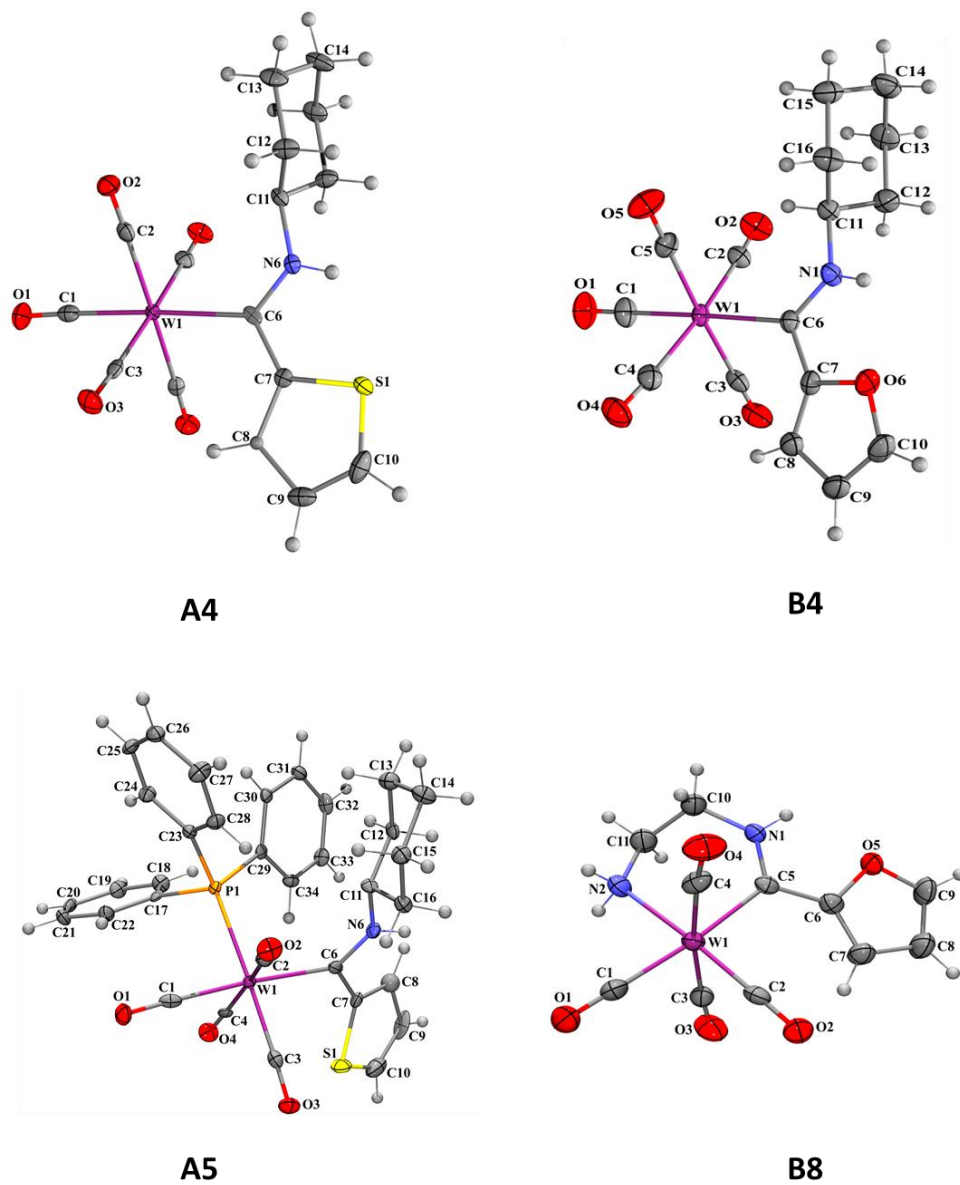
FIGURE 3.13: ORTEP PLOTS FOR COMPLEXES A4, A5, B4, AND B8

TABLE 3.9: SELECTED DATA FOR THE CRYSTAL STRUCTURES OF COMPLEXES A4, A5, B4 AND B8				
R=Cyclohexyl				
	Complex A4	**Complex B4**	**Complex A5**	**Complex B8**
Bond Length (Å)				
W-C5	2.269	2.251	2.246	2.231
W-C$_C$O	2.006	2.000	1.986	2.027
W-C$_A$O	2.048	2.040	2.025	2.031
W-C$_B$O	2.048	2.040	1.990	1.939
C5-C4	1.473	1.467	1.493	1.453
C4-C3	1.411	1.350	1.373	1.345
C3-C2	1.452	1.424	1.545	1.415
C2-C1	1.335	1.335	1.340	1.340
C1-S or O	1.478	1.362	1.596	1.352
C4-S or O	1.427	1.392	1.701	1.389
C5-N$_c$	1.330	1.320	1.315	1.316
C$_B$-N$_B$				1.461
C$_C$-N$_C$				1.480
W-N$_B$ or P			2.558	2.305
Torsion angles (°)				
W-C5-C4-N$_C$	180.0	178.2	-179.9	176.5
W-C5-C4-C3	0.0	12.88	-30.22	13.5

The crystal structures all have octahedral geometries with distortions due to the presence of the sterically demanding carbene substituents. Complexes **A4** and **A5** showed variation in the orientation of the heteroaryl ring. The sulphur group could either face to or away from the metal in a ratio of approximately 1:1. This is not uncommon and thienyl rings are known to alter their orientation with respect to the metal centre.[30] **B8** has a six-membered chelate ring formed by the metal, carbene carbon and the ethylenediamine chelate. Six-membered rings generally take on a chair conformation; however, when a double bond is present this is not possible.[31] The ring will then take on the chair conformation as far as possible resulting in puckering. Puckering of this nature was observed in complex **B8** for the N2-C11-C10-N1-C5 portion of the structure (Figure 3.13).

In general, it was noted that the W-C5 bond is much longer than the W-CO bonds for the carbonyl groups. This indicates that the carbene bond has less double bond character than the W-CO bonds. Variations can also be seen among the lengths of the carbonyl groups. In metal pentacarbonyl

78

complexes **A4** and **B4**, the carbonyl groups *trans* to the carbene is shorter than the *cis* carbonyl ligands. This indicates that the carbene is a weaker π-acceptor ligand than the carbonyl group and thus allows for more π-donation from the metal to the *trans* carbonyl groups. In complex **A5** the W-C_BO and W-C_CO bond lengths are approximately the same length, but shorter than W-C_AO. This suggests that the carbene and the phosphine ligands have similar π-acceptor qualities, but are weaker π-acceptors than carbonyl groups. It is interesting to note however, that in complex **B8** the bond lengths of W-C_AO and W-C_CO are much closer than in complex **A4** and **B4**. The W-C_BO bond is much shorter than the bond length of either of the other carbonyl groups. Amines are mostly σ-donors and do not have π-metal interaction.[32] Therefore the carbonyl group *trans* to the carbene will have the largest amount of π-metal donation and the shortest bond length as observed. The W-P bond length in complex **A5** is 2.558 Å, while in $W(CO)_5PPh_3$ the W-P bond length is 2.545 Å, which suggests that either less electron density is available for π-donation to the phosphine or an increase in steric ligands results in a slight increase in this bond length for **A5**.[33] If one considers the various C-N bonds, it can be clearly seen that the $C_{carbene}$-N bonds are much shorter than the C-N bonds of the chelate backbone in complex **B8**. The reduced C-N bond length for the $C_{carbene}$-N bond shows increased bond order between this carbon and nitrogen. Lastly, if one compares the bond lengths of the heteroaryl substituents, distortion of the heteroaryl ring due to electron donation from the ring to the carbene can be seen. The effect is most pronounced in **A4**. From the data it can be seen that the formal single and double bonds do not exist anymore for some of the bonds and intermediate bond lengths are observed. In the uncoordinated form the heteroaryl rings are symmetrical.[34,35] The bond lengths that were affected are C_4-C_3, C_2-C_1, C_4-S/O, and C_1-S/O.

Torsion angles observed for the complexes varies somewhat. The thienyl complex (**A4**) is completely planar, indicating that the carbene ligand and the tungsten metal centre are perfectly orientated for electron delocalisation, as was supported by the bond lengths of the thienyl ring. Also, H-bonding between the N_c-H and the sulphur atom locks this bond in place. The other complexes, in contrast, both deviated from planarity, with the effect being slightly greater in complex **B8** than in complex **B4**, and most severe for complex **A5**. In the case of complexes **A5** and **B4** steric factors may play the greatest role in this disturbance. Generally, as seen for complexes **A4** and **B4**, the carbene substituent is staggered between the carbonyl groups, allowing for minimal steric interactions. However, due to chelation in complex **B8** the heteroaryl group of the carbene is forced into an eclipsed position relative to C_AO and C_BO, resulting in steric hindrance. Consequently the heteroaryl group is forced out of the carbene plane. In complex **A5** steric interactions between the large phenyl groups and the carbene substituents are most likely the cause of the distortions. A similar argument does not hold for complex **B4**, since there are no sterically demanding groups, and the complex is not locked in position, as is the case for complex **B8**. Packing interactions or electronic interactions are known to overcome the stabilization effect. π-Delocalisation is therefore suggested as the reason for the deviation from planarity.
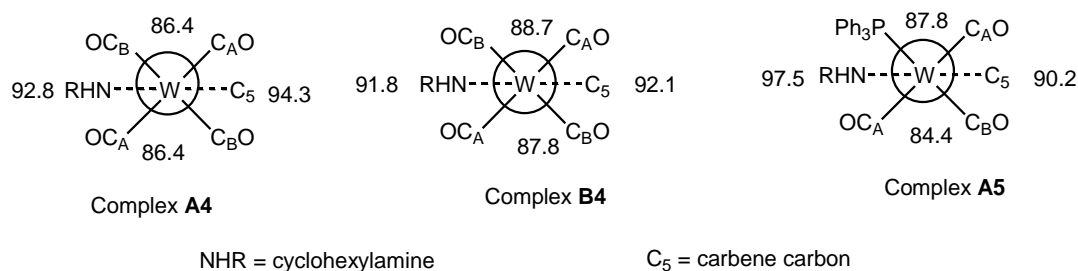
FIGURE 3.14: SELECTED BOND ANGLES (°) FOR COMPLEXES A4, B4, AND A5

Some deviations from the perfect octahedral structure were observed for the complexes. As shown in figure 3.14, the carbene ligands caused slight distortions from the optimal 90° angle for a perfect octahedron. This was seen by an increase in the bond angles in the equatorial plane for complexes **A4, A5** and **B4.** The ligands in the equatorial plane appeared to be forced apart to allow carbene substituents to nestle between the carbonyl groups. The largest deviation was observed in **A5**. Both the sterically demanding cyclohexylamino group and the phosphine ligand are located on the same side of the molecule, resulting in a 7.5° deviation from the perfect 90° octahedral geometry, to allow these groups enough space.

Complex **B8** also showed deviations from optimal octahedral geometry due to steric requirements. The C_5-W-N_B angle and the C_CO-W-C_BO angles were 95.2° and 97.5°, respectively. This clearly suggests that the steric requirements of the ethylenediamine carbene backbone and the furyl ring force the carbonyl groups away from the carbene ligand.

The W-C-O bonds of the carbonyl groups showed deviations from linearity in **A5** and **B8**. These deviations from linearity in the W-C-O bonds were most notable for the C_A-O carbonyl groups in both complexes. The W-C-O bond angles for W-C_A-O averaged 172.4° and 173.9° in **A5** and **B8**, respectively. The deviation of the W-C-O bond from 180° again shows the steric demand of the carbene ligand on these complexes.

80
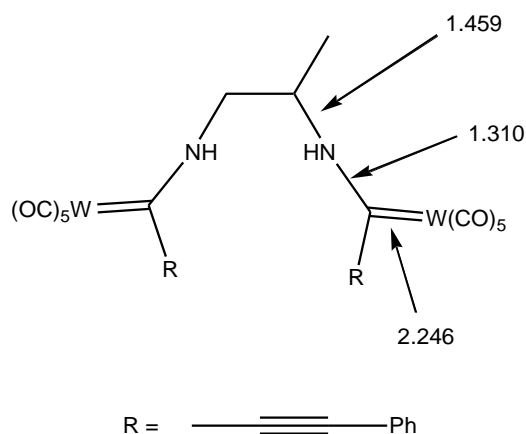
FIGURE 3.15: REPRESENTATIVE AMINO CARBENE WITH SELECTED BOND LENGTHS (Å) [17]

If the data found for complexes **A4**, **A5**, **B4** and **B8** are compared with that found in the diamino carbene complex in figure 3.15, many similarities can be seen. The bond lengths for key bonds are very similar with variations in the bond length only occurring in the second decimal. This indicates a good correlation between the literature example and the complexes discussed here.

3.7 THEORETICAL CALCULATIONS

The theoretical aspects of this chapter focused on determining the distribution of the HOMOs and LUMOs, and the corresponding gap between these two orbitals. Electrostatic potential maps were used along with the HOMO and LUMO diagrams to further explain experimental data. The size of the HOMO-LUMO gap is of importance since this energy difference can be related to the reactivity of the complexes. Once again the thienyl and furyl derivatives had similar distributions for the HOMOs and the LUMOs, thus only the orbitals of the thienyl derivatives are shown. Furthermore, calculations were done for the *trans* isomer of complex **A5**, thus allowing for comparisons. All calculations were done for the *mer* isomer of complex **A6**, since the sterically demanding complex would favour this arrangement and this would allow for continuity with chapter 2. **B7** could potentially be found in two different conformations (Figure 3.16).
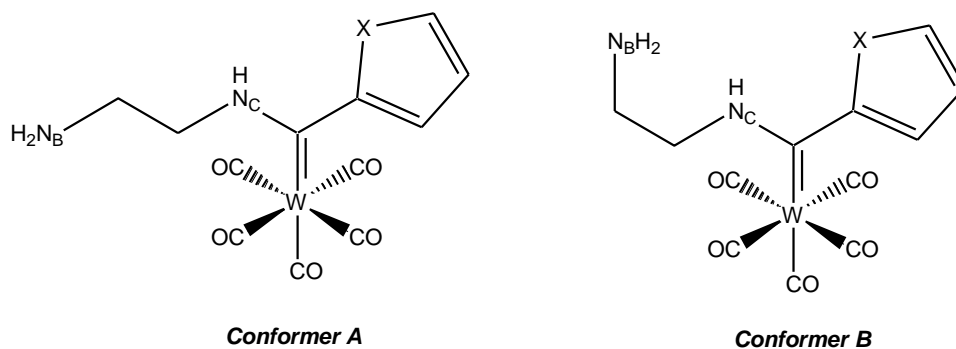
FIGURE 3.16: TWO POSSIBLE CONFORMERS OF A7 AND B7

Conformer *A* has the ethylenediamine carbene substituent orientated as a straight chain. Conformer *B,* in contrast, has the ethylenediamine substituent folded back towards the carbene centre, thus allowing for H-bonding between the hydrogen atom on N_C and N_B. Conformer *B* was 20.4 kJ/mol lower in energy than conformer *A* and consequently the preferred conformation for **A7** and **B7**. Both conformations are only shown further in this section when a significant difference was found in the theoretical properties of the two conformations.

The crystallographic structure of **B7** could not be determined uniquely. The crystals are possibly twinned and the space group could not be assigned beyond doubt. However, the best solution yielded a partial structure that was refined to an R-factor of approximately 13%, but included unresolved peaks in the difference map. The structure is included (Figure 3.17) for comparison of the structural backbone with experimental and theoretical data. It confirms that conformer *B* is the preferred conformation for the ethylenediamino substituent in solid state, as was suggested by theoretical calculations.
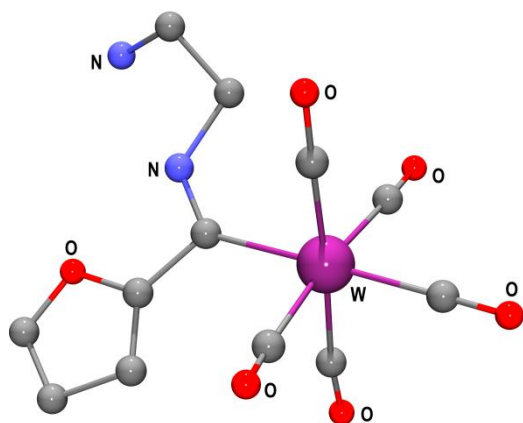
FIGURE 3.17: INCOMPLETELY REFINED CRYSTAL STRUCTURE OF COMPLEX **B7**

A4: E = -0.206 Hartrees   A5: E = -0.180 Hartrees   A5 *trans*: E = -0.177 Hartrees

A6: E = -0.168 Hartrees   A7: E = -0.203 Hartrees   A8: E = -0.178 Hartrees
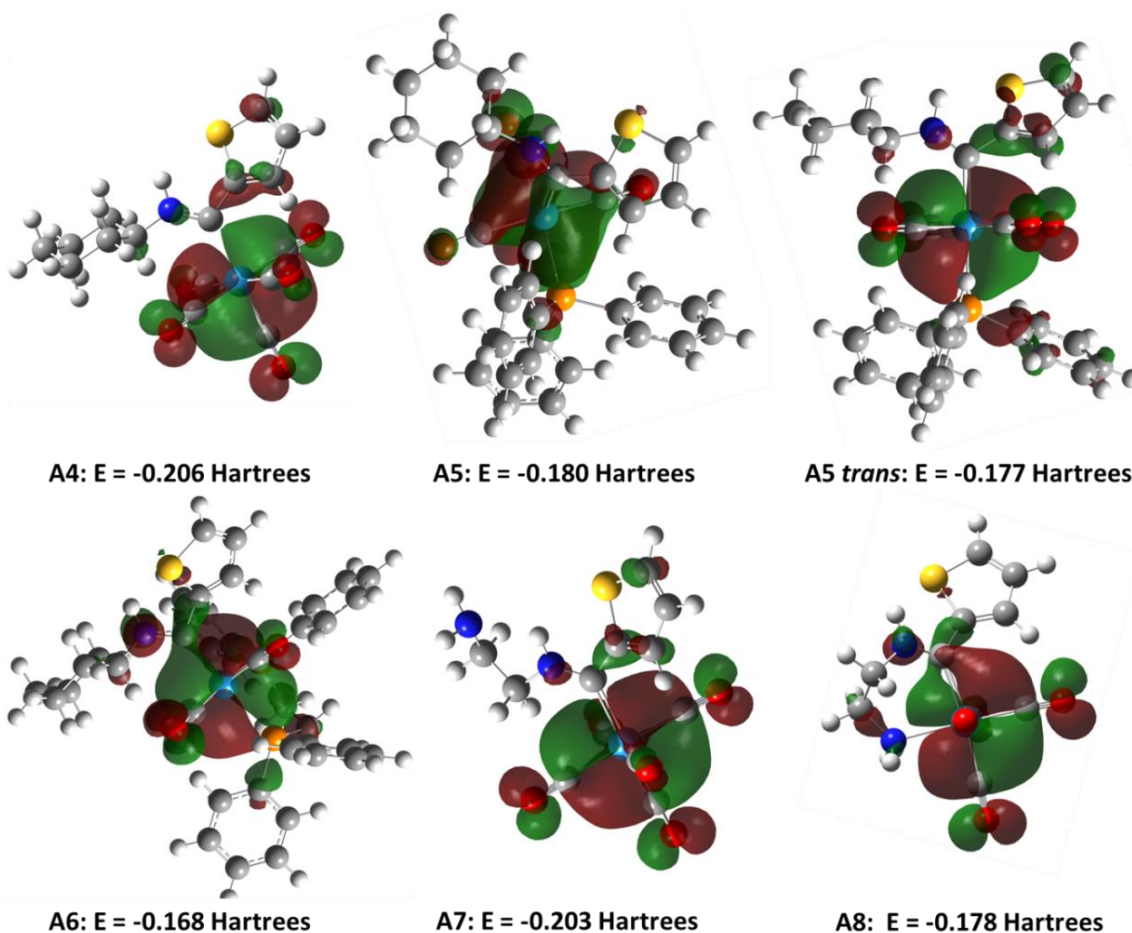
FIGURE 3.18: HOMO DIAGRAMS CALCULATED FOR OPTIMIZED COMPLEXES **A4-A8 (1** HARTREE = **2600 KJ/MOL)**

83
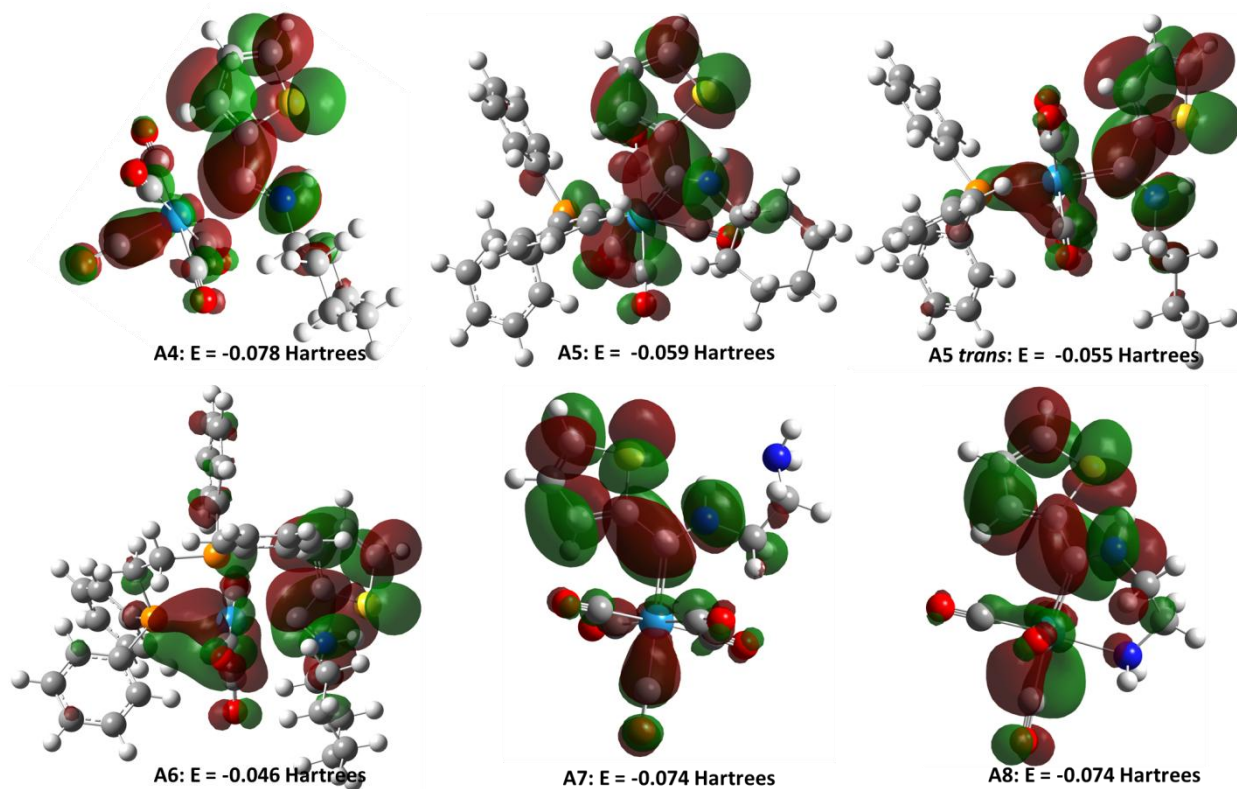
FIGURE 3.19: LUMO DIAGRAMS CALCULATED FOR OPTIMIZED COMPLEXES A4-A8 (1 HARTREE = 2600 KJ/MOL)

It is clear in figure 3.18 that the HOMO is centred on the metal in all cases. The greatest variation is found for **A8**, where the HOMO was not distributed evenly across the metal centre. Instead, the HOMO for **A8** was unsymmetrically distributed around the metal, excluding the chelate from the HOMO. The LUMO is generally located on the carbene ligand, and the metal-ligand bond *trans* to the carbene. More specifically, the LUMO is concentrated on the carbene carbon atom, heteroaryl ring and the nitrogen atoms of the carbene ligand. This suggests that electrophilic attack would occur on the metal centre, and nucleophilic attack, in contrast, would most likely be directed at the carbene. It is also interesting to note that the *trans* isomer of **A5** does not show a significant change in the location of either the HOMO or LUMO when compared to the *cis* isomer. Lastly, altering the ligand sphere does not appear to change the distribution of the HOMOs and LUMOs dramatically.

84

Complex **A4**

Complex **A6**

Complex **A5**

Complex **A5** *trans*

Electron Density
High   Low
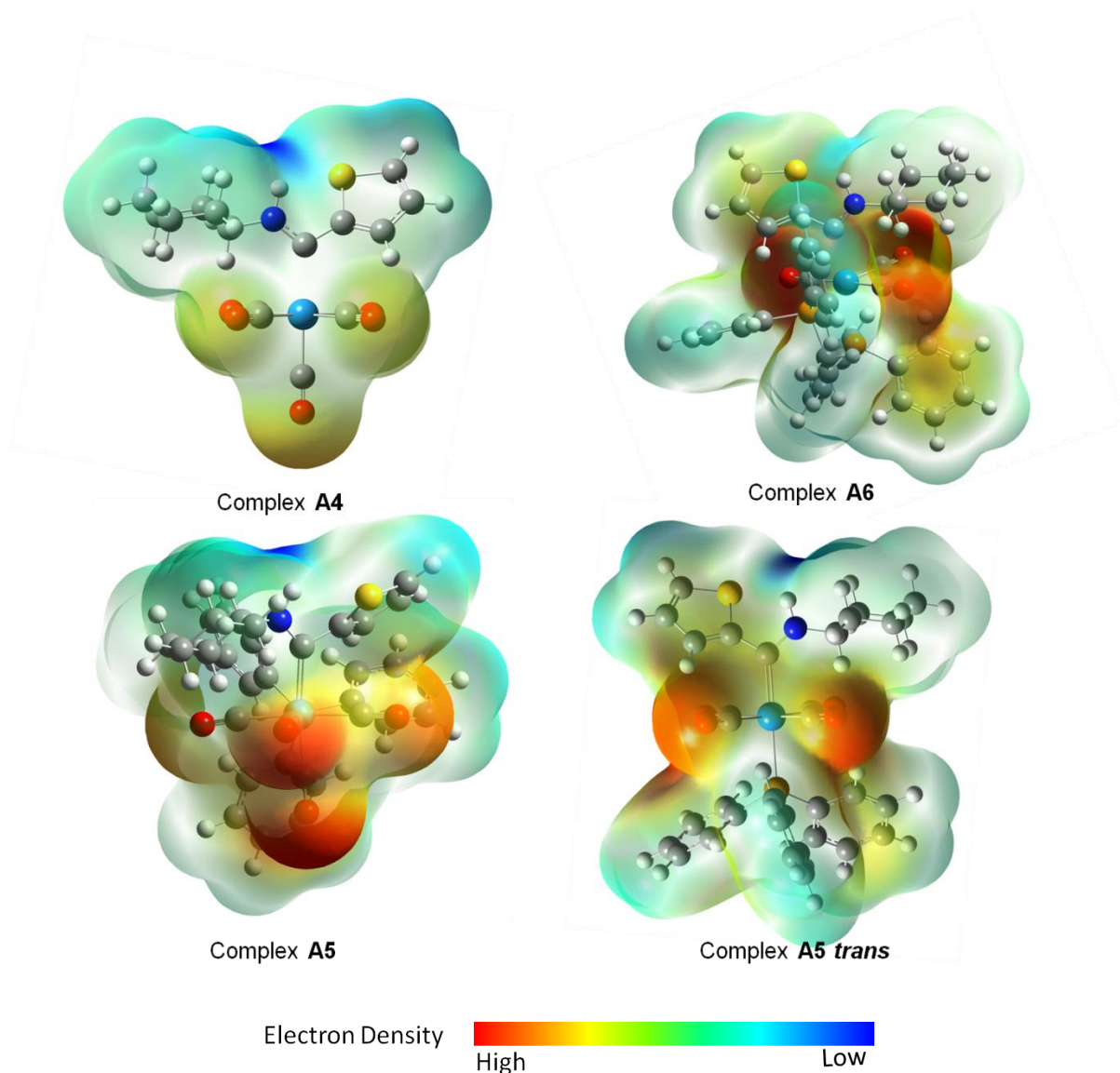
FIGURE 3.20: ESP MAPS CALCULATED FOR OPTIMIZED COMPLEXES A4-A6

The ESP maps calculated for complexes **A4**-**A6** are shown in figure 3.20. Calculations for the *trans* isomer of complex **A5** were once again included for comparative purposes. Complexes **A4**-**A6** have the highest distribution of electron density on the carbonyl groups. In contrast, the amino substituent found on the carbene ligand has the lowest concentration of electron density. For all the phosphine substituted complexes (**A5**, **A5** *trans* and **A6**), the carbonyl groups create pockets of electron density. The electron rich carbonyl groups in complex **A5** *trans* and **A6** are completely surrounded by the electron poor regions.

85
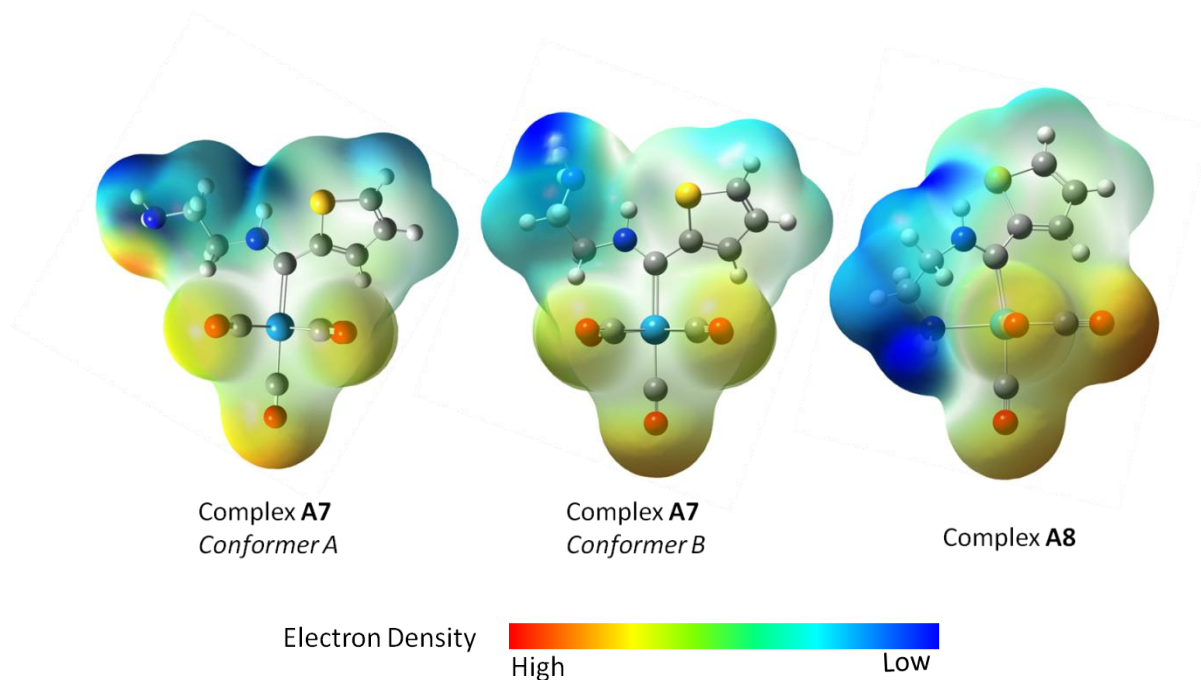
FIGURE 3.21: ESP MAPS CALCULATED FOR OPTIMIZED COMPLEX A7 AND A8

ESP maps once again indicated the difference between the two conformers proposed for complex **A7**; and between complex **A7** and **A8** (Figure 3.21). The electron density found for conformer *A* of **A7** shows the largest difference from conformer *B* on the free amine group of the ethylenediamine substituent (N_B). This clearly indicates a large difference in the electron distributions of the two conformers. For conformer *A,* a large amount of electron density is found on N_B while for conformer *B* very little electron density is found on N_B. **A8** also shows a large difference in electron density on N_B when compared to **A7**. The ESP maps clearly show that the lowest concentration of electron density is found on N_B when it is chelated to the tungsten(0) moiety. This indicates the electron withdrawing nature of the metal sphere, and corresponds well with assignments of the ^{1}H NMR shifts, which showed that proton chemical resonances associated with the amino groups moved downfield upon chelation.

If one considers the electron density of the heteroaryl ring in all the amino carbene complexes (Figures 3.20 and 3.21), it is clear that the electron density is lowest on C1. The electron density found for the heteroaryl ring substituents consequently confirms the order of the chemical shifts observed on ^{1}H NMR spectra.

TABLE 3.10: ENERGY DIFFERENCE BETWEEN HOMOS AND LUMOS	
COMPLEX	**ENERGY GAP (KJ / MOL)**
COMPLEX A4	336.1
COMPLEX A5	317.7
COMPLEX A5 *TRANS*	319.6
COMPLEX A6	302.1
COMPLEX A7	338.7
COMPLEX A8	272.8

The energy difference between the HOMOs and the LUMOs calculated for complexes **A4**-**A8** decreases as follows:

A7 > **A4** > **A5** *trans* > **A5** > **A6** > **A8**

These energy gaps are once again not significantly different between all cases but do allow for a tentative trend in reactivity to be suggested. This suggests that when phosphine complexes are considered, an increase in the number of phosphine ligands corresponds to a decrease in the HOMO-LUMO gap. Also, the amino chelate complex **A8** had the lowest HOMO-LUMO energy gap. However, this decrease in the energy gap does not necessarily correspond to an increase in reactivity of the complex, since neither the third carbonyl group nor the phosphine groups readily dissociates.[36] Therefore, reactivity may decrease. **A8** appears to be the most reactive complex, and is as a result most likely to be useful for catalytic reactions.

3.8 CONCLUSION

Synthesis and characterisation of complexes **A4**-**A8** and **B4**-**B8** could be achieved satisfactorily for most cases. These complexes clearly exhibited the unique properties that are associated with aminolysis of Fischer carbene complexes. ^{1}H-, ^{13}C- and ^{31}P NMR all confirmed that the proposed complexes were synthesised successfully. Further evidence confirming the proposed molecular structures was obtained with XRD characterisation of complexes **A4**, **A5**, **B4** and **B8**. Theoretical calculations suggested that the HOMOs were centred on the metal centre, while the LUMOs were located on the carbene ligand. The metal centre will thus be the preferred location for electrophilic attack, and the carbene ligand the preferred location for nucleophilic attack. ESP maps indicated that the highest concentration of electron density is always found on the carbonyl ligands. Lastly, complex **A8** is likely to be the most reactive complex, if one considers the HOMO-LUMO energy difference. It can thus be concluded that varying the metal-ligand sphere and the carbene substituents is handy for altering the characteristics of the tungsten Fischer carbene complexes, and may be used to tune reactivity patterns. Future work from these studies would include determination of the structure of **A7**. The effects which allow for multiple conformers of complex **A4** and **B4**, will also be studied. Lastly,

87

experimental data which allows for the comparison of complexes **A4**-**A8** and **B4**-**B8** is needed to confirm the expected reactivity trends, and is thus suggested for future studies.

3.9 REFERENCES

(1)   Dötz, K. H. *Angew. Chem. Int. Ed.* **1984**, *23*, 587.

(2)   Kotha, S.; Dipak, M. K. *Tetrahedron* **2012**, *68*, 397.

(3)   de Frémont, P.; Marion, N.; Nolan, S. P. *Coor. Chem. Rev.* **2009**, *253*, 862.

(4)   Dötz, K. H.; Tomuschat, P. *Chem. Soc. Rev.* **1999**, *28*, 187.

(5)   Andrada, D. M.; Jimenez-Halla, J. O. C.; Solà, M. *J. Org. Chem.* **2010**, *75*, 5821.

(6)   Heckl, B.; Werner, H.; Fischer, E. O. *Angew. Chem. Int. Edit* **1968**, *7*, 817.

(7)   Bernasconi, C. F.; Stronach, M. W. *J. Am. Chem. Soc.* **1993**, *115*, 1341.

(8)   Imwinkelried, R.; Hegedus, L. S. *Organometallics* **1988**, *7*, 702.

(9)   Fischer, E. O.; Winkler, E.; Kreiter, C. G.; Huttner, G.; Krieg, B. *Angew. Chem. Int. Edit* **1971**, *10*, 922.

(10)   Maiorana, S.; Seneci, P.; Rossi, T.; Bladoli, C.; Ciraco, M.; de Magistris, E.; Licandro, E.; Papagni, A.; Provera, S.; Baldoli, C.; Povera, S. *Tetrahedron Lett.* **1999**, *40*, 3635.

(11)   Fernandez, I.; Sierra, M. A.; Gomez-Gallego, M.; Mancheno, M. J.; Cossío, F. P. *Angew. Chem.* **2006**, *118*, 131.

(12)   Sabaté, R.; Schick, U.; Moreto, J. M.; Ricart, S. *Organometallics* **1996**, *15*, 3611.

(13)   Stumpf, R.; Burzlaff, N.; Weibert, B.; Fischer, H. *J. Organomet. Chem.* **2002**, *651*, 66.

(14)   Streubel, R.; Priemer, S.; Jones, P. G. *J. Organomet. Chem.* **2001**, *618*, 423.

(15)   Reinheimer, E. W.; Kantardjieff, K. A.; Ouyang, X.; Herron, S. R.; Lu, T.; Casalnuovo, J. A. *J. Chem. Crystallogr.* **2007**, *37*, 507.

(16)   Fischer, E. O.; Aumann, R. *Angew. Chem. Int. Edit* **1967**, *6*, 879.

(17)   Moreto, J. M.; Ricart, S.; Dötz, K. H.; Molins, E. *Organometallics* **2001**, *20*, 62.

(18)   Hafner, A.; Hegedus, L. S.; de Weck, G.; Hawkins, B.; Dötz, K. H. *J. Chem. Soc.* **1988**, *110*, 8413.

(19)   Fischer, E. O.; Fischer, H. *Chem. Ber.* **1974**, *107*, 657.

(20)   Cardin, D. J.; Cetinkaya, B.; Lappert, M. F. *Chem. Rev.* **1972**, *72*, 545.

(21)   Darensbourg, M. Y.; Darensbourg, D. J. *Inorg. Chem.* **1970**, *9*, 32.

(22)   Connor, J. A.; Jones, M.; Randall, E. W.; Rosenberg, E. *J.Chem.Soc. Dalton Trans* **1972**, 2419.

(23)   Connor, J. A.; Jones, M. *J. Chem. Soc. (A)* **1971**, 1974.

(24)   Bezuidenhout, D. I. Synthesis and structural investigations of manganese carbene complexes, University of Pretoria, **2006**.

(25)   Lotz, S.; Landman, M.; Bezuidenhout, D. I.; Oliver, A. J.; Liles, D. C.; van Rooyen, P. H. *J. Organomet. Chem.* **2005**, *690*, 5929.

(26)   Moser, E.; Fischer, E. O. *J. Organomet. Chem.* **1969**, *16*, 275.

(27)   Bodner, G. M.; Kahl, S. B.; BOrk, K.; Storhoff, B. N.; Wuller, J. E. *Inorg. Chem.* **1973**, *12*, 1071.

(28)   Schenk, W. A.; Buchner, W. *Inorg. Chim. Acta* **1983**, *70*, 189.

(29)   Guns, M. F.; Claeys, E. G.; Van Der Kelen, G. P. *J. Mol. Struct* **1979**, *54*, 101.

(30)   Landman, M.; van Rooyen, P. H.; Wessels, H.; Thompson, *Unpublished results* **2012**.

(31)   Clayden, J.; Greeves, N.; Warren, S.; Wothers, P. *Organic Chemistry*; Oxford University Press: Oxford, **2001**.

(32)   Braterman, P. S. *Metal Carbonyl Spectra*; 1st ed.; Academic Press Inc.: London, **1975**.

(33)   Aroney, M. J.; Buys, E.; Davies, M. S.; Hambley, T. W. *J. Chem. Soc. Dalton Trans.* **1994**, 2827.

(34)   Liecheski, P. B.; Rankin, D. W. H. *J. Mol. Struct.* **1989**, *196*, 1.

(35)   Harshbarger, W. R.; Bauer, S. H. *Acta Crystallogr.* **1970**, *B26*, 1010.

(36)   Arrieta, A.; Cossío, F. P.; Fernandez, I.; Gomez-Gallego, M.; Lecea, B.; Mancheno, M. J.; Sierra, M. A. *J. Am. Chem. Soc.* **2000**, *122*, 11509.

CHAPTER 4:

N-HETEROCYCLIC CARBENE DERIVATIVES OF TUNGSTEN(0): A THEORETICAL DISCUSSION

4.1 INTRODUCTION

N-heterocyclic carbenes are currently a very popular class of ligands. This is mostly due to the excellent catalytic properties NHC metal complexes possess, and the advantages these ligands present when compared to phosphines.[1–4] NHCs are at times described as an extreme case of diamino Fischer carbenes, since they are merely diheteroatom substituted Fischer type complexes.[5] However, differences in both the nature of the metal carbene bond as well as reactivity patterns, allow NHCs a class of their own. In view of the fact that both phosphine and amine derivatives of Fischer carbenes were discussed in Chapter 2 and 3, and the similarities between NHCs and these two classes of ligands, it was logical to conclude this study by examining N-heterocyclic carbene complexes of tungsten(0).

The first NHCs were synthesised by Wanzlick[6] and Öfele[7] (Figure 4.1). Öfele achieved the synthesis of his novel carbene by *in situ* deprotonation of the azolium NHC precursor by the basic chromium metallate, as shown in figure 4.1. However, the field of NHC chemistry only truly developed after Arduengo isolated the first free carbenes in 1991.[8,9] NHCs are used widely in catalysis today due to the many similarities with phosphine ligands. Extensive theoretical studies have thus been done on these complexes to allow comparison between NHCs and phosphines, as well as to the properties of NHCs to be predicted.[5,10,11]
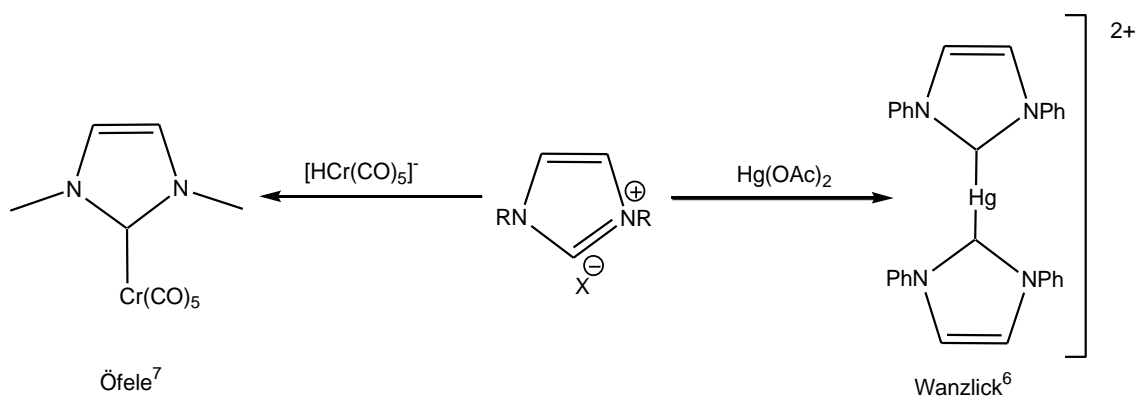
FIGURE 4.1: FIRST NHC COMPLEXES SYNTHESISED BY ÖFELE[7] AND WANZLICK[6]

Several synthetic routes have been developed for the synthesis of NHC ligands and complexes since 1968.[1,9] Most NHC metal complexes can be synthesised using mainly three basic methods.[12] Firstly, in situ deprotonation of NHC precursors may be used. This method is especially useful when the carbene is unstable. Next, complexation of free, pre-formed NHCs may be used to synthesise the NHC complex.[12] This method is very useful since few limitations are placed on the type of metal used, and the nature of the ligands found on the metal.[12] Lastly, NHC metal complexes can be synthesised by cleaving electron-rich olefins.[12] However, deprotonation of heterocyclic NHC precursors is the most common method used for synthesis of both free NHCs and NHC complexes.[1,12] Synthesis of the imidazolium precursors, used to produce free carbenes, can be divided into three different methods, as described by Benhamou *et.al.*[1] These can be distinguished by the order in which the different units of the NHC ligand are linked:

1. The NHC ring can be closed by adding the carbene centre as the final step;
2. The NHC-backbone can be used to close the heteroaryl ring by addition to the N-C=N group;
3. Introduction of the amino group may be used to allow for ring closure.

Recently a fourth method was introduced by Kim *et.al.*[13] This method allows for the synthesis of Group 6 NHC complexes from ethoxy Fischer carbenes, by replacement of the Fischer carbene with a free NHC.
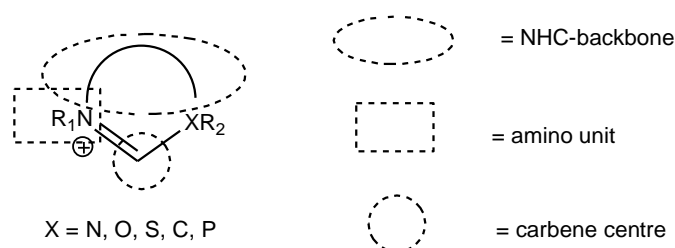
FIGURE 4.2: CLASSIFICATION OF THE NHC LIGAND PRECURSORS FOR DIFFERENTIATION OF SYNTHETIC ROUTES TO NHC PRECURSORS[1]

Of these methods, route 1, which was used by Arduengo for synthesis of the first imidazolium salts and free carbene, is still the most preferred method to produce NHC precursors.[1] Many variations for the synthesis of the NHC-backbone amino unit exist.[1,9,12] An assortment of precursor molecules used for synthesis of NHCs, which contain nitrogen as the only heteroatom in the heterocyclic ring, can be seen in figure 4.3. Additionally, several routes may be used to introduce the carbene centre during the final step.[1,2,9] These methods include the use of paraformaldehyde, trialkyl orthoformate, cyclization making use of a formamide already present in the molecule, and 1,1-bis(electrophile) compounds.[1] 1,1-Bis(electrophiles) are methylene complexes that contain two leaving groups, such as chloromethyl ethers and *gem*-dihalides.
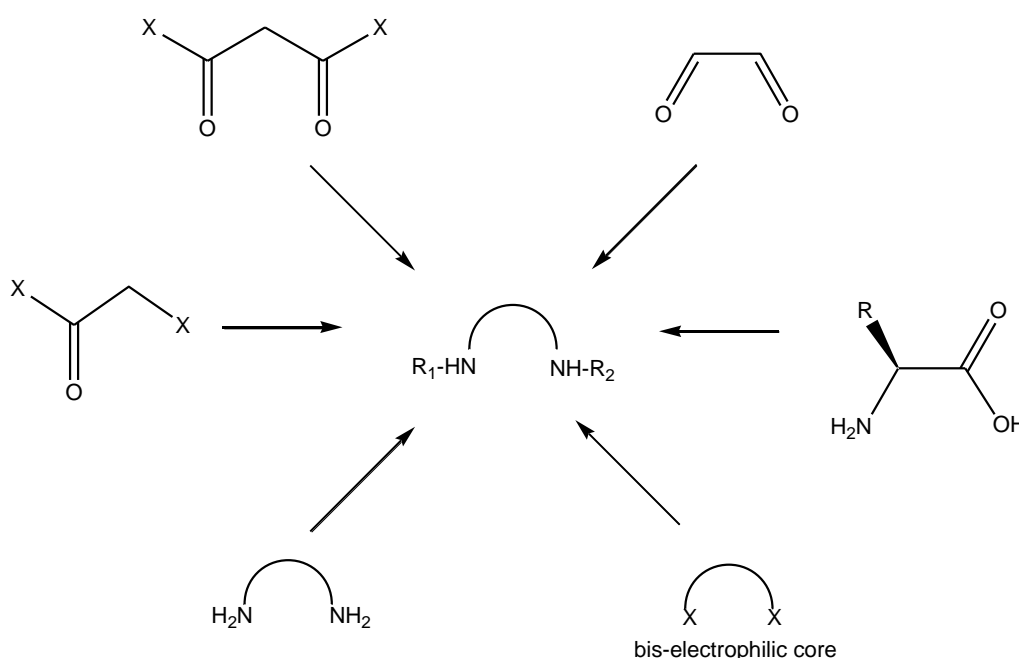
FIGURE 4.3: VARIOUS PRECURSORS THAT MAY BE USED FOR THE SYNTHESIS OF THE NHC-AMINO BACKBONE

For the purposes of this study, which focuses on tungsten(0) complexes, it is also important to note that the first work done by Öfele made use of chromium(0),[7] also a Group 6 metal. Öfele and others continued the study on coordinating Group 6 metals to NHCs, and several new complexes have been synthesised since 1968, of which a few recent examples are shown in figure 4.4.[14–17] However, when compared to metals such as Ru and Pd, much less development has occurred for Group 6 metals. The shift in focus is largely due to the application NHC complexes found in catalysis[5] after the development of the Grubbs catalysts. Much attention was thus given to altering known catalytic systems by replacing phosphine groups with NHCs, as was seen in the progression from the Grubbs 1 to the second generation Grubbs catalyst.

Kreiter *et.al.*[15]

Herrmann *et.al.*[17]

Nonnenmacher *et.al.*[14]

Ku *et.al.*[16]
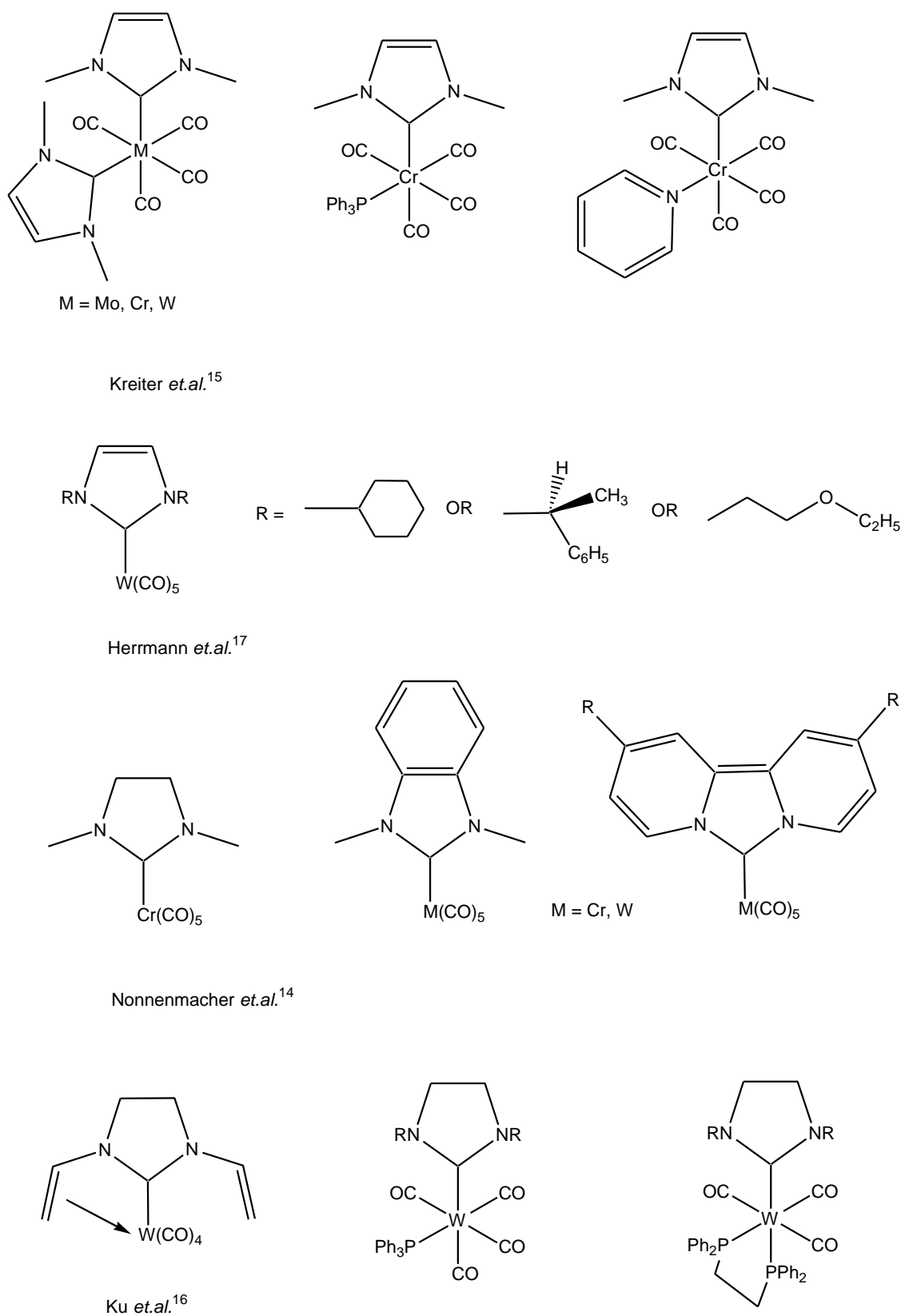
FIGURE 4.4: SELECTED LITERATURE EXAMPLES OF GROUP 6 METAL COMPLEXES

93

4.2 FOCUS OF THIS STUDY

Complex **C**[17]
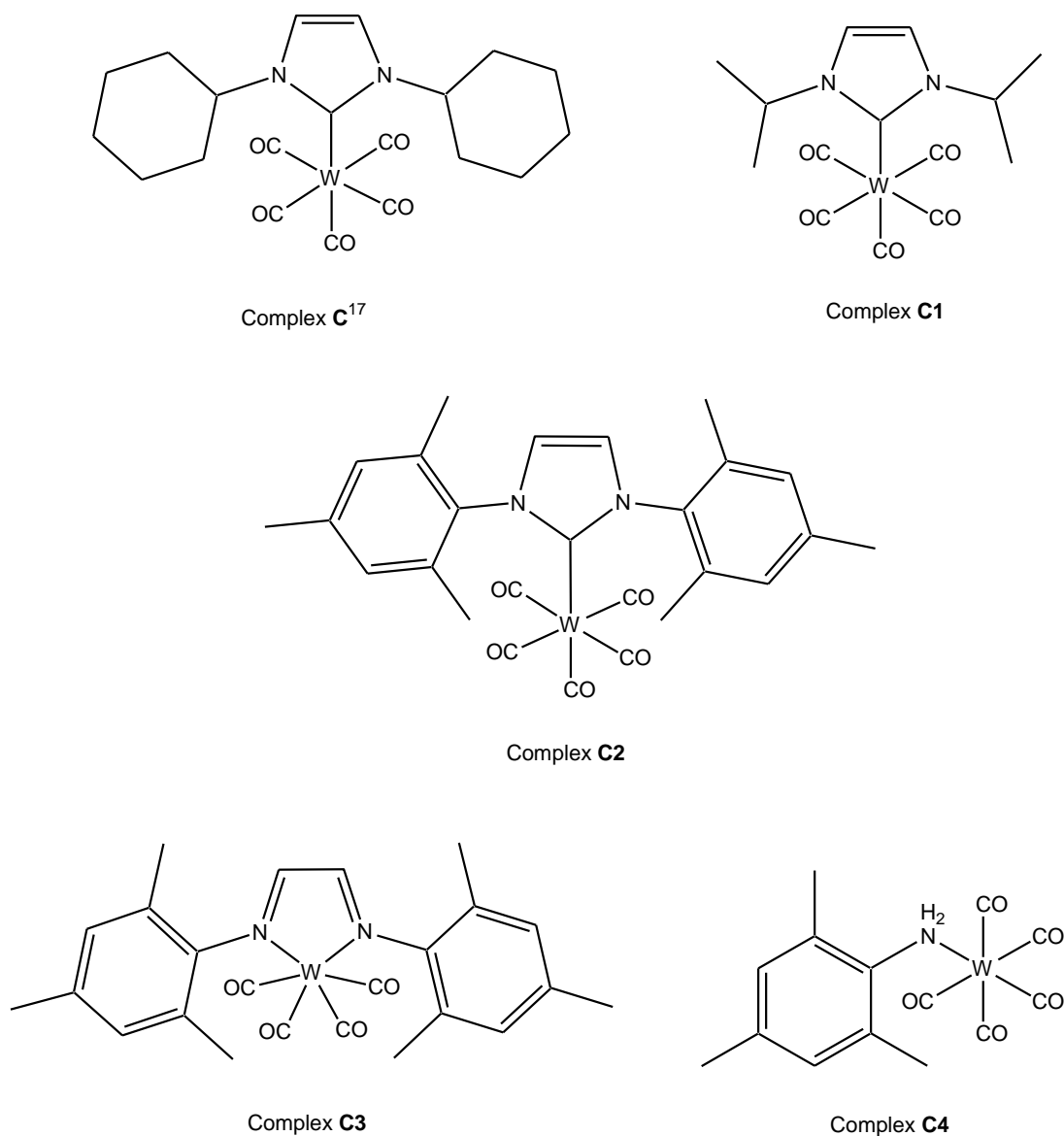
Complex **C1**

Complex **C2**

Complex **C3**

Complex **C4**

NHCs have many similarities with both Fischer carbenes and phosphines,[5] and thus are complementary to the ligands studied in chapters 2 and 3. The synthesis of novel NHC tungsten(0) complexes was thus proposed (complexes **C1** and **C2**). However, negligible yield was found in the reaction to synthesise complex **C1**, and several novel side-products were observed for complex **C2**. Unfortunately, even though complexes **C1** and **C2** appeared to be formed in the crude product, these complexes could not be characterised due to exceptionally low yields after purification. The low yields

were a result of decomposition that occurred during cleaning. The isolation of both complexes **C1** and **C2** could not be satisfactorily achieved. Theoretical studies of the proposed complexes (**C1** and **C2**), as well as a known literature example, complex **C**, synthesised by Herrmann.*et.al.*,[17] were however undertaken. Complex **C** was used as the literature comparison since it allows for a range of complexes in which the influence of steric bulkiness (comparison **C** vs **C1**) and altered saturation of NHC substituents (complex **C** vs **C2**) can be compared.

4.3 SYNTHESIS

R = Isopropyl   **C1**
R = Mesityl   **C2**
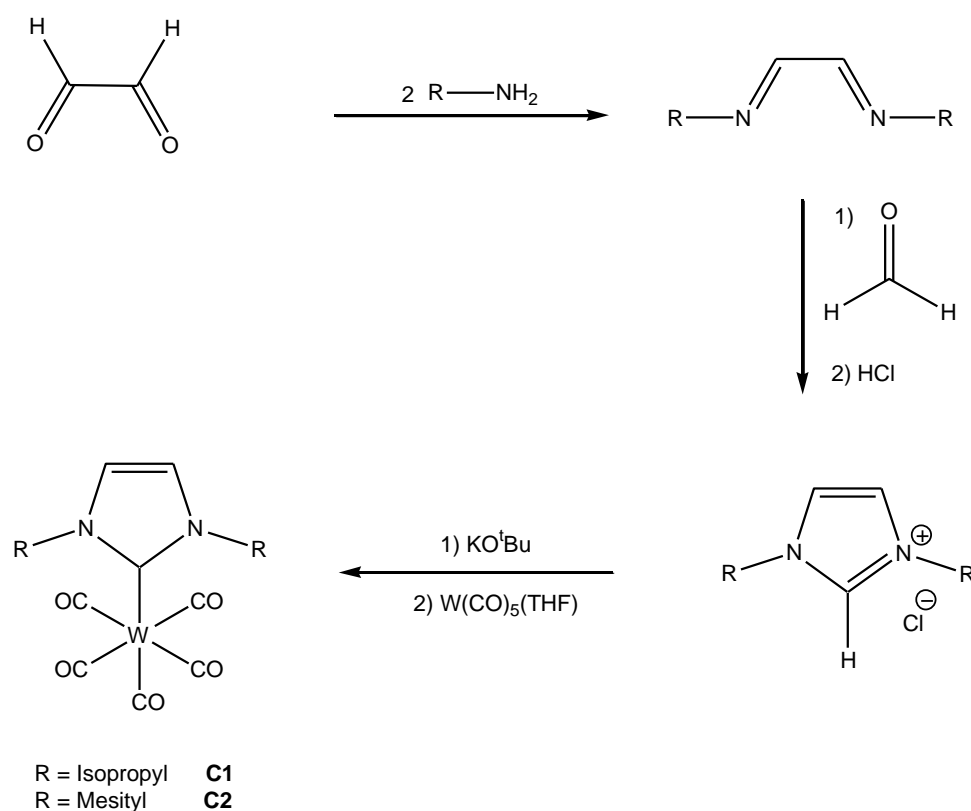
SCHEME 4.1: SYNTHETIC ROUTE PROPOSED FOR PENTACARBONYL NHC COMPLEXES OF TUNGSTEN(0)

The synthetic route shown in scheme 4.1 is similar to that used by Nonnenmacher *et.al.*[14] It is possible to purchase the imidazolium chloride salt and thus only the final step needs to be considered. Initially the full synthetic method was attempted for **C2**. However, the target complex was obtained in a low yield, due to decomposition. Upon coordination of the free NHC to $W(CO)_5THF$, decomposition products (**C3** and **C4**) were obtained as main products. The yield of the target complex was too low for characterisation purposes. For complex **C1**, very low yields were again obtained,

95

since the complex also appeared to be sensitive to DCM, while being poorly soluble in non-polar solvents. These factors resulted in incomplete characterisation of **C1**.

Target complex (**C2**)   Decomposition product (**C3**)
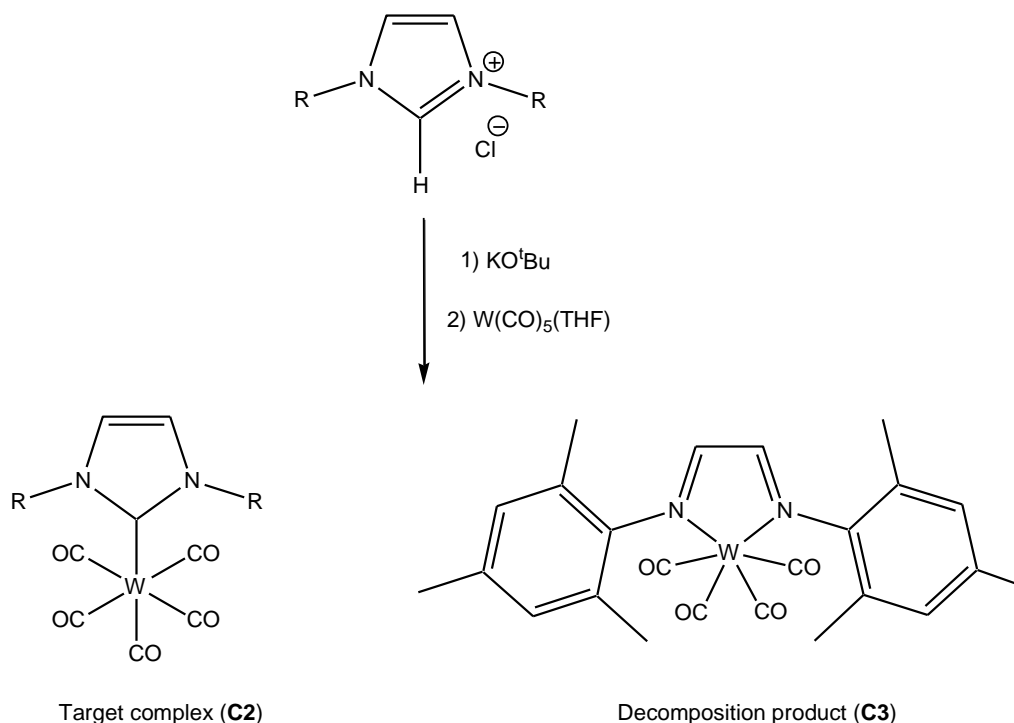
SCHEME 4.2: FORMATION OF COMPLEX C3

The formation of complex **C3** was unexpected (Scheme 4.2). The crude product obtained during the reaction was bright yellow, as would be expected for the target complex, but became bright pink when silica gel was added for dry loading during column chromatography. However, minimal amounts of pink (**C3**) was present on TLC, and yellow spots were found corresponding to the expected position of **C2**. This suggests that the decomposition of **C2** or its precursor may be catalysed by acidic conditions, such as exposure to silica gel. **C2** could thus be synthesised in crude form but not purified. Purification on aluminium oxide was attempted as an alternative. Once again, complex **C3** was obtained as the main product, and minimal amounts of **C2** were obtained. Decomposition of the crude product was, however, much less significant when aluminium oxide was used than when silica gel was used. The formation of complex **C3** is unique and suggests that a carbon extraction may occur as a decomposition route of the NHC precursor. To our knowledge, no similar decomposition routes have been reported, and a detailed investigation into the mechanism of this reaction will be the topic of future work. Also, synthesis of the free carbene was not done in a glove box, and is suggested for future attempts in synthesising **C1** and **C2**. Due to the reactive nature of free carbenes, it is possible that these compounds underwent decomposition before being added to the metal. However, since

96

comparisons could be made from the theoretical calculations, synthesis of **C1** and **C2** and optimisation of the reaction conditions were not attempted further.

Complex **C3**   Complex **C4**
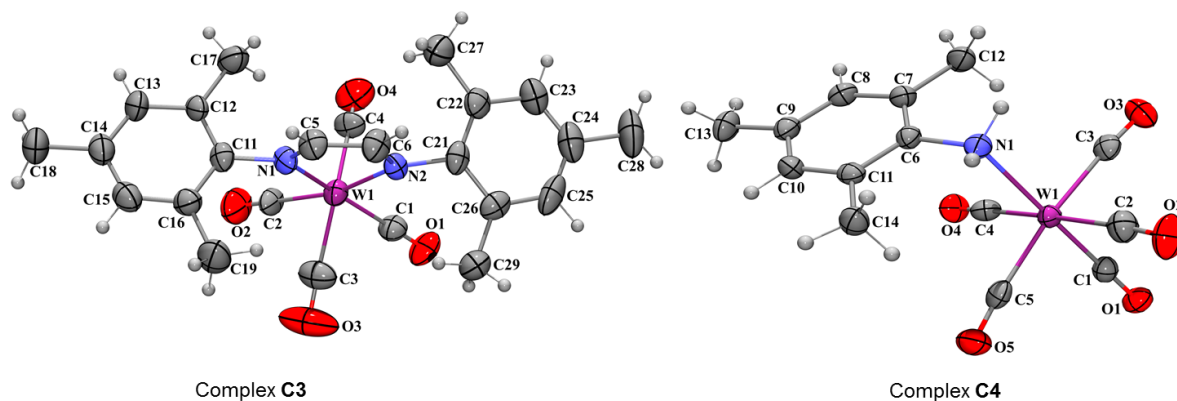
FIGURE 4.6: ORTEP PLOTS OF COMPLEXES C3 AND C4

4.4 THEORETICAL STUDY

Even though the synthesis of the novel tungsten pentacarbonyl NHC complexes (**C1** and **C2**) proved challenging, these complexes and a literature example were modelled using the Gaussian 03 software package. This allowed for comparison of the HOMOs and LUMOs, electrostatic potential maps and energy differences between the HOMOs and LUMOs of complexes **C**, **C1** and **C2**. The literature example chosen was the ICyc pentacarbonyl tungsten derivative (complex **C**) synthesised by Herrmann *et.al.*[17] (Figures 4.4 and 4.5). It was chosen since it was similar to both **C1** and **C2**, while posing sufficient differences to allow for general trends to be observed.

As a starting point, a summary of the HOMOs and LUMOs calculated for the complexes are shown in figure 4.7. The electrostatic potential maps are shown in figure 4.8, and the discussion is concluded with the energy differences between the HOMOs and LUMOs (Table 4.1).

HOMO C: E = -0.200 Hartrees   **HOMO C1: E = -0.201 Hartrees**   **HOMO C2: E = -0.194 Hartrees**

LUMO C: E = -0.043 Hartrees   **LUMO C1: E = -0.043 Hartrees**   **LUMO C2: E = -0.039 Hartrees**
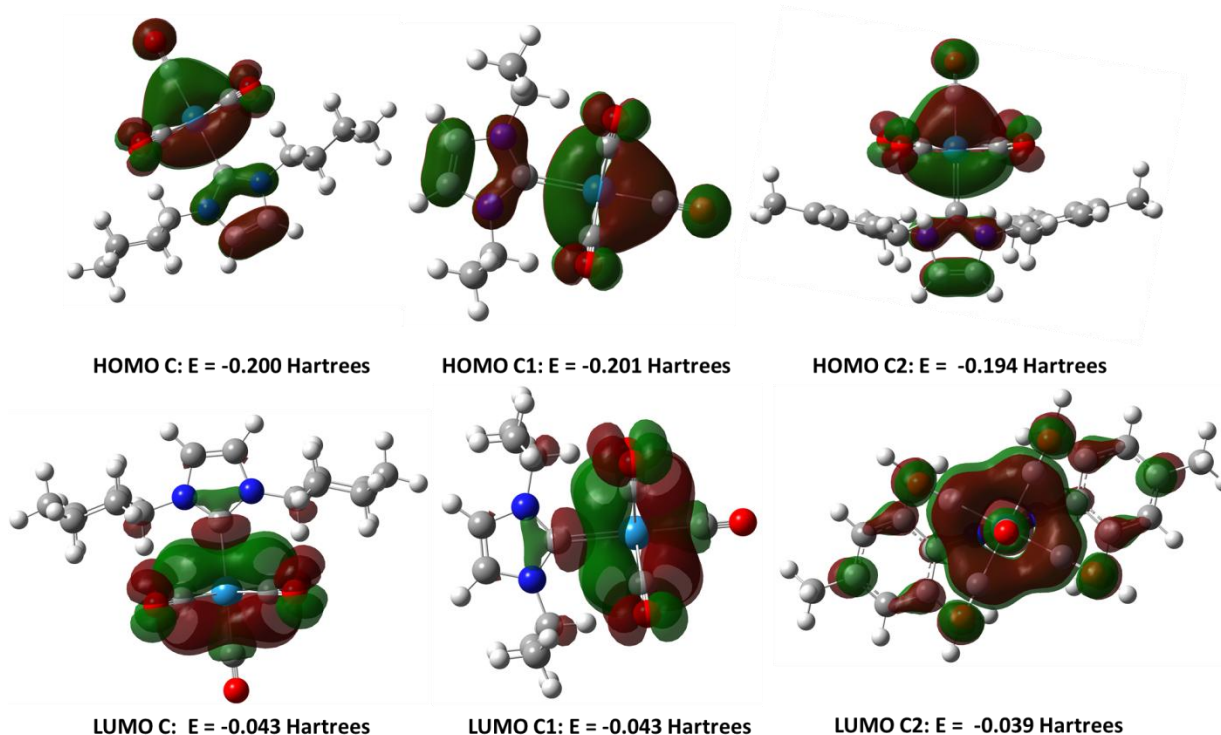
FIGURE 4.7: CALCULATED HOMOS AND LUMOS FOR OPTIMIZED COMPLEXES C, C1 AND C2 (1 HARTREE = 2600 KJ/MOL)

The main contribution to the HOMOs of **C**, **C1** and **C2** were all centred on the tungsten carbonyl moiety. Some of the HOMO was also located on the heterocyclic core of the NHC ligand. The LUMOs were again located mostly on the metal centre as well as on the carbonyl ligands, excluding the *trans* carbonyl ligand and the metal centre itself. In the case of complexes **C** and **C1**, both of which contain saturated alkyl substituents on the NHC, a very small portion of the LUMO appeared to be located on the NHC ligand. Complex **C2**, however, had a larger portion of the LUMO located across the mesityl NHC substituents. The location of the HOMO and LUMO indicate that both electrophilic and nucleophilic attacks are most likely to occur on the metal centre. This suggests that, unlike Fischer carbene complexes, in which the carbene carbon is susceptible to nucleophilic attack, it is likely that the metal sphere, of the NHC complexes discussed here, will be involved in nucleophilic attack. The calculations also agree well with the reactivity of NHC complexes as noted in literature. It is known that NHC ligands are not as reactive as other carbene lignads and thus do not react readily.[2] This difference in reactivity when NHCs are compared to other carbenes is naturally also reflected by the applications for which NHC are used. Metathesis requires that a double bond can coordinate to the metal centre and displaces one of the ligands. Donation of π-electrons from unsaturated bonds is seen as a nucleophilic attack. If one draws an analogy between nucleophilic attack of a double bond and the coordination of a double bond to a metal centre, then coordination may also be seen as a nucleophilic attack. The metal-centred LUMO is thus ideal for coordination of an unsaturated complex,

98

the initial step required for metathesis. Complex **C**, **C1** and **C2**, consequently, have prospective applications as metathesis catalysts.
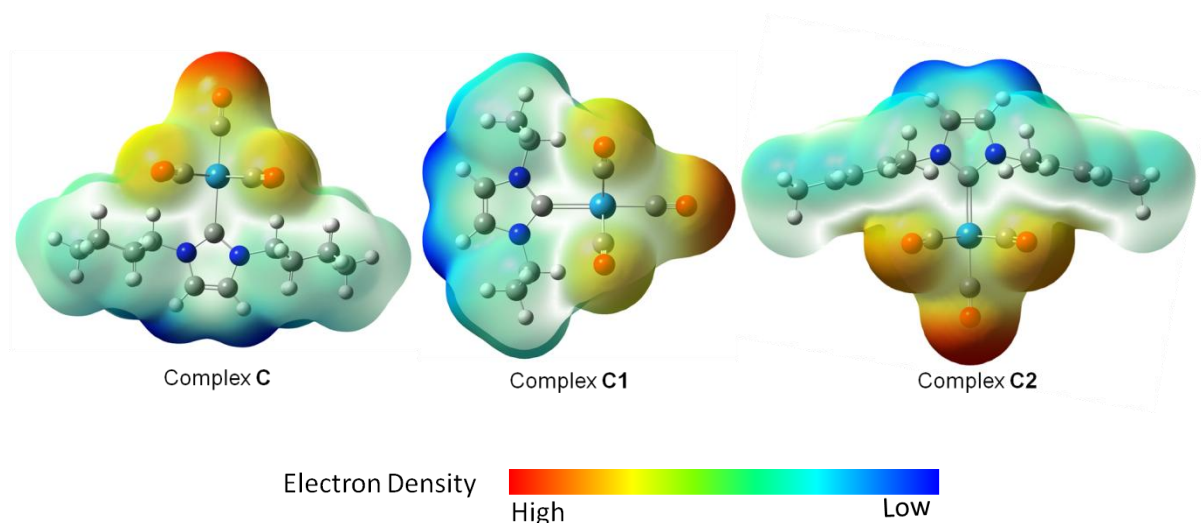
FIGURE 4.8: CALCULATED ELECTROSTATIC POTENTIAL MAPS FOR OPTIMIZED COMPLEXES C, C1 AND C2

Electrostatic potential maps were calculated for complexes **C**, **C1** and **C2**, and are represented in figure 4.8. All the NHCs considered indicate that electron density is not spread evenly across the molecules. The uneven electron distribution suggests that the complexes have a dipole. The highest concentration of electron density is found on the carbonyl ligands. The NHC ligand has the least amount of electron density concentrated on it. This suggests that electron density is drained from the NHC ligand to the metal centre.

TABLE 4.1: ENERGY DIFFERENCE BETWEEN HOMOS AND LUMOS	
COMPLEX	**ENERGY GAP (KJ / MOL)**
C	412.2
C1	414.8
C2	407.0

The energy difference between the HOMOs and the LUMOs is summarised in Table 4.1. The size of this energy difference decreases in the order **C1** > **C** > **C2**. The difference between the HOMO-LUMO energy gaps is not very large, but does allow tentative predictions for the relative reactivity of the complexes to be made. It appears that the differences in the energy gap are related to the size and the aromaticity of the NHC substituents. The larger the substituents, the smaller the energy difference between the HOMO and the LUMO. If **C** and **C2** are compared, the influence of aromatic versus

99

saturated substituents can be seen. It appears that aromaticity of the NHC substituent allows for a slight decrease in the energy gap between the HOMOs and the LUMOs. As mentioned in chapter 2, the energy difference between the HOMO and LUMOs can be related to the reactivity of the complex.[18] The trend noted above for **C**, **C1** and **C2** suggests that bulky and aromatic substituents are likely to decrease the HOMO-LUMO gap, and thus increase the reactivity of the molecule. Increased reactivity for a complex, when combined with a LUMO localised on the metal centre, as explained above, should result in an excellent catalyst. The trend also suggests that the reactivity of NHC complexes can be tuned by modification of the ligands, as shown in literature.[11]

4.5 CONCLUSION

Synthesis of complexes **C1** and **C2** could not be achieved satisfactorily due to challenging purification which was accompanied by decomposition. However, two novel compounds, **C3** and **C4**, were found as by-products of the proposed synthetic procedures. Compound **C3** is of great interest since it may be formed in a reaction representing a novel decomposition pathway, which includes carbon extraction. Determining how complex **C3** formed is therefore an important avenue of future study. Theoretical studies of complexes **C**, **C1** and **C2** could, none the less, be completed. The theoretical studies indicate that the HOMOs and LUMOs of **C**, **C1** and **C2** are found mostly on the metal centre, in contrast to the Fischer carbenes discussed in chapters 2 and 3, which had the HOMOs centred around the metal and the LUMOs centred on the carbene ligand and the bond *trans* to it. Electrostatic potential maps, however, indicate that the most electron density is found on the carbonyl ligands, as was found for the Fischer carbene complexes of chapters 2 and 3. Lastly, a tentative trend could be proposed from the energy difference between the HOMO and the LUMO. The energy difference suggests that larger, aromatic substituted NHC complexes have smaller energy gaps, indicating greater reactivity. A comparison of a larger range of NHC complexes is needed to determine whether this trend does in fact hold, and which factors contribute most.

4.6 REFERENCES

(1)   Benhamou, L.; Chardon, E.; Lavigne, G.; C, V. *Chem. Rev.* **2011**, 2705

(2)   Herrmann, W. A.; Weskamp, T.; Böhm, V. P. W. *Adv. Organomet. Chem.* **2001**, *48*, 1.

(3)   Zinn, F. K.; Viciu, M. S.; Nolan, S. P. *Annu. Rep. Prog. Chem. Sect. B.. Chem. Sect. B.* **2004**, *100*, 231.

(4)   Singh, R.; Nolan, S. P. *Annu. Rep. Prog. Chem., Sect. B* **2006**, *102*, 168.

(5)   Fey, N.; Haddow, M. F.; Harvey, J. N.; Mcmullin, C. L.; Orpen, A. G. *Dalton Trans.* **2009**, 8183.

(6)   Wanzlick, H. W.; Schoenherr, H. J. *Angew. Chem. Int. Ed. Engl.* **1968**, *7*, 141.

(7)   Öfele, K. *J. Organomet. Chem.* **1968**, *12*, 42.

(8)   Lee, M.-tsung; Hu, C.-han *Organometallics* **2004**, *23*, 976.

(9)   de Frémont, P.; Marion, N.; Nolan, S. P. *Coord. Chem. Rev.* **2009**, *253*, 862.

(10)   Lai, C.-liang; Guo, W.-hsin; Lee, M.-tsung; Hu, C.-han *J. Organomet. Chem.* **2005**, *690*, 5867.

(11)   Jacobsen, H.; Correa, A.; Poater, A.; Constable, C.; Cavallo, L. *Coord. Chem. Rev.* **2009**, *253*, 687.

(12)   Herrmann, W. A.; Weskamp, T.; Böhm, V. P. W. *J. Organomet. Chem.* **2000**, *600*, 12.

(13)   Kim, S.; Choi, S. Y.; Lee, T. L.; Park, K. H.; Sitzmann, H.; Chung, Y. K. *J. Organomet. Chem.* **2007**, *692*, 5390.

(14)   Nonnenmacher, M.; Kunz, D.; Rominger, F.; Oeser, T. *J. Organomet. Chem.* **2005**, *690*, 5647.

(15)   Kreiter, C. G.; Öfele, K.; Wieser, G. W. *Chem. Ber.* **1976**, *109*, 1749.

(16)   Ku, R.; Huang, J.; Cho, J.; Kiang, F.; Reddy, K. R.; Chen, Y.; Lee, K.; Lee, J.; Lee, G.; Peng, S.; Liu, S. *Organometallics* **1999**, *18*, 2145.

(17)   Herrmann, W. A.; Köcher, C.; Gooßen, L. J.; Artus, G. R. J. *Chem. Eur. J.* **1996**, *2*, 1627.

(18)   Arrieta, A.; Cossío, F. P.; Fernández, I.; Gomez-Gallego, M.; Lecea, B.; Mancheno, M. J.; Sierra, M. A. *J. Am. Chem. Soc.* **2000**, *122*, 11509.

CHAPTER 5:

CONCLUSIONS AND FUTURE WORK

Eighteen novel complexes, including decomposition products, were synthesised in this study. This included sixteen novel ethoxy and amino tungsten(0) carbonyl carbene derivatives of thiophene (**A1-A8**) and furan (**B1-B8**). Of these complexes, six novel ethoxy phosphine tungsten(0) carbene complexes (**A1**-**A3** and **B1**-**B3**) were synthesised. Novel amino carbenes that were synthesised can be divided according to substitution patterns as follows: four pentacarbonyl tungsten(0) carbene complexes (**A4**, **A7**, **B4** and **B7**) two amine chelate tungsten(0) carbene complexes (**A8** and **B8**) and four phosphine tungsten (0) carbene complexes (**A5**-**A6** and **B5**-**B6**). Lastly, two side-products (**C3** and **C4**) were obtained from the attempted synthesis of complex **C2**.

The Fischer carbene complexes were synthesised from complexes **A** and **B** by substitution of either the metal ligands or the carbene substituents (Figure 5.1).
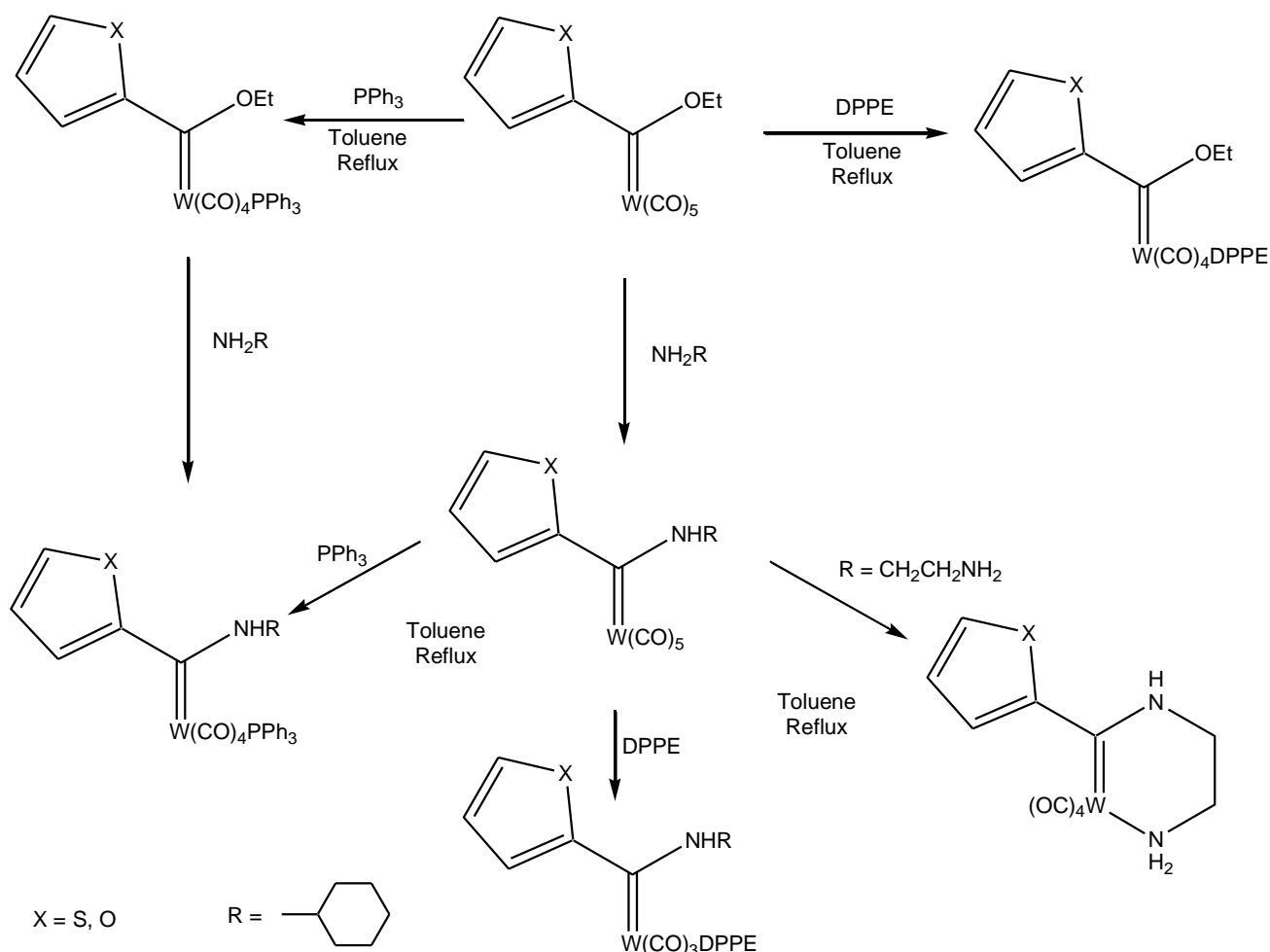
SCHEME 5.1: SYNTHETIC ROUTES TO NOVEL FISCHER CARBENE COMPLEXES SYNTHESISED (A1-A8 AND B1-B8)

Characterisation of NHC carbene complexes **C1** and **C2** was not achieved, due to low yields and decomposition of the crude products during purification. Two novel complexes, **C3** and **C4**, were obtained. The decomposition of complex **C2** to complex **C3** has, however, not been reported in literature before. Studies relating to this unique decomposition route are to be undertaken in future work.

Characterisation of the complexes clearly indicated the influence of the various modifications on the nature of the carbene complex. This was most clearly reflected by comparison of the carbene carbon resonance in the ^{13}C NMR spectra of all the carbene complexes. Ethoxy carbene carbon chemical shifts were observed between 277 ppm and 295 ppm, while amino carbene carbon resonance shifts were observed between 218 ppm and 247 ppm. This illustrates the greater π-donation from the amino substituent on the carbene than from the ethoxy substituent. Carbonyl carbon shifts were useful to

103

distinguish between *cis* and *trans* isomers. The ^{1}J(W-C$_{Carbonyl}$) couplings found for complex **B1** were also indicative of the *trans* influence of the carbene ligand, and suggested that the carbene ligand is a stronger *trans* influencing ligand, than carbonyl ligands.[1] Thus ligands *trans* to the carbene substituents should have longer bonds than the same ligand in a position *cis* to the carbene ligand and *trans* to a carbonyl. A complete set of ^{1}J(W-C) couplings were not observed for any other complex, and thus the *trans* influence for amino carbene tungsten(0) complexes could not be determined. Future work will thus include more sensitive NMR studies to determine these coupling constants, in order to have a more complete range of complexes to deduce a general trend.

The pentacarbonyl amino carbenes (**A4**, **B4, A7** and **B7**) had lower wavenumbers for the carbonyl stretching frequencies when compared to the ethoxy carbene analogues (**A** and **B**). A decrease in wavenumbers associated with carbonyl stretching frequencies upon aminolysis is expected, and a known trend in literature.[2–5] Amino carbenes require less π-backbonding from the metal for stabilization, due to an increase in π-donation from the amino group when compared to the ethoxy carbenes. A decrease in metal-carbene π-bonding permits an increase in π-donation from the metal to the carbonyl groups. This increase in π-donation would subsequently decrease the bond order between the carbon and the oxygen of the carbonyl group, thereby decreasing the wavenumbers observed for the carbonyl stretching frequencies. Both the tetracarbonyl (**A5**, **B5**, **A8** and **B8**) and tricarbonyl (**A6** and **B6**) amino carbene complexes also showed a shift to lower wavenumbers when compared with the ethoxy carbene complexes (**A4**, **B4**, **A7**, **B7**, **A3** and **B3**).

Eight complexes (W(CO)$_4$DPPE, **A3**, **A4**, **B4**, **A5**, **B8**, **C3** and **C4**) could be characterised by means of X-ray diffraction studies. The crystal structure of **A3** indicated that the W-P bonds, did in fact, follow the trend expected from the *trans* influence deduced from NMR studies. The W-P bond *trans* to the carbene in complex **A3** was longer than the W-P bond *trans* to a carbonyl ligand in complex **A3.** Further XRD studies of complexes **A1**-**A2**, **A6**, **B1**-**B3** and **B5-B6** would assist in determining the *trans* influence of the carbene ligand relative to carbonyl and phosphine ligands, when combined with NMR data. The unresolved crystal structure of complex **B7** was included for comparative reasons only. Due to possible twinning in this structure an R-factor of approximately 13% was obtained. Therefore, no crystallographic data of this structure was included.

Synthesis of all Fischer carbene complexes was successful. All complexes could be purified and characterised successfully. The reactions were not always fully optimized, however, the aim of the study was the initial development of synthetic routes to the various complexes. Optimisation of the various synthetic routes used is thus an avenue of future work. Also, development of a synthetic route to NHC complexes **C1** and **C2** are envisioned for future work.

104

Theoretical calculations were useful for comparison between the Fischer carbene complexes mutually, as well as with NHC complexes. It should firstly be noted that theoretical calculations of vibrational spectra were used for assignments of the IR active stretching modes that were observed in the experimental data for all Fischer carbene complexes studied. Also, only the theoretical data for the thienyl Fischer carbene complexes (**A1**-**A8**) was shown, since the furyl complexes followed the same trends (**B1**-**B8**). The distribution of the HOMOs and LUMOs were significantly different between the Fischer complexes (**A1**-**A8**) and the NHC complexes (**C-C2**) studied. Both the ethoxy (**A1**-**A3**) and the amino (**A5**-**A8**) Fischer carbene complexes showed the HOMO to be localised on the metal centre and the LUMO was located on the carbene ligands and the bond *trans* to it. In the NHC complexes (**C-C2**) both the HOMO and the LUMO were found to be on the metal centre. This clearly suggests that the NHC complexes will have markedly different reactivity patterns than the Fischer carbene complexes. The olefin metathesis mechanism requires that one of the ligands on the metal centre is replaced by the incoming alkene, in what can be seen as a nucleophilic attack.[6] This would require that the LUMO be located on the metal centre, thus suggesting that NHC complexes will be the most useful for this type of transformation reaction. Also, the presence of both the HOMO and the LUMO on the metal centre of the NHC complexes suggests that these complexes will be the most useful for catalytic transformations which require the metal centre to play an active role in the forming and breaking of bonds, to allow the transformation to occur.

ESP maps illustrated that, for all the complexes studied the highest amount of electron density is always found on the carbonyl ligands. Lastly, the HOMO-LUMO energy gaps calculated ranged from 272 kJ/mol to 415 kJ/mol. The complexes can be placed in order of decreasing HOMO-LUMO energy gap as follows:

C1 > **C** > **C2** > **A7** > **A4** > **A5** *trans* > **A5** > **A6** > **A2** > **A1** > **A3** > **A8**

These energy gaps are not significantly different for all cases but do allow for a tentative trend in reactivity to be predicted and for comparisons between classes of complexes. This trend suggests that the NHC complexes (**C-C2**) are less reactive than the Fischer carbene complexes (**A1**-**A8**). Furthermore, in general, the amino carbene complexes (**A4**-**A7**) will be less reactive than the ethoxy carbene complexes (**A1-A3**), with the exception of complex **A8**. Also, in monophosphine substituted Fischer carbene complexes the *trans* isomers (**A2** and **A5** *trans*) are less reactive than the *cis* isomers (**A1** and **A5**). Diphosphinated Fischer carbene complexes (**A6** and **A3**) have a lower energy gap, but due to the high number of carbonyl ligands that have been substituted, these complexes are known to be less reactive than the monophosphine Fischer carbene complexes.[7] Lastly, from complex **A8** it can be concluded that amine substituted Fischer carbene complexes are the more reactive than phosphine substituted Fischer carbene complexes. Thus, the HOMO-LUMO energy gap, in contrast to the HOMO and LUMO orbital distributions suggests that the NHC complexes will be the least

reactive. However, this does not imply that NHC complexes will not be useful for catalytic transformations; it merely points towards higher activation energy barriers. Experimental studies are thus vital to determine the best applications and the reactivity patterns of the Fischer and NHC tungsten(0) complexes studied. On this point, it is suggested that for olefin metathesis purposes the NHC complexes will be most useful, while the Fischer carbene complexes will be useful for carbene-centred reactions.

5. 1 REFERENCES

(1)   Buchner, W.; Schenk, W. A. *Inorg. Chem.,* **1984**, *23*, 132

(2)   Cardin, D. J.; Cetinkaya, B.; Lappert, M. F. *Chem. Rev.,* **1972**, *72*, 545

(3)   Hafner, A.; Hegedus, L. S.; de Weck, G.; Hawkins, B.; Dötz, K. H. *J. of Amer. Chem. Soc.,* **1988**, *110*, 8413

(4)   Connor, J. A.; Jones, M.; Randall, E. W.; Rosenberg, E. *J.Chem.Soc., Dalton Trans.,* **1972**, 2419.

(5)   Connor, J. A.; Jones, M. *J. Chem. Soc. (A)* **1971**, 1974

(6)   Elschenbroich, C. *Organometallics*; 3rd ed.; Wiley - VCH: Weinheim, **2011**.

(7)   Arrieta, A.; Cossío, F. P.; Fernández, I.; Gomez-Gallego, M.; Lecea, B.; Mancheno, M. J.; Sierra, M. A. *J. Am. Chem. Soc.* **2000**, *122*, 11509

CHAPTER 6:

EXPERIMENTAL

6.1 GENERAL

6.1.1 Apparatus and standard procedures

All reactions, unless otherwise noted, were performed under inert nitrogen or argon atmospheres using standard Schlenk techniques.[1] All solvents were freshly distilled, dried and collected under inert conditions, with the exception of toluene. Toluene was not dried, but used after bubbling nitrogen gas through the solvent for 5 to 10 min. All other reagents were used directly. Column chromatography was carried out under inert nitrogen and argon atmospheres using silica gel (particle size 0.063-0.200mm) as the stationary phase. All percentage yields were calculated relative to the limiting reactant. All crystallization was done using hexane:DCM diffusion methods.

6.1.2 Characterisation

NMR Spectroscopy

All ^{13}C and ^{31}P NMR spectra were proton decoupled.

NMR spectra were recorded using deuterated solvent peaks as the internal references (Table 6.1).

TABLE 6.1: REFERENCE PEAKS FOR DEUTERATED SOLVENTS USED		
Solvent	^{1}H (ppm)	^{13}C (ppm)
CDCl$_3$	7.24	77.2
CD$_2$Cl$_2$	5.32	54.0
CD$_3$CN	1.94	1.9
		118.7

NMR spectra were recorded on a Bruker ARX-300, Bruker Ultra Shield 400 Plus AVANCE III, and a Bruker AVANCE 500 (Table 6.2).

TABLE 6.2: NMR SPECTROMETER SPECIFICATIONS		
Spectrometer	^{1}H-NMR (MHz)	^{13}C-NMR (MHz)
Bruker ARX-300	300.1	75.5
Bruker Ultra Shield 400 Plus AVANCE III	400.2	100.6
Bruker AVANCE 500	500.1	125.8

Infrared Spectroscopy

IR spectra were recorded on a Perkin Elmer Spectrum RXI FT-IR spectrophotometer. All spectra were recorded as KBr pellets.

Mass Spectrometry

Mass spectra were recorded on a SYNAPT G2 HDMS with the following parameters:

> TOF-MS method

> Sampling time: 4min, with direct infusion inlet method

> Source: Electron spray ionization

> Positive polarity acquisition mode

> Resolution: Analyzer mode

X-ray Crystallography

X-ray data was recorded at several institutions and the specifications of the diffractometers are available on request.

6.1.3 Theoretical Calculations

All calculations were executed using GAUSSIAN 03 software.[2] All calculations were modelled using ground state DFT calculations with the B3LYP functional and the GEN basis set (6-31G* for C, H, O,

108

P, S, N and LANL2DZ for W) with a neutral charge and the singlet spin state. The DFT-B3LYP method was selected since it allows for an increase in accuracy with only a small increase in computation time.[3] Two different basis sets were used for the molecules. The LANL2DZ basis set was used to optimise the W metal centre. LANL2DZ includes relativistic effects which is significant for heavy atoms. In contrast, the 6-31G* basis set was used for all the other atoms found in the complexes. This basis set was chosen, since it allowed for the needed level of accuracy for the smaller atoms, while optimising time costs. This methodology is similar to those found in literature and has been shown to be effective for similar complexes.[4,5,6,7]

Calculations for most molecules were performed on molecules constructed with Gaussview 4.1, with the exception of complexes **B4** and **B8** that were based on crystal structure data. RMS (Root mean square) values were determined for comparison of the crystal structures obtained and theoretical calculations for these complexes using the structure overlay function found in the Mercury software package. This allowed for comparisons of the theoretical and experimental data in cases where experimental data became available after calculations were performed. The RMS values for complexes **A3**, **A4**, **B4**, **A5**, and **B8** vary from 0.100 Å to 1.39 Å. The values and corresponding images for visualizing the RMS determinations can be found in appendix I. Input and output files used for calculations can be found in appendix J.

6.2 SYNTHETIC PROCEDURES

Complex A[8]
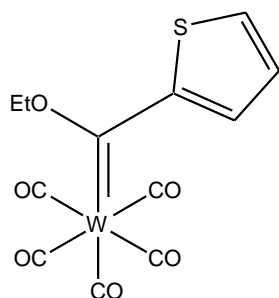
This synthetic method deviated from that published in literature. Thiophene (0.240 mL, 2.995 mmol) in ± 20 mL of THF was cooled to -79 °C. To this solution, ^{n}BuLi (1.5M, 2 mL, 3.00 mmol) was added dropwise. The reaction mixture was allowed to stir at this temperature for 1 hr, and then at RT for 5 min, resulting in a pale yellow solution. $W(CO)_6$ (1.066g, 3.03 mmol) was added to the reaction mixture at -76 °C and stirred at this temperature for 15 min. A bright yellow solution was obtained. The reaction mixture was then allowed to stir at RT for 20 min. The solution was red-orange. The solvent

was then removed, yielding a bright orange oil. 15 mL of DCM was added to the product and the solution was cooled to -68°C. Et_3OBF_4 in DCM (0.0670 g/mL, 8.60 mL, 3.03 mmol) was added slowly, and the reaction allowed to stir cold for 30 min, and then at RT for a further 30 min. The solution was a dark red brown. The crude product was filtered through silica gel, and washed off with DCM. A dark red brown solid was obtained after the solvent was removed. The product was purified on silica gel using hexane:DCM gradients.

Yield: 1.067 g, 2.30 mmol, 76.6%, red solid.

M.S.(m/z): 464 [M^+]; 435 [M^+(-Et)]; 408 [M^+(-2CO)]; 380 [M^+(-3CO)];

^{1}H NMR: Table 2.2 ^{13}C NMR: Table 2.5   IR: Table 2.9

Complex B[9,10]
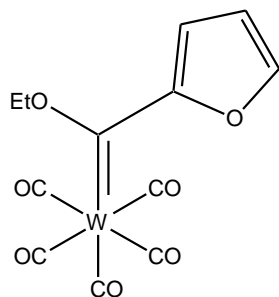
This synthetic method deviated from that published in literature. Furan (0.32 mL, 4.37 mmol) in 15 mL THF was cooled to -35 °C, and ^{n}BuLi (1.5M, 3.13 mL, 4.70 mmol) was added dropwise, resulting in a pale yellow solution. The reaction was allowed to stir at -35 °C for 40 min. $W(CO)_6$ (1.755 g, 4.99 mmol) was added and the reaction allowed to stir cold for a further 20 min (bright yellow solution), and then at RT for 1 hr (dark red brown solution). The solvent was then removed, and a dark brown oil obtained. This product was dissolved in 30 mL of DCM and cooled to -40 °C. Et_3OBF_4 in DCM (0.2454 g/mL, 5 mL, 6.46 mmol) was added to the reaction mixture and allowed to stir for 30 min. The reaction was then allowed to stir at RT for 1 hr, yielding a dark red-brown solution which was filtered through silica gel and rinsed off with DCM. A dark red-brown solid was obtained after solvent removal. The product was purified on silica gel with hexane:DCM gradients.

Yield: Monocarbene: 1.046g, 2.33 mmol, 54%, red solid

M.S. (m/z): 419 [M^+(-Et)]

^{1}H NMR: Table 2.3 ^{13}C NMR: Table 2.6   IR: Table 2.9

W(CO)₄DPPE
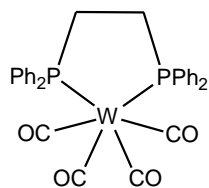
W(CO)$_6$ (0.530 g, 1.51 mmol) and DPPE (0.606 g, 1.52 mmol) were mixed in ± 15 mL of diglyme. The reaction mixture was refluxed for 5 hrs. Initially the solution was pale yellow but gradually became green. Methanol (± 20 mL) was then added to the reaction mixture, causing white crystals to precipitate out. This was left for 3 days to allow for crystallization. The crystals were filtered off from the mother liquor. The crystals obtained in this manner were dissolved in minimal DCM, and double that volume of MeOH was added to induce crystallization. This mixture was allowed to stand in the dark for several days. Pale green crystals (0.209 g) were obtained after filtration of the mother liquor. The mother liquor was then concentrated and cooled, resulting in a second crop of white crystals (0.0026 g).

Yield: 0.212 g, 0.305 mmol, 20.2%, greenish white crystals

M.S. (*m/z*): 385 [M$^+$(-4Ph)]; 302 [M$^+$(-4Ph, -3CO)]; 274 [M$^+$(-4Ph; -4CO)]

^{1}H NMR: Table 2.1 ^{13}C NMR: Table 2.4   IR: Table 2.9

XRD data in appendix A

Complexes A1 and A2

A1   **A2**
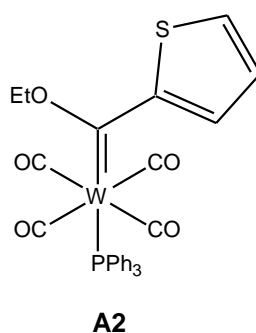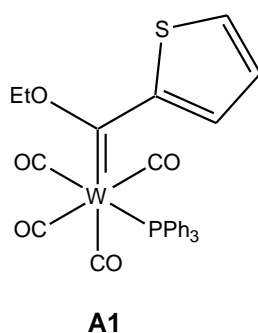
Complex **A** (1.393 g, 3.00 mmol) and PPh$_3$ (0.945 g, 3.60 mmol) were dissolved in 30 mL of toluene (wine red solution). This mixture was left to reflux overnight (dark brown solution), and the solvent was removed (dark brown solid). The crude product was purified on silica gel using hexane:DCM gradients. Unreacted carbene **A** (0.285 g, 0.614 mmol, 20.5 %) and two products were obtained according to TLC. The two products were identified as the *cis* and *trans* isomers of the product. The *trans* product, **A2**, is yellow-brown in solution and elutes after the starting carbene **A**. The cis product,

111

A1, eluted directly after the *trans* isomer, **A2**, as a dark red-brown solution. The bands corresponding to the isomers could not be completely separated and thus fractions were collected and combined as necessary.

Yield: **A1**: 0.590 g, 0.845 mmol, 28.2%, reddish-brown solid

   A2: 0.040 g, 0.057 mmol, 1.9%, yellow-brown solid

M.S. (*m/z*):   **A1:** 557 [M$^+$(-Et, -4CO)]; 327 [M$^+$(-4Ph, -Et, -4CO)]

   A2: 352 [M$^+$(-Et, -PPh$_3$, -2CO)]; 327 [M$^+$(-4Ph, -Et, -4CO)]

A1 and **A2:** ^{1}H NMR: Table 2.2 ^{13}C NMR: Table 2.5 ^{31}P NMR: Table 2.8   IR: Table 2.9

Complexes B1 and B2
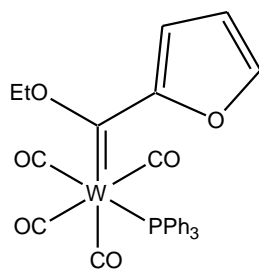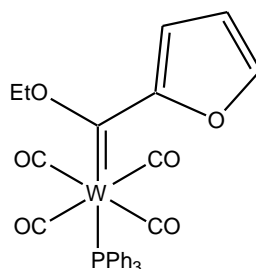
B1   **B2**

Complex **B** (0.868 g, 1.94 mmol) and PPh$_3$ (0.566 g, 2.14 mmol) were dissolved in 40 mL of toluene (wine red solution) and left to reflux for 7 hrs (brown solution). The solvent was then removed, yielding a brown solid as the crude product. TLC indicated starting monocarbene **B** and two products (*cis* and *trans* isomers as for thiophene analogues, **A1** and **A2**) were present. Starting monocarbene **B** was removed from the products on a silica gel filter using hexane:DCM gradient elution. The isomers were then separated on a cooled silica gel column using hexane:DCM gradient elution. Elution patterns and colours for the isomers were the same as for the thiophene analogues (**A1** and **A2**).

Yield: **B1**: 0.615 g, 0.901 mmol, 46.6%, red-brown solid

   B2: 0.030 g, 0.044 mmol, 3.33%, yellow-brown solid

M.S. (*m/z*):   **B1:** 654 [M$^+$]; 541 [M$^+$(-4CO; -Et)]; 310 [M$^+$(-3Ph, -4CO, -Et)]; 308 [M$^+$(-PPh$_3$, -4CO)]; 279 [M$^+$(-PPh$_3$, -4CO, -Et)]

B1 and **B2:** ^{1}H-NMR: Table 2.3 ^{13}C-NMR: Table 2.6 ^{31}P NMR: Table 2.8   IR: Table 2.9

Complex A3

A3
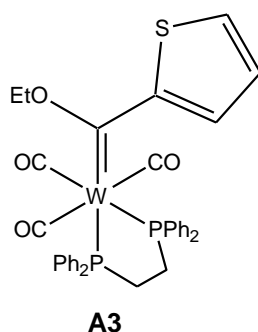
Complex **A** (0.464 g, 1.00 mmol) and DPPE (0.412 g, 1.03 mmol) were dissolved in ± 40 mL of toluene (wine red solution). The mixture was then left to reflux until all the starting carbene had reacted (dark brown solution). TLC indicated two products were present; a brown-yellow compound and a more polar brown-red compound. The solvent was removed, yielding a brown solid. The crude product was dissolved in minimal DCM and purified by diffusion crystallization methods with hexane. Large, clumpy, black (*mer* isomer of target molecule) and fine white crystals (W(CO)$_4$DPPE) were obtained. These were separated by sonication of the sample in hexane and then removing the suspension that formed, leaving large black crystals. TLC indicated that the black crystals obtained corresponded to the first yellow brown compound in the crude product. Separation by silica gel chromatography was attempted, however, the products could not be separated and decomposition occurred, therefore only crystallization was used as a purification method.

Yield: 0.312 g, 0.387 mmol, 38.7%, black crystals

M.S. (*m/z*): 806 [M$^+$]

^{1}H-NMR: Table 2.2 ^{13}C-NMR: Table 2.7 ^{31}P NMR: Table 2.8   IR: Table 2.9

XRD data in appendix B

113

Complex B3

B3
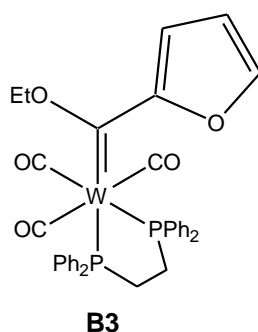
Complex **B** (0.534 g, 1.19 mmol) and DPPE (0.748 g, 1.88 mmol) were dissolved in 30 mL of toluene (wine red solution). This mixture was left to reflux until no more starting carbene (complex **B**) was present on TLC (dark brown solution). The solvent was then removed, yielding a dark brown solid that contained two products. A yellow-brown product, later identified as the *mer* isomer of the target complex, and a more polar brown-red product were present. The crude product was dissolved in minimal DCM and purified by diffusion crystallization with hexane. The crystals obtained were a mixture of black (*mer* isomer) and white (W(CO)$_4$DPPE) crystals. These were cleaned in the same manner as complex **A3**, with the exception that the larger white crystals were manually separated from the product after the hexane wash.

Yield: 0.378 g, 0.478 mmol, 40.2%, black crystals

M.S. (*m/z*): 790 [M$^+$]; 453 [M$^+$(-4Ph, -Et)]; 425 [M$^+$(-4Ph; -CO; -Et)]; 397 [M$^+$(-4Ph; -2CO; -Et)]

^{1}H-NMR: Table 2.3 ^{13}C-NMR: Table 2.7 ^{31}P NMR: Table2.8   IR: Table 2.9

Complex A4

A4
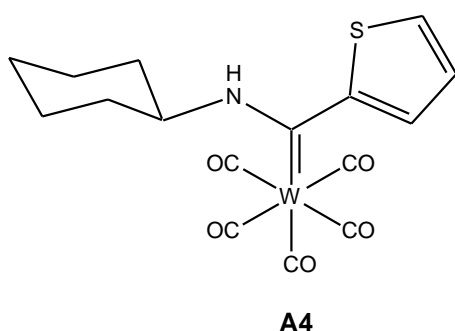
Complex **A** (0.464 g, 1.00 mmol) was dissolved in 20 mL of THF and 0.245 g of cyclohexylamine was added in two portions over a 1 hr period. The solution was allowed to stir for 2 hrs, gradually changing colour from dark red to bright yellow. Solvent was removed and a bright yellow crystalline solid with an oily residue was obtained. The product was purified on a silica gel column with hexane:DCM gradient elution.

114

Yield: 0.455 g, 0.880 mmol, 88%, bright orange yellow solid

M.S. (*m/z*): 433 [M$^+$(-3CO)]; 280 [M$^+$(-5CO; -Cyclohexylamine)]

^{1}H-NMR: Table 3.1 ^{13}C-NMR: Table 3.3   IR: Table 3.8

XRD data in appendix C

Complex B4
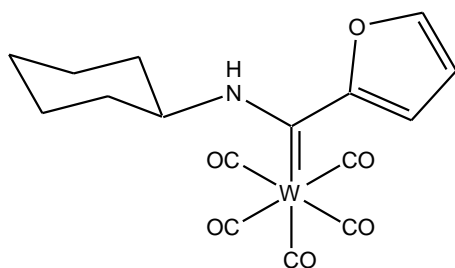
B4

Complex **B** (0.448 g, 1.00 mmol) was dissolved in 30 mL of ether, and cyclohexylamine (0.38 mL, 3.32 mmol) was added in two portions over an hour time period. The reaction mixture, initially, was wine red and gradually became lighter until it was golden yellow. The solution was allowed to stir for approximately 2 hr in total. Solvent was then removed, resulting in a bright yellow crystalline substance with some oily residue. The product was purified on a silica gel column with hexane:DCM gradient elution.

Yield: 0.474 g, 0.946 mmol, 94.6 %, bright yellow solid

M.S. (*m/z*): 280 [M$^+$(-5CO; -Cyclohexyl)]

^{1}H-NMR: Table 3.2 ^{13}C-NMR: Table 3.4   IR: Table 3.8

XRD data in appendix D

115

Complex A5

A5
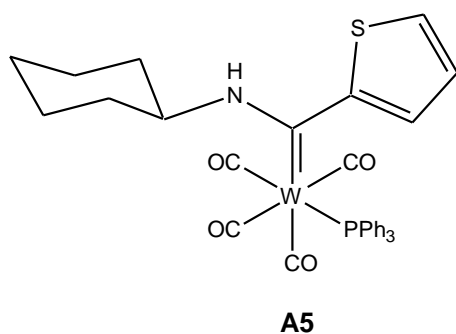
Complex **A4** (0.258 g, 0.51 mmol) and PPh$_3$ (0.264 g, 1.01 mmol) was dissolved in 40 mL of toluene, resulting in a bright yellow solution. The reaction mixture was allowed to reflux, with stirring for 4 hrs. At this point, decomposition products were evident as a brown precipitate was formed, and thus the solution was cooled immediately and the solvent removed. A bright orange solid was obtained. The crude product was then purified on a silica gel column using hexane:DCM gradient elution. Two fractions were collected. The first fraction was **A4** (0.207g, 0.41mmol). The second fraction was bright orange and contained the product. The product was obtained as a pale orange crystalline solid.

Yield: 0.162 g, 0.216 mmol, 42.02%, pale orange crystalline solid

^{1}H-NMR: Table 3.1 ^{13}C-NMR: Table 3.3 ^{31}P NMR: Table 3.5   IR: Table 3.8

XRD data in appendix E

Complex B5

B5
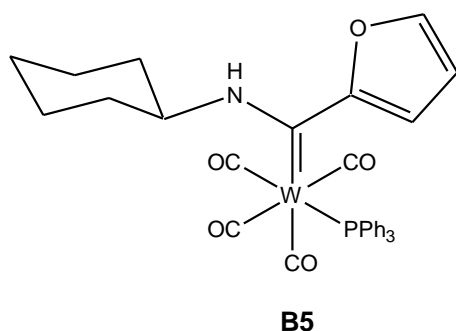
Complex **B1** (0.144 g, 0.21 mmol) was dissolved in 20 mL of ether, resulting in a dark brown-red solution. Cyclohexylamine (0.02 mL, 0.35 mmol) was added to the solution in two equal portions, one hour apart. The reaction was allowed to stir overnight. The crude product was then purified on a silica gel column using hexane:DCM gradient elution. Two bands were isolated. The first band was the starting complex **B1**. The second band was bright orange and identified as the target compound. A pale orange crystalline solid was obtained after the solvent was removed.

Yield: 0.060 g, 0.082 mmol, 39%, pale orange crystalline solid

¹H-NMR: Table 3.2   ¹³C-NMR: Table 3.4   ³¹P NMR: Table 3.5   IR: Table 3.8

Complex A6

A6
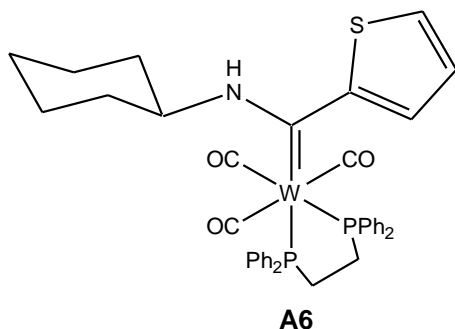
Complex **A4** (0.260 g, 0.503 mmol) and DPPE (0.249 g, 0.625 mmol) were dissolved in 20 mL of toluene, and allowed to reflux with stirring for 24 hrs. The reaction mixture was initially bright yellow and gradually became a dark wine red solution. TLC indicated the presence of both the *fac* and *mer* isomers. The solvent was removed, yielding a dark red solid as the crude product. Purification by crystallization was attempted as for the ethoxy analogues. However, this proved to be unsuccessful. The crude product was thus purified on a silica gel column using hexane:DCM gradient elution. Yield was very low and thus estimated.

Yield: ±15 %, orange solid

¹H-NMR: Table 3.1   ¹³C-NMR: Table 3.3   ³¹P NMR: Table 3.5   IR: Table 3.8

Complex B6

B6
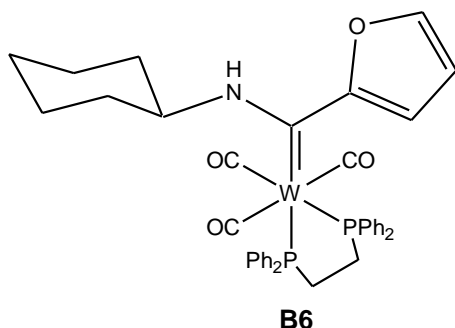
Complex **B4** (0.375 g, 0.748 mmol) and DPPE (0.305 g, 0.766 mmol) were dissolved in 30 mL of toluene. This mixture was allowed to reflux with stirring for 24 hrs. The solution, initially, was bright yellow and became dark red. The solvent was removed, and TLC indicated the presence of starting material, **B4**, and two red products. Purification by crystallization failed in this case as for the thienyl-

117

analogue. The crude product was thus purified on a silica gel column using hexane:DCM gradient elution. 2 bands were collected, namely, the starting cycloaminocarbene, **B4**, and the target complex, **B6**. Due to extremely low yield, the percentage yield could only be estimated.

Yield: ±10%, orange solid

M.S. (*m/z*): 843 [M$^+$]; 453 [M$^+$(-4Ph;-CO; -Cyclohexyl)]; 425 [M$^+$(-4Ph;-2CO; -Cyclohexyl)]; 397 [M$^+$(-4Ph;-3CO; -Cyclohexyl)]

^{1}H-NMR: Table 3.2 ^{31}P NMR: Table 3.5   IR: Table 3.8.

Complex A7
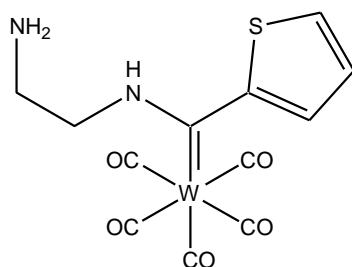
A7

Ethylenediamine (0.05 mL, 0.75 mmol) was dissolved in 10 mL of DCM, and complex **A** (0.232g, 0.50 mmol) was added to the solution while maintaining vigorous stirring. Initially the reaction mixture was dark red, but gradually became bright yellow. The solvent was removed, yielding a bright yellow crystalline solid.

Yield : 0.136 g, 0.284 mmol, 56.89%, bright yellow crystalline solid

^{1}H-NMR: Table 3.6 ^{13}C-NMR: Table 3.7   IR: Table 3.8

Complex B7
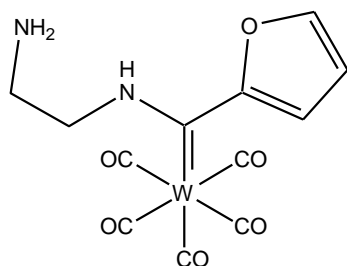
B7

Ethylenediamin (0.05 mL, 0.75 mmol) was dissolved in 10 mL of DCM. Complex **B** (0.224 g, 0.50 mmol) dissolved in 10 mL of DCM (bright red solution), was added dropwise, with vigorous stirring, to the ethylenediamine solution. The solution immediately turned bright yellow. The solvent was removed, yielding a bright yellow crystalline solid.

Yield: 0.164 g, 0.355 mmol, 70.8 %, bright yellow crystalline solid

M.S. (*m/z*): 279 [M$^+$(-EtNH$_2$; -5CO)]

^{1}H-NMR: Table 3.6 ^{13}C-NMR: Table 3.7   IR: Table 3.8

Complex A8
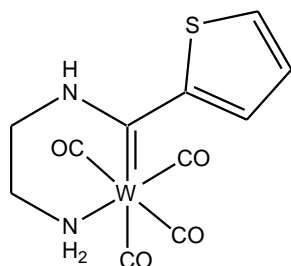
A8

Ethylenediamine (0.0763 g, 1.27 mmol) was dissolved in 30 mL of toluene and placed in a heated oil bath at 105°C. Complex **A** (0.465 g, 1.00 mmol) was added to the solution, forming a dark red solution. The reaction mixture was allowed to reflux for 1 ½ hrs, with stirring. The solution was dark orange-red and an orange precipitate formed. The reaction mixture was allowed to cool, while the precipitate was allowed to settle. The solvent was decanted and the resulting orange precipitate washed with cold hexane. This precipitate was found to be only mildly soluble in DCM. It was completely soluble in THF and acetonitrile.

Yield: 0.228 g, 0.507 mmol, bright orange solid

^{1}H-NMR: Table 3.6 ^{13}C-NMR: Table 3.7   IR: Table 3.8

Complex B8
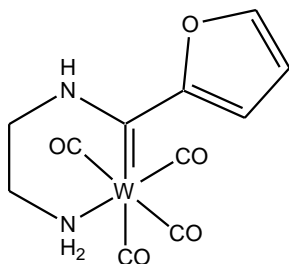
B8

Ethylenediamine (0.075 g, 1.25 mmol) was dissolved in 40 mL of toluene and heated at 110 °C for 5 min. Complex **B** (0.448 g, 1.00 mmol) was added to the heated solution. The reaction was allowed to reflux for 5 hrs until no more starting material was observed on TLC. The solution was initially yellow, and became dark red with time. Once reflux was completed, a large amount of orange precipitate was observed, with a yellow-orange solution above. The reaction mixture was cooled and the precipitate allowed to settle overnight. The solvent was carefully decanted, yielding a bright orange solid which was further washed with cold hexane. This precipitate was partially soluble in DCM, and completely soluble in THF and acetonitrile.

Yield: 0.214 g, 0.49 mmol, 49.30 %, bright orange solid

^{1}H-NMR: Table 3.6 ^{13}C-NMR: Table 3.7   IR: Table 3.8

XRD data in appendix F

1,3-Bis-(2,4,6-trimethyl-phenyl)-imidazolium chloride[11]
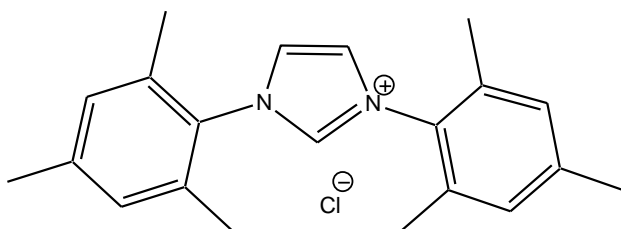
This synthesis deviated from that published in literature. Paraformaldehyde (0.16 g, 5.33 mmol) and glyoxalbis(2,4,6-trimethylphenyl)imine (1.467 g, 5.02 mmol) were mixed in 50mL of toluene and allowed to reflux with stirring for 5 hrs. The mixture remained bright yellow throughout. The reaction

120

mixture was then allowed to cool. HCl (6M, 4 ml, 24 mmol) was mixed with dioxane (2 mL) and added dropwise to the reaction mixture. The reaction mixture was then allowed to stir for 5 days. Initially this reaction mixture was yellow with a white precipitate that formed; however, it finally was a brown-white suspension. The solution was filtered, and the filtrate washed several times with cold THF. This was repeated until no more filtrate was obtained. Two distinct filtrates were thus obtained, and both were air dried. The first crop was a beige powdery substance, and the second, a fine white feathery crystalline substance. The filtrates were combined and dissolved in minimal warm EtOH. Ether was then added slowly to the solution until crystallization started. The solution was placed in an ice bath and allowed to cool. Fine white feathery crystals were obtained after filtration and air drying.

Yield: 0.764 g, 2.24 mmol, 45%, white crystalline solid

Complex C1

C1
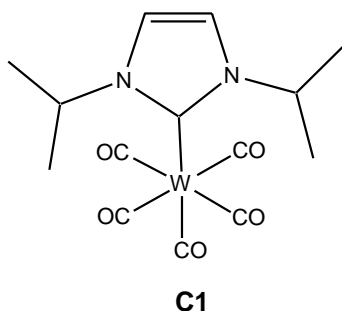
a) W(CO)$_6$ (0.396 g, 1.13 mmol) was dissolve in 40 mL of THF and photolysed for 4 ½ hrs, resulting in a green-yellow solution.

b) 1,3-Di-i-propylimidazolium chloride (0.139 g, 1.00 mmol) was placed in 30 mL of THF and cooled to -30 °C. KO^{t}Bu (0.139 g, 1.18 mmol) was added to this suspension, and the reaction mixture was stirred at -30°C for 30 min, forming a beige suspension.

Reaction mixture (a) was added to reaction mixture (b) at -30 °C. This mixture was allowed to stir at this cold temperature for 1hr, and was then stirred at RT. for another 2 hrs. A bright yellow solution with a white precipitate was obtained. The solvent was removed yielding the crude product as a greenish yellow solid. The crude product was purified on a silica gel column with hexane:DCM gradient elution, and finally washed with ether. A single yellow fraction was collected. This product was minimally soluble in CDCl$_3$ and was sensitive to CD$_2$Cl$_2$. Minimal yield was obtained, and thus it was only estimated. A green yellow solid was obtained after the solvent was removed. No characterisation could be done due to the limited yield.

Yield: < 5%, green yellow crystalline solid

121

Complex C2

Method A: Purchased 1,3-Bis(2,4,6-trimethylphenyl)imidazolium chloride
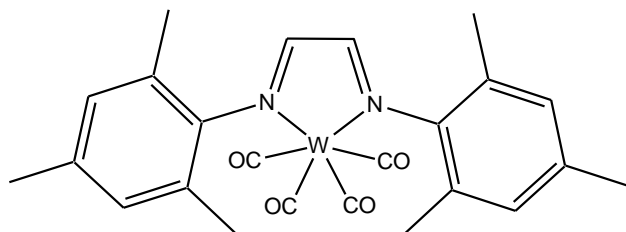
C3

a) W(CO)$_6$ (0.530 g, 1.51 mmol) was placed in 5 mL of THF and 50 mL of hexane. Photolysis was carried out on this solution for 5hr. A dark yellow solution was obtained.

b) 1,3-Bis(2,4,6-trimethylphenyl)imidazolium chloride (0.375 g, 1.10 mmol) and KO^{t}Bu (0.138 g, 1.18 mmol) were dissolved in 20 mL of THF, and allowed to stir at RT for 30 min. A bright yellow solution was obtained.

Solution (a) was mixed with solution (b) and then allowed to stir for 3 hr. The reaction mixture was bright orange. The solvent was removed and the crude product purified on silica using a hexane: DCM gradient. Upon addition of silica to a DCM solution of the crude product, for dry loading, the solution became dark pink. The product eluted in a non polar gradient as a bright pink band. A bright pink solid, **C3**, was obtained after evaporation. Several other bands were visible; however, none were obtained in large enough quantities for characterisation.

Yield: 10%, dark pink solid

^{1}H-NMR (δ, ppm) (CDCl$_3$): 2.06 (s, 12 H, CH$_3$), 2.34 (s, 6 H, CH$_3$),7.02 (s, 4H, CH) ,7.05 (s, 2H, N=CH)

^{13}C-NMR (δ, ppm) (CDCl$_3$): 17.9 (*ortho*, CH$_3$), 21.1 (*para*, CH$_3$) 123.4 (*ortho*), 129.5 (*meta*), 135.6 (*para*), 137.7 (C=C), 139.8 (N-C$_{arom}$)

IR (ν, cm^{-1}): 1873, 1908, 1963, 2057

XRD data found in appendix G

Method B: 1,3-Bis(2,4,6-trimethylphenyl)imidazolium chloride synthesised as described above.
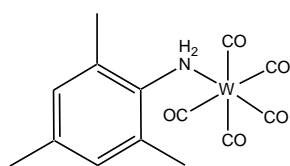
C4

a) $W(CO)_6$ (0.530 g, 1.51 mmol) was dissolved in a THF:hexane mixture (5 mL:50 mL). This solution was photolysed for 5 hrs, resulting in a bright yellow solution.

b) KO^{t}Bu (0.138 g, 1.23 mmol) and 1,3-bis(2,4,6-trimethylphenyl)imidazolium chloride (0.375 g, 1.10 mmol) were mixed in THF and allowed to stir for 30 min, at RT. The solution was beige coloured.

Reaction mixture (a) was then added to reaction mixture (b), and the resultant solution was allowed to stir for 3 hrs at RT. The mixture was initially bright yellow and progressively became yellow-green. The solvent was removed, and a green-yellow solid obtained. The crude product was purified on silica using hexane:DCM gradient elution. A single yellow band was obtained. A yellow solid, **C4**, was obtained after removal of the solvent. Minimal yields were obtained, and thus this was only estimated.

Yield: 5%, yellow crystalline solid

^{1}H-NMR (δ; ppm) (CDCl$_3$): 2.25 (s, 3H, CH$_3$), 2.34 (s, 6H, CH$_3$), 4.25 (s, NH$_2$), 6.83 (s,2H,CH)

^{13}C-NMR (δ; ppm) (CDCl$_3$): 17.4 (*ortho*, CH$_3$), 20.5 (*para*, CH$_3$) 124.9 (*ortho*), 130.1 (*meta*), 134.1 (*para*), 140.4 (N-C$_{arom}$)

IR (ν, cm^{-1}): 1844, 1867, 1910, 1943, 2071

XRD data in appendix H

123

6.3 REFERENCES

(1)   Schriver, D. F.; Drezdzon, M. A. *The manipulation of Air-Sensitive Compounds*; 2 nd.; Wiley: New York, **1980**.

(2)   Frisch, M. J., Trucks, G. W., Schlegel, H. B., Scuseria, G. E., Robb, M. A., Cheeseman, J. R., Montgomery Jr, J. A., Vreven, T., Kudin, K. N., Burant, J. C., Millam, J. M., Lyengar, S. S., Tomasi, J., Barone, V., Mennucci, B., Cossi, M., Scalmani, G., Rega, N., Petersson, G. A., Nakatsuji, H., Hada, M., Ehara, M., Toyota, K., Fukuda, R., Hasegawa, J., Ishida, M., Nakajima, T., Honda, Y., Kitao, O., Nakai, H., Klene, M., Li, X., Knox, J. E., Hratchian, H. P., Cross, J. B., Bakken, V., Adamo, C., Jaramillo, J., Gomperts, R., Stratmann, R. E., Yazyev, O., Austin, A. J., Cammi, R., Pomelli, C., Ochterski, J. W., Ayala, P. Y., Morokuma, K., Voth, G. A., Salvador, P., Dannenberg, J. J., Zakrzewski, V. G., Dapprich, S., Daniels, A. D., Strain, M. C., Farkas, O., Malick, D. K., Rabuck, A. D., Raghavachari, K., Foresman, J. B., Ortiz, J. V., Cui, Q. Baboul, A. G., Clifford, S., Cioslowski, J., Stefanov, B. B., Liu, G., Liashenko, A., Piskorz, P., Komaromi, I., Martin, R. L., Fox, D. J., Keith, T., Al-Laham, M. A., Peng, C. Y., Nanayakkara, A., Challacombe, M., Gill, P. M., Johnson, W. B., Chen, W., Wong, M. W., Gonzalez, C., Pople, J. A.,*Gaussian 03*, revision D.01 Gaussian, Inc., Wallingford CT, **2004**.

(3)   Foresman, J.B.; Frisch, Æ. *Exploring chemistry with electronic structure methods*; 2nd ed.; Gaussian Inc.: Pittsburgh, **1996**

(4)   Cramer, C.J.; Truhlar, D.G. *Phys. Chem. Chem. Phys.* **2009**, *11*, 10757

(5)   Landman, M.; Barnard, W.; van Rooyen, P.H.; Liles, D.C. *J. Mol. Struct.* **2012**, *1021,* 76

(6)   Arrieta, A.; Cossío, F. P.; Fernández, I.; Gomez-Gallego, M.; Lecea, B.; Mancheno, M. J.; Sierra, M. A. *J. Am. Chem. Soc.* **2000**, *122*, 11509.

(7)   Bezuidenhout, D.I. Multimetal complexes of Fischer carbenes, University of Pretoria, **2010**

(8)   Aoki, S.; Fujimura, T.; Nakamura, E. *J. Am. Chem. Soc.* **1992**, *114*, 2985

(9)   Crause, C. Synthesis and application of carbene complexes with heteroaromatic substituents, University of Pretoria, **2004**

(10)   Crause, C.; Lotz, S. *Dalton Trans.* **2005**, *9*, 1649

(11)   Hintermann, L. *Beilstein Journal of Organic Chemistry* **2007**, *5*, 2

124

APPENDIX A:

CRYSTALLOGRAPHIC DATA OF W(CO)₄DPPE
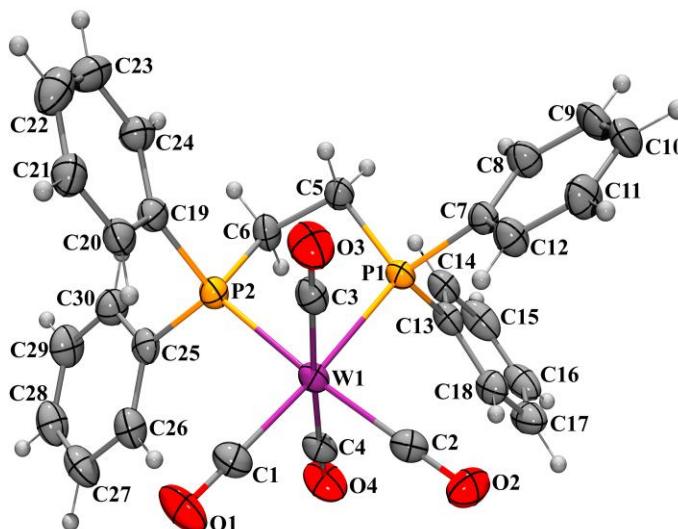
Table 1. Crystal data and structure refinement for W(CO)$_4$DPPE.

Identification code	up1207	
Empirical formula	C30 H24 O4 P2 W	
Formula weight	694.28	
Temperature	180(2) K	
Wavelength	0.71073 Å	
Crystal system	Orthorhombic	
Space group	Pbca	
Unit cell dimensions	a = 16.7462(2) Å	$\square$= 90°.
	b = 14.4634(2) Å	$\square$= 90°.
	c = 22.3021(4) Å	$\square$ = 90°.
Volume	5401.73(14) Å^3	
Z	8	
Density (calculated)	1.707 Mg/m^3	

Absorption coefficient	$4.430\ mm^{-1}$
F(000)	2720
Crystal size	$0.16 \times 0.10 \times 0.02\ mm^3$
Theta range for data collection	3.57 to 27.87°.
Index ranges	-19<=h<=22, -18<=k<=18, -29<=l<=29
Reflections collected	42908
Independent reflections	6401 [R(int) = 0.0749]
Completeness to theta = 27.87°	99.7 %
Absorption correction	Semi-empirical from equivalents
Max. and min. transmission	0.930 and 0.740
Refinement method	Full-matrix least-squares on F^2
Data / restraints / parameters	6401 / 0 / 334
Goodness-of-fit on F^2	1.017
Final R indices [I>2sigma(I)]	R1 = 0.0351, wR2 = 0.0628
R indices (all data)	R1 = 0.0701, wR2 = 0.0715
Extinction coefficient	0
Largest diff. peak and hole	1.778 and $-1.425\ e.Å^{-3}$

126

Table 2.   Atomic coordinates (x 10^4) and equivalent isotropic displacement parameters (Å^{2}x 10^3) for W(CO)₄DPPE.   U(eq) is defined as one third of the trace of the orthogonalized U^{ij} tensor.

	x	y	z	U(eq)
W(1)	183(1)	3961(1)	3817(1)	26(1)
C(1)	557(3)	5267(3)	3746(2)	36(1)
O(1)	792(2)	6017(2)	3702(2)	55(1)
C(2)	448(2)	3924(3)	4681(2)	31(1)
O(2)	573(2)	3890(2)	5193(1)	44(1)
C(3)	1282(3)	3504(3)	3578(2)	30(1)
O(3)	1902(2)	3242(2)	3441(2)	49(1)
C(4)	-938(3)	4348(3)	4065(2)	34(1)
O(4)	-1578(2)	4519(2)	4202(2)	50(1)
P(1)	-292(1)	2327(1)	3825(1)	26(1)
P(2)	-346(1)	3845(1)	2774(1)	29(1)
C(5)	-515(2)	1978(3)	3049(2)	31(1)
C(6)	-942(2)	2777(3)	2722(2)	33(1)
C(7)	327(2)	1395(3)	4124(2)	29(1)
C(8)	75(3)	474(3)	4087(2)	38(1)
C(9)	518(3)	-213(3)	4368(2)	45(1)
C(10)	1213(3)	0(3)	4668(2)	43(1)
C(11)	1468(3)	903(3)	4691(2)	40(1)
C(12)	1025(2)	1590(3)	4422(2)	35(1)
C(13)	-1218(2)	2139(3)	4243(2)	31(1)
C(14)	-1886(3)	1689(3)	4011(2)	36(1)
C(15)	-2545(3)	1550(3)	4372(3)	46(1)
C(16)	-2549(3)	1833(3)	4955(2)	45(1)
C(17)	-1902(3)	2294(3)	5189(2)	43(1)
C(18)	-1243(3)	2447(3)	4836(2)	35(1)
C(19)	403(3)	3738(3)	2175(2)	32(1)
C(20)	1084(2)	4285(3)	2217(2)	34(1)
C(21)	1689(3)	4223(3)	1792(2)	39(1)
C(22)	1615(3)	3621(4)	1319(2)	50(1)
C(23)	936(3)	3076(4)	1270(2)	47(1)
C(24)	337(3)	3134(3)	1691(2)	36(1)

C(25)	-1050(2)	4725(3)	2498(2)	30(1)
C(26)	-1113(3)	5565(3)	2788(2)	38(1)
C(27)	-1656(3)	6235(3)	2587(2)	48(1)
C(28)	-2142(3)	6047(3)	2105(2)	45(1)
C(29)	-2086(3)	5215(3)	1815(2)	44(1)
C(30)	-1542(2)	4557(3)	2009(2)	39(1)

_____

Table 3.   Bond lengths [Å] and angles [°] for W(CO)$_4$DPPE.

_____

W(1)-C(2)	1.978(4)	C(14)-C(15)	1.380(6)
W(1)-C(1)	1.996(4)	C(14)-H(14)	0.9500
W(1)-C(3)	2.027(5)	C(15)-C(16)	1.365(7)
W(1)-C(4)	2.036(5)	C(15)-H(15)	0.9500
W(1)-P(1)	2.4940(10)	C(16)-C(17)	1.374(6)
W(1)-P(2)	2.4964(11)	C(16)-H(16)	0.9500
C(1)-O(1)	1.158(5)	C(17)-C(18)	1.374(6)
C(2)-O(2)	1.161(5)	C(17)-H(17)	0.9500
C(3)-O(3)	1.147(5)	C(18)-H(18)	0.9500
C(4)-O(4)	1.140(5)	C(19)-C(20)	1.390(6)
P(1)-C(7)	1.827(4)	C(19)-C(24)	1.394(6)
P(1)-C(13)	1.830(4)	C(20)-C(21)	1.390(6)
P(1)-C(5)	1.841(4)	C(20)-H(20)	0.9500
P(2)-C(19)	1.838(4)	C(21)-C(22)	1.372(7)
P(2)-C(25)	1.840(4)	C(21)-H(21)	0.9500
P(2)-C(6)	1.843(4)	C(22)-C(23)	1.389(7)
C(5)-C(6)	1.542(5)	C(22)-H(22)	0.9500
C(5)-H(5A)	0.9900	C(23)-C(24)	1.375(6)
C(5)-H(5B)	0.9900	C(23)-H(23)	0.9500
C(6)-H(6A)	0.9900	C(24)-H(24)	0.9500
C(6)-H(6B)	0.9900	C(25)-C(26)	1.380(6)
C(7)-C(12)	1.374(6)	C(25)-C(30)	1.388(6)
C(7)-C(8)	1.399(6)	C(26)-C(27)	1.403(6)
C(8)-C(9)	1.389(6)	C(26)-H(26)	0.9500
C(8)-H(8)	0.9500	C(27)-C(28)	1.375(7)
C(9)-C(10)	1.378(6)	C(27)-H(27)	0.9500
C(9)-H(9)	0.9500	C(28)-C(29)	1.369(6)
C(10)-C(11)	1.375(6)	C(28)-H(28)	0.9500
C(10)-H(10)	0.9500	C(29)-C(30)	1.387(6)
C(11)-C(12)	1.378(6)	C(29)-H(29)	0.9500
C(11)-H(11)	0.9500	C(30)-H(30)	0.9500
C(12)-H(12)	0.9500		
C(13)-C(14)	1.394(6)	C(2)-W(1)-C(1)	91.85(17)
C(13)-C(18)	1.396(6)	C(2)-W(1)-C(3)	92.57(17)

129

C(1)-W(1)-C(3)	90.16(16)	C(5)-C(6)-H(6A)	109.6
C(2)-W(1)-C(4)	87.15(18)	P(2)-C(6)-H(6A)	109.6
C(1)-W(1)-C(4)	92.92(17)	C(5)-C(6)-H(6B)	109.6
C(3)-W(1)-C(4)	176.91(15)	P(2)-C(6)-H(6B)	109.6
C(2)-W(1)-P(1)	92.26(12)	H(6A)-C(6)-H(6B)	108.1
C(1)-W(1)-P(1)	175.83(13)	C(12)-C(7)-C(8)	118.7(4)
C(3)-W(1)-P(1)	88.98(11)	C(12)-C(7)-P(1)	120.5(3)
C(4)-W(1)-P(1)	87.96(12)	C(8)-C(7)-P(1)	120.6(3)
C(2)-W(1)-P(2)	170.44(12)	C(9)-C(8)-C(7)	119.6(4)
C(1)-W(1)-P(2)	95.80(13)	C(9)-C(8)-H(8)	120.2
C(3)-W(1)-P(2)	93.13(13)	C(7)-C(8)-H(8)	120.2
C(4)-W(1)-P(2)	86.75(13)	C(10)-C(9)-C(8)	120.7(4)
P(1)-W(1)-P(2)	80.18(3)	C(10)-C(9)-H(9)	119.7
O(1)-C(1)-W(1)	178.4(4)	C(8)-C(9)-H(9)	119.7
O(2)-C(2)-W(1)	177.3(4)	C(11)-C(10)-C(9)	119.6(4)
O(3)-C(3)-W(1)	179.7(4)	C(11)-C(10)-H(10)	120.2
O(4)-C(4)-W(1)	176.5(4)	C(9)-C(10)-H(10)	120.2
C(7)-P(1)-C(13)	100.70(18)	C(10)-C(11)-C(12)	120.1(4)
C(7)-P(1)-C(5)	104.82(18)	C(10)-C(11)-H(11)	120.0
C(13)-P(1)-C(5)	105.48(19)	C(12)-C(11)-H(11)	120.0
C(7)-P(1)-W(1)	121.38(13)	C(7)-C(12)-C(11)	121.4(4)
C(13)-P(1)-W(1)	114.50(13)	C(7)-C(12)-H(12)	119.3
C(5)-P(1)-W(1)	108.53(13)	C(11)-C(12)-H(12)	119.3
C(19)-P(2)-C(25)	104.64(19)	C(14)-C(13)-C(18)	118.5(4)
C(19)-P(2)-C(6)	104.73(19)	C(14)-C(13)-P(1)	124.0(3)
C(25)-P(2)-C(6)	102.26(18)	C(18)-C(13)-P(1)	117.4(3)
C(19)-P(2)-W(1)	116.10(14)	C(15)-C(14)-C(13)	119.5(5)
C(25)-P(2)-W(1)	119.50(14)	C(15)-C(14)-H(14)	120.2
C(6)-P(2)-W(1)	107.85(14)	C(13)-C(14)-H(14)	120.2
C(6)-C(5)-P(1)	109.4(3)	C(16)-C(15)-C(14)	121.1(4)
C(6)-C(5)-H(5A)	109.8	C(16)-C(15)-H(15)	119.5
P(1)-C(5)-H(5A)	109.8	C(14)-C(15)-H(15)	119.5
C(6)-C(5)-H(5B)	109.8	C(15)-C(16)-C(17)	120.2(4)
P(1)-C(5)-H(5B)	109.8	C(15)-C(16)-H(16)	119.9
H(5A)-C(5)-H(5B)	108.2	C(17)-C(16)-H(16)	119.9
C(5)-C(6)-P(2)	110.3(3)	C(16)-C(17)-C(18)	119.7(5)

130

C(16)-C(17)-H(17)	120.2	C(23)-C(24)-H(24)	119.7
C(18)-C(17)-H(17)	120.2	C(19)-C(24)-H(24)	119.7
C(17)-C(18)-C(13)	120.9(4)	C(26)-C(25)-C(30)	118.5(4)
C(17)-C(18)-H(18)	119.5	C(26)-C(25)-P(2)	120.1(3)
C(13)-C(18)-H(18)	119.5	C(30)-C(25)-P(2)	121.4(3)
C(20)-C(19)-C(24)	118.2(4)	C(25)-C(26)-C(27)	120.5(4)
C(20)-C(19)-P(2)	117.7(3)	C(25)-C(26)-H(26)	119.8
C(24)-C(19)-P(2)	124.2(3)	C(27)-C(26)-H(26)	119.8
C(19)-C(20)-C(21)	121.1(4)	C(28)-C(27)-C(26)	119.8(5)
C(19)-C(20)-H(20)	119.5	C(28)-C(27)-H(27)	120.1
C(21)-C(20)-H(20)	119.5	C(26)-C(27)-H(27)	120.1
C(22)-C(21)-C(20)	119.9(4)	C(29)-C(28)-C(27)	120.2(4)
C(22)-C(21)-H(21)	120.0	C(29)-C(28)-H(28)	119.9
C(20)-C(21)-H(21)	120.0	C(27)-C(28)-H(28)	119.9
C(21)-C(22)-C(23)	119.6(4)	C(28)-C(29)-C(30)	120.1(4)
C(21)-C(22)-H(22)	120.2	C(28)-C(29)-H(29)	120.0
C(23)-C(22)-H(22)	120.2	C(30)-C(29)-H(29)	120.0
C(24)-C(23)-C(22)	120.6(5)	C(29)-C(30)-C(25)	121.0(4)
C(24)-C(23)-H(23)	119.7	C(29)-C(30)-H(30)	119.5
C(22)-C(23)-H(23)	119.7	C(25)-C(30)-H(30)	119.5
C(23)-C(24)-C(19)	120.6(4)		

_____

131

Table 4.   Anisotropic displacement parameters (Å²x 10³)for W(CO)₄DPPE.   The anisotropic displacement factor exponent takes the form: $-2\pi^2[\,h^2a^{*2}U^{11} + ... + 2\,h\,k\,a^*\,b^*\,U^{12}\,]$

	U^{11}	U^{22}	U^{33}	U^{23}	U^{13}	U^{12}
W(1)	25(1)	22(1)	30(1)	-1(1)	-1(1)	-1(1)
C(1)	33(2)	30(2)	44(3)	-3(2)	-2(2)	3(2)
O(1)	52(2)	26(2)	86(3)	2(2)	1(2)	-11(1)
C(2)	27(2)	28(2)	37(3)	-6(2)	-1(2)	1(2)
O(2)	41(2)	55(2)	36(2)	-9(2)	-6(2)	5(2)
C(3)	32(3)	25(2)	35(2)	1(2)	-2(2)	-3(2)
O(3)	36(2)	48(2)	62(2)	4(2)	7(2)	7(2)
C(4)	35(3)	26(2)	41(3)	-4(2)	-1(2)	-3(2)
O(4)	32(2)	43(2)	75(3)	0(2)	8(2)	6(1)
P(1)	27(1)	21(1)	29(1)	-1(1)	0(1)	-1(1)
P(2)	30(1)	26(1)	30(1)	1(1)	-2(1)	-1(1)
C(5)	36(2)	27(2)	29(2)	0(2)	-2(2)	-4(2)
C(6)	36(3)	31(2)	33(3)	6(2)	-6(2)	-4(2)
C(7)	31(3)	25(2)	30(2)	1(2)	3(2)	-1(2)
C(8)	40(3)	30(2)	42(3)	-2(2)	-5(2)	-4(2)
C(9)	60(3)	21(2)	54(3)	3(2)	-4(3)	3(2)
C(10)	54(3)	32(3)	42(3)	4(2)	-8(2)	13(2)
C(11)	38(3)	42(3)	41(3)	1(2)	-12(2)	2(2)
C(12)	35(3)	29(2)	41(3)	1(2)	-4(2)	-2(2)
C(13)	29(2)	23(2)	41(3)	4(2)	0(2)	1(2)
C(14)	35(3)	29(2)	44(3)	1(2)	-1(2)	0(2)
C(15)	23(2)	34(3)	80(4)	6(3)	1(3)	-1(2)
C(16)	35(3)	32(3)	68(4)	6(3)	17(3)	5(2)
C(17)	48(3)	34(2)	47(3)	-3(2)	13(2)	2(2)
C(18)	33(2)	32(2)	39(3)	1(2)	6(2)	-3(2)
C(19)	34(2)	32(2)	30(2)	3(2)	0(2)	7(2)
C(20)	36(3)	30(2)	35(3)	4(2)	0(2)	2(2)
C(21)	38(3)	42(3)	37(3)	6(2)	4(2)	2(2)
C(22)	42(3)	67(3)	40(3)	8(3)	8(2)	10(3)
C(23)	49(3)	56(3)	35(3)	-9(2)	2(2)	10(3)
C(24)	37(3)	37(2)	35(2)	-3(2)	-1(2)	2(2)

132

C(25)	26(2)	31(2)	34(2)	6(2)	3(2)	-3(2)
C(26)	35(3)	36(3)	43(3)	7(2)	-4(2)	-2(2)
C(27)	47(3)	32(2)	64(4)	8(2)	0(3)	6(2)
C(28)	34(3)	44(3)	57(3)	15(3)	-5(2)	1(2)
C(29)	38(3)	50(3)	45(3)	6(2)	-12(2)	0(2)
C(30)	40(3)	41(3)	37(3)	1(2)	-5(2)	-2(2)

_____

Table 5.   Hydrogen coordinates (x 10^4) and isotropic displacement parameters (Å^{2}x 10^3) for W(CO)$_4$DPPE.

	x	y	z	U(eq)
H(5A)	-13	1823	2837	37
H(5B)	-860	1422	3050	37
H(6A)	-1474	2879	2905	40
H(6B)	-1022	2611	2296	40
H(8)	-396	320	3872	45
H(9)	340	-836	4353	54
H(10)	1514	-473	4858	51
H(11)	1951	1053	4893	48
H(12)	1206	2212	4444	42
H(14)	-1888	1481	3607	43
H(15)	-3003	1252	4211	55
H(16)	-3000	1710	5201	54
H(17)	-1912	2505	5592	52
H(18)	-797	2767	4999	42
H(20)	1136	4707	2540	41
H(21)	2153	4596	1829	47
H(22)	2026	3578	1027	60
H(23)	884	2659	944	56
H(24)	-125	2759	1650	44
H(26)	-786	5690	3127	45
H(27)	-1688	6817	2782	57
H(28)	-2517	6495	1973	54
H(29)	-2420	5089	1481	53
H(30)	-1506	3982	1805	47

134

Table 6.   Torsion angles [°] for W(CO)$_4$DPPE.

_____

C(2)-W(1)-P(1)-C(7)	-52.2(2)
C(3)-W(1)-P(1)-C(7)	40.3(2)
C(4)-W(1)-P(1)-C(7)	-139.3(2)
P(2)-W(1)-P(1)-C(7)	133.68(16)
C(2)-W(1)-P(1)-C(13)	68.91(19)
C(3)-W(1)-P(1)-C(13)	161.4(2)
C(4)-W(1)-P(1)-C(13)	-18.1(2)
P(2)-W(1)-P(1)-C(13)	-105.20(16)
C(2)-W(1)-P(1)-C(5)	-173.57(18)
C(3)-W(1)-P(1)-C(5)	-81.03(19)
C(4)-W(1)-P(1)-C(5)	99.37(19)
P(2)-W(1)-P(1)-C(5)	12.32(14)
C(1)-W(1)-P(2)-C(19)	74.62(19)
C(3)-W(1)-P(2)-C(19)	-15.86(18)
C(4)-W(1)-P(2)-C(19)	167.23(18)
P(1)-W(1)-P(2)-C(19)	-104.28(15)
C(1)-W(1)-P(2)-C(25)	-52.30(19)
C(3)-W(1)-P(2)-C(25)	-142.78(18)
C(4)-W(1)-P(2)-C(25)	40.31(18)
P(1)-W(1)-P(2)-C(25)	128.80(14)
C(1)-W(1)-P(2)-C(6)	-168.31(19)
C(3)-W(1)-P(2)-C(6)	101.22(18)
C(4)-W(1)-P(2)-C(6)	-75.70(18)
P(1)-W(1)-P(2)-C(6)	12.79(14)
C(7)-P(1)-C(5)-C(6)	-172.4(3)
C(13)-P(1)-C(5)-C(6)	81.7(3)
W(1)-P(1)-C(5)-C(6)	-41.4(3)
P(1)-C(5)-C(6)-P(2)	54.5(3)
C(19)-P(2)-C(6)-C(5)	82.0(3)
C(25)-P(2)-C(6)-C(5)	-169.0(3)
W(1)-P(2)-C(6)-C(5)	-42.2(3)
C(13)-P(1)-C(7)-C(12)	-119.0(4)
C(5)-P(1)-C(7)-C(12)	131.7(4)
W(1)-P(1)-C(7)-C(12)	8.6(4)

135

C(13)-P(1)-C(7)-C(8)	56.9(4)
C(5)-P(1)-C(7)-C(8)	-52.5(4)
W(1)-P(1)-C(7)-C(8)	-175.6(3)
C(12)-C(7)-C(8)-C(9)	2.1(7)
P(1)-C(7)-C(8)-C(9)	-173.8(4)
C(7)-C(8)-C(9)-C(10)	-1.7(7)
C(8)-C(9)-C(10)-C(11)	0.2(7)
C(9)-C(10)-C(11)-C(12)	0.9(7)
C(8)-C(7)-C(12)-C(11)	-1.0(7)
P(1)-C(7)-C(12)-C(11)	174.9(3)
C(10)-C(11)-C(12)-C(7)	-0.4(7)
C(7)-P(1)-C(13)-C(14)	-100.2(4)
C(5)-P(1)-C(13)-C(14)	8.7(4)
W(1)-P(1)-C(13)-C(14)	127.9(3)
C(7)-P(1)-C(13)-C(18)	78.2(3)
C(5)-P(1)-C(13)-C(18)	-173.0(3)
W(1)-P(1)-C(13)-C(18)	-53.8(3)
C(18)-C(13)-C(14)-C(15)	-0.9(6)
P(1)-C(13)-C(14)-C(15)	177.4(3)
C(13)-C(14)-C(15)-C(16)	-1.0(7)
C(14)-C(15)-C(16)-C(17)	2.3(7)
C(15)-C(16)-C(17)-C(18)	-1.7(7)
C(16)-C(17)-C(18)-C(13)	-0.2(7)
C(14)-C(13)-C(18)-C(17)	1.5(6)
P(1)-C(13)-C(18)-C(17)	-177.0(3)
C(25)-P(2)-C(19)-C(20)	92.5(3)
C(6)-P(2)-C(19)-C(20)	-160.3(3)
W(1)-P(2)-C(19)-C(20)	-41.5(4)
C(25)-P(2)-C(19)-C(24)	-88.7(4)
C(6)-P(2)-C(19)-C(24)	18.5(4)
W(1)-P(2)-C(19)-C(24)	137.3(3)
C(24)-C(19)-C(20)-C(21)	-0.9(6)
P(2)-C(19)-C(20)-C(21)	178.0(3)
C(19)-C(20)-C(21)-C(22)	0.7(7)
C(20)-C(21)-C(22)-C(23)	-0.2(7)
C(21)-C(22)-C(23)-C(24)	0.0(7)

136

C(22)-C(23)-C(24)-C(19)	-0.3(7)
C(20)-C(19)-C(24)-C(23)	0.7(6)
P(2)-C(19)-C(24)-C(23)	-178.1(4)
C(19)-P(2)-C(25)-C(26)	-113.9(3)
C(6)-P(2)-C(25)-C(26)	137.1(3)
W(1)-P(2)-C(25)-C(26)	18.2(4)
C(19)-P(2)-C(25)-C(30)	67.8(4)
C(6)-P(2)-C(25)-C(30)	-41.2(4)
W(1)-P(2)-C(25)-C(30)	-160.1(3)
C(30)-C(25)-C(26)-C(27)	-0.8(6)
P(2)-C(25)-C(26)-C(27)	-179.1(3)
C(25)-C(26)-C(27)-C(28)	1.5(7)
C(26)-C(27)-C(28)-C(29)	-1.3(7)
C(27)-C(28)-C(29)-C(30)	0.5(7)
C(28)-C(29)-C(30)-C(25)	0.2(7)
C(26)-C(25)-C(30)-C(29)	0.0(6)
P(2)-C(25)-C(30)-C(29)	178.2(3)

_____

Symmetry transformations used to generate equivalent atoms:

137

APPENDIX B:

CRYSTALLOGRAPHIC DATA OF COMPLEX A3
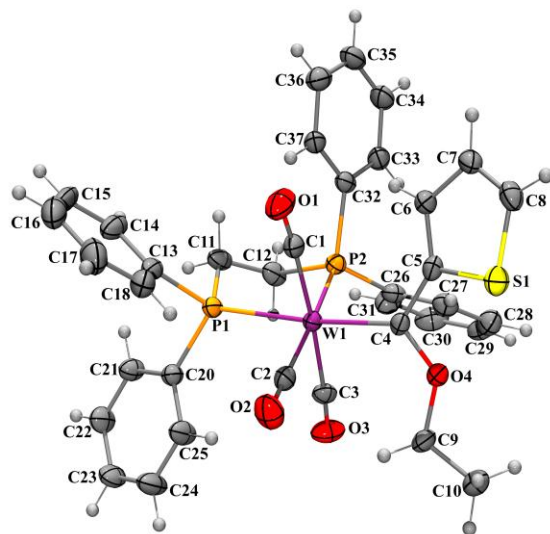
Table 1. Crystal data and structure refinement for **A3**.

Identification code	up1108
Empirical formula	$C_{36}H_{32}O_4P_2SW$
Formula weight	806.47
Temperature	180(2) K
Wavelength	0.71069 Å
Crystal system	Monoclinic
Space group	$P2_1/n$
Unit cell dimensions	a = 15.9555(2) Å α = 90°.
	b = 11.7418(2) Å β = 96.264(1)°.
	c = 17.1911(3) Å γ = 90°.
Volume	3201.46(9) Å^3
Z	4
Density (calculated)	1.673 Mg/m^3
Absorption coefficient	3.813 mm^{-1}
F(000)	1600
Crystal size	0.18 x 0.07 x 0.02 mm^3

θ range for data collection	3.67 to 32.04°.
Index ranges	-23<=h<=23, -10<=k<=17, -25<=l<=25
Reflections collected	42725
Independent reflections	11098 [R(int) = 0.0719]
Completeness to θ = 32.04°	99.5 %
Absorption correction	Semi-empirical from equivalents
Max. and min. transmission	0.9276 and 0.5469
Refinement method	Full-matrix least-squares on F^2
Data / restraints / parameters	11098 / 0 / 398
Goodness-of-fit on F^2	1.020
Final R indices [I>2σ(I)]	R1 = 0.0419, wR2 = 0.0751
R indices (all data)	R1 = 0.0803, wR2 = 0.0846
Extinction coefficient	0
Largest diff. peak and hole	1.151 and -1.187 e.Å^{-3}

Table 2.   Atomic coordinates (x 10^4) and equivalent isotropic displacement parameters (Å^2x 10^3) for **A3**.   U(eq) is defined as one third of the trace of the orthogonalized U^{ij} tensor.

	x	y	z	U(eq)
W(1)	673(1)	1705(1)	7197(1)	23(1)
C(1)	330(2)	1556(3)	6037(2)	30(1)
O(1)	151(2)	1555(3)	5370(2)	48(1)
C(2)	1245(2)	3131(3)	6934(2)	30(1)
O(2)	1590(2)	3939(2)	6751(2)	48(1)
C(3)	968(2)	1949(3)	8353(2)	29(1)
O(3)	1070(2)	2089(3)	9021(2)	44(1)
C(4)	1799(2)	845(3)	7006(2)	23(1)
O(4)	2596(2)	980(2)	7352(1)	31(1)
C(5)	1894(2)	50(3)	6371(2)	25(1)
C(6)	1309(2)	-620(3)	5934(2)	29(1)
C(7)	1673(3)	-1326(3)	5389(2)	32(1)
C(8)	2503(3)	-1190(3)	5404(2)	34(1)
S(1)	2892(1)	-217(1)	6090(1)	36(1)
C(9)	2824(2)	1722(3)	8022(2)	33(1)
C(10)	3776(2)	1684(3)	8147(2)	37(1)
P(1)	-713(1)	2651(1)	7282(1)	27(1)
P(2)	-136(1)	65(1)	7687(1)	26(1)
C(11)	-1483(2)	1572(3)	7541(2)	36(1)
C(12)	-1045(2)	707(3)	8109(2)	34(1)
C(13)	-1262(2)	3349(3)	6411(2)	32(1)
C(14)	-2128(3)	3283(4)	6216(3)	45(1)
C(15)	-2498(3)	3875(5)	5551(3)	56(1)
C(16)	-2029(3)	4516(4)	5101(3)	54(1)
C(17)	-1168(3)	4582(4)	5303(3)	54(1)
C(18)	-792(3)	4007(3)	5944(2)	41(1)
C(20)	-802(2)	3803(3)	8000(2)	27(1)
C(21)	-1557(2)	4090(3)	8271(2)	34(1)
C(22)	-1599(2)	4997(3)	8791(2)	39(1)
C(23)	-886(3)	5612(3)	9031(2)	42(1)
C(24)	-136(3)	5343(4)	8759(3)	50(1)
C(25)	-92(2)	4442(3)	8244(3)	43(1)

140

C(26)	407(2)	-777(3)	8488(2)	29(1)
C(27)	1213(3)	-1169(3)	8422(2)	35(1)
C(28)	1627(3)	-1874(3)	8990(2)	38(1)
C(29)	1237(3)	-2182(4)	9636(2)	40(1)
C(30)	444(3)	-1778(4)	9717(2)	46(1)
C(31)	24(3)	-1085(4)	9146(2)	41(1)
C(32)	-681(2)	-1027(3)	7056(2)	27(1)
C(33)	-808(2)	-2130(3)	7317(2)	33(1)
C(34)	-1266(3)	-2915(3)	6832(3)	41(1)
C(35)	-1604(3)	-2608(4)	6092(3)	43(1)
C(36)	-1485(3)	-1525(3)	5825(2)	39(1)
C(37)	-1022(2)	-730(3)	6302(2)	30(1)

141

Table 3.   Bond lengths [Å] and angles [°] for **A3**.

_____

W(1)-C(2)	1.982(4)	C(11)-H(11B)	0.9900
W(1)-C(3)	2.012(4)	C(12)-H(12A)	0.9900
W(1)-C(1)	2.017(4)	C(12)-H(12B)	0.9900
W(1)-C(4)	2.117(3)	C(13)-C(14)	1.388(5)
W(1)-P(1)	2.4930(9)	C(13)-C(18)	1.391(6)
W(1)-P(2)	2.5145(9)	C(14)-C(15)	1.411(6)
C(1)-O(1)	1.151(4)	C(14)-H(14)	0.9500
C(2)-O(2)	1.158(4)	C(15)-C(16)	1.362(7)
C(3)-O(3)	1.155(4)	C(15)-H(15)	0.9500
C(4)-O(4)	1.353(4)	C(16)-C(17)	1.381(7)
C(4)-C(5)	1.459(5)	C(16)-H(16)	0.9500
O(4)-C(9)	1.457(4)	C(17)-C(18)	1.374(6)
C(5)-C(6)	1.379(5)	C(17)-H(17)	0.9500
C(5)-S(1)	1.741(3)	C(18)-H(18)	0.9500
C(6)-C(7)	1.421(5)	C(20)-C(21)	1.379(5)
C(6)-H(6)	0.9500	C(20)-C(25)	1.385(5)
C(7)-C(8)	1.332(5)	C(21)-C(22)	1.397(5)
C(7)-H(7)	0.9500	C(21)-H(21)	0.9500
C(8)-S(1)	1.710(4)	C(22)-C(23)	1.372(5)
C(8)-H(8)	0.9500	C(22)-H(22)	0.9500
C(9)-C(10)	1.512(5)	C(23)-C(24)	1.368(5)
C(9)-H(9A)	0.9900	C(23)-H(23)	0.9500
C(9)-H(9B)	0.9900	C(24)-C(25)	1.386(5)
C(10)-H(10A)	0.9800	C(24)-H(24)	0.9500
C(10)-H(10B)	0.9800	C(25)-H(25)	0.9500
C(10)-H(10C)	0.9800	C(26)-C(27)	1.382(5)
P(1)-C(13)	1.842(4)	C(26)-C(31)	1.392(5)
P(1)-C(20)	1.848(4)	C(27)-C(28)	1.392(5)
P(1)-C(11)	1.852(4)	C(27)-H(27)	0.9500
P(2)-C(26)	1.834(4)	C(28)-C(29)	1.379(5)
P(2)-C(32)	1.836(4)	C(28)-H(28)	0.9500
P(2)-C(12)	1.851(4)	C(29)-C(30)	1.373(6)
C(11)-C(12)	1.525(6)	C(29)-H(29)	0.9500
C(11)-H(11A)	0.9900	C(30)-C(31)	1.389(6)

142

C(30)-H(30)	0.9500	C(6)-C(5)-C(4)	130.8(3)
C(31)-H(31)	0.9500	C(6)-C(5)-S(1)	109.4(3)
C(32)-C(33)	1.393(5)	C(4)-C(5)-S(1)	119.8(3)
C(32)-C(37)	1.393(5)	C(5)-C(6)-C(7)	113.0(3)
C(33)-C(34)	1.395(5)	C(5)-C(6)-H(6)	123.5
C(33)-H(33)	0.9500	C(7)-C(6)-H(6)	123.5
C(34)-C(35)	1.374(6)	C(8)-C(7)-C(6)	113.3(4)
C(34)-H(34)	0.9500	C(8)-C(7)-H(7)	123.4
C(35)-C(36)	1.372(6)	C(6)-C(7)-H(7)	123.4
C(35)-H(35)	0.9500	C(7)-C(8)-S(1)	112.2(3)
C(36)-C(37)	1.400(5)	C(7)-C(8)-H(8)	123.9
C(36)-H(36)	0.9500	S(1)-C(8)-H(8)	123.9
C(37)-H(37)	0.9500	C(8)-S(1)-C(5)	92.15(18)
		O(4)-C(9)-C(10)	104.8(3)
C(2)-W(1)-C(3)	92.32(15)	O(4)-C(9)-H(9A)	110.8
C(2)-W(1)-C(1)	86.00(15)	C(10)-C(9)-H(9A)	110.8
C(3)-W(1)-C(1)	176.18(14)	O(4)-C(9)-H(9B)	110.8
C(2)-W(1)-C(4)	87.03(13)	C(10)-C(9)-H(9B)	110.8
C(3)-W(1)-C(4)	96.27(14)	H(9A)-C(9)-H(9B)	108.9
C(1)-W(1)-C(4)	87.08(14)	C(9)-C(10)-H(10A)	109.5
C(2)-W(1)-P(1)	94.07(10)	C(9)-C(10)-H(10B)	109.5
C(3)-W(1)-P(1)	89.56(11)	H(10A)-C(10)-H(10B)	109.5
C(1)-W(1)-P(1)	87.13(10)	C(9)-C(10)-H(10C)	109.5
C(4)-W(1)-P(1)	174.02(10)	H(10A)-C(10)-H(10C)	109.5
C(2)-W(1)-P(2)	171.53(11)	H(10B)-C(10)-H(10C)	109.5
C(3)-W(1)-P(2)	81.46(10)	C(13)-P(1)-C(20)	98.78(16)
C(1)-W(1)-P(2)	99.85(11)	C(13)-P(1)-C(11)	103.36(19)
C(4)-W(1)-P(2)	99.31(9)	C(20)-P(1)-C(11)	103.82(17)
P(1)-W(1)-P(2)	80.22(3)	C(13)-P(1)-W(1)	119.77(12)
O(1)-C(1)-W(1)	174.9(3)	C(20)-P(1)-W(1)	119.90(12)
O(2)-C(2)-W(1)	176.8(3)	C(11)-P(1)-W(1)	108.99(12)
O(3)-C(3)-W(1)	174.6(3)	C(26)-P(2)-C(32)	102.79(16)
O(4)-C(4)-C(5)	103.5(3)	C(26)-P(2)-C(12)	104.56(17)
O(4)-C(4)-W(1)	130.5(2)	C(32)-P(2)-C(12)	100.10(16)
C(5)-C(4)-W(1)	125.5(2)	C(26)-P(2)-W(1)	116.52(12)
C(4)-O(4)-C(9)	123.9(3)	C(32)-P(2)-W(1)	124.32(12)

143

C(12)-P(2)-W(1)	105.83(13)
C(12)-C(11)-P(1)	109.9(3)
C(12)-C(11)-H(11A)	109.7
P(1)-C(11)-H(11A)	109.7
C(12)-C(11)-H(11B)	109.7
P(1)-C(11)-H(11B)	109.7
H(11A)-C(11)-H(11B)	108.2
C(11)-C(12)-P(2)	110.1(3)
C(11)-C(12)-H(12A)	109.6
P(2)-C(12)-H(12A)	109.6
C(11)-C(12)-H(12B)	109.6
P(2)-C(12)-H(12B)	109.6
H(12A)-C(12)-H(12B)	108.2
C(14)-C(13)-C(18)	118.5(4)
C(14)-C(13)-P(1)	122.9(3)
C(18)-C(13)-P(1)	118.5(3)
C(13)-C(14)-C(15)	119.1(4)
C(13)-C(14)-H(14)	120.4
C(15)-C(14)-H(14)	120.4
C(16)-C(15)-C(14)	121.7(4)
C(16)-C(15)-H(15)	119.2
C(14)-C(15)-H(15)	119.2
C(15)-C(16)-C(17)	118.8(5)
C(15)-C(16)-H(16)	120.6
C(17)-C(16)-H(16)	120.6
C(18)-C(17)-C(16)	120.6(5)
C(18)-C(17)-H(17)	119.7
C(16)-C(17)-H(17)	119.7
C(17)-C(18)-C(13)	121.3(4)
C(17)-C(18)-H(18)	119.3
C(13)-C(18)-H(18)	119.3
C(21)-C(20)-C(25)	118.8(3)
C(21)-C(20)-P(1)	122.5(3)
C(25)-C(20)-P(1)	118.6(3)
C(20)-C(21)-C(22)	120.4(4)
C(20)-C(21)-H(21)	119.8

C(22)-C(21)-H(21)	119.8
C(23)-C(22)-C(21)	119.9(4)
C(23)-C(22)-H(22)	120.1
C(21)-C(22)-H(22)	120.1
C(24)-C(23)-C(22)	120.2(4)
C(24)-C(23)-H(23)	119.9
C(22)-C(23)-H(23)	119.9
C(23)-C(24)-C(25)	120.1(4)
C(23)-C(24)-H(24)	119.9
C(25)-C(24)-H(24)	119.9
C(20)-C(25)-C(24)	120.6(4)
C(20)-C(25)-H(25)	119.7
C(24)-C(25)-H(25)	119.7
C(27)-C(26)-C(31)	118.4(4)
C(27)-C(26)-P(2)	119.1(3)
C(31)-C(26)-P(2)	122.5(3)
C(26)-C(27)-C(28)	121.0(4)
C(26)-C(27)-H(27)	119.5
C(28)-C(27)-H(27)	119.5
C(29)-C(28)-C(27)	120.0(4)
C(29)-C(28)-H(28)	120.0
C(27)-C(28)-H(28)	120.0
C(30)-C(29)-C(28)	119.6(4)
C(30)-C(29)-H(29)	120.2
C(28)-C(29)-H(29)	120.2
C(29)-C(30)-C(31)	120.6(4)
C(29)-C(30)-H(30)	119.7
C(31)-C(30)-H(30)	119.7
C(30)-C(31)-C(26)	120.4(4)
C(30)-C(31)-H(31)	119.8
C(26)-C(31)-H(31)	119.8
C(33)-C(32)-C(37)	118.4(3)
C(33)-C(32)-P(2)	122.3(3)
C(37)-C(32)-P(2)	119.1(3)
C(32)-C(33)-C(34)	120.5(4)
C(32)-C(33)-H(33)	119.8

144

C(34)-C(33)-H(33)	119.8		C(35)-C(36)-C(37)	120.3(4)
C(35)-C(34)-C(33)	120.5(4)		C(35)-C(36)-H(36)	119.8
C(35)-C(34)-H(34)	119.8		C(37)-C(36)-H(36)	119.8
C(33)-C(34)-H(34)	119.8		C(32)-C(37)-C(36)	120.4(4)
C(36)-C(35)-C(34)	119.9(4)		C(32)-C(37)-H(37)	119.8
C(36)-C(35)-H(35)	120.1		C(36)-C(37)-H(37)	119.8
C(34)-C(35)-H(35)	120.1			

_____

Table 4.   Anisotropic displacement parameters (Å^{2}x 10^3)for **A3**.   The anisotropic displacement factor exponent takes the form: -2p^2[h^{2}a*^{2}U^{11} + ... + 2 h k a* b* U^{12}]

	U^{11}	U^{22}	U^{33}	U^{23}	U^{13}	U^{12}
W(1)	18(1)	25(1)	25(1)	-5(1)	2(1)	1(1)
C(1)	26(2)	32(2)	31(2)	-7(2)	0(2)	6(2)
O(1)	42(2)	69(2)	30(2)	-6(1)	-2(1)	11(2)
C(2)	21(2)	29(2)	39(2)	-3(2)	2(2)	1(2)
O(2)	44(2)	32(2)	69(2)	4(2)	13(2)	-5(1)
C(3)	24(2)	30(2)	33(2)	-5(2)	3(2)	-8(2)
O(3)	42(2)	62(2)	30(1)	-13(1)	5(1)	-14(2)
C(4)	20(2)	23(2)	27(2)	3(1)	1(1)	1(1)
O(4)	25(1)	34(1)	32(1)	-8(1)	-2(1)	4(1)
C(5)	22(2)	29(2)	25(2)	2(2)	2(1)	4(2)
C(6)	26(2)	31(2)	29(2)	-5(2)	1(2)	3(2)
C(7)	36(2)	32(2)	26(2)	-7(2)	-2(2)	6(2)
C(8)	40(2)	33(2)	30(2)	-2(2)	8(2)	9(2)
S(1)	26(1)	42(1)	42(1)	-7(1)	7(1)	4(1)
C(9)	24(2)	41(2)	32(2)	-6(2)	-5(2)	1(2)
C(10)	27(2)	40(2)	43(2)	-4(2)	-1(2)	-3(2)
P(1)	21(1)	28(1)	33(1)	-10(1)	1(1)	1(1)
P(2)	22(1)	27(1)	28(1)	-5(1)	3(1)	-1(1)
C(11)	22(2)	37(2)	50(2)	-18(2)	6(2)	-4(2)
C(12)	25(2)	35(2)	44(2)	-11(2)	14(2)	-5(2)
C(13)	27(2)	35(2)	34(2)	-16(2)	-2(2)	8(2)
C(14)	29(2)	62(3)	43(2)	-22(2)	-4(2)	10(2)
C(15)	34(3)	73(3)	56(3)	-32(3)	-21(2)	27(2)
C(16)	61(3)	53(3)	46(3)	-12(2)	-11(2)	26(3)
C(17)	68(4)	44(3)	47(3)	3(2)	-1(2)	17(2)
C(18)	40(2)	38(2)	43(2)	-4(2)	-6(2)	8(2)
C(20)	25(2)	28(2)	28(2)	-4(2)	2(2)	-1(2)
C(21)	26(2)	40(2)	36(2)	-11(2)	6(2)	-4(2)
C(22)	29(2)	44(2)	46(2)	-12(2)	11(2)	2(2)
C(23)	37(2)	41(2)	46(2)	-22(2)	5(2)	1(2)
C(24)	34(2)	47(2)	68(3)	-31(2)	6(2)	-6(2)
C(25)	23(2)	45(2)	60(3)	-24(2)	9(2)	-2(2)

146

C(26)	29(2)	30(2)	28(2)	-7(2)	3(2)	-7(2)
C(27)	37(2)	33(2)	34(2)	-2(2)	6(2)	-5(2)
C(28)	35(2)	38(2)	40(2)	3(2)	1(2)	0(2)
C(29)	42(3)	43(2)	31(2)	5(2)	-8(2)	-9(2)
C(30)	52(3)	61(3)	25(2)	1(2)	7(2)	-19(2)
C(31)	38(2)	56(3)	29(2)	-3(2)	5(2)	0(2)
C(32)	21(2)	28(2)	33(2)	-8(2)	6(2)	-2(2)
C(33)	27(2)	31(2)	40(2)	-3(2)	3(2)	-2(2)
C(34)	37(2)	28(2)	57(3)	-8(2)	0(2)	-3(2)
C(35)	37(2)	36(2)	56(3)	-18(2)	2(2)	-3(2)
C(36)	33(2)	47(2)	35(2)	-9(2)	0(2)	0(2)
C(37)	26(2)	27(2)	35(2)	-4(2)	-1(2)	0(2)

_____

Table 5. Hydrogen coordinates (x 10^4) and isotropic displacement parameters (Å^2x 10^3) for **A3**.

	x	y	z	U(eq)
H(6)	723	-610	5990	35
H(7)	1356	-1844	5049	38
H(8)	2840	-1588	5071	41
H(9A)	2578	1440	8490	39
H(9B)	2623	2508	7908	39
H(10A)	3978	2172	8591	55
H(10B)	4006	1955	7675	55
H(10C)	3962	899	8257	55
H(11A)	-1944	1950	7784	43
H(11B)	-1733	1178	7061	43
H(12A)	-1449	102	8217	41
H(12B)	-848	1087	8610	41
H(14)	-2466	2845	6526	54
H(15)	-3091	3826	5415	68
H(16)	-2289	4910	4655	65
H(17)	-833	5030	4995	65
H(18)	-199	4059	6071	49
H(21)	-2052	3668	8102	41
H(22)	-2120	5188	8978	47
H(23)	-913	6226	9387	50
H(24)	355	5774	8924	60
H(25)	430	4262	8056	51
H(27)	1489	-953	7981	42
H(28)	2179	-2144	8933	46
H(29)	1516	-2669	10023	48
H(30)	179	-1974	10168	55
H(31)	-528	-820	9206	49
H(33)	-581	-2349	7829	39
H(34)	-1345	-3667	7014	49
H(35)	-1919	-3145	5766	52
H(36)	-1719	-1313	5313	47
H(37)	-939	16	6111	36

148

Table 6.   Torsion angles [°] for **A3**.

_____

C(2)-W(1)-C(4)-O(4)	58.3(3)	C(3)-W(1)-P(2)-C(26)	-43.80(16)
C(3)-W(1)-C(4)-O(4)	-33.7(3)	C(1)-W(1)-P(2)-C(26)	139.84(16)
C(1)-W(1)-C(4)-O(4)	144.5(3)	C(4)-W(1)-P(2)-C(26)	51.21(16)
P(2)-W(1)-C(4)-O(4)	-116.0(3)	P(1)-W(1)-P(2)-C(26)	-134.83(13)
C(2)-W(1)-C(4)-C(5)	-112.6(3)	C(3)-W(1)-P(2)-C(32)	-173.63(18)
C(3)-W(1)-C(4)-C(5)	155.4(3)	C(1)-W(1)-P(2)-C(32)	10.02(17)
C(1)-W(1)-C(4)-C(5)	-26.4(3)	C(4)-W(1)-P(2)-C(32)	-78.61(17)
P(2)-W(1)-C(4)-C(5)	73.1(3)	P(1)-W(1)-P(2)-C(32)	95.34(14)
C(5)-C(4)-O(4)-C(9)	179.1(3)	C(3)-W(1)-P(2)-C(12)	71.90(17)
W(1)-C(4)-O(4)-C(9)	6.7(5)	C(1)-W(1)-P(2)-C(12)	-104.46(17)
O(4)-C(4)-C(5)-C(6)	162.3(4)	C(4)-W(1)-P(2)-C(12)	166.91(16)
W(1)-C(4)-C(5)-C(6)	-24.8(5)	P(1)-W(1)-P(2)-C(12)	-19.13(14)
O(4)-C(4)-C(5)-S(1)	-14.5(4)	C(13)-P(1)-C(11)-C(12)	164.7(2)
W(1)-C(4)-C(5)-S(1)	158.36(18)	C(20)-P(1)-C(11)-C(12)	-92.6(3)
C(4)-C(5)-C(6)-C(7)	-177.0(3)	W(1)-P(1)-C(11)-C(12)	36.3(3)
S(1)-C(5)-C(6)-C(7)	0.1(4)	P(1)-C(11)-C(12)-P(2)	-55.4(3)
C(5)-C(6)-C(7)-C(8)	-0.8(5)	C(26)-P(2)-C(12)-C(11)	171.8(3)
C(6)-C(7)-C(8)-S(1)	1.1(4)	C(32)-P(2)-C(12)-C(11)	-82.1(3)
C(7)-C(8)-S(1)-C(5)	-0.9(3)	W(1)-P(2)-C(12)-C(11)	48.2(3)
C(6)-C(5)-S(1)-C(8)	0.4(3)	C(20)-P(1)-C(13)-C(14)	-88.1(3)
C(4)-C(5)-S(1)-C(8)	177.9(3)	C(11)-P(1)-C(13)-C(14)	18.5(3)
C(4)-O(4)-C(9)-C(10)	-174.5(3)	W(1)-P(1)-C(13)-C(14)	139.9(3)
C(2)-W(1)-P(1)-C(13)	62.01(18)	C(20)-P(1)-C(13)-C(18)	89.5(3)
C(3)-W(1)-P(1)-C(13)	154.31(17)	C(11)-P(1)-C(13)-C(18)	-164.0(3)
C(1)-W(1)-P(1)-C(13)	-23.78(17)	W(1)-P(1)-C(13)-C(18)	-42.6(3)
P(2)-W(1)-P(1)-C(13)	-124.29(14)	C(18)-C(13)-C(14)-C(15)	0.4(5)
C(2)-W(1)-P(1)-C(20)	-60.12(18)	P(1)-C(13)-C(14)-C(15)	178.0(3)
C(3)-W(1)-P(1)-C(20)	32.18(17)	C(13)-C(14)-C(15)-C(16)	-0.5(6)
C(1)-W(1)-P(1)-C(20)	-145.90(18)	C(14)-C(15)-C(16)-C(17)	0.1(7)
P(2)-W(1)-P(1)-C(20)	113.59(14)	C(15)-C(16)-C(17)-C(18)	0.4(7)
C(2)-W(1)-P(1)-C(11)	-179.42(18)	C(16)-C(17)-C(18)-C(13)	-0.4(6)
C(3)-W(1)-P(1)-C(11)	-87.12(17)	C(14)-C(13)-C(18)-C(17)	0.0(6)
C(1)-W(1)-P(1)-C(11)	94.80(17)	P(1)-C(13)-C(18)-C(17)	-177.7(3)
P(2)-W(1)-P(1)-C(11)	-5.71(14)	C(13)-P(1)-C(20)-C(21)	71.0(3)

C(11)-P(1)-C(20)-C(21)	-35.2(4)		C(26)-C(27)-C(28)-C(29)	-0.8(6)
W(1)-P(1)-C(20)-C(21)	-157.1(3)		C(27)-C(28)-C(29)-C(30)	-0.7(6)
C(13)-P(1)-C(20)-C(25)	-105.5(3)		C(28)-C(29)-C(30)-C(31)	1.5(6)
C(11)-P(1)-C(20)-C(25)	148.3(3)		C(29)-C(30)-C(31)-C(26)	-0.9(6)
W(1)-P(1)-C(20)-C(25)	26.5(4)		C(27)-C(26)-C(31)-C(30)	-0.5(6)
C(25)-C(20)-C(21)-C(22)	-1.0(6)		P(2)-C(26)-C(31)-C(30)	176.3(3)
P(1)-C(20)-C(21)-C(22)	-177.5(3)		C(26)-P(2)-C(32)-C(33)	16.9(3)
C(20)-C(21)-C(22)-C(23)	0.4(6)		C(12)-P(2)-C(32)-C(33)	-90.7(3)
C(21)-C(22)-C(23)-C(24)	0.4(7)		W(1)-P(2)-C(32)-C(33)	152.1(2)
C(22)-C(23)-C(24)-C(25)	-0.5(7)		C(26)-P(2)-C(32)-C(37)	-166.8(3)
C(21)-C(20)-C(25)-C(24)	1.0(6)		C(12)-P(2)-C(32)-C(37)	85.6(3)
P(1)-C(20)-C(25)-C(24)	177.5(4)		W(1)-P(2)-C(32)-C(37)	-31.6(3)
C(23)-C(24)-C(25)-C(20)	-0.2(7)		C(37)-C(32)-C(33)-C(34)	0.0(5)
C(32)-P(2)-C(26)-C(27)	89.7(3)		P(2)-C(32)-C(33)-C(34)	176.4(3)
C(12)-P(2)-C(26)-C(27)	-166.1(3)		C(32)-C(33)-C(34)-C(35)	-0.5(6)
W(1)-P(2)-C(26)-C(27)	-49.7(3)		C(33)-C(34)-C(35)-C(36)	0.5(6)
C(32)-P(2)-C(26)-C(31)	-87.2(3)		C(34)-C(35)-C(36)-C(37)	0.0(6)
C(12)-P(2)-C(26)-C(31)	17.0(4)		C(33)-C(32)-C(37)-C(36)	0.5(5)
W(1)-P(2)-C(26)-C(31)	133.4(3)		P(2)-C(32)-C(37)-C(36)	-176.0(3)
C(31)-C(26)-C(27)-C(28)	1.4(6)		C(35)-C(36)-C(37)-C(32)	-0.5(6)
P(2)-C(26)-C(27)-C(28)	-175.7(3)			

_____

150

APPENDIX C:

CRYSTALLOGRAPHIC DATA OF COMPLEX A4
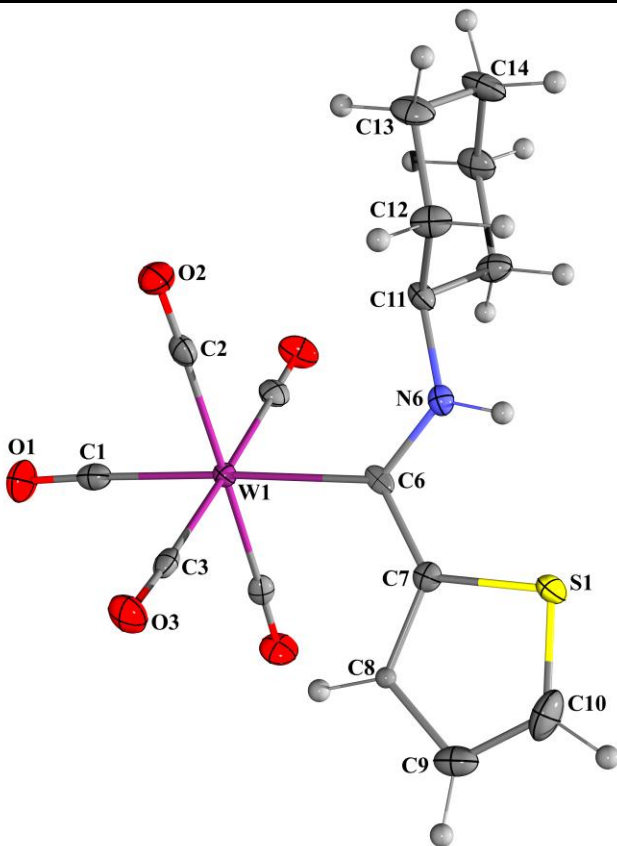
Table 1. Crystal data and structure refinement for **A4**.

Identification code	mo_11fm_rp02
Empirical formula	$C_{16}H_{15}NO_5SW$
Formula weight	517.20
Temperature	100(2) K
Wavelength	0.71073 Å
Crystal system	monoclinic
Space group	$P2_1/m$
Unit cell dimensions	a = 9.5736(8) Å α = 90°.
	b = 9.6865(8) Å β = 112.472(2)°.
	c = 9.9936(8) Å γ = 90°.

Volume	856.38(12) $Å^3$
Z	2
Density (calculated)	2.006 Mg/m^3
Absorption coefficient	6.891 mm^{-1}
F(000)	496
Crystal size	0.19 x 0.18 x 0.13 mm^3
Θ range for data collection	2.21 to 28.40°.
Index ranges	-12<=h<=12, -12<=k<=8, -10<=l<=13
Reflections collected	4935
Independent reflections	2269 [R(int) = 0.0326]
Completeness to θ = 25.24°	99.9 %
Absorption correction	Semi-empirical from equivalents
Max. and min. transmission	0.475 and 0.360
Refinement method	Full-matrix least-squares on F^2
Data / restraints / parameters	2269 / 8 / 134
Goodness-of-fit on F^2	0.997
Final R indices [I>2σ(I)]	R1 = 0.0257, wR2 = 0.0468
R indices (all data)	R1 = 0.0299, wR2 = 0.0480
Extinction coefficient	0
Largest diff. peak and hole	0.709 and -1.181 $e.Å^{-3}$

Table 2. Atomic coordinates (x 10^4) and equivalent isotropic displacement parameters ($Å^2$x 10^3) for **A4**. U(eq) is defined as one third of the trace of the orthogonalized U^{ij} tensor.

	x	y	z	U(eq)
W(1)	5487(1)	2500	8564(1)	12(1)
C(1)	4999(6)	2500	10346(6)	19(1)
O(1)	4769(4)	2500	11398(4)	28(1)
C(2)	3929(4)	4032(4)	7691(4)	18(1)
O(2)	3071(3)	4893(3)	7234(3)	25(1)
C(3)	7012(4)	950(4)	9469(4)	15(1)
O(3)	7824(3)	64(3)	9992(3)	25(1)
C(6)	6150(5)	2500	6614(5)	12(1)
N(6)	5195(5)	2500	5237(4)	15(1)
C(7)	7740(5)	2500	6758(5)	14(1)
S(1)	8322(3)	2500	5349(5)	22(1)
C(8)	9064(14)	2500	8030(13)	8(4)
S(1A)	9142(5)	2500	8379(6)	16(1)
C(8A)	8404(19)	2500	5700(20)	40(10)
C(9)	10460(6)	2500	7778(6)	23(1)
C(10)	10074(7)	2500	6345(7)	33(1)
C(11)	3558(6)	2500	4660(5)	16(1)
C(12)	2961(4)	3799(4)	3745(4)	20(1)
C(13)	1236(4)	3799(4)	3104(4)	23(1)
C(14)	611(7)	2500	2227(6)	27(1)

153

Table 3. Bond lengths [Å] and angles [°] for **A4**.
_____

W(1)-C(1)	2.006(6)	C(13)-H(13B)	0.9900
W(1)-C(2)#1	2.048(4)	C(14)-C(13)#1	1.520(5)
W(1)-C(2)	2.048(4)	C(14)-H(14A)	0.9900
W(1)-C(3)#1	2.048(4)	C(14)-H(14B)	0.9900
W(1)-C(3)	2.048(4)		
W(1)-C(6)	2.269(5)	C(1)-W(1)-C(2)#1	89.98(14)
C(1)-O(1)	1.153(6)	C(1)-W(1)-C(2)	89.98(14)
C(2)-O(2)	1.137(4)	C(2)#1-W(1)-C(2)	92.9(2)
C(3)-O(3)	1.142(4)	C(1)-W(1)-C(3)#1	88.65(14)
C(6)-N(6)	1.330(6)	C(2)#1-W(1)-C(3)#1	178.46(14)
C(6)-C(7)	1.473(7)	C(2)-W(1)-C(3)#1	86.38(13)
N(6)-C(11)	1.449(6)	C(1)-W(1)-C(3)	88.65(13)
N(6)-H(6)	0.8800	C(2)#1-W(1)-C(3)	86.38(13)
C(7)-C(8)	1.411(12)	C(2)-W(1)-C(3)	178.46(14)
C(7)-C(8A)	1.428(16)	C(3)#1-W(1)-C(3)	94.30(19)
C(7)-S(1A)	1.663(7)	C(1)-W(1)-C(6)	177.43(19)
C(7)-S(1)	1.701(6)	C(2)#1-W(1)-C(6)	91.79(13)
S(1)-C(10)	1.590(7)	C(2)-W(1)-C(6)	91.79(13)
C(8)-C(9)	1.451(13)	C(3)#1-W(1)-C(6)	89.60(12)
C(8)-H(8)	0.9500	C(3)-W(1)-C(6)	89.60(12)
S(1A)-C(9)	1.591(7)	O(1)-C(1)-W(1)	177.7(4)
C(8A)-C(10)	1.477(17)	O(2)-C(2)-W(1)	178.6(3)
C(8A)-H(8A)	0.9500	O(3)-C(3)-W(1)	177.5(3)
C(9)-C(10)	1.335(8)	N(6)-C(6)-C(7)	112.2(4)
C(9)-H(9)	0.9500	N(6)-C(6)-W(1)	125.5(4)
C(10)-H(10)	0.9500	C(7)-C(6)-W(1)	122.3(3)
C(11)-C(12)	1.532(4)	C(6)-N(6)-C(11)	128.6(4)
C(11)-C(12)#1	1.532(4)	C(6)-N(6)-H(6)	115.7
C(11)-H(11)	1.0000	C(11)-N(6)-H(6)	115.7
C(12)-C(13)	1.526(5)	C(8)-C(7)-C(6)	128.8(6)
C(12)-H(12A)	0.9900	C(8A)-C(7)-C(6)	131.6(8)
C(12)-H(12B)	0.9900	C(8A)-C(7)-S(1A)	107.4(8)
C(13)-C(14)	1.520(5)	C(6)-C(7)-S(1A)	121.0(4)
C(13)-H(13A)	0.9900	C(8)-C(7)-S(1)	106.2(6)

C(6)-C(7)-S(1)	124.9(4)		N(6)-C(11)-H(11)	109.0
C(10)-S(1)-C(7)	94.8(4)		C(12)-C(11)-H(11)	109.0
C(7)-C(8)-C(9)	114.4(9)		C(12)#1-C(11)-H(11)	109.0
C(7)-C(8)-H(8)	122.8		C(13)-C(12)-C(11)	110.3(3)
C(9)-C(8)-H(8)	122.8		C(13)-C(12)-H(12A)	109.6
C(9)-S(1A)-C(7)	95.4(4)		C(11)-C(12)-H(12A)	109.6
C(7)-C(8A)-C(10)	113.0(13)		C(13)-C(12)-H(12B)	109.6
C(7)-C(8A)-H(8A)	123.5		C(11)-C(12)-H(12B)	109.6
C(10)-C(8A)-H(8A)	123.5		H(12A)-C(12)-H(12B)	108.1
C(10)-C(9)-C(8)	106.9(7)		C(14)-C(13)-C(12)	111.4(4)
C(10)-C(9)-S(1A)	118.1(5)		C(14)-C(13)-H(13A)	109.3
C(10)-C(9)-H(9)	126.6		C(12)-C(13)-H(13A)	109.3
C(8)-C(9)-H(9)	126.6		C(14)-C(13)-H(13B)	109.3
S(1A)-C(9)-H(9)	115.4		C(12)-C(13)-H(13B)	109.3
C(9)-C(10)-C(8A)	106.1(8)		H(13A)-C(13)-H(13B)	108.0
C(9)-C(10)-S(1)	117.7(5)		C(13)#1-C(14)-C(13)	111.8(4)
C(9)-C(10)-H(10)	121.2		C(13)#1-C(14)-H(14A)	109.3
C(8A)-C(10)-H(10)	132.7		C(13)-C(14)-H(14A)	109.3
S(1)-C(10)-H(10)	121.2		C(13)#1-C(14)-H(14B)	109.3
N(6)-C(11)-C(12)	109.7(3)		C(13)-C(14)-H(14B)	109.3
N(6)-C(11)-C(12)#1	109.7(3)		H(14A)-C(14)-H(14B)	107.9
C(12)-C(11)-C(12)#1	110.4(4)			

_____

Symmetry transformations used to generate equivalent atoms: #1 x,-y+1/2,z

Table 4.   Anisotropic displacement parameters (Å^{2}x 10^3)for **A4**.   The anisotropic displacement factor exponent takes the form: -2p^2[h^{2}a*^{2}U^{11} + ... + 2 h k a* b* U^{12}]

	U^{11}	U^{22}	U^{33}	U^{23}	U^{13}	U^{12}
W(1)	12(1)	11(1)	11(1)	0	4(1)	0
C(1)	15(3)	14(3)	24(3)	0	3(2)	0
O(1)	35(2)	28(2)	27(2)	0	20(2)	0
C(2)	19(2)	19(2)	14(2)	-5(1)	4(2)	-3(2)
O(2)	24(2)	22(2)	26(2)	-2(1)	5(1)	8(1)
C(3)	17(2)	15(2)	17(2)	-3(1)	9(2)	-6(2)
O(3)	26(2)	18(2)	25(2)	6(1)	5(1)	5(1)
C(6)	19(3)	2(2)	11(2)	0	1(2)	0
N(6)	18(2)	14(2)	13(2)	0	6(2)	0
C(7)	16(2)	10(2)	16(2)	0	6(2)	0
S(1)	16(2)	36(2)	11(2)	0	3(1)	0
S(1A)	17(2)	24(2)	7(2)	0	6(2)	0
C(9)	16(3)	17(3)	30(3)	0	2(2)	0
C(10)	36(3)	38(4)	38(4)	0	29(3)	0
C(11)	18(3)	16(3)	11(2)	0	3(2)	0
C(12)	17(2)	15(2)	26(2)	2(1)	5(2)	-1(2)
C(13)	23(2)	15(2)	24(2)	6(2)	1(2)	4(2)
C(14)	25(3)	23(3)	20(3)	0	-6(2)	0

Table 5.   Hydrogen coordinates (x 10^4) and isotropic displacement parameters (Å^2x 10^3) for **A4**.

	x	y	z	U(eq)
H(6)	5613	2500	4591	18
H(8)	9044	2500	8973	9
H(8A)	7832	2500	4685	48
H(9)	11457	2500	8495	28
H(10)	10820	2500	5934	39
H(11)	3207	2500	5482	19
H(12A)	3334	4629	4355	24
H(12B)	3342	3830	2953	24
H(13A)	860	3864	3897	27
H(13B)	869	4618	2475	27
H(14A)	-504	2500	1895	32
H(14B)	873	2500	1360	32

157

Table 6.   Torsion angles [°] for **A4**

_____

C(2)#1-W(1)-C(6)-N(6)	46.49(10)	C(8)-C(7)-S(1A)-C(9)	0
C(2)-W(1)-C(6)-N(6)	-46.49(10)	C(8A)-C(7)-S(1A)-C(9)	0
C(3)#1-W(1)-C(6)-N(6)	-132.85(9)	C(6)-C(7)-S(1A)-C(9)	180
C(3)-W(1)-C(6)-N(6)	132.85(9)	S(1)-C(7)-S(1A)-C(9)	0
C(2)#1-W(1)-C(6)-C(7)	-133.51(10)	C(8)-C(7)-C(8A)-C(10)	0
C(2)-W(1)-C(6)-C(7)	133.51(10)	C(6)-C(7)-C(8A)-C(10)	180
C(3)#1-W(1)-C(6)-C(7)	47.15(9)	S(1A)-C(7)-C(8A)-C(10)	0
C(3)-W(1)-C(6)-C(7)	-47.15(9)	S(1)-C(7)-C(8A)-C(10)	180
C(7)-C(6)-N(6)-C(11)	180	C(7)-C(8)-C(9)-C(10)	0
W(1)-C(6)-N(6)-C(11)	0	C(7)-C(8)-C(9)-S(1A)	180
N(6)-C(6)-C(7)-C(8)	180	C(7)-S(1A)-C(9)-C(10)	0
W(1)-C(6)-C(7)-C(8)	0	C(7)-S(1A)-C(9)-C(8)	0
N(6)-C(6)-C(7)-C(8A)	0	C(8)-C(9)-C(10)-C(8A)	0
W(1)-C(6)-C(7)-C(8A)	180	S(1A)-C(9)-C(10)-C(8A)	0
N(6)-C(6)-C(7)-S(1A)	180	C(8)-C(9)-C(10)-S(1)	0
W(1)-C(6)-C(7)-S(1A)	0	S(1A)-C(9)-C(10)-S(1)	0
N(6)-C(6)-C(7)-S(1)	0	C(7)-C(8A)-C(10)-C(9)	0
W(1)-C(6)-C(7)-S(1)	180	C(7)-C(8A)-C(10)-S(1)	180
C(8)-C(7)-S(1)-C(10)	0	C(7)-S(1)-C(10)-C(9)	0
C(8A)-C(7)-S(1)-C(10)	0	C(7)-S(1)-C(10)-C(8A)	0
C(6)-C(7)-S(1)-C(10)	180	C(6)-N(6)-C(11)-C(12)	119.2(3)
S(1A)-C(7)-S(1)-C(10)	0	C(6)-N(6)-C(11)-C(12)#1	-119.2(3)
C(8A)-C(7)-C(8)-C(9)	0	N(6)-C(11)-C(12)-C(13)	178.9(3)
C(6)-C(7)-C(8)-C(9)	180	C(12)#1-C(11)-C(12)-C(13)	57.8(5)
S(1A)-C(7)-C(8)-C(9)	180	C(11)-C(12)-C(13)-C(14)	-56.0(5)
S(1)-C(7)-C(8)-C(9)	0	C(12)-C(13)-C(14)-C(13)#1	54.5(6)

_____

Symmetry transformations used to generate equivalent atoms: #1 x,-y+1/2,z

158

Table 7.   Hydrogen bonds for **A4** [Å and °].

D-H...A	d(D-H)	d(H...A)	d(D...A)	<(DHA)
N(6)-H(6)...S(1)	0.88	2.41	2.952(5)	120

APPENDIX D:

CRYSTALLOGRAPHIC DATA OF COMPLEX B4
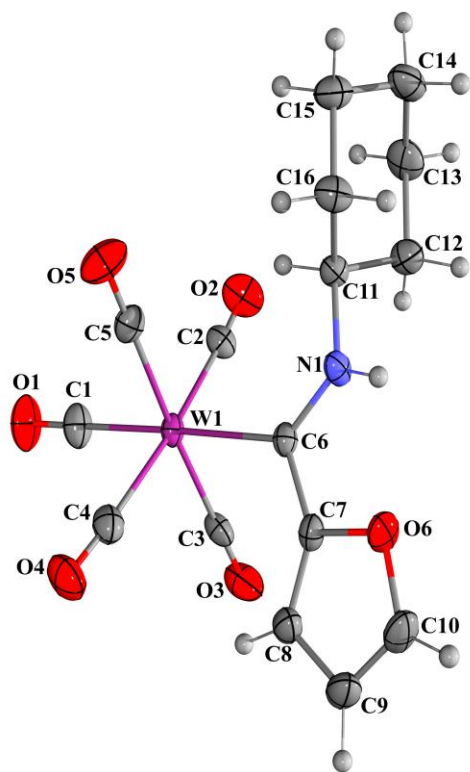
Table 1.   Crystal data and structure refinement for **B4**

Identification code	12m_up1	
Empirical formula	$C_{16}H_{15}N\ O_6W$	
Formula weight	501.14	
Temperature	296(2) K	
Wavelength	0.71069 Å	
Crystal system	Triclinic	
Space group	*P*-1	
Unit cell dimensions	a = 6.643(5) Å	α = 74.975(5)°.
	b = 9.372(5) Å	β = 86.258(5)°.
	c = 15.311(5) Å	γ = 69.921(5)°.

Volume	864.4(8) Å^3
Z	2
Density (calculated)	1.925 Mg/m^3
Absorption coefficient	6.712 mm^{-1}
F(000)	480
Crystal size	0.314 x 0.264 x 0.133 mm^3
θ range for data collection	1.38 to 28.00°.
Index ranges	$-8 \leq h \leq 8$, $-12 \leq k \leq 12$, $-20 \leq l \leq 20$
Reflections collected	21842
Independent reflections	4192 [R(int) = 0.1134]
Completeness to $\theta = 28.00°$	100.0 %
Absorption correction	Analytical
Max. and min. transmission	0.404 and 0.132
Refinement method	Full-matrix least-squares on F^2
Data / restraints / parameters	4192 / 0 / 220
Goodness-of-fit on F^2	1.109
Final R indices [I>2σ(I)]	R1 = 0.0299, wR2 = 0.0707
R indices (all data)	R1 = 0.0313, wR2 = 0.0715
Extinction coefficient	0
Largest diff. peak and hole	2.858 and -2.175 e.Å^{-3}

Table 2.   Atomic coordinates (x 10^4) and equivalent isotropic displacement parameters (Å^2x 10^3) for **B4**.   U(eq) is defined as one third of the trace of the orthogonalized U^{ij} tensor.

	x	y	z	U(eq)
W(1)	4353(1)	1954(1)	2784(1)	19(1)
C(1)	6591(6)	-23(5)	2624(3)	33(1)
O(1)	7895(6)	-1158(5)	2530(3)	49(1)
C(2)	6590(6)	3012(5)	2341(2)	26(1)
O(2)	7933(5)	3523(5)	2086(2)	41(1)
C(3)	5433(6)	1515(5)	4070(3)	27(1)
O(3)	6067(6)	1268(5)	4790(2)	45(1)
C(4)	2324(7)	694(5)	3195(3)	29(1)
O(4)	1268(6)	-55(4)	3393(2)	42(1)
C(5)	3107(6)	2528(5)	1510(3)	27(1)
O(5)	2344(6)	2855(5)	798(2)	45(1)
C(6)	1749(5)	4127(5)	2983(2)	20(1)
N(1)	1286(5)	5571(4)	2466(2)	23(1)
C(7)	282(5)	4039(4)	3738(2)	23(1)
C(8)	264(6)	2926(5)	4499(2)	28(1)
C(9)	-1527(7)	3600(5)	5003(3)	34(1)
C(10)	-2487(6)	5071(5)	4520(3)	35(1)
O(6)	-1437(4)	5403(3)	3741(2)	29(1)
C(11)	2435(5)	6130(4)	1683(2)	22(1)
C(12)	3488(7)	7203(6)	1911(3)	30(1)
C(13)	4663(7)	7845(6)	1088(3)	37(1)
C(14)	3156(7)	8671(5)	271(3)	36(1)
C(15)	2136(6)	7601(5)	52(2)	32(1)
C(16)	919(6)	6972(5)	861(2)	28(1)

162

Table 3.　Bond lengths [Å] and angles [°] for **B4**.

_____

W(1)-C(1)	2.000(4)	C(14)-H(14B)	0.9700
W(1)-C(3)	2.031(4)	C(15)-C(16)	1.535(5)
W(1)-C(5)	2.035(4)	C(15)-H(15A)	0.9700
W(1)-C(2)	2.045(4)	C(15)-H(15B)	0.9700
W(1)-C(4)	2.051(5)	C(16)-H(16A)	0.9700
W(1)-C(6)	2.251(4)	C(16)-H(16B)	0.9700
C(1)-O(1)	1.154(6)		
C(2)-O(2)	1.153(5)	C(1)-W(1)-C(3)	90.87(17)
C(3)-O(3)	1.144(5)	C(1)-W(1)-C(5)	93.11(17)
C(4)-O(4)	1.129(6)	C(3)-W(1)-C(5)	176.01(14)
C(5)-O(5)	1.153(5)	C(1)-W(1)-C(2)	86.20(19)
C(6)-N(1)	1.320(5)	C(3)-W(1)-C(2)	88.68(15)
C(6)-C(7)	1.466(5)	C(5)-W(1)-C(2)	91.81(16)
N(1)-C(11)	1.457(4)	C(1)-W(1)-C(4)	88.04(19)
N(1)-H(1)	0.83(5)	C(3)-W(1)-C(4)	92.15(15)
C(7)-C(8)	1.350(5)	C(5)-W(1)-C(4)	87.76(16)
C(7)-O(6)	1.392(4)	C(2)-W(1)-C(4)	174.19(15)
C(8)-C(9)	1.424(5)	C(1)-W(1)-C(6)	177.81(14)
C(8)-H(8)	0.9300	C(3)-W(1)-C(6)	89.17(15)
C(9)-C(10)	1.336(6)	C(5)-W(1)-C(6)	86.85(15)
C(9)-H(9)	0.9300	C(2)-W(1)-C(6)	95.99(16)
C(10)-O(6)	1.362(4)	C(4)-W(1)-C(6)	89.78(16)
C(10)-H(10)	0.9300	O(1)-C(1)-W(1)	179.4(4)
C(11)-C(12)	1.523(6)	O(2)-C(2)-W(1)	175.9(4)
C(11)-C(16)	1.525(4)	O(3)-C(3)-W(1)	179.1(4)
C(11)-H(11)	0.9800	O(4)-C(4)-W(1)	176.2(4)
C(12)-C(13)	1.537(5)	O(5)-C(5)-W(1)	178.0(3)
C(12)-H(12A)	0.9700	N(1)-C(6)-C(7)	111.9(3)
C(12)-H(12B)	0.9700	N(1)-C(6)-W(1)	127.3(3)
C(13)-C(14)	1.537(5)	C(7)-C(6)-W(1)	120.8(3)
C(13)-H(13A)	0.9700	C(6)-N(1)-C(11)	127.8(3)
C(13)-H(13B)	0.9700	C(6)-N(1)-H(1)	120(3)
C(14)-C(15)	1.499(6)	C(11)-N(1)-H(1)	112(3)
C(14)-H(14A)	0.9700	C(8)-C(7)-O(6)	109.0(3)

C(8)-C(7)-C(6)	134.2(3)		C(14)-C(13)-C(12)	110.9(3)
O(6)-C(7)-C(6)	116.6(3)		C(14)-C(13)-H(13A)	109.5
C(7)-C(8)-C(9)	107.3(4)		C(12)-C(13)-H(13A)	109.5
C(7)-C(8)-H(8)	126.4		C(14)-C(13)-H(13B)	109.5
C(9)-C(8)-H(8)	126.4		C(12)-C(13)-H(13B)	109.5
C(10)-C(9)-C(8)	106.4(3)		H(13A)-C(13)-H(13B)	108.0
C(10)-C(9)-H(9)	126.8		C(15)-C(14)-C(13)	111.2(4)
C(8)-C(9)-H(9)	126.8		C(15)-C(14)-H(14A)	109.4
C(9)-C(10)-O(6)	111.2(3)		C(13)-C(14)-H(14A)	109.4
C(9)-C(10)-H(10)	124.4		C(15)-C(14)-H(14B)	109.4
O(6)-C(10)-H(10)	124.4		C(13)-C(14)-H(14B)	109.4
C(10)-O(6)-C(7)	106.1(3)		H(14A)-C(14)-H(14B)	108.0
N(1)-C(11)-C(12)	109.2(3)		C(14)-C(15)-C(16)	111.2(3)
N(1)-C(11)-C(16)	110.5(3)		C(14)-C(15)-H(15A)	109.4
C(12)-C(11)-C(16)	111.3(3)		C(16)-C(15)-H(15A)	109.4
N(1)-C(11)-H(11)	108.6		C(14)-C(15)-H(15B)	109.4
C(12)-C(11)-H(11)	108.6		C(16)-C(15)-H(15B)	109.4
C(16)-C(11)-H(11)	108.6		H(15A)-C(15)-H(15B)	108.0
C(11)-C(12)-C(13)	110.3(3)		C(11)-C(16)-C(15)	109.8(3)
C(11)-C(12)-H(12A)	109.6		C(11)-C(16)-H(16A)	109.7
C(13)-C(12)-H(12A)	109.6		C(15)-C(16)-H(16A)	109.7
C(11)-C(12)-H(12B)	109.6		C(11)-C(16)-H(16B)	109.7
C(13)-C(12)-H(12B)	109.6		C(15)-C(16)-H(16B)	109.7
H(12A)-C(12)-H(12B)	108.1		H(16A)-C(16)-H(16B)	108.2

_____

164

Table 4.   Anisotropic displacement parameters (Å^{2}x 10^3)for **B4**.   The anisotropic displacement factor exponent takes the form: -2p^2[h^{2}a*^{2}U^{11} + ... + 2 h k a* b* U^{12}]

	U^{11}	U^{22}	U^{33}	U^{23}	U^{13}	U^{12}
W(1)	16(1)	16(1)	24(1)	-8(1)	-1(1)	-2(1)
C(1)	25(2)	27(2)	45(2)	-13(2)	-6(2)	-2(2)
O(1)	37(2)	31(2)	75(2)	-28(2)	0(2)	6(2)
C(2)	22(2)	24(2)	30(2)	-4(1)	-2(1)	-6(2)
O(2)	23(1)	47(2)	52(2)	-7(2)	-2(1)	-13(1)
C(3)	28(2)	21(2)	33(2)	-2(2)	-4(1)	-12(2)
O(3)	63(2)	47(2)	33(2)	3(1)	-17(1)	-34(2)
C(4)	32(2)	25(2)	30(2)	-6(2)	-5(1)	-8(2)
O(4)	48(2)	39(2)	47(2)	-6(1)	-4(1)	-28(2)
C(5)	21(2)	29(2)	30(2)	-12(2)	4(1)	-6(2)
O(5)	39(2)	66(3)	29(1)	-16(2)	-6(1)	-14(2)
C(6)	18(2)	17(2)	23(1)	-7(1)	-2(1)	-3(1)
N(1)	18(1)	18(2)	30(1)	-6(1)	5(1)	-4(1)
C(7)	20(2)	21(2)	28(2)	-11(1)	3(1)	-6(1)
C(8)	33(2)	27(2)	31(2)	-12(2)	7(1)	-15(2)
C(9)	39(2)	38(2)	34(2)	-15(2)	15(2)	-23(2)
C(10)	29(2)	40(2)	42(2)	-22(2)	19(2)	-15(2)
O(6)	23(1)	27(2)	37(1)	-14(1)	11(1)	-5(1)
C(11)	18(2)	21(2)	25(2)	-5(1)	3(1)	-6(1)
C(12)	29(2)	34(2)	29(2)	-9(2)	2(1)	-15(2)
C(13)	33(2)	40(3)	45(2)	-11(2)	7(2)	-24(2)
C(14)	35(2)	30(2)	37(2)	-1(2)	10(2)	-11(2)
C(15)	30(2)	34(2)	25(2)	-3(2)	2(1)	-6(2)
C(16)	19(2)	30(2)	28(2)	-2(1)	-1(1)	-6(1)

165

Table 5.   Hydrogen coordinates (x 10^4) and isotropic displacement parameters (Å^2x 10^3) for **B4**.

	x	y	z	U(eq)
H(1)	200(70)	6280(60)	2560(30)	27
H(8)	1240	1909	4663	34
H(9)	-1945	3112	5559	41
H(10)	-3714	5777	4693	42
H(11)	3560	5223	1546	26
H(12A)	4499	6623	2415	35
H(12B)	2403	8069	2090	35
H(13A)	5252	8575	1230	44
H(13B)	5843	6986	949	44
H(14A)	2049	9586	391	43
H(14B)	3947	9027	-245	43
H(15A)	3236	6728	-114	38
H(15B)	1151	8169	-462	38
H(16A)	-257	7834	999	33
H(16B)	325	6249	713	33

166

Table 6. Torsion angles [°] for **B4**.

_____

C(3)-W(1)-C(6)-N(1)	127.0(3)	C(7)-C(8)-C(9)-C(10)	0.2(5)
C(5)-W(1)-C(6)-N(1)	-53.0(3)	C(8)-C(9)-C(10)-O(6)	-0.5(5)
C(2)-W(1)-C(6)-N(1)	38.4(3)	C(9)-C(10)-O(6)-C(7)	0.5(5)
C(4)-W(1)-C(6)-N(1)	-140.8(3)	C(8)-C(7)-O(6)-C(10)	-0.4(4)
C(3)-W(1)-C(6)-C(7)	-54.9(3)	C(6)-C(7)-O(6)-C(10)	-176.6(3)
C(5)-W(1)-C(6)-C(7)	125.0(3)	C(6)-N(1)-C(11)-C(12)	-111.8(4)
C(2)-W(1)-C(6)-C(7)	-143.5(3)	C(6)-N(1)-C(11)-C(16)	125.5(4)
C(4)-W(1)-C(6)-C(7)	37.2(3)	N(1)-C(11)-C(12)-C(13)	-178.5(3)
C(7)-C(6)-N(1)-C(11)	176.9(3)	C(16)-C(11)-C(12)-C(13)	-56.2(4)
W(1)-C(6)-N(1)-C(11)	-4.9(5)	C(11)-C(12)-C(13)-C(14)	55.7(5)
N(1)-C(6)-C(7)-C(8)	-168.8(4)	C(12)-C(13)-C(14)-C(15)	-56.7(5)
W(1)-C(6)-C(7)-C(8)	12.9(6)	C(13)-C(14)-C(15)-C(16)	57.4(4)
N(1)-C(6)-C(7)-O(6)	6.1(4)	N(1)-C(11)-C(16)-C(15)	178.1(3)
W(1)-C(6)-C(7)-O(6)	-172.2(2)	C(12)-C(11)-C(16)-C(15)	56.5(4)
O(6)-C(7)-C(8)-C(9)	0.1(4)	C(14)-C(15)-C(16)-C(11)	-57.0(4)
C(6)-C(7)-C(8)-C(9)	175.3(4)		

_____

Table 7.   Hydrogen bonds for **B4** [Å and °].

D-H...A	d(D-H)	d(H...A)	d(D...A)	<(DHA)
N(1)-H(1)...O(6)	0.83(5)	2.17(4)	2.585(4)	111(4)
N(1)-H(1)...O(1)#1	0.83(5)	2.35(5)	3.141(5)	158(4)

Symmetry transformations used to generate equivalent atoms: #1 x-1, y+1, z

APPENDIX E:

CRYSTALLOGRAPHIC DATA OF COMPLEX A5
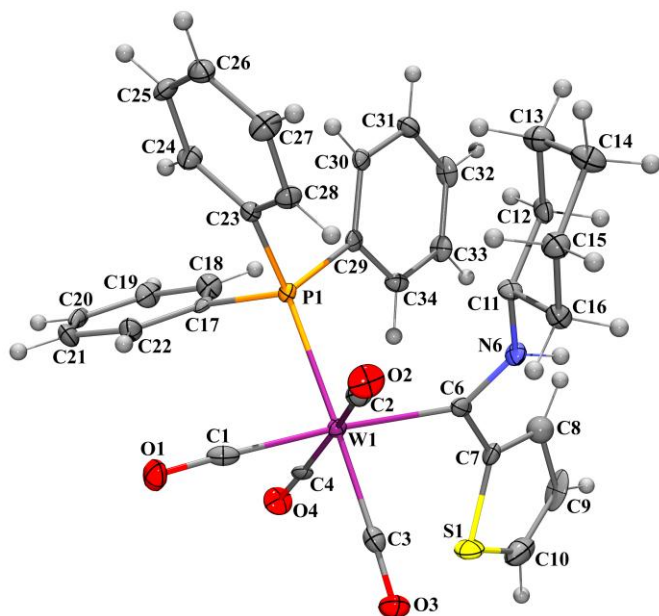
Table 1. Crystal data and structure refinement for **A5**.

Identification code	rp77tpc	
Empirical formula	$C_{33}H_{29}N\,O_4PSW$	
Formula weight	750.45	
Temperature	100(2) K	
Wavelength	0.71073 Å	
Crystal system	Monoclinic	
Space group	*Cc*	
Unit cell dimensions	a = 18.2055(16) Å	$\alpha = 90°.$
	b = 15.3430(14) Å	$\beta = 93.649(1)°.$
	c = 10.7537(10) Å	$\gamma = 90°.$
Volume	2997.7(5) Å^3	
Z	4	
Density (calculated)	1.663 Mg/m^3	

Absorption coefficient	4.015 mm^{-1}
F(000)	1484
Crystal size	0.23 x 0.12 x 0.06 mm^3
θ range for data collection	1.74 to 28.84°.
Index ranges	-23<=h<=24, -20<=k<=19, -14<=l<=6
Reflections collected	9549
Independent reflections	4822 [R(int) = 0.0318]
Completeness to θ = 25.24°	100.0 %
Absorption correction	Semi-empirical from equivalents
Max. and min. transmission	0.7947 and 0.4534
Refinement method	Full-matrix least-squares on F^2
Data / restraints / parameters	4822 / 2 / 379
Goodness-of-fit on F^2	0.945
Final R indices [I>2sigma(I)]	R1 = 0.0247, wR2 = 0.0484
R indices (all data)	R1 = 0.0286, wR2 = 0.0504
Absolute structure parameter	0.013(6)
Extinction coefficient	0
Largest diff. peak and hole	1.094 and -0.554 e.Å^{-3}

170

Table 2.   Atomic coordinates (x 10^4) and equivalent isotropic displacement parameters ($Å^2$x 10^3) for **A5**.   U(eq) is defined as one third of the trace of the orthogonalized U^{ij} tensor.

	x	y	z	U(eq)
W(1)	-61(1)	3067(1)	2398(1)	11(1)
C(1)	-649(3)	2734(3)	851(5)	17(1)
O(1)	-1013(2)	2548(3)	-38(4)	25(1)
C(2)	394(3)	3979(3)	1331(5)	18(1)
O(2)	577(2)	4507(2)	647(4)	25(1)
C(3)	-798(3)	3990(3)	2692(5)	16(1)
O(3)	-1234(2)	4527(2)	2821(4)	23(1)
C(4)	-686(3)	2178(3)	3246(5)	15(1)
O(4)	-1098(2)	1685(2)	3624(4)	23(1)
C(6)	520(3)	3448(3)	4222(5)	15(1)
N(6)	1180(2)	3788(3)	4423(4)	15(1)
C(7)	176(3)	3339(3)	5436(5)	15(1)
S(1)	-746(2)	3455(3)	5584(4)	23(1)
C(8)	531(11)	3174(14)	6574(19)	25(7)
S(1A)	683(4)	3132(4)	6782(5)	18(1)
C(8A)	-561(10)	3375(14)	5640(20)	12(5)
C(9)	5(6)	3120(3)	7607(5)	30(2)
C(10)	-670(4)	3258(4)	7073(7)	33(2)
C(11)	1713(3)	3980(3)	3497(5)	14(1)
C(12)	2484(3)	3692(4)	3976(5)	17(1)
C(13)	3038(3)	3911(4)	3003(5)	23(1)
C(14)	3024(3)	4875(4)	2690(5)	23(1)
C(15)	2242(3)	5175(3)	2249(5)	19(1)
C(16)	1692(3)	4953(3)	3198(5)	17(1)
P(1)	847(1)	1836(1)	2025(1)	11(1)
C(17)	384(2)	778(3)	1750(4)	12(1)
C(18)	507(3)	70(3)	2578(5)	20(1)
C(19)	151(3)	-718(3)	2310(6)	20(1)
C(20)	-298(3)	-823(3)	1229(5)	20(1)
C(21)	-402(3)	-127(3)	419(5)	20(1)
C(22)	-73(3)	664(3)	685(5)	17(1)
C(23)	1425(3)	1894(3)	689(5)	14(1)

171

C(24)	1647(3)	1134(3)	78(5)	17(1)
C(25)	2132(3)	1192(4)	-859(5)	19(1)
C(26)	2403(3)	1987(3)	-1220(5)	19(1)
C(27)	2191(3)	2739(4)	-621(5)	22(1)
C(28)	1700(3)	2689(3)	318(5)	16(1)
C(29)	1511(3)	1568(3)	3307(5)	13(1)
C(30)	2247(3)	1329(3)	3141(5)	14(1)
C(31)	2717(3)	1097(3)	4160(5)	18(1)
C(32)	2472(4)	1098(4)	5343(6)	20(1)
C(33)	1749(3)	1335(3)	5528(5)	18(1)
C(34)	1284(3)	1573(3)	4522(5)	15(1)

_____

Table 3.   Bond lengths [Å] and angles [°] for **A5**.

_____

W(1)-C(1)	1.986(6)	C(13)-H(13B)	0.9900
W(1)-C(3)	1.990(5)	C(14)-C(15)	1.543(7)
W(1)-C(2)	2.021(5)	C(14)-H(14A)	0.9900
W(1)-C(4)	2.028(5)	C(14)-H(14B)	0.9900
W(1)-C(6)	2.246(5)	C(15)-C(16)	1.513(7)
W(1)-P(1)	2.5580(13)	C(15)-H(15A)	0.9900
C(1)-O(1)	1.165(6)	C(15)-H(15B)	0.9900
C(2)-O(2)	1.157(6)	C(16)-H(16A)	0.9900
C(3)-O(3)	1.158(6)	C(16)-H(16B)	0.9900
C(4)-O(4)	1.158(6)	P(1)-C(29)	1.821(5)
C(6)-N(6)	1.314(6)	P(1)-C(23)	1.837(5)
C(6)-C(7)	1.493(7)	P(1)-C(17)	1.844(5)
N(6)-C(11)	1.465(6)	C(17)-C(22)	1.384(7)
N(6)-H(6)	0.8800	C(17)-C(18)	1.413(7)
C(7)-C(8)	1.370(19)	C(18)-C(19)	1.393(7)
C(7)-C(8A)	1.376(19)	C(18)-H(18)	0.9500
C(7)-S(1A)	1.696(9)	C(19)-C(20)	1.388(8)
C(7)-S(1)	1.706(7)	C(19)-H(19)	0.9500
S(1)-C(10)	1.626(9)	C(20)-C(21)	1.384(8)
C(8)-C(9)	1.51(2)	C(20)-H(20)	0.9500
C(8)-H(8)	0.9500	C(21)-C(22)	1.376(7)
S(1A)-C(9)	1.564(12)	C(21)-H(21)	0.9500
C(8A)-C(10)	1.57(2)	C(22)-H(22)	0.9500
C(8A)-H(8A)	0.9500	C(23)-C(28)	1.386(7)
C(9)-C(10)	1.340(12)	C(23)-C(24)	1.410(7)
C(9)-H(9)	0.9500	C(24)-C(25)	1.384(7)
C(10)-H(10)	0.9500	C(24)-H(24)	0.9500
C(11)-C(16)	1.527(7)	C(25)-C(26)	1.381(7)
C(11)-C(12)	1.528(8)	C(25)-H(25)	0.9500
C(12)-C(13)	1.536(8)	C(26)-C(27)	1.389(7)
C(12)-H(12A)	0.9900	C(26)-H(26)	0.9500
C(12)-H(12B)	0.9900	C(27)-C(28)	1.393(7)
C(13)-C(14)	1.517(7)	C(27)-H(27)	0.9500
C(13)-H(13A)	0.9900	C(28)-H(28)	0.9500

C(29)-C(34)	1.395(7)	C(11)-N(6)-H(6)	116.3
C(29)-C(30)	1.411(7)	C(8)-C(7)-C(8A)	105.9(14)
C(30)-C(31)	1.393(7)	C(8)-C(7)-C(6)	127.0(10)
C(30)-H(30)	0.9500	C(8A)-C(7)-C(6)	127.1(11)
C(31)-C(32)	1.375(8)	C(8)-C(7)-S(1A)	4.9(11)
C(31)-H(31)	0.9500	C(8A)-C(7)-S(1A)	110.7(10)
C(32)-C(33)	1.390(8)	C(6)-C(7)-S(1A)	122.1(4)
C(32)-H(32)	0.9500	C(8)-C(7)-S(1)	110.3(10)
C(33)-C(34)	1.380(7)	C(8A)-C(7)-S(1)	5.3(10)
C(33)-H(33)	0.9500	C(6)-C(7)-S(1)	122.7(4)
C(34)-H(34)	0.9500	S(1A)-C(7)-S(1)	115.2(4)
		C(10)-S(1)-C(7)	92.8(4)
C(1)-W(1)-C(3)	89.0(2)	C(7)-C(8)-C(9)	112.4(14)
C(1)-W(1)-C(2)	85.5(2)	C(7)-C(8)-H(8)	123.8
C(3)-W(1)-C(2)	84.4(2)	C(9)-C(8)-H(8)	123.8
C(1)-W(1)-C(4)	85.2(2)	C(9)-S(1A)-C(7)	94.6(5)
C(3)-W(1)-C(4)	90.2(2)	C(7)-C(8A)-C(10)	109.7(14)
C(2)-W(1)-C(4)	169.3(2)	C(7)-C(8A)-H(8A)	125.2
C(1)-W(1)-C(6)	175.52(19)	C(10)-C(8A)-H(8A)	125.2
C(3)-W(1)-C(6)	87.8(2)	C(10)-C(9)-C(8)	106.4(8)
C(2)-W(1)-C(6)	97.3(2)	C(10)-C(9)-S(1A)	119.4(5)
C(4)-W(1)-C(6)	91.7(2)	C(8)-C(9)-S(1A)	12.9(8)
C(1)-W(1)-P(1)	89.91(15)	C(10)-C(9)-H(9)	126.8
C(3)-W(1)-P(1)	177.81(15)	C(8)-C(9)-H(9)	126.8
C(2)-W(1)-P(1)	97.45(15)	S(1A)-C(9)-H(9)	113.8
C(4)-W(1)-P(1)	87.77(14)	C(9)-C(10)-C(8A)	105.5(9)
C(6)-W(1)-P(1)	93.17(13)	C(9)-C(10)-S(1)	118.0(6)
O(1)-C(1)-W(1)	177.8(4)	C(8A)-C(10)-S(1)	12.8(7)
O(2)-C(2)-W(1)	172.1(5)	C(9)-C(10)-H(10)	121.0
O(3)-C(3)-W(1)	177.7(5)	C(8A)-C(10)-H(10)	133.4
O(4)-C(4)-W(1)	172.6(5)	S(1)-C(10)-H(10)	121.0
N(6)-C(6)-C(7)	109.3(5)	N(6)-C(11)-C(16)	109.3(4)
N(6)-C(6)-W(1)	128.4(4)	N(6)-C(11)-C(12)	110.3(4)
C(7)-C(6)-W(1)	122.3(3)	C(16)-C(11)-C(12)	111.3(4)
C(6)-N(6)-C(11)	127.3(4)	C(11)-C(12)-C(13)	109.6(5)
C(6)-N(6)-H(6)	116.3	C(11)-C(12)-H(12A)	109.7

174

C(13)-C(12)-H(12A)	109.7		C(18)-C(17)-P(1)	121.6(4)
C(11)-C(12)-H(12B)	109.7		C(19)-C(18)-C(17)	119.0(5)
C(13)-C(12)-H(12B)	109.7		C(19)-C(18)-H(18)	120.5
H(12A)-C(12)-H(12B)	108.2		C(17)-C(18)-H(18)	120.5
C(14)-C(13)-C(12)	111.2(4)		C(20)-C(19)-C(18)	121.0(5)
C(14)-C(13)-H(13A)	109.4		C(20)-C(19)-H(19)	119.5
C(12)-C(13)-H(13A)	109.4		C(18)-C(19)-H(19)	119.5
C(14)-C(13)-H(13B)	109.4		C(21)-C(20)-C(19)	119.2(5)
C(12)-C(13)-H(13B)	109.4		C(21)-C(20)-H(20)	120.4
H(13A)-C(13)-H(13B)	108.0		C(19)-C(20)-H(20)	120.4
C(13)-C(14)-C(15)	111.1(4)		C(22)-C(21)-C(20)	120.6(5)
C(13)-C(14)-H(14A)	109.4		C(22)-C(21)-H(21)	119.7
C(15)-C(14)-H(14A)	109.4		C(20)-C(21)-H(21)	119.7
C(13)-C(14)-H(14B)	109.4		C(21)-C(22)-C(17)	121.0(5)
C(15)-C(14)-H(14B)	109.4		C(21)-C(22)-H(22)	119.5
H(14A)-C(14)-H(14B)	108.0		C(17)-C(22)-H(22)	119.5
C(16)-C(15)-C(14)	111.3(4)		C(28)-C(23)-C(24)	118.3(5)
C(16)-C(15)-H(15A)	109.4		C(28)-C(23)-P(1)	120.2(4)
C(14)-C(15)-H(15A)	109.4		C(24)-C(23)-P(1)	121.3(4)
C(16)-C(15)-H(15B)	109.4		C(25)-C(24)-C(23)	120.1(5)
C(14)-C(15)-H(15B)	109.4		C(25)-C(24)-H(24)	120.0
H(15A)-C(15)-H(15B)	108.0		C(23)-C(24)-H(24)	120.0
C(15)-C(16)-C(11)	110.7(4)		C(26)-C(25)-C(24)	121.1(5)
C(15)-C(16)-H(16A)	109.5		C(26)-C(25)-H(25)	119.4
C(11)-C(16)-H(16A)	109.5		C(24)-C(25)-H(25)	119.4
C(15)-C(16)-H(16B)	109.5		C(25)-C(26)-C(27)	119.3(5)
C(11)-C(16)-H(16B)	109.5		C(25)-C(26)-H(26)	120.4
H(16A)-C(16)-H(16B)	108.1		C(27)-C(26)-H(26)	120.4
C(29)-P(1)-C(23)	102.5(2)		C(26)-C(27)-C(28)	120.0(5)
C(29)-P(1)-C(17)	101.4(2)		C(26)-C(27)-H(27)	120.0
C(23)-P(1)-C(17)	101.3(2)		C(28)-C(27)-H(27)	120.0
C(29)-P(1)-W(1)	116.92(16)		C(23)-C(28)-C(27)	121.2(5)
C(23)-P(1)-W(1)	119.68(17)		C(23)-C(28)-H(28)	119.4
C(17)-P(1)-W(1)	112.42(15)		C(27)-C(28)-H(28)	119.4
C(22)-C(17)-C(18)	119.1(5)		C(34)-C(29)-C(30)	117.3(5)
C(22)-C(17)-P(1)	119.3(4)		C(34)-C(29)-P(1)	119.1(4)

175

C(30)-C(29)-P(1)	123.6(4)		C(31)-C(32)-H(32)	120.1
C(31)-C(30)-C(29)	120.5(5)		C(33)-C(32)-H(32)	120.1
C(31)-C(30)-H(30)	119.7		C(34)-C(33)-C(32)	119.7(5)
C(29)-C(30)-H(30)	119.7		C(34)-C(33)-H(33)	120.1
C(32)-C(31)-C(30)	120.6(5)		C(32)-C(33)-H(33)	120.1
C(32)-C(31)-H(31)	119.7		C(33)-C(34)-C(29)	122.0(5)
C(30)-C(31)-H(31)	119.7		C(33)-C(34)-H(34)	119.0
C(31)-C(32)-C(33)	119.9(5)		C(29)-C(34)-H(34)	119.0

_____

Table 4.   Anisotropic displacement parameters ($\text{Å}^2\text{x }10^3$)for **A5**.   The anisotropic displacement factor exponent takes the form: $-2p^2[\ h^2a^{*2}U^{11} + ... + 2\ h\ k\ a^*\ b^*\ U^{12}\ ]$

	U^{11}	U^{22}	U^{33}	U^{23}	U^{13}	U^{12}
W(1)	11(1)	10(1)	11(1)	0(1)	1(1)	0(1)
C(1)	14(3)	16(3)	21(3)	8(2)	6(2)	4(2)
O(1)	29(2)	26(2)	18(2)	-4(2)	-8(2)	6(2)
C(2)	17(3)	20(3)	17(3)	-1(2)	1(2)	3(2)
O(2)	30(2)	18(2)	27(2)	8(2)	5(2)	1(2)
C(3)	15(3)	19(3)	15(3)	1(2)	-1(2)	-4(2)
O(3)	19(2)	23(2)	27(2)	0(2)	-1(2)	8(2)
C(4)	10(2)	19(3)	15(3)	-3(2)	-2(2)	8(2)
O(4)	22(2)	20(2)	29(2)	3(2)	7(2)	-7(2)
C(6)	12(2)	9(2)	23(3)	-2(2)	1(2)	0(2)
N(6)	17(2)	17(2)	10(2)	-1(2)	2(2)	-1(2)
C(7)	18(3)	12(2)	14(2)	-4(2)	3(2)	-1(2)
S(1)	16(2)	32(2)	21(2)	-1(1)	7(2)	5(2)
S(1A)	24(3)	24(2)	7(2)	0(2)	3(2)	-4(2)
C(9)	62(5)	24(3)	4(5)	0(2)	3(5)	-4(3)
C(10)	33(4)	24(3)	42(4)	-8(3)	18(3)	-3(3)
C(11)	12(2)	18(3)	14(2)	1(2)	5(2)	-3(2)
C(12)	17(3)	20(3)	12(3)	-2(2)	-2(2)	-4(2)
C(13)	18(3)	27(3)	23(3)	1(2)	3(2)	2(2)
C(14)	17(3)	27(3)	26(3)	6(2)	2(2)	-1(2)
C(15)	19(3)	21(3)	17(3)	1(2)	3(2)	-1(2)
C(16)	16(3)	15(3)	18(3)	2(2)	-1(2)	0(2)
P(1)	12(1)	12(1)	10(1)	-1(1)	1(1)	0(1)
C(17)	12(2)	12(2)	12(2)	-3(2)	7(2)	-1(2)
C(18)	21(3)	20(3)	19(3)	3(2)	1(2)	-1(2)
C(19)	22(3)	15(3)	24(3)	1(2)	5(3)	-4(2)
C(20)	15(2)	17(3)	28(3)	-13(2)	8(2)	-6(2)
C(21)	14(2)	22(3)	23(3)	-5(2)	-5(2)	0(2)
C(22)	17(3)	14(3)	19(3)	0(2)	-3(2)	2(2)
C(23)	11(2)	16(3)	14(2)	-2(2)	1(2)	-1(2)
C(24)	18(3)	17(3)	17(3)	0(2)	5(2)	-3(2)
C(25)	19(3)	20(3)	20(3)	-7(2)	7(2)	1(2)

177

C(26)	16(2)	27(3)	16(3)	-1(2)	4(2)	-1(2)
C(27)	28(3)	18(3)	20(3)	3(2)	7(2)	1(2)
C(28)	17(3)	13(2)	19(3)	1(2)	2(2)	3(2)
C(29)	15(2)	7(2)	15(3)	-1(2)	0(2)	-2(2)
C(30)	14(2)	12(2)	15(3)	-2(2)	2(2)	-4(2)
C(31)	13(2)	19(3)	23(3)	-1(2)	-1(2)	0(2)
C(32)	27(3)	16(3)	14(3)	6(2)	-8(3)	-2(2)
C(33)	24(3)	19(3)	11(2)	3(2)	0(2)	-1(2)
C(34)	13(2)	14(3)	19(3)	2(2)	2(2)	2(2)

_____

Table 5.   Hydrogen coordinates (x 10^4) and isotropic displacement parameters (Å^2x 10^3) for **A5**.

	x	y	z	U(eq)
H(6)	1316	3914	5202	18
H(8)	1049	3102	6700	30
H(8A)	-947	3458	5014	15
H(9)	129	3010	8464	36
H(10)	-1092	3242	7550	39
H(12A)	2487	3057	4137	20
H(12B)	2625	3995	4768	20
H(13A)	3539	3745	3330	27
H(13B)	2918	3569	2236	27
H(14A)	3364	4991	2026	28
H(14B)	3197	5214	3435	28
H(15A)	2242	5812	2109	23
H(15B)	2093	4888	1447	23
H(16A)	1191	5116	2866	20
H(16B)	1807	5291	3970	20
H(18)	828	130	3305	24
H(19)	217	-1190	2877	24
H(20)	-531	-1366	1048	24
H(21)	-704	-196	-328	23
H(22)	-161	1139	129	20
H(24)	1464	582	310	20
H(25)	2281	676	-1261	23
H(26)	2731	2019	-1871	23
H(27)	2381	3289	-852	26
H(28)	1551	3208	712	20
H(30)	2423	1327	2328	16
H(31)	3211	937	4036	22
H(32)	2795	936	6033	23
H(33)	1577	1332	6344	22
H(34)	795	1746	4661	18

Table 6.   Torsion angles [°] for **A5**.

_____

C(3)-W(1)-C(6)-N(6)	-115.2(5)	C(7)-S(1A)-C(9)-C(8)	0(4)
C(2)-W(1)-C(6)-N(6)	-31.2(5)	C(8)-C(9)-C(10)-C(8A)	1.7(13)
C(4)-W(1)-C(6)-N(6)	154.6(5)	S(1A)-C(9)-C(10)-C(8A)	1.6(10)
P(1)-W(1)-C(6)-N(6)	66.8(4)	C(8)-C(9)-C(10)-S(1)	-1.3(11)
C(3)-W(1)-C(6)-C(7)	64.5(4)	S(1A)-C(9)-C(10)-S(1)	-1.4(8)
C(2)-W(1)-C(6)-C(7)	148.6(4)	C(7)-C(8A)-C(10)-C(9)	-2.9(15)
C(4)-W(1)-C(6)-C(7)	-25.6(4)	C(7)-C(8A)-C(10)-S(1)	165(5)
P(1)-W(1)-C(6)-C(7)	-113.5(4)	C(7)-S(1)-C(10)-C(9)	1.9(6)
C(7)-C(6)-N(6)-C(11)	178.2(4)	C(6)-N(6)-C(11)-C(16)	100.9(6)
W(1)-C(6)-N(6)-C(11)	-2.0(7)	C(6)-N(6)-C(11)-C(12)	-136.4(5)
N(6)-C(6)-C(7)-C(8)	-31.1(13)	N(6)-C(11)-C(12)-C(13)	-179.2(4)
W(1)-C(6)-C(7)-C(8)	149.1(12)	C(16)-C(11)-C(12)-C(13)	-57.6(6)
N(6)-C(6)-C(7)-C(8A)	149.6(12)	C(11)-C(12)-C(13)-C(14)	56.9(6)
W(1)-C(6)-C(7)-C(8A)	-30.2(13)	C(12)-C(13)-C(14)-C(15)	-55.7(6)
N(6)-C(6)-C(7)-S(1A)	-31.3(6)	C(13)-C(14)-C(15)-C(16)	55.0(6)
W(1)-C(6)-C(7)-S(1A)	148.9(4)	C(14)-C(15)-C(16)-C(11)	-55.4(6)
N(6)-C(6)-C(7)-S(1)	146.1(4)	N(6)-C(11)-C(16)-C(15)	179.6(4)
W(1)-C(6)-C(7)-S(1)	-33.7(6)	C(12)-C(11)-C(16)-C(15)	57.5(6)
C(8)-C(7)-S(1)-C(10)	-1.9(11)	C(1)-W(1)-P(1)-C(29)	-168.1(2)
C(6)-C(7)-S(1)-C(10)	-179.5(5)	C(3)-W(1)-P(1)-C(29)	-107(4)
C(8A)-C(7)-C(8)-C(9)	-1.6(19)	C(2)-W(1)-P(1)-C(29)	106.5(2)
C(6)-C(7)-C(8)-C(9)	179.0(7)	C(4)-W(1)-P(1)-C(29)	-82.9(2)
S(1A)-C(7)-C(8)-C(9)	-179(100)	C(6)-W(1)-P(1)-C(29)	8.6(2)
S(1)-C(7)-C(8)-C(9)	1.5(17)	C(1)-W(1)-P(1)-C(23)	67.1(2)
C(8)-C(7)-S(1A)-C(9)	1(13)	C(3)-W(1)-P(1)-C(23)	129(4)
C(8A)-C(7)-S(1A)-C(9)	-1.9(11)	C(2)-W(1)-P(1)-C(23)	-18.3(2)
C(6)-C(7)-S(1A)-C(9)	178.9(4)	C(4)-W(1)-P(1)-C(23)	152.4(2)
S(1)-C(7)-S(1A)-C(9)	1.3(5)	C(6)-W(1)-P(1)-C(23)	-116.1(2)
C(8)-C(7)-C(8A)-C(10)	2.6(18)	C(1)-W(1)-P(1)-C(17)	-51.5(2)
C(6)-C(7)-C(8A)-C(10)	-177.9(7)	C(3)-W(1)-P(1)-C(17)	10(4)
S(1A)-C(7)-C(8A)-C(10)	2.9(16)	C(2)-W(1)-P(1)-C(17)	-136.9(2)
C(7)-C(8)-C(9)-C(10)	-0.2(17)	C(4)-W(1)-P(1)-C(17)	33.7(2)
C(7)-C(8)-C(9)-S(1A)	179(6)	C(6)-W(1)-P(1)-C(17)	125.3(2)
C(7)-S(1A)-C(9)-C(10)	0.0(6)	C(29)-P(1)-C(17)-C(22)	-168.1(4)

180

C(23)-P(1)-C(17)-C(22)	-62.7(4)
W(1)-P(1)-C(17)-C(22)	66.3(4)
C(29)-P(1)-C(17)-C(18)	9.5(4)
C(23)-P(1)-C(17)-C(18)	114.9(4)
W(1)-P(1)-C(17)-C(18)	-116.2(4)
C(22)-C(17)-C(18)-C(19)	-1.4(7)
P(1)-C(17)-C(18)-C(19)	-179.0(4)
C(17)-C(18)-C(19)-C(20)	2.3(7)
C(18)-C(19)-C(20)-C(21)	-1.2(7)
C(19)-C(20)-C(21)-C(22)	-0.8(7)
C(20)-C(21)-C(22)-C(17)	1.6(8)
C(18)-C(17)-C(22)-C(21)	-0.5(7)
P(1)-C(17)-C(22)-C(21)	177.1(4)
C(29)-P(1)-C(23)-C(28)	-94.9(4)
C(17)-P(1)-C(23)-C(28)	160.6(4)
W(1)-P(1)-C(23)-C(28)	36.4(5)
C(29)-P(1)-C(23)-C(24)	80.1(5)
C(17)-P(1)-C(23)-C(24)	-24.4(5)
W(1)-P(1)-C(23)-C(24)	-148.6(4)
C(28)-C(23)-C(24)-C(25)	0.5(8)
P(1)-C(23)-C(24)-C(25)	-174.6(4)
C(23)-C(24)-C(25)-C(26)	-0.4(8)
C(24)-C(25)-C(26)-C(27)	0.7(8)
C(25)-C(26)-C(27)-C(28)	-1.1(8)
C(24)-C(23)-C(28)-C(27)	-0.8(8)
P(1)-C(23)-C(28)-C(27)	174.3(4)
C(26)-C(27)-C(28)-C(23)	1.2(8)
C(23)-P(1)-C(29)-C(34)	172.3(4)
C(17)-P(1)-C(29)-C(34)	-83.3(4)
W(1)-P(1)-C(29)-C(34)	39.3(4)
C(23)-P(1)-C(29)-C(30)	-9.5(5)
C(17)-P(1)-C(29)-C(30)	94.9(4)
W(1)-P(1)-C(29)-C(30)	-142.5(4)
C(34)-C(29)-C(30)-C(31)	0.9(7)
P(1)-C(29)-C(30)-C(31)	-177.3(4)
C(29)-C(30)-C(31)-C(32)	0.0(8)

C(30)-C(31)-C(32)-C(33)	-0.3(8)
C(31)-C(32)-C(33)-C(34)	-0.4(8)
C(32)-C(33)-C(34)-C(29)	1.3(8)
C(30)-C(29)-C(34)-C(33)	-1.6(7)
P(1)-C(29)-C(34)-C(33)	176.7(4)

Table 7.   Hydrogen bonds for **A5** [Å and °].

D-H...A	d(D-H)	d(H...A)	d(D...A)	<(DHA)
N(6)-H(6)...S(1A)	0.88	2.43	2.926(7)	116.1

APPENDIX F:

CRYSTALLOGRAPHIC DATA OF B8
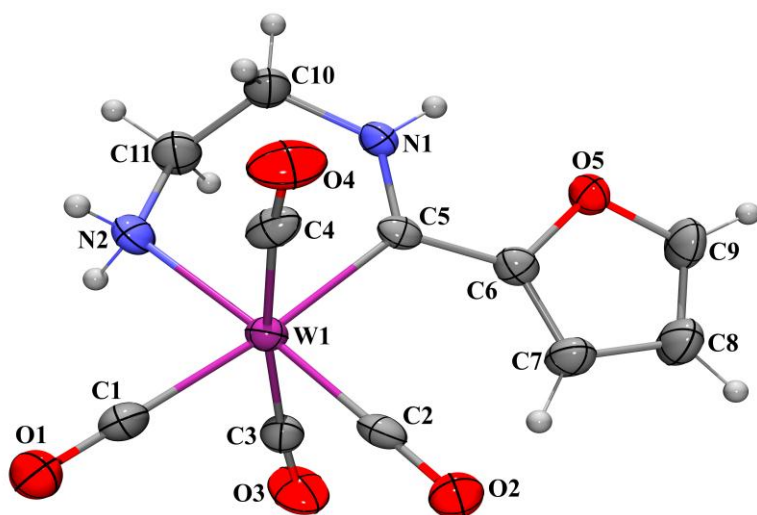
Table 1. Crystal data and structure refinement for **B8**.

Identification code	up1208
Empirical formula	$C_{11}H_{10}N_2O_5W$
Formula weight	434.06
Temperature	180(2) K
Wavelength	0.71070 Å
Crystal system	Monoclinic
Space group	*C*2/*c*
Unit cell dimensions	a = 15.2071(3) Å α = 90°.
	b = 6.40370(10) Å β = 92.1400(10)°.
	c = 26.5845(7) Å γ = 90°.
Volume	2587.04(9) Å^3
Z	8

Density (calculated)	2.229 Mg/m^3
Absorption coefficient	8.948 mm^{-1}
F(000)	1632
Crystal size	0.50 x 0.05 x 0.01 mm^3
θ range for data collection	3.53 to 27.85°.
Index ranges	-19<=h<=19, -7<=k<=8, -34<=l<=34
Reflections collected	14471
Independent reflections	3044 [R(int) = 0.0696]
Completeness to θ = 27.85°	99.1 %
Absorption correction	Semi-empirical from equivalents
Max. and min. transmission	0.924 and 0.716
Refinement method	Full-matrix least-squares on F^2
Data / restraints / parameters	3044 / 0 / 172
Goodness-of-fit on F^2	1.003
Final R indices [I>2σ(I)]	R1 = 0.0332, wR2 = 0.0459
R indices (all data)	R1 = 0.0608, wR2 = 0.0513
Extinction coefficient	0
Largest diff. peak and hole	0.827 and -0.821 e.Å^{-3}

Table 2. Atomic coordinates (x 10^4) and equivalent isotropic displacement parameters (Å^2x 10^3) for **B8**. U(eq) is defined as one third of the trace of the orthogonalized U^{ij} tensor.

	x	y	z	U(eq)
W(1)	5230(1)	8328(1)	4023(1)	23(1)
C(1)	4134(4)	9219(8)	4352(2)	34(1)
O(1)	3502(2)	9710(7)	4550(2)	50(1)
C(2)	4641(3)	5755(8)	3825(2)	26(1)
O(2)	4275(2)	4191(5)	3706(2)	35(1)
C(3)	4768(3)	9471(8)	3350(2)	29(1)
O(3)	4479(3)	9912(7)	2960(2)	50(1)
C(4)	5687(3)	6809(9)	4649(2)	28(1)
O(4)	5935(3)	5811(6)	4982(2)	45(1)
C(5)	6522(3)	7651(7)	3687(2)	23(1)
N(1)	7274(2)	8449(7)	3856(2)	26(1)
N(2)	5858(3)	11473(7)	4259(2)	33(1)
O(5)	7461(2)	5608(5)	3158(2)	33(1)
C(6)	6612(3)	6175(7)	3277(2)	27(1)
C(7)	6036(4)	5220(9)	2957(2)	35(1)
C(8)	6520(4)	4011(9)	2618(3)	43(2)
C(9)	7365(4)	4281(9)	2764(2)	40(2)
C(10)	7362(3)	10010(9)	4255(2)	35(1)
C(11)	6785(3)	11911(8)	4145(2)	38(1)

Table 3.   Bond lengths [Å] and angles [°] for **B8**.

_____

W(1)-C(2)	1.939(5)	C(2)-W(1)-C(3)	85.7(2)
W(1)-C(1)	1.993(6)	C(1)-W(1)-C(3)	90.8(2)
W(1)-C(4)	2.027(5)	C(4)-W(1)-C(3)	172.3(2)
W(1)-C(3)	2.035(6)	C(2)-W(1)-C(5)	97.5(2)
W(1)-C(5)	2.231(5)	C(1)-W(1)-C(5)	173.83(19)
W(1)-N(2)	2.305(4)	C(4)-W(1)-C(5)	87.5(2)
C(1)-O(1)	1.157(6)	C(3)-W(1)-C(5)	89.9(2)
C(2)-O(2)	1.183(6)	C(2)-W(1)-N(2)	176.92(17)
C(3)-O(3)	1.147(6)	C(1)-W(1)-N(2)	88.60(18)
C(4)-O(4)	1.145(6)	C(4)-W(1)-N(2)	94.06(19)
C(5)-N(1)	1.316(6)	C(3)-W(1)-N(2)	92.90(18)
C(5)-C(6)	1.452(7)	C(5)-W(1)-N(2)	85.24(16)
N(1)-C(10)	1.462(7)	O(1)-C(1)-W(1)	178.7(6)
N(1)-H(1)	0.8800	O(2)-C(2)-W(1)	179.4(5)
N(2)-C(11)	1.480(7)	O(3)-C(3)-W(1)	173.0(5)
N(2)-H(2A)	0.9200	O(4)-C(4)-W(1)	174.7(5)
N(2)-H(2B)	0.9200	N(1)-C(5)-C(6)	113.7(4)
O(5)-C(9)	1.352(6)	N(1)-C(5)-W(1)	123.7(4)
O(5)-C(6)	1.389(6)	C(6)-C(5)-W(1)	122.5(3)
C(6)-C(7)	1.347(7)	C(5)-N(1)-C(10)	124.6(4)
C(7)-C(8)	1.416(8)	C(5)-N(1)-H(1)	117.7
C(7)-H(7)	0.9500	C(10)-N(1)-H(1)	117.7
C(8)-C(9)	1.339(8)	C(11)-N(2)-W(1)	119.9(3)
C(8)-H(8)	0.9500	C(11)-N(2)-H(2A)	107.4
C(9)-H(9)	0.9500	W(1)-N(2)-H(2A)	107.4
C(10)-C(11)	1.523(7)	C(11)-N(2)-H(2B)	107.4
C(10)-H(10A)	0.9900	W(1)-N(2)-H(2B)	107.4
C(10)-H(10B)	0.9900	H(2A)-N(2)-H(2B)	106.9
C(11)-H(11A)	0.9900	C(9)-O(5)-C(6)	105.5(4)
C(11)-H(11B)	0.9900	C(7)-C(6)-O(5)	109.0(5)
		C(7)-C(6)-C(5)	133.8(5)
C(2)-W(1)-C(1)	88.7(2)	O(5)-C(6)-C(5)	117.2(4)
C(2)-W(1)-C(4)	87.5(2)	C(6)-C(7)-C(8)	108.0(5)
C(1)-W(1)-C(4)	92.6(2)	C(6)-C(7)-H(7)	126.0

C(8)-C(7)-H(7)	126.0		N(1)-C(10)-H(10B)	109.3
C(9)-C(8)-C(7)	105.1(5)		C(11)-C(10)-H(10B)	109.3
C(9)-C(8)-H(8)	127.5		H(10A)-C(10)-H(10B)	107.9
C(7)-C(8)-H(8)	127.5		N(2)-C(11)-C(10)	110.8(4)
C(8)-C(9)-O(5)	112.4(5)		N(2)-C(11)-H(11A)	109.5
C(8)-C(9)-H(9)	123.8		C(10)-C(11)-H(11A)	109.5
O(5)-C(9)-H(9)	123.8		N(2)-C(11)-H(11B)	109.5
N(1)-C(10)-C(11)	111.7(4)		C(10)-C(11)-H(11B)	109.5
N(1)-C(10)-H(10A)	109.3		H(11A)-C(11)-H(11B)	108.1
C(11)-C(10)-H(10A)	109.3			

_____

187

Table 4. Anisotropic displacement parameters ($Å^2$x 10^3)for **B8**. The anisotropic displacement factor exponent takes the form: $-2p^2[h^2a^{*2}U^{11} + ... + 2 h k a^* b^* U^{12}]$

	U^{11}	U^{22}	U^{33}	U^{23}	U^{13}	U^{12}
W(1)	19(1)	25(1)	24(1)	0(1)	-1(1)	0(1)
C(1)	27(3)	35(3)	38(4)	-11(3)	-7(3)	-2(2)
O(1)	29(2)	69(3)	53(3)	-27(2)	10(2)	-5(2)
C(2)	16(3)	35(3)	26(3)	3(2)	-1(2)	5(2)
O(2)	29(2)	31(2)	43(3)	-3(2)	3(2)	-6(2)
C(3)	25(3)	29(3)	34(4)	-4(2)	3(3)	-2(2)
O(3)	48(3)	67(3)	34(3)	9(2)	-6(2)	17(2)
C(4)	27(3)	38(3)	20(3)	-1(3)	2(2)	-9(3)
O(4)	47(3)	50(3)	37(3)	14(2)	-13(2)	-5(2)
C(5)	22(3)	23(3)	25(3)	6(2)	-2(2)	3(2)
N(1)	19(2)	31(2)	27(3)	-4(2)	2(2)	3(2)
N(2)	27(2)	30(2)	42(3)	-4(2)	-3(2)	8(2)
O(5)	24(2)	35(2)	41(3)	-10(2)	7(2)	0(2)
C(6)	24(3)	27(3)	31(3)	2(2)	4(2)	-2(2)
C(7)	27(3)	41(3)	37(4)	-6(3)	2(3)	-7(3)
C(8)	41(4)	47(4)	42(4)	-18(3)	5(3)	-3(3)
C(9)	45(4)	40(4)	37(4)	-14(3)	11(3)	1(3)
C(10)	24(3)	38(3)	43(4)	-11(3)	1(3)	-4(3)
C(11)	30(3)	36(3)	47(4)	-5(3)	4(3)	-5(3)

Table 5.   Hydrogen coordinates (x 10^4) and isotropic displacement parameters ($Å^2$x 10^3) for **B8**.

	x	y	z	U(eq)
H(1)	7758	8012	3718	31
H(2A)	5519	12514	4112	40
H(2B)	5809	11601	4601	40
H(7)	5413	5336	2958	42
H(8)	6295	3187	2345	52
H(9)	7842	3614	2609	48
H(10A)	7984	10456	4292	42
H(10B)	7195	9376	4578	42
H(11A)	7002	13105	4351	45
H(11B)	6822	12300	3786	45

Table 6. Torsion angles [°] for **B8**.

_____

C(2)-W(1)-C(5)-N(1)	-153.3(4)	C(9)-O(5)-C(6)-C(7)	-0.7(6)
C(4)-W(1)-C(5)-N(1)	-66.2(4)	C(9)-O(5)-C(6)-C(5)	-178.7(5)
C(3)-W(1)-C(5)-N(1)	121.0(4)	N(1)-C(5)-C(6)-C(7)	-169.9(6)
N(2)-W(1)-C(5)-N(1)	28.1(4)	W(1)-C(5)-C(6)-C(7)	13.6(9)
C(2)-W(1)-C(5)-C(6)	22.8(4)	N(1)-C(5)-C(6)-O(5)	7.4(7)
C(4)-W(1)-C(5)-C(6)	109.9(4)	W(1)-C(5)-C(6)-O(5)	-169.0(3)
C(3)-W(1)-C(5)-C(6)	-62.9(4)	O(5)-C(6)-C(7)-C(8)	-0.4(6)
N(2)-W(1)-C(5)-C(6)	-155.8(4)	C(5)-C(6)-C(7)-C(8)	177.1(6)
C(6)-C(5)-N(1)-C(10)	178.2(5)	C(6)-C(7)-C(8)-C(9)	1.4(7)
W(1)-C(5)-N(1)-C(10)	-5.3(7)	C(7)-C(8)-C(9)-O(5)	-1.9(7)
C(1)-W(1)-N(2)-C(11)	177.4(4)	C(6)-O(5)-C(9)-C(8)	1.7(7)
C(4)-W(1)-N(2)-C(11)	84.9(4)	C(5)-N(1)-C(10)-C(11)	-53.7(7)
C(3)-W(1)-N(2)-C(11)	-91.8(4)	W(1)-N(2)-C(11)-C(10)	-42.9(6)
C(5)-W(1)-N(2)-C(11)	-2.2(4)	N(1)-C(10)-C(11)-N(2)	78.4(6)

_____

Table 7. Hydrogen bonds for **B8** [Å and °].

D-H...A	d(D-H)	d(H...A)	d(D...A)	<(DHA)
N(1)-H(1)...O(5)	0.88	2.18	2.621(6)	111
N(1)-H(1)...O(2)#1	0.88	2.43	3.119(5)	136
N(2)-H(2A)...O(2)#2	0.92	2.40	3.274(5)	159
N(2)-H(2B)...O(1)#3	0.92	2.59	3.365(7)	142

Symmetry transformations used to generate equivalent atoms: #1 x+1/2,y+1/2,z   #2 x,y+1,z
#3 -x+1,-y+2,-z+1

191

APPENDIX G:

CRYSTALLOGRAPHIC DATA OF C3
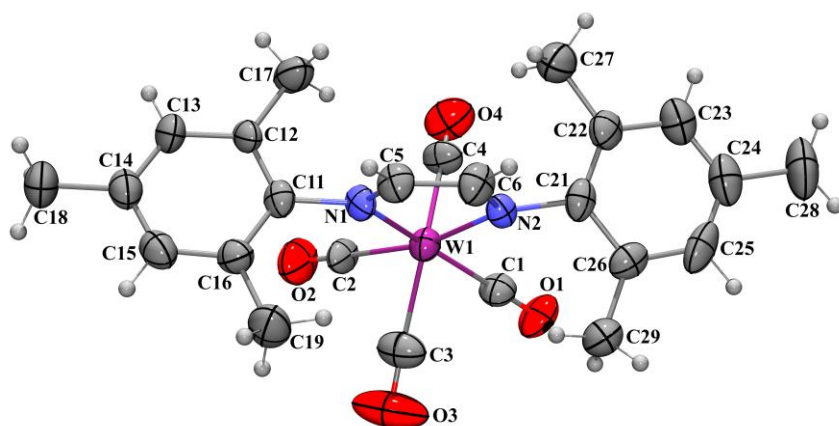
Table 1. Crystal data and structure refinement for **C3**.

Identification code	ml07_cc
Empirical formula	$C_{24}H_{24}N_2O_4W$
Formula weight	588.30
Temperature	293(2) K
Wavelength	0.71073 Å
Crystal system	Monoclinic
Space group	*Cc*
Unit cell dimensions	a = 19.6167(16) Å α = 90°.
	b = 7.5755(6) Å β = 100.932(1)°.
	c = 15.9243(13) Å γ = 90°.
Volume	2323.5(3) Å^3
Z	4
Density (calculated)	1.682 Mg/m^3

Absorption coefficient	5.003 mm^{-1}
F(000)	1152
Crystal size	0.17 x 0.14 x 0.13 mm^3
Θ range for data collection	2.61 to 26.60°.
Index ranges	-23<=h<=18, -5<=k<=9, -19<=l<=19
Reflections collected	6087
Independent reflections	3577 [R(int) = 0.0312]
Completeness to θ = 25.24°	99.2 %
Absorption correction	Semi-empirical from equivalents
Max. and min. transmission	0.552 and 0.424
Refinement method	Full-matrix least-squares on F^2
Data / restraints / parameters	3577 / 2 / 287
Goodness-of-fit on F^2	1.133
Final R indices [I>2σ(I)]	R1 = 0.0340, wR2 = 0.0899
R indices (all data)	R1 = 0.0365, wR2 = 0.0920
Absolute structure parameter	0.08(2)
Extinction coefficient	0
Largest diff. peak and hole	1.135 and -0.822 e.Å^{-3}

193

Table 2. Atomic coordinates (x 10^4) and equivalent isotropic displacement parameters (Å^2x 10^3) for **C3**. U(eq) is defined as one third of the trace of the orthogonalized U^{ij} tensor.

	x	y	z	U(eq)
W(1)	5843(1)	7430(1)	4050(1)	39(1)
C(1)	4987(5)	8771(11)	3546(6)	47(2)
O(1)	4488(4)	9497(9)	3290(5)	68(2)
C(2)	6541(5)	9377(11)	4080(7)	46(2)
O(2)	6940(4)	10444(10)	4100(6)	81(2)
C(3)	5684(6)	8661(14)	5135(6)	63(3)
O(3)	5574(7)	9532(12)	5660(6)	119(4)
C(4)	5979(6)	7225(12)	2792(6)	50(2)
O(4)	6049(6)	7342(10)	2127(7)	78(3)
N(1)	6572(3)	5567(8)	4752(4)	39(2)
N(2)	5320(3)	4933(8)	4048(4)	36(1)
C(5)	6342(5)	3998(10)	4877(6)	45(2)
C(6)	5653(5)	3603(11)	4460(6)	50(2)
C(11)	7287(4)	5967(9)	5147(5)	39(2)
C(12)	7795(4)	5801(11)	4644(5)	40(2)
C(13)	8478(5)	6227(12)	5019(6)	53(2)
C(14)	8652(5)	6764(12)	5852(7)	52(2)
C(15)	8140(5)	6847(13)	6331(6)	52(2)
C(16)	7457(5)	6463(11)	6001(5)	44(2)
C(17)	7617(6)	5152(16)	3736(7)	61(3)
C(18)	9395(7)	7217(15)	6244(10)	70(3)
C(19)	6924(6)	6563(17)	6564(7)	68(3)
C(21)	4662(4)	4484(10)	3483(6)	43(2)
C(22)	4673(5)	3592(11)	2722(6)	49(2)
C(23)	4053(5)	3255(14)	2174(7)	58(2)
C(24)	3431(6)	3781(13)	2370(7)	63(3)
C(25)	3426(5)	4644(13)	3111(8)	65(3)
C(26)	4031(5)	5038(11)	3691(6)	47(2)
C(27)	5339(6)	2948(15)	2469(9)	68(3)
C(28)	2761(6)	3469(18)	1729(10)	92(4)
C(29)	4010(6)	5943(14)	4518(7)	58(3)

Table 3.   Bond lengths [Å] and angles [°] for **C3**.
_____

W(1)-C(1)	1.996(10)	C(19)-H(19A)	0.9600
W(1)-C(2)	2.007(8)	C(19)-H(19B)	0.9600
W(1)-C(3)	2.039(11)	C(19)-H(19C)	0.9600
W(1)-C(4)	2.077(10)	C(21)-C(22)	1.391(13)
W(1)-N(2)	2.152(6)	C(21)-C(26)	1.406(12)
W(1)-N(1)	2.163(6)	C(22)-C(23)	1.380(13)
C(1)-O(1)	1.130(11)	C(22)-C(27)	1.518(15)
C(2)-O(2)	1.122(10)	C(23)-C(24)	1.375(15)
C(3)-O(3)	1.118(12)	C(23)-H(23)	0.9300
C(4)-O(4)	1.097(14)	C(24)-C(25)	1.351(16)
N(1)-C(5)	1.300(10)	C(24)-C(28)	1.522(14)
N(1)-C(11)	1.456(10)	C(25)-C(26)	1.390(14)
N(2)-C(6)	1.307(10)	C(25)-H(25)	0.9300
N(2)-C(21)	1.466(10)	C(26)-C(29)	1.492(14)
C(5)-C(6)	1.421(12)	C(27)-H(27A)	0.9600
C(5)-H(5)	0.9300	C(27)-H(27B)	0.9600
C(6)-H(6)	0.9300	C(27)-H(27C)	0.9600
C(11)-C(16)	1.390(11)	C(28)-H(28A)	0.9600
C(11)-C(12)	1.399(11)	C(28)-H(28B)	0.9600
C(12)-C(13)	1.396(12)	C(28)-H(28C)	0.9600
C(12)-C(17)	1.504(13)	C(29)-H(29A)	0.9600
C(13)-C(14)	1.368(13)	C(29)-H(29B)	0.9600
C(13)-H(13)	0.9300	C(29)-H(29C)	0.9600
C(14)-C(15)	1.374(14)		
C(14)-C(18)	1.512(15)	C(1)-W(1)-C(2)	98.8(4)
C(15)-C(16)	1.374(13)	C(1)-W(1)-C(3)	81.7(4)
C(15)-H(15)	0.9300	C(2)-W(1)-C(3)	81.8(5)
C(16)-C(19)	1.502(14)	C(1)-W(1)-C(4)	84.4(4)
C(17)-H(17A)	0.9600	C(2)-W(1)-C(4)	82.3(4)
C(17)-H(17B)	0.9600	C(3)-W(1)-C(4)	156.9(4)
C(17)-H(17C)	0.9600	C(1)-W(1)-N(2)	94.7(3)
C(18)-H(18A)	0.9600	C(2)-W(1)-N(2)	165.7(3)
C(18)-H(18B)	0.9600	C(3)-W(1)-N(2)	104.7(4)
C(18)-H(18C)	0.9600	C(4)-W(1)-N(2)	94.7(3)

C(1)-W(1)-N(1)	164.4(3)		C(15)-C(16)-C(11)	117.9(8)
C(2)-W(1)-N(1)	94.9(4)		C(15)-C(16)-C(19)	120.0(9)
C(3)-W(1)-N(1)	93.0(3)		C(11)-C(16)-C(19)	122.1(9)
C(4)-W(1)-N(1)	104.9(3)		C(12)-C(17)-H(17A)	109.5
N(2)-W(1)-N(1)	72.3(3)		C(12)-C(17)-H(17B)	109.5
O(1)-C(1)-W(1)	176.7(9)		H(17A)-C(17)-H(17B)	109.5
O(2)-C(2)-W(1)	178.8(9)		C(12)-C(17)-H(17C)	109.5
O(3)-C(3)-W(1)	170.5(9)		H(17A)-C(17)-H(17C)	109.5
O(4)-C(4)-W(1)	171.1(9)		H(17B)-C(17)-H(17C)	109.5
C(5)-N(1)-C(11)	117.2(6)		C(14)-C(18)-H(18A)	109.5
C(5)-N(1)-W(1)	117.5(5)		C(14)-C(18)-H(18B)	109.5
C(11)-N(1)-W(1)	125.1(5)		H(18A)-C(18)-H(18B)	109.5
C(6)-N(2)-C(21)	115.3(6)		C(14)-C(18)-H(18C)	109.5
C(6)-N(2)-W(1)	118.9(6)		H(18A)-C(18)-H(18C)	109.5
C(21)-N(2)-W(1)	124.7(5)		H(18B)-C(18)-H(18C)	109.5
N(1)-C(5)-C(6)	116.6(7)		C(16)-C(19)-H(19A)	109.5
N(1)-C(5)-H(5)	121.7		C(16)-C(19)-H(19B)	109.5
C(6)-C(5)-H(5)	121.7		H(19A)-C(19)-H(19B)	109.5
N(2)-C(6)-C(5)	114.4(7)		C(16)-C(19)-H(19C)	109.5
N(2)-C(6)-H(6)	122.8		H(19A)-C(19)-H(19C)	109.5
C(5)-C(6)-H(6)	122.8		H(19B)-C(19)-H(19C)	109.5
C(16)-C(11)-C(12)	121.3(7)		C(22)-C(21)-C(26)	120.7(8)
C(16)-C(11)-N(1)	120.8(8)		C(22)-C(21)-N(2)	119.4(8)
C(12)-C(11)-N(1)	117.9(7)		C(26)-C(21)-N(2)	119.8(8)
C(13)-C(12)-C(11)	117.7(8)		C(23)-C(22)-C(21)	118.9(9)
C(13)-C(12)-C(17)	121.0(8)		C(23)-C(22)-C(27)	118.2(10)
C(11)-C(12)-C(17)	121.2(8)		C(21)-C(22)-C(27)	122.9(9)
C(14)-C(13)-C(12)	121.8(9)		C(24)-C(23)-C(22)	121.2(10)
C(14)-C(13)-H(13)	119.1		C(24)-C(23)-H(23)	119.4
C(12)-C(13)-H(13)	119.1		C(22)-C(23)-H(23)	119.4
C(13)-C(14)-C(15)	118.5(9)		C(25)-C(24)-C(23)	119.4(9)
C(13)-C(14)-C(18)	120.8(10)		C(25)-C(24)-C(28)	120.9(12)
C(15)-C(14)-C(18)	120.7(10)		C(23)-C(24)-C(28)	119.6(11)
C(16)-C(15)-C(14)	122.8(9)		C(24)-C(25)-C(26)	122.5(10)
C(16)-C(15)-H(15)	118.6		C(24)-C(25)-H(25)	118.7
C(14)-C(15)-H(15)	118.6		C(26)-C(25)-H(25)	118.7

196

C(25)-C(26)-C(21)	117.2(9)		H(28A)-C(28)-H(28B)	109.5
C(25)-C(26)-C(29)	121.4(9)		C(24)-C(28)-H(28C)	109.5
C(21)-C(26)-C(29)	121.3(9)		H(28A)-C(28)-H(28C)	109.5
C(22)-C(27)-H(27A)	109.5		H(28B)-C(28)-H(28C)	109.5
C(22)-C(27)-H(27B)	109.5		C(26)-C(29)-H(29A)	109.5
H(27A)-C(27)-H(27B)	109.5		C(26)-C(29)-H(29B)	109.5
C(22)-C(27)-H(27C)	109.5		H(29A)-C(29)-H(29B)	109.5
H(27A)-C(27)-H(27C)	109.5		C(26)-C(29)-H(29C)	109.5
H(27B)-C(27)-H(27C)	109.5		H(29A)-C(29)-H(29C)	109.5
C(24)-C(28)-H(28A)	109.5		H(29B)-C(29)-H(29C)	109.5
C(24)-C(28)-H(28B)	109.5			

_____

197

Table 4. Anisotropic displacement parameters (Å^2x 10^3)for **C3**. The anisotropic displacement factor exponent takes the form: $-2p^2[\,h^2a^{*2}U^{11} + ... + 2\,h\,k\,a^*\,b^*\,U^{12}\,]$

	U^{11}	U^{22}	U^{33}	U^{23}	U^{13}	U^{12}
W(1)	36(1)	32(1)	46(1)	4(1)	5(1)	3(1)
C(1)	50(6)	36(5)	55(6)	1(4)	10(5)	7(4)
O(1)	47(4)	66(4)	90(6)	13(4)	12(4)	21(3)
C(2)	39(5)	31(4)	72(7)	-6(4)	17(5)	-10(3)
O(2)	64(5)	62(4)	119(7)	-11(4)	24(5)	-19(4)
C(3)	85(8)	59(6)	43(5)	3(5)	8(5)	21(5)
O(3)	204(12)	91(6)	66(6)	-10(5)	37(7)	57(7)
C(4)	60(7)	58(6)	30(5)	6(4)	8(5)	12(4)
O(4)	84(7)	92(7)	62(6)	19(4)	26(5)	16(4)
N(1)	37(4)	38(3)	36(4)	3(3)	-6(3)	8(3)
N(2)	38(4)	36(3)	32(3)	2(3)	7(3)	-7(3)
C(5)	46(5)	36(4)	50(5)	8(3)	0(4)	8(3)
C(6)	45(5)	38(4)	66(6)	8(4)	11(5)	-4(3)
C(11)	37(4)	33(4)	43(5)	6(3)	-3(4)	3(3)
C(12)	35(5)	45(4)	37(4)	-6(3)	-5(4)	9(3)
C(13)	34(5)	66(6)	56(6)	-9(4)	-3(4)	6(4)
C(14)	44(5)	47(5)	60(6)	-6(4)	-5(4)	2(4)
C(15)	57(6)	49(5)	46(5)	-5(4)	-4(4)	5(4)
C(16)	45(5)	49(4)	39(5)	0(4)	7(4)	7(4)
C(17)	52(6)	85(8)	47(6)	-7(5)	12(5)	14(5)
C(18)	43(6)	84(7)	76(9)	-13(6)	-5(6)	-1(5)
C(19)	62(7)	99(8)	42(6)	-3(6)	10(5)	-3(6)
C(21)	34(4)	36(4)	58(5)	13(4)	3(4)	-4(3)
C(22)	44(5)	39(4)	63(6)	0(4)	10(4)	-8(4)
C(23)	58(7)	60(6)	52(6)	4(5)	0(5)	-13(5)
C(24)	54(6)	53(5)	74(7)	9(5)	-10(5)	-14(4)
C(25)	34(5)	56(5)	107(9)	22(6)	17(6)	-5(4)
C(26)	48(5)	42(5)	54(6)	10(4)	20(4)	2(4)
C(27)	57(7)	66(6)	84(9)	-15(6)	21(6)	-6(5)
C(28)	53(7)	84(8)	124(12)	6(8)	-23(7)	-19(6)
C(29)	49(6)	64(6)	63(6)	-6(5)	15(5)	6(4)

198

Table 5. Hydrogen coordinates (x 10^4) and isotropic displacement parameters ($Å^2$x 10^3) for ML07.

	x	y	z	U(eq)
H(5)	6615	3176	5222	54
H(6)	5455	2491	4478	60
H(13)	8823	6142	4693	64
H(15)	8260	7177	6902	63
H(17A)	8025	5181	3485	91
H(17B)	7266	5897	3414	91
H(17C)	7447	3963	3730	91
H(18A)	9571	8058	5888	105
H(18B)	9673	6166	6291	105
H(18C)	9412	7714	6802	105
H(19A)	6847	7775	6694	102
H(19B)	7088	5928	7085	102
H(19C)	6497	6048	6272	102
H(23)	4056	2663	1663	69
H(25)	3002	4987	3239	78
H(27A)	5630	3940	2407	102
H(27B)	5229	2323	1936	102
H(27C)	5579	2173	2904	102
H(28A)	2685	4429	1329	138
H(28B)	2379	3395	2026	138
H(28C)	2796	2385	1427	138
H(29A)	3938	7186	4419	87
H(29B)	4441	5758	4907	87
H(29C)	3636	5470	4760	87

199

Table 6. Torsion angles [°] for **C3**.

_____

C(2)-W(1)-N(1)-C(5)	-178.2(7)	C(18)-C(14)-C(15)-C(16)	179.4(9)
C(3)-W(1)-N(1)-C(5)	99.8(7)	C(14)-C(15)-C(16)-C(11)	0.1(14)
C(4)-W(1)-N(1)-C(5)	-94.9(7)	C(14)-C(15)-C(16)-C(19)	179.4(9)
N(2)-W(1)-N(1)-C(5)	-4.7(6)	C(12)-C(11)-C(16)-C(15)	2.3(12)
C(2)-W(1)-N(1)-C(11)	6.3(7)	N(1)-C(11)-C(16)-C(15)	-179.1(7)
C(3)-W(1)-N(1)-C(11)	-75.7(7)	C(12)-C(11)-C(16)-C(19)	-176.9(9)
C(4)-W(1)-N(1)-C(11)	89.6(7)	N(1)-C(11)-C(16)-C(19)	1.7(12)
N(2)-W(1)-N(1)-C(11)	179.8(7)	C(6)-N(2)-C(21)-C(22)	-72.6(10)
C(1)-W(1)-N(2)-C(6)	-169.1(7)	W(1)-N(2)-C(21)-C(22)	95.1(8)
C(3)-W(1)-N(2)-C(6)	-86.4(7)	C(6)-N(2)-C(21)-C(26)	110.8(9)
C(4)-W(1)-N(2)-C(6)	106.2(7)	W(1)-N(2)-C(21)-C(26)	-81.6(9)
N(1)-W(1)-N(2)-C(6)	2.1(7)	C(26)-C(21)-C(22)-C(23)	-0.1(12)
C(1)-W(1)-N(2)-C(21)	23.7(7)	N(2)-C(21)-C(22)-C(23)	-176.7(7)
C(3)-W(1)-N(2)-C(21)	106.3(7)	C(26)-C(21)-C(22)-C(27)	-179.4(9)
C(4)-W(1)-N(2)-C(21)	-61.1(7)	N(2)-C(21)-C(22)-C(27)	4.0(12)
N(1)-W(1)-N(2)-C(21)	-165.2(7)	C(21)-C(22)-C(23)-C(24)	-0.2(14)
C(11)-N(1)-C(5)-C(6)	-177.5(8)	C(27)-C(22)-C(23)-C(24)	179.1(9)
W(1)-N(1)-C(5)-C(6)	6.6(10)	C(22)-C(23)-C(24)-C(25)	0.1(15)
C(21)-N(2)-C(6)-C(5)	168.9(7)	C(22)-C(23)-C(24)-C(28)	176.9(10)
W(1)-N(2)-C(6)-C(5)	0.5(11)	C(23)-C(24)-C(25)-C(26)	0.4(15)
N(1)-C(5)-C(6)-N(2)	-4.7(12)	C(28)-C(24)-C(25)-C(26)	-176.4(9)
C(5)-N(1)-C(11)-C(16)	-81.6(10)	C(24)-C(25)-C(26)-C(21)	-0.6(13)
W(1)-N(1)-C(11)-C(16)	93.9(8)	C(24)-C(25)-C(26)-C(29)	-178.1(9)
C(5)-N(1)-C(11)-C(12)	97.1(9)	C(22)-C(21)-C(26)-C(25)	0.5(12)
W(1)-N(1)-C(11)-C(12)	-87.4(8)	N(2)-C(21)-C(26)-C(25)	177.1(7)
C(16)-C(11)-C(12)-C(13)	-2.8(12)	C(22)-C(21)-C(26)-C(29)	177.9(9)
N(1)-C(11)-C(12)-C(13)	178.5(7)	N(2)-C(21)-C(26)-C(29)	-5.4(12)
C(16)-C(11)-C(12)-C(17)	176.0(8)		
N(1)-C(11)-C(12)-C(17)	-2.7(12)		
C(11)-C(12)-C(13)-C(14)	1.0(14)		
C(17)-C(12)-C(13)-C(14)	-177.8(9)		
C(12)-C(13)-C(14)-C(15)	1.3(14)		
C(12)-C(13)-C(14)-C(18)	180.0(9)		
C(13)-C(14)-C(15)-C(16)	-1.9(15)		

APPENDIX H:

CRYSTALLOGRAPHIC DATA OF C4
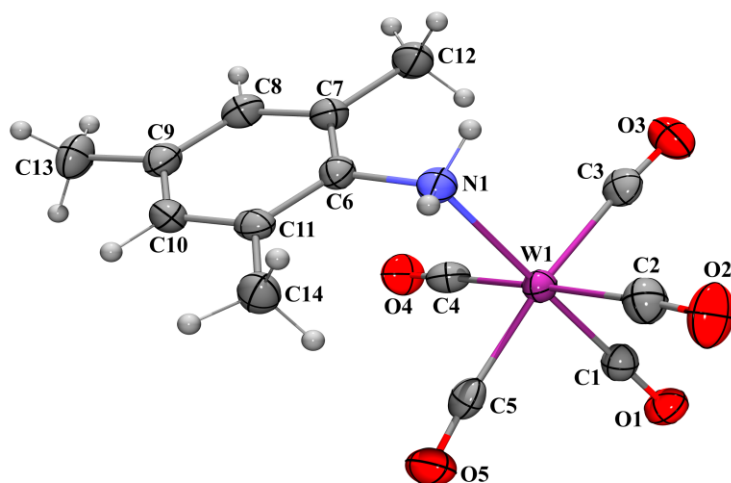
Table 1. Crystal data and structure refinement for **C4**.

Identification code	12m_up2
Empirical formula	$C_{14}H_{13}NO_5W$
Formula weight	459.10
Temperature	173(2) K
Wavelength	0.71073 Å
Crystal system	monoclinic
Space group	$P2_1/n$
Unit cell dimensions	a = 11.6233(6) Å α = 90°.
	b = 11.7269(7) Å β = 112.206(1)°.
	c = 12.1499(7) Å γ = 90°.
Volume	1533.26(15) Å^3
Z	4
Density (calculated)	1.989 Mg/m^3
Absorption coefficient	7.553 mm^{-1}
F(000)	872

Crystal size	0.30 x 0.18 x 0.11 mm^3
Θ range for data collection	2.07 to 27.99°.
Index ranges	-15<=h<=15, -15<=k<=15, -16<=l<=14
Reflections collected	15278
Independent reflections	3710 [R(int) = 0.1338]
Completeness to θ = 27.99°	100.0 %
Absorption correction	Analytical
Max. and min. transmission	0.490 and 0.210
Refinement method	Full-matrix least-squares on F^2
Data / restraints / parameters	3710 / 0 / 193
Goodness-of-fit on F^2	0.957
Final R indices [I>2σ(I)]	R1 = 0.0365, wR2 = 0.0787
R indices (all data)	R1 = 0.0491, wR2 = 0.0839
Extinction coefficient	0
Largest diff. peak and hole	1.394 and -2.196 e.Å^{-3}

202

Table 2. Atomic coordinates (x 10^4) and equivalent isotropic displacement parameters (Å^2x 10^3) for **C4**. U(eq) is defined as one third of the trace of the orthogonalized U^{ij} tensor.

	x	y	z	U(eq)
W(1)	3530(1)	2087(1)	2039(1)	26(1)
C(1)	3312(5)	841(5)	3016(5)	32(1)
O(1)	3151(4)	91(4)	3572(3)	40(1)
C(2)	1645(6)	2067(5)	1087(5)	40(1)
O(2)	608(4)	1980(5)	596(4)	56(1)
C(3)	3240(6)	3182(5)	3226(5)	35(1)
O(3)	3041(4)	3733(4)	3905(4)	48(1)
C(4)	5401(6)	2041(5)	3011(5)	33(1)
O(4)	6437(4)	1989(4)	3568(4)	43(1)
C(5)	3712(5)	861(5)	916(5)	35(1)
O(5)	3809(5)	111(4)	367(4)	49(1)
N(1)	3815(4)	3606(4)	908(4)	31(1)
C(6)	5093(5)	3798(5)	1011(4)	28(1)
C(7)	5887(5)	4461(5)	1948(4)	31(1)
C(8)	7114(5)	4547(5)	2063(5)	34(1)
C(9)	7572(5)	4020(5)	1287(5)	33(1)
C(10)	6738(6)	3401(5)	358(5)	34(1)
C(11)	5501(5)	3284(5)	187(4)	29(1)
C(12)	5433(6)	5047(5)	2815(5)	43(2)
C(13)	8910(5)	4095(6)	1445(5)	43(2)
C(14)	4622(6)	2613(5)	-876(5)	38(1)

Table 3.   Bond lengths [Å] and angles [°] for **C4**.
_____

W(1)-C(1)	1.959(6)		
W(1)-C(4)	2.047(6)	C(1)-W(1)-C(4)	89.0(2)
W(1)-C(5)	2.048(6)	C(1)-W(1)-C(5)	87.1(2)
W(1)-C(3)	2.052(6)	C(4)-W(1)-C(5)	90.6(2)
W(1)-C(2)	2.055(7)	C(1)-W(1)-C(3)	87.0(2)
W(1)-N(1)	2.349(4)	C(4)-W(1)-C(3)	91.8(2)
C(1)-O(1)	1.167(7)	C(5)-W(1)-C(3)	173.6(2)
C(2)-O(2)	1.129(8)	C(1)-W(1)-C(2)	88.7(2)
C(3)-O(3)	1.137(7)	C(4)-W(1)-C(2)	177.7(2)
C(4)-O(4)	1.138(7)	C(5)-W(1)-C(2)	88.5(2)
C(5)-O(5)	1.135(7)	C(3)-W(1)-C(2)	88.8(3)
N(1)-C(6)	1.460(7)	C(1)-W(1)-N(1)	178.63(19)
N(1)-H(1A)	0.9200	C(4)-W(1)-N(1)	90.18(19)
N(1)-H(1B)	0.9200	C(5)-W(1)-N(1)	94.0(2)
C(6)-C(11)	1.397(7)	C(3)-W(1)-N(1)	91.9(2)
C(6)-C(7)	1.399(7)	C(2)-W(1)-N(1)	92.0(2)
C(7)-C(8)	1.383(8)	O(1)-C(1)-W(1)	178.1(5)
C(7)-C(12)	1.511(8)	O(2)-C(2)-W(1)	175.1(6)
C(8)-C(9)	1.391(8)	O(3)-C(3)-W(1)	175.6(5)
C(8)-H(8)	0.9500	O(4)-C(4)-W(1)	178.0(5)
C(9)-C(10)	1.384(8)	O(5)-C(5)-W(1)	173.8(5)
C(9)-C(13)	1.496(8)	C(6)-N(1)-W(1)	115.5(3)
C(10)-C(11)	1.379(8)	C(6)-N(1)-H(1A)	108.4
C(10)-H(10)	0.9500	W(1)-N(1)-H(1A)	108.4
C(11)-C(14)	1.528(7)	C(6)-N(1)-H(1B)	108.4
C(12)-H(12A)	0.9800	W(1)-N(1)-H(1B)	108.4
C(12)-H(12B)	0.9800	H(1A)-N(1)-H(1B)	107.5
C(12)-H(12C)	0.9800	C(11)-C(6)-C(7)	121.6(5)
C(13)-H(13A)	0.9800	C(11)-C(6)-N(1)	118.8(5)
C(13)-H(13B)	0.9800	C(7)-C(6)-N(1)	119.5(5)
C(13)-H(13C)	0.9800	C(8)-C(7)-C(6)	117.5(5)
C(14)-H(14A)	0.9800	C(8)-C(7)-C(12)	121.0(5)
C(14)-H(14B)	0.9800	C(6)-C(7)-C(12)	121.5(5)
C(14)-H(14C)	0.9800	C(7)-C(8)-C(9)	122.9(5)

204

C(7)-C(8)-H(8)	118.5		H(12A)-C(12)-H(12C)	109.5
C(9)-C(8)-H(8)	118.5		H(12B)-C(12)-H(12C)	109.5
C(10)-C(9)-C(8)	117.1(5)		C(9)-C(13)-H(13A)	109.5
C(10)-C(9)-C(13)	120.6(5)		C(9)-C(13)-H(13B)	109.5
C(8)-C(9)-C(13)	122.2(5)		H(13A)-C(13)-H(13B)	109.5
C(11)-C(10)-C(9)	123.0(5)		C(9)-C(13)-H(13C)	109.5
C(11)-C(10)-H(10)	118.5		H(13A)-C(13)-H(13C)	109.5
C(9)-C(10)-H(10)	118.5		H(13B)-C(13)-H(13C)	109.5
C(10)-C(11)-C(6)	117.8(5)		C(11)-C(14)-H(14A)	109.5
C(10)-C(11)-C(14)	120.3(5)		C(11)-C(14)-H(14B)	109.5
C(6)-C(11)-C(14)	121.9(5)		H(14A)-C(14)-H(14B)	109.5
C(7)-C(12)-H(12A)	109.5		C(11)-C(14)-H(14C)	109.5
C(7)-C(12)-H(12B)	109.5		H(14A)-C(14)-H(14C)	109.5
H(12A)-C(12)-H(12B)	109.5		H(14B)-C(14)-H(14C)	109.5
C(7)-C(12)-H(12C)	109.5			

_____

205

Table 4.   Anisotropic displacement parameters ($\text{Å}^2 \times 10^3$) for **C4**. The anisotropic displacement factor exponent takes the form: $-2p^2[\,h^2 a^{*2} U^{11} + ... + 2\,h\,k\,a^*\,b^*\,U^{12}\,]$

	U^{11}	U^{22}	U^{33}	U^{23}	U^{13}	U^{12}
W(1)	23(1)	26(1)	30(1)	1(1)	10(1)	1(1)
C(1)	29(3)	37(3)	30(3)	-1(2)	11(2)	-2(2)
O(1)	47(2)	37(2)	38(2)	2(2)	19(2)	-7(2)
C(2)	37(4)	45(4)	40(3)	6(3)	16(3)	4(3)
O(2)	27(3)	84(4)	50(3)	10(2)	9(2)	-1(2)
C(3)	40(3)	35(3)	33(3)	10(2)	18(2)	1(3)
O(3)	54(3)	49(3)	47(2)	-1(2)	26(2)	11(2)
C(4)	38(3)	26(3)	33(3)	-2(2)	10(2)	-2(2)
O(4)	25(2)	48(3)	48(3)	0(2)	6(2)	3(2)
C(5)	36(3)	39(3)	34(3)	5(2)	18(2)	-7(3)
O(5)	71(3)	35(2)	52(3)	-8(2)	35(2)	-5(2)
N(1)	28(2)	28(2)	36(2)	7(2)	12(2)	4(2)
C(6)	28(3)	26(3)	31(3)	4(2)	13(2)	1(2)
C(7)	35(3)	26(3)	34(3)	-2(2)	15(2)	-3(2)
C(8)	35(3)	30(3)	34(3)	0(2)	10(2)	-5(2)
C(9)	33(3)	28(3)	41(3)	6(2)	16(2)	0(2)
C(10)	41(3)	27(3)	40(3)	-2(2)	24(3)	1(2)
C(11)	38(3)	22(2)	28(3)	2(2)	14(2)	1(2)
C(12)	54(4)	37(3)	46(3)	-12(3)	29(3)	-11(3)
C(13)	31(3)	51(4)	48(3)	8(3)	17(3)	-3(3)
C(14)	41(4)	42(3)	33(3)	-10(2)	18(3)	-9(3)

Table 5.   Hydrogen coordinates (x 10^4) and isotropic displacement parameters (Å^2x 10^3) for **C4**.

	x	y	z	U(eq)
H(1A)	3333	3475	121	37
H(1B)	3529	4263	1132	37
H(8)	7668	4987	2699	40
H(10)	7029	3039	-187	40
H(12A)	4747	5563	2381	64
H(12B)	6114	5486	3388	64
H(12C)	5142	4474	3237	64
H(13A)	9386	4454	2210	64
H(13B)	8987	4552	801	64
H(13C)	9235	3326	1426	64
H(14A)	3941	3109	-1362	56
H(14B)	4283	1962	-592	56
H(14C)	5079	2338	-1356	56

207

Table 6. Torsion angles [°] for **C4**.

_____

C(4)-W(1)-N(1)-C(6)	15.0(4)	C(12)-C(7)-C(8)-C(9)	179.9(5)
C(5)-W(1)-N(1)-C(6)	-75.7(4)	C(7)-C(8)-C(9)-C(10)	1.0(8)
C(3)-W(1)-N(1)-C(6)	106.8(4)	C(7)-C(8)-C(9)-C(13)	-178.2(5)
C(2)-W(1)-N(1)-C(6)	-164.3(4)	C(8)-C(9)-C(10)-C(11)	-0.6(8)
W(1)-N(1)-C(6)-C(11)	93.3(5)	C(13)-C(9)-C(10)-C(11)	178.6(5)
W(1)-N(1)-C(6)-C(7)	-84.8(5)	C(9)-C(10)-C(11)-C(6)	-1.5(8)
C(11)-C(6)-C(7)-C(8)	-2.9(8)	C(9)-C(10)-C(11)-C(14)	178.5(5)
N(1)-C(6)-C(7)-C(8)	175.2(5)	C(7)-C(6)-C(11)-C(10)	3.3(8)
C(11)-C(6)-C(7)-C(12)	177.9(5)	N(1)-C(6)-C(11)-C(10)	-174.8(5)
N(1)-C(6)-C(7)-C(12)	-3.9(8)	C(7)-C(6)-C(11)-C(14)	-176.7(5)
C(6)-C(7)-C(8)-C(9)	0.7(8)	N(1)-C(6)-C(11)-C(14)	5.2(8)

_____

Table 7. Hydrogen bonds for **C4** [Å and °].

D-H...A	d(D-H)	d(H...A)	d(D...A)	<(DHA)
N(1)-H(1A)...O(4)#1	0.92	2.36	3.204(6)	152.6
N(1)-H(1B)...O(1)#2	0.92	2.33	3.121(6)	144.4

Symmetry transformations used to generate equivalent atoms: #1 x-1/2,-y+1/2,z-1/2 #2 -x+1/2,y+1/2,-z+1/2

APPENDIX I:

RMS Data
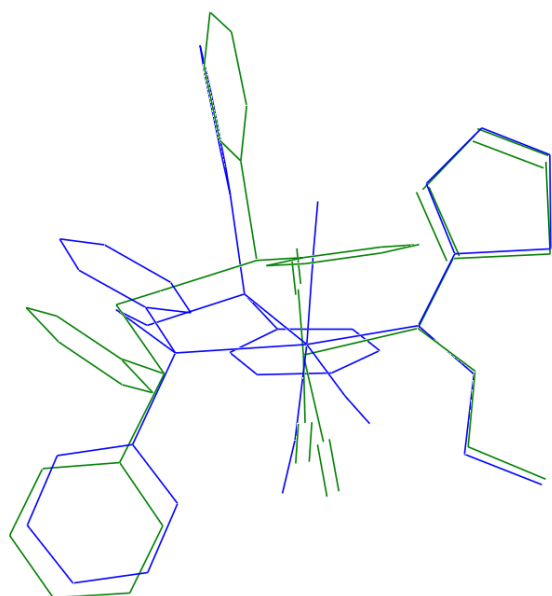
Key: ▬ **Theoretical structure**
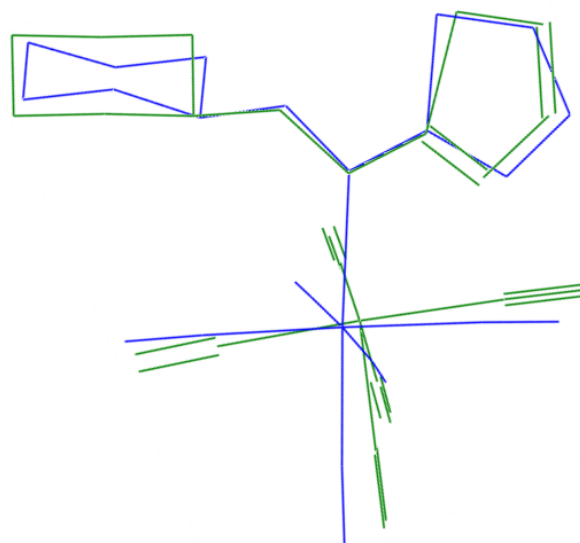   ▬ **Crystal structure**

Figure A. Complex **A3** (RMS: 1.39 Å)
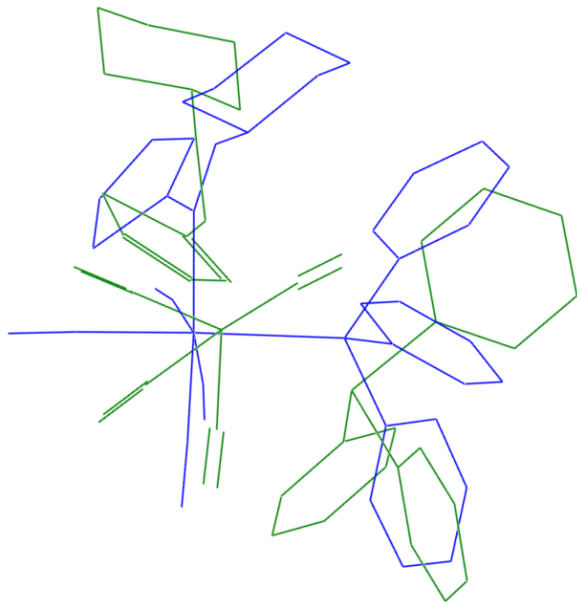

Figure A. Complex **A4** (RMS: 0.353 Å)

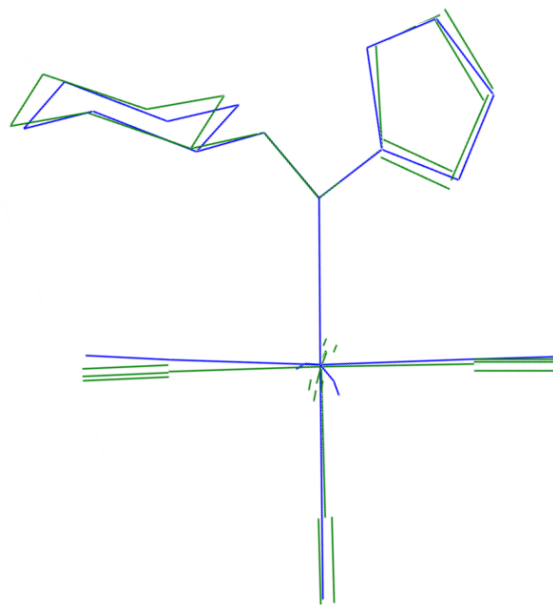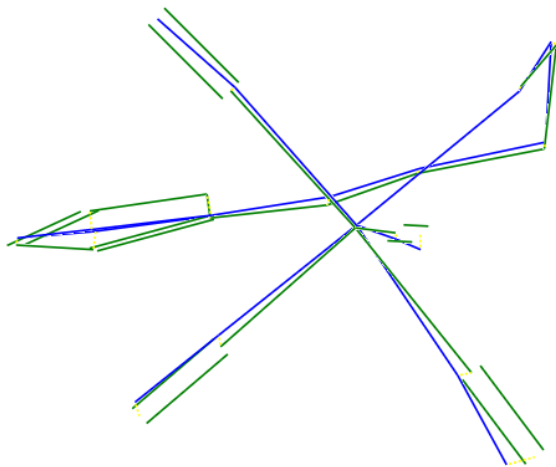Figure A. Complex **A5** (RMS: 0.849 Å)

Figure A. Complex **B4** (RMS: 0.100 Å)

Figure A. Complex **B8** (RMS: 0.126 Å)